Quantitative Nucleic Acid Measurements Inform Strategies to Mitigate Viral Outbreaks

Thesis by

Alexander Viloria Winnett

In Partial Fulfillment of the Requirements for

the Degree of

Doctorate of Biology

CALIFORNIA INSTITUTE OF TECHNOLOGY

Pasadena, California

2025

(Defended September 17, 2024)

Alexander Viloria Winnett
ORCID: 0000-0002-7338-5605

TABLE OF CONTENTS

ACKNOWLEDGEMENTS

I wish to first acknowledge the over seven million individuals lost to the devastating COVID-19 pandemic, which continues to take the lives of thousands across the globe today and cause chronic illness in survivors. I'd also like to acknowledge the individuals from Pasadena and its surrounding communities who participated in our Caltech COVID-19 Study: your diligence and support of science enabled important lessons for how to best detect SARS-CoV-2 infection to prevent further spread and development of additional variants. This fundamental role of the community in science is recognized and not taken for granted. Additionally, I wish to thank the essential workers, from healthcare workers to grocery store clerks, who labored to sustain us all throughout the danger and uncertainty of the COVID-19 pandemic.

Several mentors have guided my training and the subsequent research work, most notably my advisor, Dr. Rustem F. Ismagilov. My thesis committee members—Dr. Valerie Arboleda, Dr. Matt Thomson, and Dr. Ellen Rothenberg—have also provided enormously valuable guidance.

In addition to co-authors of published work presented in this thesis, and I also wish to thank the following individuals for technical guidance on various aspects of the research work:

Dr. Michael K Porter, Dr. Natasha Shelby, Reid Akana, Dr. Matthew Bidwell Goetz, Dr. Annabelle De St Maurice, Dr. Christopher Graber, Dr. David Beenhouwer, Dr. Timothy Stenzel, Dr. Andy Lim, Dr. Karen Heichman, Dr. Omai Garner, Dr. Robert Schlaberg, Dr. Jennifer Fulcher, Dr. Debika Bhattacharya, Dr. Allison Rhines, Dr. Dan Wattendorf, Dr. Doug Rains, Dr. Issy Lin, Kenin Quian, Dr. Mildred Galvez, Dr. Prashant Bhat, Lindsay Hartson, Dr. Izabela Ragan, Dr. David Boyle, Dr. Jason Andrews, Dr. Christopher Mason, Dr. Daniel Butler, Namita Dahlmer Dr. Andrew Grosovsky, Dr. Molly Franke, Dr. Laura Leubbert, Dr. Lior Pachter, Dr. Mikhail Shapiro, Dr. Diane Newman, Dr. Victoria Orphan, Han Zhang, Anna Romano, Henry (Hengyu) Wang, Minkyo Lee, Sasha Tabachnikova, and Kerrie Greene.

I wish to thank the following individuals for auxiliary support in completion of the research work:

Liz Ayala, Raina Beaven, Sohee Lee, Mi Kyung Kim, Supresh Gupta, Lucy Viramontes, Shannon Yamashita, Lauriane Quenee, Grace Fisher-Adams, Junie Hildebrandt, Megan Hayashi, RuthAnne Bevier, Chantal D'Apuzzo, Victor Rivera, Gary Waters, Leonard Edwards, Gaylene Ursua,

Cynthia Ramos, Shannon Yamashita Prabhu Gounder, Tony Chang, Jennifer Howes, Sarah Weinstein, Nari Shin, and Lesli and Will.

Finally, I wish to thank the following individuals for general guidance and support through the completion of my doctorate:

Anny Viloria Winnett, Nic Zenquis, Larissa DeSouza, Dr. Diego Almanza, Jessica Soule, Meghan Mahoney, Colton Smith, Nicole Ocasio Martinez, Samantha Kelley, Jacob Winnett, Nadia Barredos, Martin Soto Cardenas, Claudia Almonacid Sara, Dakotah Tyler, Jocelyn White, Elijah Catalan, Dr. Ricardo Rosales, Dr. Jay Gill, Dr. Sarah Andebrehan, Dr. Richard Kesseli, Claudia Heske, Dr. Elaine Bearer, Dr. David Dawson, Dr. Olujimi Ajijola, Familia Viloria y Rodriguez Zambrano, Chinenye Wachuku, Yuna Farah, Natasha Reich, Devon Dobbs, Levi Palmer, Melina Mastrodimos, Noah Okada, Joshua Chaj, Andrew Lu, Delaney Sullivan, Jessica Jacobs Li.

Funding for my research work has been provided by the following sources:

The Center for Environmental Microbial Interactions at Caltech, Geffen Scholarship from the University of California Los Angeles, National Institutes of Health (NIH) F30 Award (NIAID F30AI16752), Bill and Melinda Gates Foundation (INV-023124), Ronald and Maxine Linde Center for New Initiatives at the California Institute of Technology, and NIH T32GM008042 to the UCLA-Caltech Medical Scientist Training Program.

ABSTRACT

Humans have always been and continue to be at risk of infection by pathogens that surround us. However, recent advancements in quantitative nucleic acid technologies have allowed for more detailed study of these pathogens, how they spread among individuals, and how our immune systems respond to infection. In this thesis, I describe the design and execution of the Caltech COVID-19 Study, which used quantitative nucleic acid measurements to investigate the natural history of SARS-CoV-2 infection and inform strategies for diagnostics and vaccine development to reduce viral transmission. The Caltech COVID-19 Study enrolled participants in the Los Angeles area between September 2020 and April 2022 who were at risk of SARS-CoV-2 infection due to recent exposure to a household contact with acute infection. Participants collected paired upper respiratory specimens (saliva, nasal swabs, and throat swabs) daily or twice daily for approximately two weeks. These specimens underwent SARS-CoV-2 viral load quantification to assess transmission risk and determine whether to extend or terminate study enrollment. For participants who initially tested negative for SARS-CoV-2 RNA but later developed sustained infection, we tracked viral load from the very start of infection. These measurements were then used to evaluate the performance of various COVID-19 diagnostic tests. Our findings revealed a significant advantage of high-analytical-sensitivity tests over those with lower sensitivity, as well as the benefit of testing both the throat and nose rather than just the nose. In addition to viral load quantification, we sequenced human mRNA from these specimens to assess gene expression. Analyzing these changes allowed us to study how the mucosal immune system responds to acute viral infection across multiple anatomical sites over time, providing insights that could improve mucosal vaccine design. Notably, our data showed that, contrary to current models of localized paracrine interferon signaling, distinct compartments of the upper respiratory mucosa exhibited synchronized interferon stimulation during early infection—even in the absence of detectable local viral replication. Mucosal vaccines capable of triggering this coordinated interferon response, maintaining CD8+ T memory cells to rapidly execute effector functions upon viral exposure, may be key to achieving sterilizing immunity. Findings from quantitative nucleic acid measurements in this thesis inform strategies to more effectively mitigate viral outbreaks.

PUBLISHED CONTENT AND CONTRIBUTIONS

Referenced in Chapter I: Dora AV*, Winnett A*, Jatt LP, Davar K, Watanabe M, Sohn L, Kern HS, Graber CJ, Goetz MB. Universal and Serial Laboratory Testing for SARS-CoV-2 at a Long-Term Care Skilled Nursing Facility for Veterans — Los Angeles, California, 2020 (May 2020). CDC Morbidity and Mortality Weekly Report. http://dx.doi.org/10.15585/mmwr.mm6921e1

Extracted and coded participant data. Outbreak investigation activities. Data analysis. Generation of Table 1. Literature review. Maintained reference library. Drafted and revised manuscript with AVD.

Referenced in Chapter I: Dora AV*, Winnett A*, Fulcher JA, Sohn L, Feliza C, Lee-Chang I, Ghadishah E, Schwartzman WA, Beenhouwer DO, Vallone J, Graber CJ, Goetz MB, Bhattacharya D. Using Serologic Testing to Assess the Effectiveness of Outbreak Control Efforts, Serial PCR Testing, and Cohorting of Positive SARS-CoV-2 Patients in a Skilled Nursing Facility (Aug 2020). Clinical Infectious Disease. http://dx.doi.org/10.1093/cid/ciaa1286

Extracted and coded participant data. Data analysis. Generation of Figure 1. Literature review. Maintained reference library. Drafted and revised manuscript with AVD.

Referenced in Chapter I: Winnett A, Jatt LP, Sohn L, Lysaght M, Yoshiwaka T, Simon SR, Graber CJ, Goetz MB. Coordinated outreach for veterans in long-term care facilities by an integrated Veterans Affairs healthcare system during the COVID-19 pandemic (May 2020). Infection Control and Hospital Epidemiology. https://doi.org/10.1017/ice.2020.326

Conceptualization with MBG. Literature review. Managed reference library. Drafted and revised manuscript.

Referenced in Chapter I: Jatt LP, Winnett A, Graber CJ, Vallone J, Beenhouwer DO, Goetz MB. Widespread severe acute respiratory coronavirus virus 2 (SARS-CoV-2) laboratory surveillance program to minimize asymptomatic transmission in high-risk inpatient and congregate living settings (April 2020). Infection Control and Hospital Epidemiology. https://doi.org/10.1017/ice.2020.301

Validated underlying data with LPJ. Literature review. Revised manuscript with JLP.

Referenced in Chapter I: Schoepp NG, Liaw EJ, Winnett A, Savela ES, Ismagilov RF. Differential DNA Accessibility to Polymerase Enables 30-minute Phenotypic β-lactam Antibiotic Susceptibility Testing of Carbapenem-resistant Enterobacteriaceae (Dec 2019). PLoS Biology. https://doi.org/10.1371/journal.pbio.3000652

NGS, EJL, AW, ESS, and RFI contributed to conceiving the method, revising the manuscript, and interpretation of experimental results. NGS and AW tested clinical samples using the modified workflow. Revised manuscript with co-authors.

Referenced in Chapter I: Viloria Winnett A, Srinivasan V, Davis M, Vijayan T, Uslan DZ, Garner OB, de St Maurice A. The Path of More Resistance: a Comparison of National Healthcare Safety Network and Clinical Laboratory Standards Institute Criteria in Developing Cumulative Antimicrobial Susceptibility Test Reports and Institutional Antibiograms (Feb 2022). Journal of Clinical Microbiology. https://doi.org/10.1128/jcm.01366-21

Compiled and cleaned clinical laboratory data, and clinical chart data. Designed analytical approach. Prepared Figure 1, Table 1, Table 2, Table S1, Table S2, and Figure S1. Performed analyses for and prepared Figures 2-6 with VS. Literature review. Managed reference library. Outlined and drafted manuscript. Revised manuscript with VS and ADSM.

Referenced in Chapter I: Kenin Qian K, Viloria Winnett A, Abhyankar V, Keo D, Wang C, Ismagilov RF, Toy T, Eskin E, Arboleda VA. Nucleic acid extraction methods for oro-

respiratory specimens undergoing clinical metagenomic sequencing (July 2024). In submission at American Journal of Clinical Pathology.

AVW and RFI compiled and analyzed data shown in Figure 2, and reported in *Human upper respiratory specimen types exhibit multiple pre-analytical variables* subsection of Results.

Chapter II: Viloria Winnett A*, Porter MK*, Romano AE, Savela ES, Akana R, Shelby TS, Reyes JA, Schlenker NW, Cooper MM, Carter AM, Ji J, Barlow JT, Tognazzini C, Feaster M, Goh YY, Ismagilov. Morning SARS-CoV-2 testing yields better detection of infection due to higher viral loads in saliva and nasal-swabs upon waking (March 2022). Microbiology Spectrum. https://doi.org/10.1101/2022.03.02.22271724

Collaborated with MMC, NS, RFI, YG, MF on initial study design and recruitment strategies; co-wrote IRB protocol and informed consent with MMC and NS; co-wrote enrollment questionnaire with NS and JJ; co-wrote participant informational sheets with NS and JAR and digital survey; developed and validated methods for saliva and nasal-swab specimen collection; developed and validated methods for RT-qPCR analysis for saliva and swab specimens with AER, ESS, MMC; reagents and supplies acquisition; funding acquisition; developed laboratory specimen processing workflow with AER, ESS, and MMC; performed specimen logging and QC, nucleic acid extraction, RT-qPCR; assembled Table 1 with NS; analyzed viral load timeseries data to visualize trends (Figure 1) with MKP; assisted MKP in the preparation of Figure 2; analyzed viral load data to generate Figure 3 with MKP; analyzed specimen collection data for Figure S1; generated longitudinal RT-qPCR plot array for Figure S2, Figure S3 with MKP; analyzed data for Figure S4. Verified the underlying data with MKP and NS. Outlined and wrote manuscript with MKP.

Chapter III: Savela ES*, Viloria Winnett A*, Romano AE*, Porter MK, Shelby T, Akana R, Ji Jenny, Cooper MM, Schlenker NW, Reyes JA, Carter AM, Barlow JT, Tognazzini C, Feaster M, Goh YY, Ismagilov RF. Quantitative SARS-CoV-2 Viral-Load Curves in Paired

Saliva Samples and Nasal Swabs Inform Appropriate Respiratory Sampling Site and Analytical Test Sensitivity Required for Earliest Viral Detection (Feb 2022). Journal of Clinical Microbiology. https://doi.org/10.1128/jcm.01785-21

Collaborated with MMC, NS, RFI, YG, MF on initial study design and recruitment strategies; co-wrote IRB protocol and informed consent with MMC and NS; co-wrote enrollment questionnaire with NS and JJ; co-wrote participant informational sheets with NS and JAR and digital survey; developed and validated methods for saliva and nasal-swab sample collection; developed and validated methods for RT-qPCR and RT-digital droplet PCR analysis for saliva and swab samples with AER, ESS, MMC; reagents and supplies acquisition; funding acquisition; developed laboratory sample processing workflow with AER, ESS, and MMC; performed specimen logging and QC, nucleic acid extraction, RT-qPCR, data processing—including experimental data generation for saliva calibration curve (Figure 1, Figure S2) designed with MMC and AER, establishment of nasal swab limit of detection (Figure S1), and viral load timeseries data (Figure 2) with ESS, AER, MKP, and AMC; interpreted sequencing data with AER; analyzed viral load timeseries data to visualize trends (Figure 3, Figure S4) with ESS; generated, analyzed and visualized data to assess degradation of viral RNA in saliva and nasal swab samples with RA, ESS, and AER (Figure S3); literature analysis with RA, ESS, and MKP; co-wrote sections of the manuscript outlined by ESS and RFI, edited the manuscript. Verified the underlying data with ESS.

Chapter IV: Viloria Winnett A*, Akana R*, Shelby N*, Romano AE, Davich H, Caldera S, Kim MK, Carter AM, Yamada T, Reyna JR, Ji J, Reyes JA, Cooper MM, Thomson M, Tognazzini C, Feaster M, Goh YY, Ismagilov. SARS-CoV-2 Omicron variant exhibits extreme differences in early viral loads among respiratory specimen types resulting in higher sensitivity by nasal-oropharyngeal combination specimens (March 2023). PNAS Nexus. https://doi.org/10.1093/pnasnexus/pgad033

Collaborated with NS, RFI, YG, MF on initial study design and recruitment strategies; co-wrote IRB protocol and informed consent with NS; co-wrote enrollment questionnaire and

post-study questionnaire with NS; co-developed participant keep/drop criteria with NS; funding acquisition; designed and coordinated LOD validation experiments; selected and prepared specimen for viral-variant sequencing with NS, YC, and AER; assisted with the inventory and archiving of >6,000 specimen at Caltech with AER and AMC; minor role supporting outreach by HD and NS; minor role supporting kit-making by AER, HD and AMC; verified the underlying data with NS and RA; assembled Figures 1–2 with NS; performed analysis and prepared Figures 4–7, Table S1, Figure S1, S2, S6, S7, S8, S9. Major contributor to the selection of references. Co-wrote and edited the manuscript with NS and RA.

Chapter V: Porter MK, Viloria Winnett A, Hao L, Shelby N, Reyes JA, Schlenker NW, Romano AE, Tognazzini C, Feaster M, Goh YY, Gale M, Ismagilov RF. The ratio between SARS-CoV-2 RNA viral load and culturable viral titer differs depending on stage of infection (Nov 2023). Access Microbiology. https://doi.org/10.1099/acmi.0.000732.v1

Conceptualization of nested study with MKP and RFI. Literature review with MKP. Co-wrote biosafety protocols for receipt and processing of live specimens with MKP. Reagent and supply acquisition. Determined and validated live specimen collection methods with MKP. Received, logged, and aliquoted live specimens with MKP. Performed nucleic acid extractions and RNaseP and N gene RT-qPCR. Coordinated and prepared shipments of nucleic acids for viral sequencing. Coordinated and prepared shipments of live specimens to collaborators for viral culture. Interpreted paired viral load and culture data with MKP and LH. Outlined and co-wrote manuscript with MKP. Provided feedback on the design of Figures 1, S1, and S2. Validated underlying data with MKP.

Chapter VI: Viloria Winnett A*, Akana R*, Shelby N*, Romano AE, Davich H, Caldera S, Kim MK, Carter AM, Yamada T, Reyna JR, Ji J, Reyes JA, Cooper MM, Thomson M, Tognazzini C, Feaster M, Goh YY, Ismagilov. Daily SARS-CoV-2 Nasal Rapid Antigen Testing Poorly Detects Infected and Infectious Individuals (March 2023). Microbiology Spectrum. https://doi.org/10.1128/spectrum.01295-23

Collaborated with NS, RFI, YG, MF on initial study design and recruitment strategies; co-wrote IRB protocol and informed consent with NS; co-wrote enrollment questionnaire and poststudy questionnaire with NS; co-developed participant keep/drop criteria with NS; funding acquisition; designed and coordinated LOD validation experiments; selected and prepared specimen for viral-variant sequencing with NS, YC, and AER; assisted with the inventory and archiving of >6,000 specimen at Caltech with AER and AMC; minor role supporting outreach by HD and NS; minor role supporting kit-making by AER, HD and AMC; verified the underlying data with NS and RA; major contributor to reference organization and selection; assembled Figure 1 with NS; made Figure 4 with NS; performed analysis and prepared Figure 2, Figure 6, Figure 7, Figure S1, and Table S2. Cowrote and edited the manuscript with NS and RA.

Chapter VII: Carter AM*, Viloria Winnett A*, Romano AE, Akana R, Shelby N, Ismagilov RF. Laboratory Evaluation Links Some False-Positive COVID-19 Antigen Test Results Observed in a Field Study to a Specific Lot of Test Strips (Jan 2023). Open Forum Infectious Diseases. https://doi.org/10.1093/ofid/ofac701

Collaborated with MMC, NS, RFI, YG, MF on initial study design and recruitment strategies; co-wrote IRB protocol and informed consent with MMC and NS; co-wrote enrollment questionnaire with NS and JJ; co-wrote participant informational sheets with NS and JAR and digital survey; developed and validated methods for saliva and nasal-swab sample collection; developed and validated methods for RT-qPCR and RT-digital droplet PCR analysis for saliva and swab samples with AER, ESS, MMC; reagents and supplies acquisition; funding acquisition; developed laboratory sample processing workflow with AER, ESS, and MMC; performed specimen logging and QC, nucleic acid extraction, RT-qPCR, data processing—including experimental data generation for saliva calibration curve (Figure 1, Figure S2) designed with MMC and AER, establishment of nasal swab limit of detection (Figure S1), and viral load timeseries data (Figure 2) with ESS, AER, MKP, and AMC; interpreted sequencing data with AER; analyzed viral load timeseries data to visualize trends (Figure 3) with ESS; generated, analyzed, and visualized

data to assess degradation of viral RNA in saliva and nasal swab samples (Figure S3) with RA, ESS, and AER; literature analysis with RA, ESS, and MKP; co-wrote sections of the manuscript outlined by ESS and RFI, edited the manuscript. Verified the underlying data with ESS.

Chapter VIII: Ji J*, Viloria Winnett A*, Shelby N, Reyes JA, Schlenker NW, Davich H, Caldera S, Tognazzini C, Goh YY, Feaster M, Ismagilov RF. Index Cases First Identified by Nasal-Swab Rapid COVID-19 Tests Had More Transmission to Household Contacts Than Cases Identified by Other Test Types. PLoS ONE. https://doi.org/10.1371%2Fjournal.pone.0292389

Conceptualization of study with JJ and RFI. Contributed to overall study design and recruitment strategies. Co-wrote enrollment questionnaire with NS and JJ. Data curation and analysis. Assigned vaccination status for each participant. Assigned infection status from viral load data. Assigned index case with JJ, NS, and NWS. Prepared Figure 1, 2, and 3 with JJ. Prepared Table 1 with JJ. Verified underlying data and analyses performed by JJ. Study-specific literature review with JJ. Outlined manuscript with JJ. Drafted initial manuscript. Revised manuscript with JJ.

Chapter IX: Viloria Winnett A, Stenzel T, Ismagilov RF. Validating Combination Throat-Nasal Swab Specimens for Coronavirus Disease 2019 Tests Would Improve Early Detection, Especially for the Most Vulnerable (July 2024). Clinical Infectious Diseases. https://doi.org/10.1093/cid/ciae381

Conceptualization of piece with RFI. Literature review. Generation of Figure 1. Preparation of Table S1 with TS. Drafted and revised manuscript.

Referenced in Conclusions: Laura L, Sullivan DK, Carilli M, Hjörleifsson KE, Viloria Winnett A, Chari T, Pachter L (May 2024). bioRxiv. https://doi.org/10.1101/2023.12.11.571168

Generated data shown in Figure 3A. Revised manuscript with LL.

LIST OF ILLUSTRATIONS AND/OR TABLES

Supplemental Figures

Supplemental Tables

Chapter 1

ADVANCING STRATEGIES TO PREVENT VIRAL TRANSMISSION

Physician-scientist training in a pandemic

In December 2019, the first known cases of pneumonia of unknown origin were reported in Wuhan, China, and some of those affected would succumb to a fatal pneumonia.[1] Electron microscopy revealed coronaviral morphology,[2] and emerging viral pathogen monitoring groups began sounding the alarm in January 2020.[3] As cases and fatalities appeared and rose in other countries, the World Health Organization (WHO) officially declared the COVID-19 pandemic on March 11 2020.[4]

At the time, I had completed two years of medical school and was halfway through my first year as a PhD student in the Ismagilov Laboratory at Caltech. I had always been passionate, scientifically and morally, to use my time on this Earth to research infectious diseases and reduce their burden on human health. Since beginning my PhD, I had been working on developing an assay that could rapidly determine the phenotypic beta-lactam antibiotic susceptibility of pathogenic *Enterobacteriaceae* in specimens from individuals with urinary tract infections.[5] These susceptibility results could quickly guide directed antibiotic therapy to reduce the emergence of microbes for which we have no treatments.[6] Prior to beginning my training as a physician-scientist, I had worked in a clinical *Mycobacterium tuberculosis* laboratory, evaluated monoclonal antibody therapeutics for Dengue virus, and studied unknown protein functions associated with the inner membrane complex of *Toxoplasma gondii*, as well as how methicillin resistant *Staphylococcus aureus* uses quorum sensing to regulate virulence inside the phagosomes of polymorphonuclear neutrophils. In high school I saved up money from work as a cashier at McDonald's to get trained, certified, and hired as a lifeguard. During my undergraduate studies, I would transition from late-night shifts as a server and bartender to work overnight as General Medicine Unit Coordinator at the Massachusetts General Hospital, and opt-in to serve on the Emergency Department's Hazardous Materials Response Team.

In early March 2020, as supply chains faltered, grocery stores emptied, states of emergency declared, and "lockdowns" initiated, I felt compelled to support the response however I could and however necessary. Clinical mentors connected me to Dr. Matthew Bidwell Goetz and Dr. Steven Simon, the Chief of Infectious Disease and Chief of Staff respectively, at the Greater Los Angeles Veteran's Affairs Healthcare System (GLAVAHS). I was asked to step into a loosely defined, ad hoc role, assisting with the healthcare system's response to COVID-19. On March 18, 2020, I attended my first 8 a.m. daily briefing: a small group of leaders from different areas of the hospital system sat around a table in a carpeted conference room to identify key emerging issues and make challenging decisions to coordinate swift but effective measures. The weight of the pandemic grew, as did the sentiment of these

meetings. One of my tasks would include preparation of daily situation-in-numbers updates for this meeting: waking up before sunrise to prepare an increasingly grim report the number of COVID-19 cases, hospitalizations, and deaths at the hospital, in Los Angeles, in California, in the USA, and globally. I would highlight where particularly large or deadly outbreaks were emerging. The likeness of this task to that of plague doctors before me was not lost, and occasionally, when I found a spare moment, I would quickly re-read pages from *The Plague* by Albert Camus.

As the pandemic exploded, so too did information about the novel virus. In tandem with my counterpart, Lauren Jatt (now, Dr. Lauren Jatt), I was to find, compile, and summarize emerging information on COVID-19 to inform the design of infection control policies that would best protect patients and staff (e.g., use of personal protective equipment [PPE] in clinical contexts with differential risk, alternate materials for or methods to decontaminate PPE upon shortages, staffing algorithms, patient placement and diagnostic testing workflows). Upon the release of a policy, I would circulate among staff—nurses, custodial, physicians, social workers, etc.—to explain the rationale, answer questions, and collect their reactions and feedback. I'd then bring this feedback to the team and propose revisions. The questions and reactions raised by staff guided and energized my search for the most up-to-date information and necessitated my rapid improvement of skills in crisis communication.

Guidance from the WHO, U.S. Centers for Disease Control and Prevention (CDC), California Department of Public Health, and Los Angeles County Department of Public Health were being updated by the minute. Literature was emerging in peer-reviewed journals, on pre-print servers, and on social media constantly. Zhou et al. reported that of 191 patients hospitalized since the start of the outbreak in Wuhan, 62% developed severe or critical disease, and 28% died.[1] Similarly, a report from King County Washington demonstrated that during a nursing home outbreak, 81 of approximately 130 residents became infected, 22 of whom (27%) died.[7] These high transmission and mortality rates raised substantial concern for what might happen if an outbreak were to occur among residents of the long-term care facilities on the GLAVAHS campus.

Diagnostic testing to combat the COVID-19 pandemic

The Chief of Laboratory Medicine and Pathology, Dr. John Vallone, took the lead on getting any available COVID-19 diagnostic testing up and running at GLAVAHS. Initially, specimens were submitted to an external laboratory (Quest Diagnostics) for testing. Many institutions were utilizing this external laboratory, and sending more and more samples for testing, resulting in turnaround times upwards of three days, and as high as 14 days. Heroic effort from the Department of Laboratory Medicine and Pathology at GLAVAHS and sister VA campuses brought in-house testing workflows online in rapid time, but both throughputs and reagents were limited. Given these constraints, we faced difficulty allocating testing resources between staff presenting with symptoms, ambulatory patients arriving

to the emergency department, admitted inpatients, individuals scheduled to undergo procedures, and other populations.[8]

Then, the moment we had feared arrived. At approximately 4:45 p.m. on March 28, 2020, the phone rang in the Office of the Chief of Infectious Disease. The Chief of Laboratory Medicine had an urgent result: following our testing algorithm, a resident (A0.1) of a nursing home ward had become symptomatic, tested negative by a panel of 17 non-SARS-CoV-2 respiratory viruses,[9] and reflex testing for SARS-CoV-2 had resulted positive. This was the first case of COVID-19 in the long-term care facility at GLAVAHS. Hospital engineering staff had been working round-the-clock to convert units of the hospital to COVID-19 acute care areas, with added infection control features such as antechambers and increased ventilation. Nursing home staff quickly and carefully transported the patient (A0.1, Figure 1-1) to one of these units, where despite best efforts, they would succumb to the infection. An additional resident of that nursing home ward had begun to experience COVID-19-like symptoms (A0.2, Figure 1-1), and subsequently tested positive. We anticipated that there would be more infected nursing home residents, and that the potential for a devastating outbreak was imminent.

While nursing home staff had implemented enhanced symptom screening of all residents, a recent epidemiological investigation had just revealed that unlike influenza or SARS-CoV-1, transmission of SARS-CoV-2 often occurs prior to symptom onset.[10] Flagging this evidence, we recognized that symptom screening alone might not prompt isolation of infected residents early enough to prevent transmission. Asymptomatic screening testing would likely be necessary to mitigate the outbreak.

Fortunately, that same weekend the Veterans Affairs Long Beach Healthcare System brought online a high-capacity Roche cobas 6800/8800 instrument to expand testing capacity for regional VA hospitals.[8] Given this opportunity, the decision was made to expend testing resources on a universal, serial screening testing approach. In this strategy, all nursing home residents, regardless of symptoms, would undergo nasopharyngeal swab collection and SARS-CoV-2 testing with an RT-PCR test. Infected individuals would be transported immediately to the hospital for isolation. This process would be repeated approximately every week until the outbreak was mitigated.[11]

Among three nursing home facilities at GLAVAHS, two wards (Wards A and C) experienced outbreaks. After symptomatic index cases were initially identified in each of these two facilities, Ward A had an additional four infected residents (A1.1-4), and Ward C had an additional 12 infected residents (C1.1-10, C2.1-2). Of the 16 infected residents identified by universal, serial screening testing, 13 (81%) were asymptomatic when identified. After the first two rounds of testing, no additional cases were identified. It appeared that the testing and isolation strategy, in combination with heightened infection control practices, had successfully mitigated the outbreak.[11] Serological

evaluation of residents two to three months after this outbreak revealed no infected individuals had been missed by this testing strategy.[12]

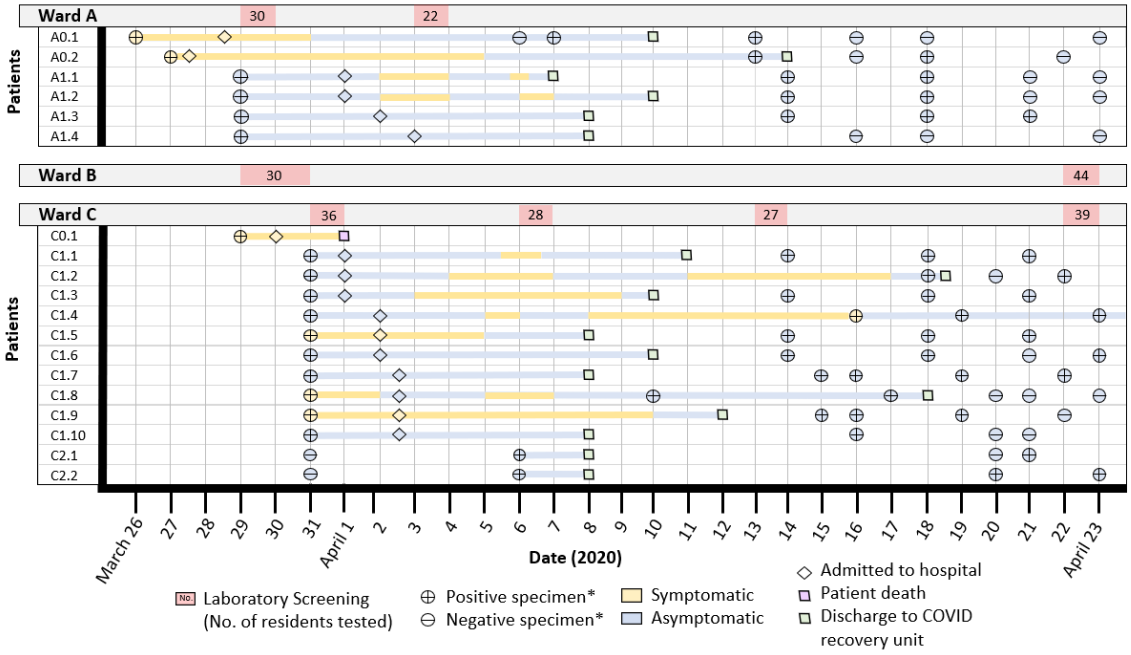

Figure 1-1. Timeline of COVID-19 outbreak and universal serial screening testing among VAGLAHS skilled nursing facility residents in March–April 2020.

The events of this outbreak demonstrated how a successful diagnostic testing strategy can facilitate targeted infection control interventions and rapid mitigation of an outbreak. However, the use of universal serial screening testing to guide infection control (as well as treatment initiation) is not limited to COVID-19. For example, the CDC recommends universal screening testing for Human Immunodeficiency Virus (HIV) infection by venipuncture at least once a year for individuals with certain risk factors[13] and every three months for individuals taking Pre-Exposure Prophylaxis.[14]

While universal serial screening testing by weekly RT-PCR on nasopharyngeal swab specimens mitigated this SARS-CoV-2 outbreak in under three weeks, other testing strategies might have been more effective and/or better optimize the use of available testing resources. These alternate strategies could employ a different frequency of testing (e.g., every five days versus every seven days), a different specimen type for testing (e.g., saliva, oropharyngeal or anterior nares swab instead of nasopharyngeal swab), or a different COVID-19 test type (e.g., rapid antigen diagnostic tests [Ag-RDTs] instead of a nucleic acid amplification test).

When infection control policies were generally settled and COVID-19 prevalence declined during the summer of 2020, I transitioned out of my role at GLAVAHS and returned my focus to research and my graduate studies at

Caltech. I was fortunate that Professor Ismagilov was also compelled to step up in response to the COVID-19 pandemic. As we discussed how to respond, we identified a question that critically needed an answer: how do we best achieve early detection of SARS-CoV-2 infection to limit transmission and mitigate outbreaks? With a worthwhile question identified, we set out to define the data needed to answer that question.

The data we need, to inform COVID-19 diagnostic testing strategies

Detection by a diagnostic test is dependent on whether the concentration of target is at or above the concentration necessary to generate a response by the assay that is discernable from noise. The lowest concentration of a diagnostic target that will reliably (at least 95% of the time) yield a positive result is known as the limit of detection of the test (LOD).[15] The efficiency of the test chemistry to extract or purify the diagnostic target from the sample and other engineered properties of the test determine the LOD of the test, though test performance can vary for specimen types with different physical or chemical characteristics. For example, saliva can be viscous, have a high abundance of bacteria, and contain food debris that interferes with some test chemistries. COVID-19 molecular diagnostic tests detect viral RNA, while COVID-19 AgRDTs detect viral surface proteins. COVID-19 tests have been developed to detect these viral components in a variety of specimen types, though acute infection is typically diagnosed using upper respiratory specimen types such as nasopharyngeal swabs, anterior nares or midturbinate nasal swabs, saliva, or oropharyngeal swabs.

The amount of these SARS-CoV-2 targets in specimens is dynamic over time. Starting from undetectable levels, virus proliferates by several orders of magnitude, and then decreases gradually (if effectively cleared by the immune system). Without treatment, this rise and fall of SARS-CoV-2 and the associated clinical features is known as the "natural history of infection." By measuring quantity of virus throughout the natural history of infection, one can predict the periods of infection that would prompt a positive result if tested by a diagnostic test with a given LOD. During the first year of the COVID-19 pandemic, nearly all available data describing the natural history of SARS-CoV-2 infection began at symptom onset, thus missing the early, presymptomatic period of infection. However, identification of infected individuals during the early period of SARS-CoV-2 infection is critically important to reduce transmission and/or maximize the efficacy of antiviral treatment.[16] Viral load measurements during the early period of infection were critically needed. Additionally, evidence was emerging that SARS-CoV-2 could infect multiple anatomical sites in the upper respiratory tract (such as the nasopharynx, anterior nares, midturbinate meatus, oropharynx, oral cavity, and salivary glands). It was unknown whether the amount of SARS-CoV-2 in each of these specimen types followed similar trajectories, such that the choice of specimen type for diagnostic testing had little impact on sensitivity.

To best predict what COVID-19 testing strategies would most effectively mitigate outbreaks, we needed quantitative viral load measurements in the highest priority specimen types (saliva, nasal swabs, and throat swabs) at high frequency (at least daily) starting from the very beginning and through the natural history of infection. From these data, we could infer how effectively different diagnostic tests, and population-level diagnostic testing strategies would prevent or mitigate SARS-CoV-2 outbreaks with similar dynamics of viral proliferation.

The Caltech COVID-19 Study

Obtaining daily, quantitative SARS-CoV-2 viral loads from paired specimen types (saliva, nasal swab, throat swab) from the very beginning of infection requires a thoughtful and strategic study design. In contrast to many diagnostic studies that enrolled participants presenting testing sites after symptom onset or upon admission to a hospital, prospective specimen collection (collection of specimens from individuals with unknown infection status) from asymptomatic individuals would be necessary to capture viral load dynamics during the very beginning of infection. We brainstormed potential study design options and sought feedback broadly. We considered a prospective cohort: 1,000 people enrolled at once, and followed for several months. However, collecting specimens every day from multiple anatomical sampling sites for several days from every participant would yield a very large number of specimens to log and process, most of which would be from individuals who do not become infected. We decided this brute force approach was insufficiently targeted. We brainstormed a "trigger" study design, where we would arrange study logistics with different facilities at heightened risk of outbreaks (e.g., military barracks, fire stations, residential care facilities, healthcare workers, grocery store workers, etc.), and upon identification of one infected individual at the facility, we would enroll all residents to collect daily specimens. We considered that during an outbreak, these facilities may be heavily burdened and that we'd need to pre-arrange with a large number of facilities, as very few might actually experience an outbreak during the study period. This led us to think about where more frequent, but smaller "outbreaks" occur.

Evidence from SARS-CoV-2[17] and other respiratory viruses[18] has indicated that the majority of transmissions occur among household contacts. We realized that if we could identify households where one resident had recently become infected, we could very quickly enroll household members and screen for infection. With key input and support from leaders at the Pasadena Public Health Department and others, we decided to execute this design: a case-ascertained household transmission study.

To connect with households that might experience transmission, we established partnerships with contact tracers at the Pasadena Public Health Department, various COVID-19 testing companies, and clinics servicing the Los Angeles area. These partners informed individuals about our study and connected them to a screening questionnaire

to confirm basic eligibility, to our study coordinators to learn more and enroll. Informed consent was conducted virtually by study coordinators.

Once enrolled, participants would complete an extensive questionnaire. This questionnaire included demographic information, medical history including current or prior COVID-19 like symptoms or diagnoses, household physical environment, household contact patterns, infection control practices, and perceptions about COVID-19 and infection control.

Participants received specimen collection kits and instructions that had been pre-assembled by members of the study team, as well as community volunteers. These kits were delivered to participants' homes within hours of enrollment. Each participant collected a set of specimens immediately upon receipt of collection kits. During Phase I of the study (September 2020 to March 2021), participants then collected specimens every morning upon waking, and every evening before preparing for bed. Saliva alone was collected between September 2020 to October 2020, and nasal swab collection was added thereafter. During Phase II of the study (November 2021 to April 2022), participants then collected saliva, nasal swab, and throat swab specimens every morning upon waking. During Phase II, participants also performed a commercially available, over-the-counter nasal swab Ag-RDT following manufacturer instructions, then reported their interpretation of the result and a photo of the test strip. In both Phase I and II, participants completed a detailed symptom report, and the results of any external COVID-19 tests at every specimen collection timepoint; initially, symptom information was manually entered into a database. Except for a nested study performed during Phase I, which collected live specimens in viral transport media to assess the dynamics of replication competent virus, all specimens were collected into a nucleic acid preservation buffer which had been shown to substantially inactivate SARS-CoV-2. Participants packaged their specimen collection tubes into several layers of containment. Medical couriers retrieved these containers to deliver to the laboratory for logging and processing.

At the laboratory (Ismagilov Laboratory at Caltech during Phase I, and Pangea Laboratory during Phase II), specimens would be logged for entry into a biorepository. During Phase I, logged specimens into a custom-built laboratory information management system, which included detailed information about gross specimen characteristics. During Phase II of the study, when testing capacity was greater, all specimens underwent nucleic acid extraction, followed by RT-qPCR for targets within the SARS-CoV-2 *N* gene and human *RNase P* gene. During Phase I, we followed an algorithm to regularly process a subset of specimens from each participant. For each participant, we processed the first two saliva specimens collected, the first saliva specimen collected in the morning, and then another saliva specimen collected every third morning. Specimens would undergo nucleic acid extraction, then RT-qPCR for targets within the SARS-CoV-2 *N* gene and human *RNase P* gene. This specimen processing

workflow evolved to handle an increasingly high volume of specimens, while maintaining biosafety. Specimens were stored at 4°C temporarily, and then at -80°C to preserve RNA integrity. Results of screening testing would be reported by laboratory operators. Participants with positive RT-qPCR results who had not reported a prior positive test result were sent a kit for confirmatory COVID-19 testing through a CLIA laboratory unaffiliated with the Caltech COVID-19 Study.

RT-qPCR results from the Caltech COVID-19 study were interpreted in real-time using a pre-defined decision tree to determine the current risk of observing transmission within the household; participants' enrollment was concluded if the risk of observing household transmission was low, and extended if it was high. Participants would complete their enrollment with a post-enrollment questionnaire, providing updated information on household infection control practices, external test results, and medical care sought by household members. Participants received compensation for their time collecting specimens and reporting information to support the study.

Individuals who were negative for SARS-CoV-2 upon enrollment, but later demonstrated consistent positive RT-qPCR results were defined as having "sustained incident infection." All specimens from these participants underwent a re-extraction and RT-qPCR pipeline to quantify viral load, and a subset underwent a RT-ddPCR assay to confirm viral load quantifications. Specimens from individuals with sustained incident infection that had been collected in viral transport media were shipped to collaborators to quantify the concentration of replication competent virus by plaque assay.

Data generated throughout the study was carefully but expeditiously analyzed to glean insights into how COVID-19 diagnostic tests should be used to achieve early detection that limits transmission and mitigates outbreaks.

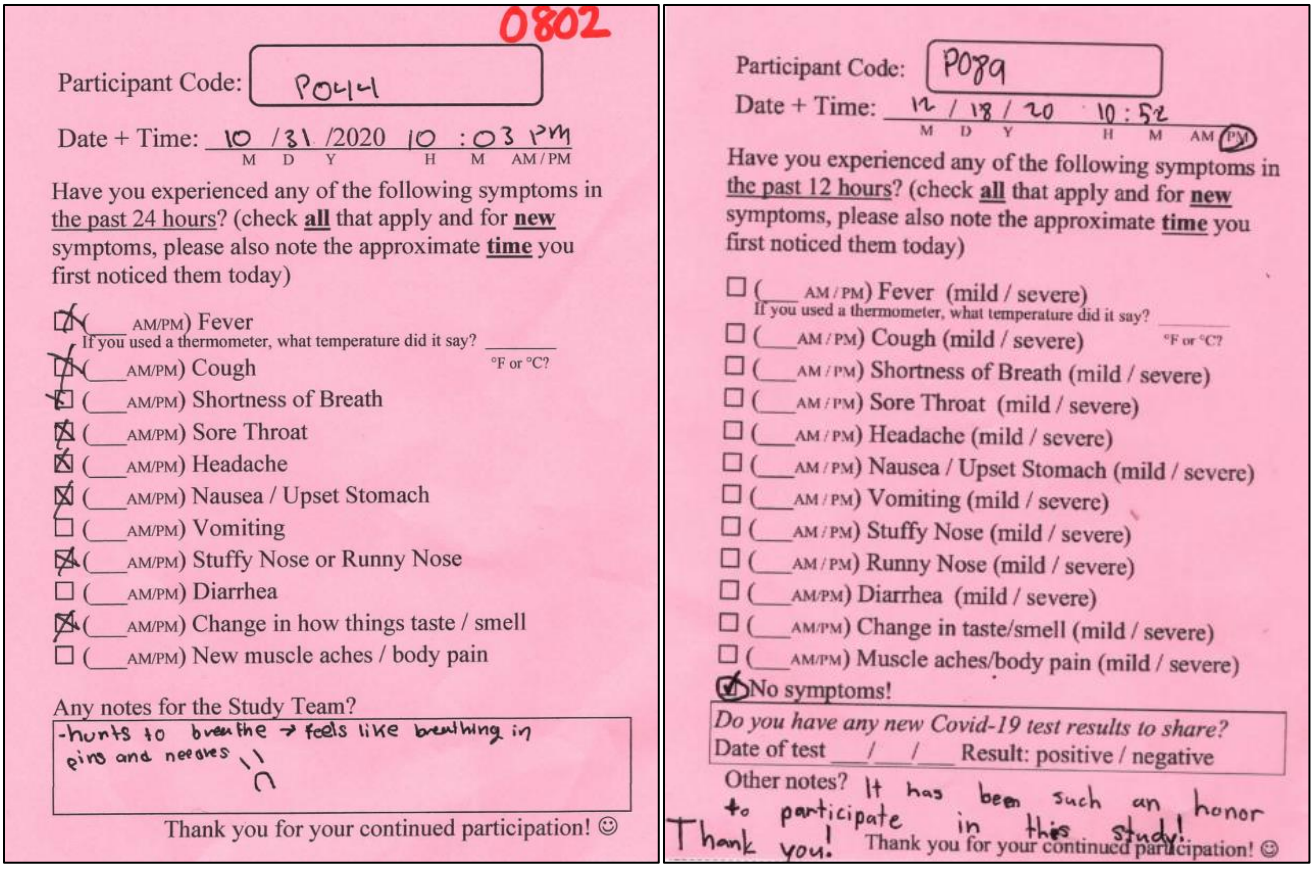

Figure 1-2. Selected specimen and symptom reporting sheets submitted by participants in Phase I of the Caltech COVID-19 Study.

An overview of how viral load dynamics informed COVID-19 testing strategies

In **Chapter II** to **Chapter IX**, I describe a series of findings about the dynamics of SARS-CoV-2 proliferation based on data generated as part of the Caltech COVID-19 Study, and the implications of these findings on diagnostic testing strategies intended to limit human-to-human transmission.

- **Chapter II** dives into the observation that SARS-CoV-2 viral loads are systematically higher in specimens collected in the morning compared to those collected in the evening, during both the rise and the fall of viral proliferation. Given this viral load pattern, we predicted that moderate to low analytical sensitivity COVID-19 tests (such as many AgRDTs) would exhibit higher clinical sensitivity if performed on morning specimens instead of evening specimens.

- In **Chapter III** and **Chapter IV**, we analyze quantitative, longitudinal viral load data in paired upper respiratory specimen types (saliva and nasal swab, or saliva and nasal swab and throat swabs, respectively) collected specifically by participants who were negative for SARS-CoV-2 RNA upon enrollment in the

study but later began testing consistently positive by a high-analytical-sensitivity RT-qPCR assay. We define these participants as individuals with sustained incident infection. **Chapter III** focuses on individuals with sustained incident infection from Phase I of the Caltech COVID-19 Study, while **Chapter IV** focuses on individuals sustained incident infection from Phase II of the Caltech COVID-19 Study. Importantly, pre-Delta variants were circulating during Phase I of the study, while Delta and then predominantly Omicron variants were circulating during Phase II. Additionally, COVID-19 vaccines were not available until the end of Phase I of the study, while many individuals in Phase II had received at least one COVID-19 vaccine dose.

- It is well established that the presence of viral RNA alone does not always indicate the presence of replication-competent, or "infectious," virus in a specimen.[19,20] Transmission of SARS-CoV-2 can only occur in an individual with shedding replication-competent virus, not viral RNA alone.[21] Since many COVID-19 diagnostic tests detect viral RNA, assessment of replication-competent virus is very laborious and time-consuming; understanding the relationship between concentration of viral RNA and of replication competent virus (viral titer) is useful to avoid unnecessary isolation of individuals with detectable viral RNA but who are not "infectious." Within Phase I of the Caltech COVID-19 study, we nested an assessment of the relationship between viral RNA and viral titer, and how that relationship changes over time throughout the natural history of infection. In **Chapter V**, we analyzed this elusive relationship in one participant in the Caltech COVID-19 study who began collecting specimens in viral transport media (which maintains SARS-CoV-2 viability) very early during very early infection.

- Within Phase II of the Caltech COVID-19 Study, we nested a field evaluation of a common at-home Ag-RDT using nasal swabs, which were an increasingly utilized and government-provided testing modality. **Chapter VI** describes the performance of this nasal swab Ag-RDT, particularly during early infection, in the context of quantitative viral load measurements from nasal swabs, throat swabs, and saliva.

- During our field evaluation of the nasal swab Ag-RDT, we noted a sudden increase in the rate of Ag-RDT positive results from individuals who were negative for SARS-CoV-2 viral RNA by RT-qPCR. Study coordinators reviewed photos of the Ag-RDT test strips, and confirmed that participants had not misreported the result, and analysis of survey submission times did not suggest that participants had incorrectly performed the test. Initially, this finding raised alarm that a novel variant may have emerged with mutations in the three regions of the SARS-CoV-2 *N* gene targeted by our RT-qPCR assay—and many other COVID-19 RT-PCR assays—causing a failure to detect (or false negative results). However, these participants did not exhibit symptoms consistent with infection, and the specimens were also negative for an additional *N*

gene region, as well as the *S* gene and *RdRp* gene. These findings suggested that the Ag-RDT more likely yielded false positive results, than the RT-qPCR assay yielded false negative results. Careful review by study coordinators revealed a common antigen test strip lot number among these false positive Ag-RDT results. We sequestered this lot of antigen test strips, and conducted a laboratory evaluation to assess whether this strip had a significantly higher false positive rate than other test strip lots, as described in **Chapter VII**. We alerted the test manufacturer and the FDA after finding that this lot indeed appeared to yield consistently false positive results.

- Our analysis of SARS-CoV-2 viral loads during early infection, and our Ag-RDT field evaluation suggested that nasal swab at home Ag-RDTs may exhibit very poor clinical sensitivity during early infection. False negative diagnostic test results would not prompt isolation of infected individuals, who might continue contact and transmit the infection to other individuals, including household members. In **Chapter VIII** we conducted an epidemiological analysis of the impact of test type used for diagnosis of COVID-19 on transmission to household contacts. Consistent with viral load and Ag-RDT field evaluation data, this analysis revealed that household index cases (first individual diagnosed with COVID-19 in a household) who were diagnosed with rapid nasal swab tests had greater transmission to household contacts.

- While nasal swab Ag-RDTs exhibited low sensitivity to identify infected or infectious individuals during early infection, our viral load data suggested that testing both the nose and the throat would improve performance by approximately 20%. Several large field evaluations comparing the results of a nasal swab Ag-RDT to the results of nasal and throat swab Ag-RDTs supported our prediction, as did numerous anecdotes on social media describing off-label use of Ag-RDTs with throat swabs (amplified by the hashtag #SwabYourThroat). At the time, however, all at home Ag-RDTs authorized for use in the USA were validated only for nasal swabs. As described in "The data we need, to inform COVID-19 diagnostic testing strategies," diagnostic test performance can be impacted by specimen type, and to ensure valid results, COVID-19 tests needed to be validated for use with throat swabs, in addition to nasal swabs. To encourage test manufacturers to perform these validations, we summarized the evidence and the importance of this step in an Invited Commentary in Clinical Infectious Diseases, co-authored with Dr. Timothy Stenzel, MD, PhD, who served as the Director of the Office of In Vitro Diagnostics for the FDA, which oversaw emergency use authorizations for COVID-19 diagnostic testing technologies. We emphasize that improving test performance would better protect the large population of individuals who remained at high risk of severe disease, including individuals with immunocompromise or advanced age. This commentary is included as **Chapter IX**.

Current limitations of systemic (humoral) vaccines for infection control

In the Spring of 2021, development, authorization, manufacturing, and distribution of systemic COVID-19 vaccines—administered through intramuscular injection—became available in Los Angeles. Eager to see the end of the COVID-19 pandemic, I spent Mondays through Saturdays advancing work presented in this thesis, and Sunday volunteering to support operations at vaccine mass distribution sites around Los Angeles (usually, a drive-through administration site hosted in the parking lot of California State University Northridge). I would walk the aisles of cars precisely guided by temporary lanes of traffic cones, checking on each vaccine recipient during their 15–30 minute observation period. As they sat waiting, many people would reflect upon what they had experienced since December 2019 and share these reflections with me. Many shared tearful stories of sickness and loss, or excitement to finally hold loved ones without the fear of their demise; others expressed a profound gratitude for the scientific achievements that were limiting the former and enabling the latter. On numerous occasions, the parking lot would erupt into applause, or sing happy birthday to someone. After so much death, we were all happy to celebrate life.

The COVID-19 vaccines had high effectiveness for preventing severe and fatal disease[22] and good safety profiles,[23] but despite our wishes, they exhibited lower effectiveness at preventing breakthrough infections which could be transmitted to others.[24] Antibody titers, the correlate of protection for humoral vaccines, were found to wane approximately 3–6 months after vaccination, such that we would regain nearly full susceptibility to infection.[25]

Since the vaccines enabled social contact but did not prevent infection, opportunities for viral mutation were abundant. New viral variants emerged, notably the Omicron variant in November 2021. Under the immunological pressure of these vaccines, emerging viral variants exhibited immune escape such that prior vaccination became less effective at preventing severe COVID-19.[26] Vaccines were redesigned, and booster doses were recommended.[27] However, vaccine booster uptake was low,[28] partially due to a low but existent risk of adverse events including cardiomyelitis[29] and post-vaccine syndrome.[30] SARS-CoV-2 continued to spread, and still more viral variants emerged.[31]

Viral transmission, evolution, and reinfection has continued through to the time of writing this thesis. Notably, more individuals are being diagnosed with “long COVID,” a chronic, pleiotropic, and often debilitating syndrome following even mild infection,[32] and the risk of developing “long COVID” has been shown to increase following repeated infections.[33]

The rapid development and distribution of humoral vaccines for COVID-19 were a pinnacle of modern innovation and an invaluable tool for pandemic mitigation, but their inability to prevent breakthrough infections left much to be desired. My experience during the acute phases of the COVID-19 pandemic have generated a strong, visceral motivation to use science and medicine to prevent or mitigate future infectious outbreaks, epidemics, and pandemics. This motivation has driven the later portion of work presented in this thesis.

The data we need, for a new generation of vaccines

I envision a future in which next-generation vaccines provide sterilizing immunity, which much more effectively blocks breakthrough infection and subsequent transmission than current humoral vaccines. It has been previously proposed that vaccines which elicit immunity at the primary site of infection may be more effective at achieving this goal.[34,35] For most pathogens, including SARS-CoV-2, the primary site of infection is a mucosal surface. While humoral vaccines generate circulating antibodies that only a small fraction of which translocate to the mucosal surface,[36,37] mucosal vaccines (or vaccines delivered to and generating immunity at a mucosal surface) could be designed to train both antibody and/or cell-mediated responses at the mucosal surface to generate sterilizing immunity.

To guide the development of mucosal vaccines that provide sterilizing immunity, I sought to study the longitudinal mucosal immune response to SARS-CoV-2 infection, the approach and results of which are presented in **Chapter X** of this thesis.

Chapter X first describes the development of methods to overcome technical challenges in human transcriptome analysis of self-collected upper respiratory clinical specimens, to generate of high-quality, robust quantitative gene expression data. This chapter then investigates the length-scale of interferon stimulation during the early phase of acute viral infection in humans—specifically, whether interferon signaling is restricted only to anatomical mucosal sites of local viral proliferation. These interpretations were made in collaboration with Professor Akiko Iwasaki and members of her laboratory at Yale University School of Medicine (Alexandra Tabachnikova, Julio Silva, Kerrie Green, and Dr. Yong Gong). These analyses seek to identify correlates for protection against sustained infection in the mucosal immune response, which can guide the development of next generation mucosal vaccine candidates.

Conclusion

Taken together, this thesis presents a body of work reflecting how sensitive, quantitative nucleic acid measurements were optimized and applied to study SARS-CoV-2 infection. Insights into the natural history of infection were then used to inform prophylactic and diagnostic strategies that reduce viral transmission and mitigate outbreaks. The findings herein are focused on SARS-CoV-2 but may be relevant for other respiratory viral pathogens with pandemic potential, including those that have yet to emerge.

References

1. Zhou F, Yu T, Du R, et al. Clinical course and risk factors for mortality of adult inpatients with COVID-19 in Wuhan, China: a retrospective cohort study. *The Lancet*. 2020;395(10229):1054-1062. doi:10.1016/S0140-6736(20)30566-3

2. Mengyang G. Novel coronavirus! Preliminary determination of the "culprit" of the unexplained pneumonia in Wuhan (Original Chinese). January 9, 2020. Accessed September 15, 2024. https://m.news.cctv.com/2020/01/09/ARTI9Vp9Lra4Tvltz3r7es96200109.shtml

3. Global Virus Network (GVN) Statement on New Strain of Coronavirus Infection in Wuhan, China - Global Virus Network. January 10, 2020. Accessed September 15, 2024. https://gvn.org/gvn-statement-on-the-new-strain-of-coronavirus-infection-in-wuhan-china/

4. Coronavirus disease (COVID-19) pandemic. Accessed September 15, 2024. https://www.who.int/europe/emergencies/situations/covid-19

5. Schoepp N, Liaw E, Winnett A, Savela E, Garner O, Ismagliov RF. Differential DNA accessibility to polymerase enables 30-minute phenotypic β-lactam antibiotic susceptibility testing of carbapenem-resistant Enterobacteriaceae | PLOS Biology. *PLoS Biol*. 2019;18(3). doi:10.1371/journal.pbio.3000652

6. Viloria Winnett A, Srinivasan V, Davis M, et al. The Path of More Resistance: a Comparison of National Healthcare Safety Network and Clinical Laboratory Standards Institute Criteria in Developing Cumulative Antimicrobial Susceptibility Test Reports and Institutional Antibiograms. *J Clin Microbiol*. 2022;60(2):e01366-21. doi:10.1128/jcm.01366-21

7. McMichael TM. COVID-19 in a Long-Term Care Facility — King County, Washington, February 27–March 9, 2020. *Morb Mortal Wkly Rep*. 2020;69. doi:10.15585/mmwr.mm6912e1

8. Jatt LP, Winnett A, Graber CJ, Vallone J, Beenhouwer DO, Goetz MB. Widespread severe acute respiratory coronavirus virus 2 (SARS-CoV-2) laboratory surveillance program to minimize asymptomatic transmission in high-risk inpatient and congregate living settings. *Infect Control Hosp Epidemiol*. 2020;41(11):1331-1334. doi:10.1017/ice.2020.301

9. Locher K, Roscoe D, Jassem A, et al. FilmArray respiratory panel assay: An effective method for detecting viral and atypical bacterial pathogens in bronchoscopy specimens. *Diagn Microbiol Infect Dis*. 2019;95(4):114880. doi:10.1016/j.diagmicrobio.2019.114880

10. He X, Lau EHY, Wu P, et al. Temporal dynamics in viral shedding and transmissibility of COVID-19. *Nat Med*. 2020;26(5):672-675. doi:10.1038/s41591-020-0869-5

11.Dora AV. Universal and Serial Laboratory Testing for SARS-CoV-2 at a Long-Term Care Skilled Nursing Facility for Veterans — Los Angeles, California, 2020. *MMWR Morb Mortal Wkly Rep*. 2020;69. doi:10.15585/mmwr.mm6921e1

12. Dora AV, Winnett A, Fulcher JA, et al. Using Serologic Testing to Assess the Effectiveness of Outbreak Control Efforts, Serial Polymerase Chain Reaction Testing, and Cohorting of Positive Severe Acute Respiratory Syndrome Coronavirus 2 Patients in a Skilled Nursing Facility. *Clin Infect Dis Off Publ Infect Dis Soc Am*. 2021;73(3):545-548. doi:10.1093/cid/ciaa1286

13. CDC. Getting Tested for HIV. HIV. September 6, 2024. Accessed September 15, 2024. https://www.cdc.gov/hiv/testing/index.html

14. Pre-Exposure Prophylaxis (PrEP). Accessed September 15, 2024. https://hivinfo.nih.gov/understanding-hiv/fact-sheets/pre-exposure-prophylaxis-prep

15. Cubas-Atienzar AI, Kontogianni K, Edwards T, et al. Limit of detection in different matrices of 19 commercially available rapid antigen tests for the detection of SARS-CoV-2. *Sci Rep*. 2021;11(1):18313. doi:10.1038/s41598-021-97489-9

16. Gottlieb RL, Vaca CE, Paredes R, et al. Early Remdesivir to Prevent Progression to Severe Covid-19 in Outpatients. *N Engl J Med*. 2022;386(4):305-315. doi:10.1056/NEJMoa2116846

17. Lee EC, Wada NI, Grabowski MK, Gurley ES, Lessler J. The engines of SARS-CoV-2 spread. *Science*. 2020;370(6515):406-407. doi:10.1126/science.abd8755

18. Dahlgren FS, Foppa IM, Stockwell M, Vargas C, LaRussa P, Reed C. Household transmission of influenza A and B within a prospective cohort during the 2013-2014 and 2014-2015 seasons - Dahlgren - 2021 - Statistics in Medicine - Wiley Online Library. *Stat Med*. 2021;40(28):6260-6276. doi:10.1002/sim.9181

19. Mina MJ, Parker R, Larremore DB. Rethinking Covid-19 Test Sensitivity — A Strategy for Containment | New England Journal of Medicine. *N Engl J Med*. 2020;383(22). doi:10.1056/NEJMp2025631

20. Perera RAPM, Tso E, Tsang OTY, et al. SARS-CoV-2 Virus Culture and Subgenomic RNA for Respiratory Specimens from Patients with Mild Coronavirus Disease. *Emerg Infect Dis*. 2020;26(11). doi:10.3201/eid2611.203219

21. Binnicker MJ. Can Testing Predict SARS-CoV-2 Infectivity? The Potential for Certain Methods To Be Surrogates for Replication-Competent Virus. *J Clin Microbiol*. 59(11):e00469-21. doi:10.1128/JCM.00469-21

22. Bernal JL, Andrews N, Gower C, et al. Effectiveness of the Pfizer-BioNTech and Oxford-AstraZeneca vaccines on covid-19 related symptoms, hospital admissions, and mortality in older adults in England: test negative case-control study. *BMJ*. 2021;373:n1088. doi:10.1136/bmj.n1088

23. Klein NP, Lewis N, Goddard K, et al. Surveillance for Adverse Events After COVID-19 mRNA Vaccination. *JAMA*. 2021;326(14):1390-1399. doi:10.1001/jama.2021.15072

24. Tan ST, Kwan AT, Rodríguez-Barraquer I, et al. Infectiousness of SARS-CoV-2 breakthrough infections and reinfections during the Omicron wave. *Nat Med*. 2023;29(2):358-365. doi:10.1038/s41591-022-02138-x

25. Menegale F, Manica M, Zardini A, et al. Evaluation of Waning of SARS-CoV-2 Vaccine–Induced Immunity: A Systematic Review and Meta-analysis. *JAMA Netw Open*. 2023;6(5):e2310650. doi:10.1001/jamanetworkopen.2023.10650

26. Paul P, El-Naas A, Hamad O, et al. Effectiveness of the pre-Omicron COVID-19 vaccines against Omicron in reducing infection, hospitalization, severity, and mortality compared to Delta and other variants: A systematic review. *Hum Vaccines Immunother*. 2023;19(1):2167410. doi:10.1080/21645515.2023.2167410

27. Staying Up to Date with COVID-19 Vaccines. September 11, 2024. Accessed September 15, 2024. https://www.cdc.gov/covid/vaccines/stay-up-to-date.html

28. Jacobs ET, Cordova-Marks FM, Farland LV, et al. Understanding low COVID-19 booster uptake among US adults. *Vaccine*. 2023;41(42):6221-6226. doi:10.1016/j.vaccine.2023.08.080

29. Kim HW, Jenista ER, Wendell DC, et al. Patients With Acute Myocarditis Following mRNA COVID-19 Vaccination. *JAMA Cardiol*. 2021;6(10):1196-1201. doi:10.1001/jamacardio.2021.2828

30. Krumholz HM, Wu Y, Sawano M, et al. Post-Vaccination Syndrome: A Descriptive Analysis of Reported Symptoms and Patient Experiences After Covid-19 Immunization. *medRxiv*. Published online November 10, 2023:2023.11.09.23298266. doi:10.1101/2023.11.09.23298266

31. Roemer C, Sheward DJ, Hisner R, et al. SARS-CoV-2 evolution in the Omicron era. *Nat Microbiol*. 2023;8(11):1952-1959. doi:10.1038/s41564-023-01504-w

32. Davis HE, McCorkell L, Vogel JM, Topol EJ. Long COVID: major findings, mechanisms and recommendations. *Nat Rev Microbiol*. 2023;21(3):133-146. doi:10.1038/s41579-022-00846-2

33. Hadley E, Yoo YJ, Patel S, et al. Insights from an N3C RECOVER EHR-based cohort study characterizing SARS-CoV-2 reinfections and Long COVID. *Nat Commun Med*. 2024;4(1):1-12. doi:10.1038/s43856-024-00539-2

34. Medzhitov R, Iwasaki A. Exploring new perspectives in immunology. *Cell*. 2024;187(9):2079-2094. doi:10.1016/j.cell.2024.03.038

35. Iwasaki A. Exploiting Mucosal Immunity for Antiviral Vaccines. *Annu Rev Immunol*. 2016;34:575-608. doi:10.1146/annurev-immunol-032414-112315

36. Neutra MR, Kozlowski PA. Mucosal vaccines: the promise and the challenge. *Nat Rev Immunol*. 2006;6(2):148-158. doi:10.1038/nri1777

37. Su F, Patel GB, Hu S, Chen W. Induction of mucosal immunity through systemic immunization: Phantom or reality? *Hum Vaccines Immunother*. 2016;12(4):1070-1079. doi:10.1080/21645515.2015.1114195

Chapter 2

MORNING SARS-COV-2 TESTING YIELDS BETTER DETECTION OF INFECTION DUE TO HIGHER VIRAL LOADS IN SALIVA AND NASAL-SWABS UPON WAKING

This chapter was originally published in “Viloria Winnett A, Porter MK, Romano AE, Savela ES, Akana R, Shelby TS, Reyes JA, Schlenker NW, Cooper MM, Carter AM, Ji J, Barlow JT, Tognazzini C, Feaster M, Goh YY, Ismagilov. Morning SARS-CoV-2 testing yields better detection of infection due to higher viral loads in saliva and nasal-swabs upon waking (March 2022). Microbiology Spectrum. https://doi.org/10.1101/2022.03.02.22271724"

Abstract

Optimizing specimen collection methods to achieve the most reliable SARSCoV-2 detection for a given diagnostic sensitivity would improve testing and minimize COVID-19 outbreaks. From September 2020 to April 2021, we performed a household-transmission study in which participants self-collected specimens every morning and evening throughout acute SARS-CoV-2 infection. Seventy mildly symptomatic participants collected saliva, and of those, 29 also collected nasal swab specimens. Viral load was quantified in 1,194 saliva and 661 nasal swab specimens using a high-analytical-sensitivity reverse transcription-quantitative PCR (RT-qPCR) assay. Viral loads in both saliva and nasal swab specimens were significantly higher in morning-collected specimens than in evening-collected specimens after symptom onset. This aspect of the biology of SARS-CoV-2 infection has implications for diagnostic testing. We infer that morning collection would have resulted in significantly improved detection and that this advantage would be most pronounced for tests with low to moderate analytical sensitivity. Collecting specimens for COVID-19 testing in the morning offers a simple and low-cost improvement to clinical diagnostic sensitivity of low- to moderate-analytical-sensitivity tests.

Importance

Our findings suggest that collecting saliva and nasal swab specimens in the morning immediately after waking yields higher SARS-CoV-2 viral loads than collection later in the day. The higher viral loads from morning specimen collection are predicted to significantly improve detection of SARS-CoV-2 in symptomatic individuals, particularly when using moderate- to low-analytical-sensitivity COVID-19 diagnostic tests, such as rapid antigen tests.

Introduction

Although vaccination has substantially reduced hospitalizations and death from COVID-19, limited vaccine uptake and availability and the potential for breakthrough infections (particularly with novel viral variants) support the continued necessity for diagnostic testing and subsequent isolation of infected individuals (1, 2). Optimizing how diagnostics are used can enhance our ability to combat the COVID-19 pandemic.

Nasopharyngeal swab, anterior nares swab, mid-turbinate swab, oropharyngeal swab, buccal swab, gingival crevicular fluid, sputum, tracheal aspirate, and saliva have all been utilized and compared as diagnostic specimens for the detection of SARS-CoV-2 infection. Work done by many groups (3–5), including ours (6), has suggested that SARS-CoV-2 is detectable, albeit at low viral loads, in saliva before anterior nares nasal

swab specimens. However, conflicting results have been reported in head-to-head comparisons of saliva to other specimen types in cross-sectional studies.

Lack of clarity on which specimen type is most reliable for SARS-CoV-2 detection is likely due to the dynamic nature of viral loads in different specimen types through the course of an infection (3, 6–11) and the differences in analytical sensitivity of diagnostic assays used in the comparisons. Currently available SARS-CoV-2 diagnostics span a wide (six orders of magnitude) range of analytical sensitivities, from the reverse transcription-PCR (RT-PCR) PerkinElmer new coronavirus nucleic acid detection kit (LOD of 180 nucleic acid amplification test detectable units [NDU]/mL) (12) to the Coris BioConcept rapid antigen lateral flow assay COVID-19 Ag Respi-Strip (LOD of ~4×10^7 copies/mL) (13). Tests with relatively moderate analytical sensitivity (LOD of 10^4 to 10^5 copies/mL of specimen) or low analytical sensitivity (LOD of 10^5 to 10^8 copies/mL of specimen) are being increasingly used, particularly for at-home and rapid screening testing and in areas of the world with limited laboratory capacity (14–16).

How specimens are collected can also affect the detectability of SARS-CoV-2 in a specimen. Because SARS-CoV-2, like other pathogens, may exhibit circadian rhythms to replication kinetics (17, 18), we hypothesized that collection time may impact SARS-CoV-2 viral load in respiratory specimens and therefore detectability of infection. Simple, low-cost changes to specimen collection protocols that significantly improve the clinical sensitivity of COVID-19 diagnostics offer an immediately actionable opportunity to improve existing diagnostics, which would be particularly valuable in settings that rely on tests with low analytical sensitivity.

We conducted a COVID-19 household transmission study (9, 19) where participants prospectively self-collected saliva and nasal swab specimens twice per day (in the morning and in the evening). From mildly symptomatic participants, we compared SARS-CoV-2 viral loads in morning- and evening-collected specimens to determine if the time of day affected viral load, and if this could be leveraged to improve detection of SARS-CoV-2 infection.

Results

Timing of morning and evening specimen collection

Viral load was quantified in 1,194 saliva specimens from 70 individuals and 661 nasal swab specimens from 29 individuals (**Table 2-1, Figure 2-1**). The distribution of collection times was roughly bimodal. Although each participant's specimen collection time varied slightly throughout enrollment, nearly all (92%) participants

had an average morning specimen collection time between 7 a.m. and 10 a.m. Evening collection time was more variable, but most participants (74%) had an average specimen collection time between 8 p.m. and 11 p.m. These patterns were used to delineate the morning and evening periods in the study: we defined sampling upon waking (4 a.m. to 12 p.m.) as morning and sampling before bed (3 p.m. to 3 a.m.) as evening (see Figure **2-S1**).

Saliva and nasal swab specimens exhibit higher viral loads in morning than evening collection across the course of acute, symptomatic illness

Saliva and nasal swab viral load profiles from most individuals (**Figure 4-S2 and 4-S3**) revealed a pattern of higher viral loads in specimens collected in the morning than in those collected in the evening. In specimens from some individuals (e.g., **Figure 2-S2A and 2-S3E**), fluctuations in both SARS-CoV-2 and human *RNase P* markers were observed, whereas in others *RNase P* remained stable and SARS-CoV-2 viral load appeared to be independent of the host marker (e.g., **Figures 2-4S2AH and 2-S3N**).

Although direct comparison between all positive morning or evening specimens demonstrates greater target abundance for both SARS-CoV-2 *N1* (**Figure 2-S4A and C**) and human *RNase P* (**Figure 2-S4B and D**), this comparison would be skewed by participants who contributed more specimens and biased by sampling at different stages of the infection. To minimize these potential biases, the time of each specimen collection was aligned relative to the date of symptom onset for that participant before plotting both individual viral load datapoints (**Figure 2-S2 and 2-S3**) and the average of log-transformed viral load values (**Figure 2-1A and B**) for all saliva and nasal swab specimens in 12-hour time bins.

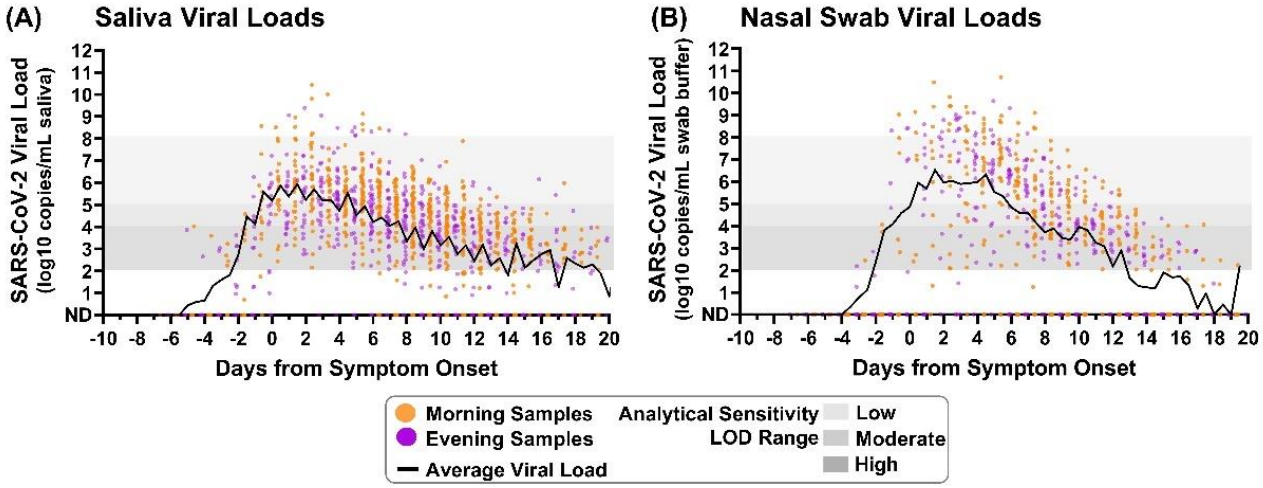

Figure 2-1. Saliva and nasal swab specimens collected in the morning and evening through the course of infection demonstrate differences in SARS-CoV-2 viral load. Black lines on each plot indicate the average viral load for each daily morning or evening specimen collection window. (A) Saliva specimen viral load (SARS-CoV-2 *N1* copies/milliliter of saliva) as measured by RT-qPCR is plotted relative to symptom onset for 1,194 specimens. (B) Nasal swab specimen viral load (*N1* copies/milliliter of swab buffer) as measured by RT-qPCR is plotted relative to symptom onset for 661 specimens. Specimens were designated morning (orange) if collected between 4 a.m. and 12 p.m. or evening (purple) if collected between 3 p.m. and 3 a.m. ND, not detected. Additional specimen details are provided in the supplemental material.

The averaged salivary viral load during each collection time point visually suggests higher viral loads in specimens collected in the morning than in the evening during both the presymptomatic and symptomatic phases of infection. This pattern was less apparent in the averaged nasal swab viral loads but can be seen when comparing the *N1* threshold cycle (C_T) values between successive time points by calculating differences in C_T (**Figure 2-2A and B**). Only reverse transcription-quantitative PCR (RT-qPCR) C_T values for pairs of successively collected morning-to-evening or evening-to-morning specimen were used to calculate the C_T difference; negative or indeterminate specimens were included only if directly followed by a positive specimen collected in the presymptomatic phase of infection. A negative difference in C_T values indicates that viral load was increasing relative to the previous measurement, whereas a positive difference indicates that viral load was decreasing relative to the previous measurement. Starting from symptom onset (day 0), saliva specimens collected in the morning typically exhibited a negative difference in C_T values relative to their preceding evening specimens, whereas evening specimens consistently had a positive difference in C_T values relative to their preceding morning specimens. This indicates that throughout the course of symptomatic infection, morning specimens typically result in relatively lower C_T values (higher viral loads) than evening specimens.

To further illustrate the pattern observed in viral loads and changes in C_T values, specimens were binned by infection stage: prior to symptom onset and in four-day intervals relative to symptom onset. The four-day interval was selected to capture reasonable resolution for infection stage while also providing sufficient measurements to observe potential differences. Significantly higher morning viral loads were not observed prior to symptom onset in either specimen type in the limited number of specimens collected during this period. However, significantly higher viral loads ($P < 0.05$, Wilcoxon matched-pair signed-rank test) were observed in saliva specimens collected in the morning for the first 16 days of symptomatic infection (**Figure 2-2C**). Differences in C_T values were also significantly lower ($P < 0.05$, Wilcoxon matched-pair signed-rank test) in morning nasal swab specimens from day 4 to day 16 of symptomatic infection (**Figure 2-2D**). Of note, nasal swab viral load appears to increase more quickly to peak than does salivary viral load (**Figure 2-1A and** B), and nasal swabs also achieve higher peak viral loads (**Figure 2-S4C**) than does saliva (**Figure 2-S4A**); the high rate of increase in viral load in nasal swabs likely obscures subtle daily fluctuations that are more apparent in saliva, where viral load rises more gradually (19). Nasal swabs appear to also be subject to more sampling variability (**Figures 2-S3 and 2-S4D**) than saliva (**Figures 2-S2 and 2-S4B**), evidenced by *RNase P* control marker C_T values.

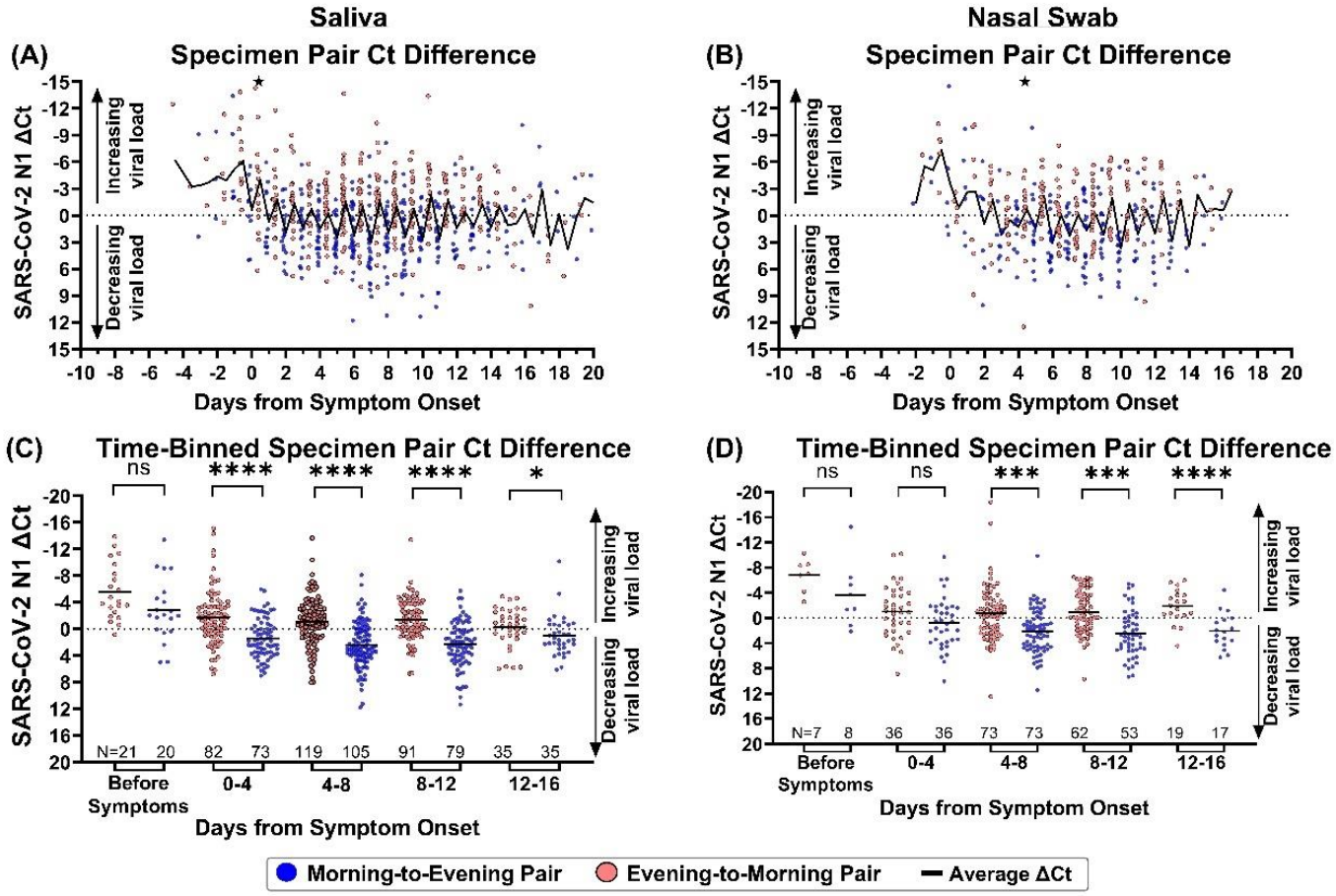

Figure 2-2. Morning viral loads are significantly higher than evening viral loads during most of SARS-CoV-2 infection**. (A and B)** The difference in N1 CT values (ΔCT) in 703 morning-to-evening and evening-to-morning successive saliva specimen pairs **(A)** and 365 morning-to-evening and evening-to-morning successive nasal swab specimen pairs **(B)**, plotted relative to symptom onset. One point in panel A and one point in panel B had ΔC_T values outside the *y* axis of the plot; these are represented as black stars at −15. (C and D) The difference in *N1* C_T values in 703 morning-to-evening and evening-to-morning sequential saliva **(C)** and nasal swab **(D)** specimen pairs relative to symptom onset. Morning-to-evening or evening-to-morning ΔC_T values were then binned into presymptomatic or four-day infection stages. The distributions of morning-to-evening and evening-to-morning ΔC_T values for each infection stage bin were then statistically compared using the Wilcoxon matched-pair signed-rank test; ns, nonsignificant or insufficient data points to perform analysis; *, $P < 0.05$; **, $P < 0.01$; ****, $P < 0.001$. Black lines indicate average viral load. ND, not detected.

Saliva and nasal swab viral loads in the range of moderate- and low-sensitivity tests underscore utility of morning sampling

The observed higher viral loads in specimens collected in the morning upon waking than in those collected later in the day led us to hypothesize that sampling in the morning could detect significantly more infected individuals than sampling in the evening. Because viral loads rise and decline throughout the course of the infection (**Figure 2-1**), we assessed this hypothesis during discrete four-day time bins following symptom onset. The presymptomatic period was not assessed, as few specimens from this period were available for analysis. Additionally, because COVID-19 diagnostics have analytical sensitivities that span several orders of magnitude, we tested this hypothesis for assays with LODs of 10^3, 10^4, 10^5, 10^6, 10^7 copies/mL; quantitative viral loads measured in each specimen were used to predict whether each specimen would reliably yield a positive result when tested by an assay of each LOD. For each time bin and each LOD, we generated two-by-two matrices to assess the detectability of morning or evening sampling within pairs of sequentially collected morning-to-evening (**Figure 2-3**) specimens. Each time bin and LOD that did not contain at least ten positive samples from saliva or nasal swab were excluded from this analysis.

For saliva specimens, the advantage of morning sampling was statistically significant in all but two comparisons (**Figure 2-3A**); the two comparisons for which a nonsignificant advantage was observed occurred in the first four days of infection, at the LODs of the lowest- and highest-analytical-sensitivity assays (LODs of 10^6 and 10^3 copies/mL, respectively). As LOD increases, fewer pairs are predicted to have detectable virus in either the morning or evening specimen; for this reason, confidence intervals widen as the LOD increases, which results in decreased power to detect significant differences in detection by assays with higher LODs. Additionally, assays with lower LODs are able to reliably detect lower viral concentrations, decreasing the impact of fluctuations in viral load from morning to evening sampling on detection.

Morning sampling with nasal swab specimens also exhibited an advantage over evening sampling after four days from symptom onset, for all LODs (**Figure 2-3B**). In the first four days of infection, a nonsignificant advantage of evening over morning sampling was observed; in this phase of the infection, viral loads in nasal swab specimens typically rise rapidly from undetectable to high (**Figure 2-1**). Therefore, during this rapid rise, the specimen collected later within a pair of successively collected specimens would improve detection; indeed, when morning-to-evening pairs were assessed (**Figure 2-3**), the later (evening) time point had improved detection but when evening-to-morning pairs were assessed (**Figure 2-S5**), the later (morning) time point resulted in improved detection.

Similarly, when viral loads are declining, one may expect the earlier time point within a pair of successively collected specimens to exhibit improved detection. We assessed whether this effect was responsible for the improved performance of morning sampling over evening sampling when pairs of successively collected morning-to-evening specimens were compared by performing an equivalent analysis of pairs of successively collected evening-to-morning specimens (**Figure 2-S5**). Even with evening-to-morning pairing, morning sampling exhibited an advantage over evening sampling for all comparisons with saliva and nearly all comparisons with nasal swabs. In the three of 12 comparisons where morning sampling with nasal swabs did not exhibit an advantage, two comparisons had equivalent detection by morning or evening sampling, and in the third comparison evening sampling exhibited only a nonsignificant advantage of less than 2% over morning sampling.

This supports that the advantage of morning sampling over evening sampling for both saliva and nasal swabs was robust to whether the morning specimen is collected prior to or following the evening specimen. These results suggest that collecting saliva or nasal swab specimens for SARS-CoV-2 testing in the morning, immediately after waking, can significantly improve detection of symptomatic, infected individuals.

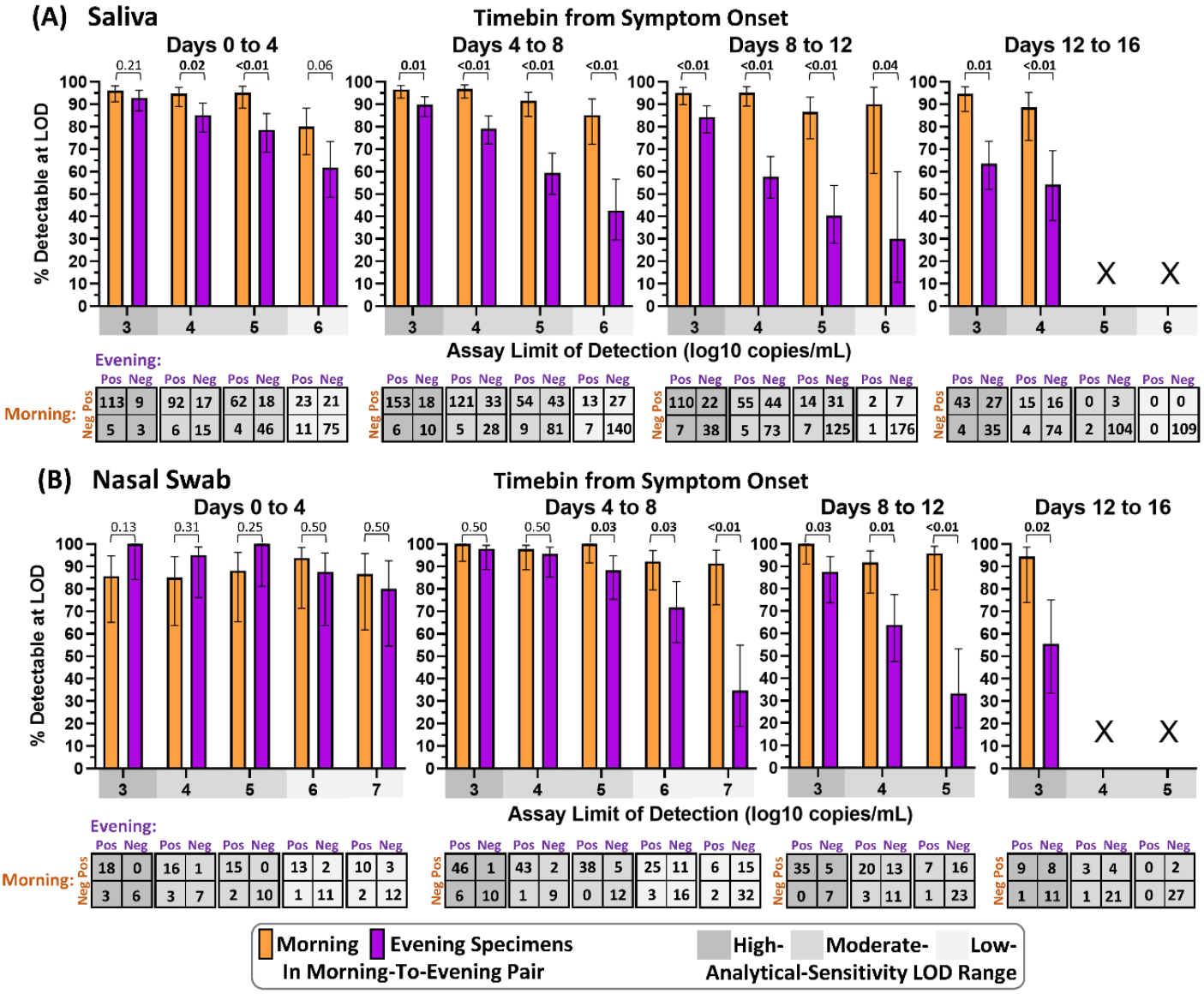

Figure 2-3. Morning saliva or nasal swab specimen collection yields improved detection across infection stages and assay analytical sensitivities. For each four-day time bin relative to symptom onset, pairs of sequentially collected morning-to-evening specimens were assessed. In each pair, the viral load in each specimen was used to predict a positive or negative result if tested by an assay with a given limit of detection (LOD) below or above the viral load, respectively. Bar plots show the fraction of pairs with a positive result in either the morning or evening specimen that would be detectable if the morning specimen (orange) or evening specimen (purple) were tested at a given LOD. Error bars indicate the 95% confidence interval. Bars are not shown (X) when fewer than 10 pairs had positive results at the given LOD during the infection time bin. Among LODs and infection time bins with more than 10 positive pairs, the percents detectable for morning versus evening specimens were compared by an upper-tailed McNemar exact test, applied to the 2 × 2 table shown below each comparison. Resulting *P* values are shown above each comparison. Boldfaced values indicate significantly higher detection with morning sampling than with evening sampling. Analysis was performed on saliva specimens **(A)** and nasal swab specimens **(B)**. Equivalent analysis for evening-to-morning pairs is shown in **Figure 2-S5** in the supplemental material. Pos, positive; Neg, negative.

Discussion

In this study, we quantitatively measured SARS-CoV-2 viral load with high frequency (twice per day) longitudinally through the course of mild COVID-19 infection in saliva for 70 individuals and in nasal swabs for 29 individuals. From these measurements, we identified a pattern of higher viral loads in saliva and nasal swab specimens collected in the morning after waking than in those collected in the evening. Although similar observations have been reported for nasopharyngeal swabs (20, 21), early morning versus spot oropharyngeal specimens (22), and early morning saliva versus nasopharyngeal swabs (23) and in wastewater surveillance (24), our study is unique and clinically relevant for three reasons: (i) we measured viral load in specimen types relevant to at-home testing using a high-analytical-sensitivity RT-qPCR assay, which enabled us to infer the performance of diagnostic tests of different analytical sensitivities at each stage of infection; (ii) we collected specimens at high temporal resolution (morning and evening) longitudinally for 2 weeks, starting from early in the course of the infection via prospective sampling of high-risk populations; and (iii) our study provides the largest data set to date that investigates daily patterns in SARS-CoV-2 viral loads, with 1,194 saliva and 661 nasal swab specimens collected longitudinally. From these data, we find compelling evidence that collecting samples for COVID-19 testing in the morning upon waking can significantly improve detection of infected individuals.

The biological and physiological reasons for higher SARS-CoV-2 viral loads in the morning remain unknown but may be due to accumulation of viral material overnight or related to viral replication and immune function. Similar to the improved performance of at-home pregnancy tests with morning urine due to accumulation of human chorionic gonadotropin (25), improved detection of SARS-CoV-2 may be the result of physical accumulation of material (e.g., cells, virions, and nucleic acids) in the upper respiratory tract due to supine positioning (aiding mucociliary clearance) and/or the decreased rate of swallowing at night (26). Higher morning viral loads being due to physical accumulation of nucleic acids is supported by an increased abundance of the constitutive human *RNase P* target in saliva and nasal swab specimens collected in the morning (see **Figures 2-S2A and 2-S3A**). Human salivary production decreases overnight (27), suggesting that higher morning viral loads could be due to a concentration of virus when saliva volume is lower. Given that some individuals exhibit this phenomenon independently of human *RNase P* target abundance (**Figures 2-S2B and 2-S3B**), a circadian rhythm in viral replication may also contribute. Regulation and responsiveness of the immune system have been linked to circadian rhythms (28, 29), shown to affect SARS-CoV-2 infection of monocytes in cell culture (30) and proposed as a modulating factor for COVID-19 severity and management (31). Others have proposed cellular interactions between viral proteins and circadian rhythm-dependent host signals (32) and demonstrated circadian rhythm-dependent entry and proliferation of SARS-CoV-2 in lung

epithelial cell types in culture (33). Regardless of mechanism, because higher viral loads are associated with replication-competent culturable virus (34, 35), these findings may also suggest a higher risk of transmission in the morning.

As many individuals remain unvaccinated and new variants emerge, it remains critical to identify infections, promptly isolate infected persons, trace and quarantine contacts, and initiate early treatment to improve efficacy. Much of the world lacks access to tests with high analytical sensitivity (36–38). Our findings suggest that strategically collecting specimens in the morning immediately after waking up may improve the performance of available low- to moderate-analytical-sensitivity tests. Morning sampling will not raise the performance of tests with low analytical sensitivity to the levels of those with higher analytical sensitivity; however, even marginal improvements in detection have been shown to reduce deaths from COVID-19 (39).

This study is subject to five main limitations. First, we had a limited number of specimens collected prior to the onset of symptoms, limiting our ability to discern a difference in detectability with morning or evening specimens during the presymptomatic phase of infection. Second, this study was performed prior to the dominance of the Delta and Omicron variants of SARS-CoV-2, which may exhibit different viral load kinetics. Host factors, including vaccination status, may also influence viral load kinetics; nearly all individuals in this cohort were unvaccinated. Third, specimens were self-collected without supervision and thus may have had a different quality from those collected by a health care professional. However, many COVID-19 diagnostics in use utilize self-collected specimens, and measurements of the human *RNase P* gene suggest consistent sampling without failure to collect sufficient material. Fourth, we quantified viral load using RT-qPCR with SARS-CoV-2 *N* gene target. Many COVID-19 diagnostics utilize *N* gene targets, and *N* gene viral loads have been shown to track with other gene targets, suggesting that *N* gene quantification to viral load conversion would be representative to demonstrate a general phenomenon relevant for diagnostics detecting other viral targets. Fifth, this analysis involves inferring positivity by assays with various analytical sensitivities (LODs), based on the quantitatively measured viral loads. A direct comparison with a specific test is needed to test real-world efficacy.

Materials and Methods

Study design

Participants were recruited for participation in a COVID-19 household transmission study as previously described (9, 19). Briefly, if at least one member of a household with two or more persons had a positive COVID-19 test result within seven days or was suspected to be positive, all household members aged six years and older were eligible to participate. Participants began collecting saliva or saliva and nasal swab specimens on the evening of enrollment and each subsequent morning and evening (as described below). COVID-19-like symptoms were reported via questionnaire with each specimen collection time point.

For participants who were SARS-CoV-2 positive when initially enrolled in the study, symptom onset was defined as the date of first symptoms reported in an enrollment questionnaire. For participants who entered the study SARS-CoV-2 negative but had unrelated symptoms, symptom onset was the first instance of a new COVID-19-like symptom or an increase in symptom severity following their first SARS-CoV-2-positive specimen.

Specimen collection

Participants self-collected anterior nares nasal swab and saliva specimens in the Spectrum SDNA-1000 Saliva Collection Kit (Spectrum Solutions LLC, Draper, UT), at home twice per day (after waking up and before going to bed), per manufacturer's guidelines (although Spectrum devices are not currently authorized for the collection of nasal swab specimens). One participant self-collected both anterior nares nasal swab and saliva specimen in Nest viral transport medium (VTM) (catalog no. NST-NST-202117; Stellar Scientific, Baltimore, MD), and three individuals collected their nasal swab specimens in VTM and their saliva specimens in the Spectrum SDNA-1000 Saliva Collection Kit. Participants were instructed not to ingest anything, smoke, or brush their teeth for at least 30 min prior to collection. For nasal swab collection, participants were asked to gently blow their noses before swabbing (four complete rotations with gentle pressure in each nostril) with sterile flocked swabs. A parent/guardian assisted minors with collection. At collection, participants recorded the date and time and any symptoms experienced in the previous 12 h. Specimens collected between 4 a.m. and 12 p.m. were defined as morning; specimens collected between 3 p.m. and 3 a.m. were defined as evening (see **Figure 2-S1** in the supplemental material).

Cohort of individuals with SARS-CoV-2 infection

Between September 2020 and April 2021, 72 participants from 39 households in southern California had acute SARS-CoV-2 infection. Of these, two never reported experiencing symptoms and were not included in subsequent analyses where viral loads are aligned with date of symptom onset. Of the 70 symptomatic individuals from 37 households included in the analyses (**Table 2-1**), all 70 collected saliva specimens while a subset of 29 individuals collected both saliva and nasal swab specimens every morning and every evening while enrolled, from which we quantified viral loads.

Individuals were enrolled at various stages of infection. Of the 70 infected, symptomatic individuals, 58 were positive for SARS-CoV-2 in the first saliva or saliva and nasal swab specimen collected upon enrollment while twelve were initially negative but became positive while enrolled in the study; of these twelve individuals, seven were collecting both saliva and nasal swabs, and the viral loads and symptoms of these individuals have been previously reported (6). Of the 58 cases positive on enrollment, 50 (86.2%) were already experiencing mild COVID-19-like symptoms and 8 (13.8%) were presymptomatic. Of the 20 individuals who were either presymptomatic (8) or negative for SARS-CoV-2 (12) on enrollment, COVID-19 symptom onset occurred an average of 1.2 days after the first SARS-CoV-2-positive saliva specimen.

The mean age of the saliva cohort was 32.8 years (standard deviation [SD], ±16.0 years), and the mean age was 33.9 years (SD, ±15.2 years) among those collecting both saliva and nasal swabs. Health conditions and medications that may have impacted viral load kinetics are provided for individual participants in the supplemental material. No participants required hospitalization. At the time of these participants' enrollment in the study (September 2020 to April 2021), vaccines were either unavailable or limited to priority groups. Only one individual (**Figures 2-S2H and 2-S3H**) reported receiving a COVID-19 vaccine (first dose of Pfizer-BioNTech COVID-19, ~3 weeks before enrollment).

Extraction and quantification of viral load by RT-qPCR

Specimen processing was performed as previously described (9). Briefly, 400 or 200 μL of fluid from each saliva or nasal swab specimen, respectively, was extracted using the MagMAX Viral/Pathogen nucleic acid isolation kit (ThermoFisher Scientific; catalog no. A42352), followed by the CDC 2019-novel coronavirus (2019-nCoV) real-time RT-PCR diagnostic panel, which targets the SARS-CoV-2 *N1* and *N2* genes, as well as a human *RNase P* control. *N1* gene C_T values were converted to viral load using an equation derived from a standard curve of heat-

inactivated SARS-CoV-2 particles spiked into human specimen matrix validated previously by independent RT-double differential PCR (ddPCR) measurement (6).

Table 2-1. Participant Demographics**.** Demographic and medical information was collected via online questionnaire upon study enrollment. All participants (No.=70) collected saliva; of these 70, 29 additionally collected nasal swabs.

	Participants Contributing Each Sample Type			
	Saliva		**Saliva and Nasal Swabs**	
	70		29	
Sex*				
Male	25	35.7%	9	31.0%
Female	45	64.3%	20	69.0%
Age				
6–11	6	8.6%	1	3.4%
12–17	9	12.9%	4	13.8%
18–24	9	12.9%	3	10.3%
25–35	17	24.3%	10	34.5%
36–45	12	17.1%	3	10.3%
46–55	11	15.7%	6	20.7%
56–65	5	7.1%	2	6.9%
65+	1	1.4%	0	0.0%
Race				
Asian/Pacific Islander	6	8.6%	2	6.9%
Black/African American	2	2.9%	2	6.9%
Native American	0	0.0%	0	0.0%
White	33	47.1%	15	51.7%
Multiple Races	4	5.7%	3	10.3%
Other/Unknown†	25	35.7%	7	24.1%
Ethnicity				
Hispanic	52	74.3%	21	72.4%
Non-Hispanic	17	24.3%	8	27.6%
Unknown	1	1.4%	0	0.0%
Tobacco Smoker or Vape User History				

Current	5	7.1%	3	10.3%
Former	15	21.4%	9	31.0%
Never	43	61.4%	16	55.2%
Unknown	7	10.0%	1	3.4%
Active Medications and Supplements				
Vitamins/Supplements	47	67.1%	21	72.4%
Acetaminophen/NSAIDs‡	33	47.1%	13	44.8%
Allergy medications/Antihistamines	11	15.7%	3	10.3%
Antibiotics/Antivirals	3	4.3%	0	0.0%
Steroid drug	3	4.3%	1	3.4%
Medical Comorbidities				
Asthma	6	8.6%	1	3.4%
Anxiety or Depression	4	5.7%	2	6.9%
Diabetes	4	5.7%	3	10.3%
Obesity	4	5.7%	2	6.9%
Hypertension	3	4.3%	1	3.4%
Immunocompromise	0	0.0%	0	0.0%
SARS-CoV-2 Vaccination Status§				
Partially vaccinated	1	1.4%	1	3.4%
Completed vaccination	0	0.0%	0	0.0%
No vaccines reported	69	98.6%	28	96.6%

Statistical analyses

Initial processing was performed in Python v3.8.2, with calculation of log-transformed averages (**Figure 2-1**). Data were exported, and differences in C_T from sequential specimens were calculated in Microsoft Excel (**Figure 2-2A to D**). Plots were prepared in GraphPad Prism 9.2.0, including calculation of medians (**Figure 2-2**). For comparison of the differences between morning and evening viral loads and differences in C_T values, the Wilcoxon matched-pair signed-rank test was performed using GraphPad (**Figure 2-2**). An upper-tailed McNemar test to compare inferred percentages of infections detectable by assays with various LODs for specimens collected in the morning or evening (**Figure 2-3 and Figure 2-S5**) was performed in Python v3.8.2 using the scipy.stats package (40).

Data availability

The data underlying the results presented in the study are available at CaltechDATA at: https://data.caltech.edu/records/20049.

Acknowledgements

We sincerely thank the study participants for making this work possible. We thank Lauriane Quenee, Grace Fisher-Adams, Junie Hildebrandt, Megan Hyashi, RuthAnne Bevier, Chantal D'Apuzzo, Ralph Adolphs, Victor Rivera, Steve Chapman, Gary Waters, Leonard Edwards, Gaylene Ursua, Cynthia Ramos, and Shannon Yamashita for their assistance and advice on study implementation and/or administration. We thank Jessica Leong, Jessica Slagle, Mika Walton, Angel Navarro, Daniel Brenner, Ojas Pradhan, Si Hyung Jin, and Mary Arrastia for volunteering their time to help with this study. We thank Angie Cheng, Susan Magdaleno, Christian Kis, Monica Herrera, and Zaina Lemeir for technical discussions regarding saliva extraction and detection. We thank Jennifer Fulcher, Debika Bhattacharya, and Matthew Bidwell Goetz for their ideas on potential study populations and early study design. We thank Omai Garner and David Beenhouwer for providing materials for initial nasal swab validation. We thank Martin Hill, Alma Sanchez, Scott Kim, Debbie Noble, Nina Paddock, Whitney Harrison, Emily Holman, Isaac Turner, Vivek Desai, Luke Wade, Tom Mayell, Stu Miller, Jennifer Howes, and Nari Shin for their support with recruitment. We thank Allison Rhines, Karen Heichman, and Dan Wattendorf for valuable discussions and guidance. We thank David Prober for discussions of circadian rhythms and feedback on the manuscript. Finally, we thank all the case investigators and contact tracers at the Pasadena Public Health Department, the City of Long Beach Department of Health & Human Services, and Caltech Student Wellness Services for their efforts in study recruitment and their work in the pandemic response.

R.F.I. is a cofounder, consultant, and a director and has stock ownership of Talis Biomedical Corp.

This study is based on research funded in part by the Bill & Melinda Gates Foundation (INV-023124). The findings and conclusions contained within are those of the authors and do not necessarily reflect positions or policies of the Bill & Melinda Gates Foundation. This work was also funded by the Ronald and Maxine Linde Center for New Initiatives at the California Institute of Technology and the Jacobs Institute for Molecular Engineering for Medicine at the California Institute of Technology. A.V.W. is supported by a UCLA DGSOM Geffen Fellowship, and M.M.C. is supported by a Caltech Graduate Student Fellowship.

References

1. Wadhwa, A., Fisher, K.A., Silver, R., Koh, M., Arons, M.M., Miller, D.A., McIntyre, A.F., Vuong, J.T., Kim, K., Takamiya, M. and Binder, A.M., 2021. Identification of presymptomatic and asymptomatic cases using cohort-based testing approaches at a large correctional facility—Chicago, Illinois, USA, May 2020. *Clinical Infectious Diseases*, *72*(5), pp. e128–e135.

2. Dora, A.V., 2020. Universal and serial laboratory testing for SARS-CoV-2 at a long-term care skilled nursing facility for veterans—Los Angeles, California, 2020. *MMWR. Morbidity and mortality weekly report*, *69*.

3. Jianyu Lai, B., German, J.R., Hong, F.H., Tai, S.H.S., McPhaul, K.M., Milton, D.K. and University of Maryland StopCOVID Research Group, 2021. Comparison of Saliva and Mid-Turbinate Swabs for Detection of COVID-19 (preprint).

4. Wyllie, A.L., Fournier, J., Casanovas-Massana, A., Campbell, M., Tokuyama, M., Vijayakumar, P., Warren, J.L., Geng, B., Muenker, M.C., Moore, A.J. and Vogels, C.B., 2020. Saliva or nasopharyngeal swab specimens for detection of SARS-CoV-2. *New England Journal of Medicine*, *383*(13), pp. 1283–1286.

5. Ke, R., Martinez, P.P., Smith, R.L., Gibson, L.L., Mirza, A., Conte, M., Gallagher, N., Luo, C.H., Jarrett, J., Conte, A. and Liu, T., 2021. Daily sampling of early SARS-CoV-2 infection reveals substantial heterogeneity in infectiousness. *medRxiv*, pp. 2021–07.

6. Wölfel, R., Corman, V.M., Guggemos, W., Seilmaier, M., Zange, S., Müller, M.A., Niemeyer, D., Jones, T.C., Vollmar, P., Rothe, C. and Hoelscher, M., 2020. Virological assessment of hospitalized patients with COVID-2019. *Nature*, *581*(7809), pp. 465–469.

7. Smith, R.L., Gibson, L.L., Martinez, P.P., Ke, R., Mirza, A., Conte, M., Gallagher, N., Conte, A., Wang, L., Fredrickson, R. and Edmonson, D.C., 2021. Longitudinal assessment of diagnostic test performance over the course of acute SARS-CoV-2 infection. *The Journal of infectious diseases*, *224*(6), pp. 976–982.

8. Singanayagam, A., Hakki, S., Dunning, J., Madon, K.J., Crone, M.A., Koycheva, A., Derqui-Fernandez, N., Barnett, J.L., Whitfield, M.G., Varro, R. and Charlett, A., 2022. Community transmission and viral load kinetics of the SARS-CoV-2 delta (B. 1.617. 2) variant in vaccinated and unvaccinated individuals in the UK: a prospective, longitudinal, cohort study. *The lancet infectious diseases*, *22*(2), pp. 183–195.

9. Savela, Emily S., Alexander Viloria Winnett, Anna E. Romano, Michael K. Porter, Natasha Shelby, Reid Akana, Jenny Ji et al. "Quantitative SARS-CoV-2 viral-load curves in paired saliva samples and nasal swabs

inform appropriate respiratory sampling site and analytical test sensitivity required for earliest viral detection." *Journal of clinical microbiology* 60, no. 2 (2022): e01785–21.

10. Kissler, S.M., Fauver, J.R., Mack, C., Tai, C.G., Breban, M.I., Watkins, A.E., Samant, R.M., Anderson, D.J., Metti, J., Khullar, G. and Baits, R., 2021. Viral dynamics of SARS-CoV-2 variants in vaccinated and unvaccinated persons. *New England Journal of Medicine*, *385*(26), pp. 2489–2491.

11. Kissler, S.M., Fauver, J.R., Mack, C., Olesen, S.W., Tai, C., Shiue, K.Y., Kalinich, C.C., Jednak, S., Ott, I.M., Vogels, C.B. and Wohlgemuth, J., 2021. Viral dynamics of acute SARS-CoV-2 infection and applications to diagnostic and public health strategies. *PLoS biology*, *19*(7), p.e3001333.

12. SARS-CoV-2 reference panel comparative data (2020) FDA. Available at: https://www.fda.gov/medical-devices/coronavirus-covid-19-and-medical-devices/sars-cov-2-reference-panel-comparative-data (Accessed: 28 May 2024).

13. Brümmer, L.E., Katzenschlager, S., Gaeddert, M., Erdmann, C., Schmitz, S., Bota, M., Grilli, M., Larmann, J., Weigand, M.A., Pollock, N.R. and Macé, A., 2021. Accuracy of novel antigen rapid diagnostics for SARS-CoV-2: A living systematic review and meta-analysis. *PLoS medicine*, *18*(8), p.e1003735.

14. Global Partnership to make available 120 million affordable, quality covid-19 rapid tests for low- and middle-income countries (2022) WHO. Available at: https://www.who.int/news/item/28-09-2020-global-partnership-to-make-available-120-million-affordable-quality-covid-19-rapid-tests-for-low--and-middle-income-countries (Accessed: 28 May 2024).

15. Connor, A., Hariharan, N., Carson, S., Sanders, K.C., Vosburg, K.B. and Sabot, O., 2021. Access to COVID-19 testing in low-and middle-income countries is still critical to achieving health equity. *Health Affairs Forefront*.

16. Global availability of COVID-19 diagnostic tests (2022) PATH. Available at: https://www.path.org/programs/diagnostics/covid-dashboard-global-availability-covid-19-diagnostic-tests/ (Accessed: 28 May 2024).

17. Borrmann, H., McKeating, J.A. and Zhuang, X., 2021. The circadian clock and viral infections. *Journal of biological rhythms*, *36*(1), pp. 9–22.

18. Diallo, A.B., Coiffard, B., Leone, M., Mezouar, S. and Mege, J.L., 2020. For whom the clock ticks: clinical chronobiology for infectious diseases. *Frontiers in immunology*, *11*, p. 533252.

19. Winnett, A., Cooper, M.M., Shelby, N., Romano, A.E., Reyes, J.A., Ji, J., Porter, M.K., Savela, E.S., Barlow, J.T., Akana, R. and Tognazzini, C., 2020. SARS-CoV-2 viral load in saliva rises gradually and to moderate levels in some humans. *medRxiv*.

20. McNaughton, C.D., Adams, N.M., Hirschie Johnson, C., Ward, M.J., Schmitz, J.E. and Lasko, T.A., 2021. Diurnal variation in SARS-CoV-2 PCR test results: test accuracy may vary by time of day. *Journal of biological rhythms*, *36*(6), pp. 595–601.

21. Liu, M., Li, Q., Zhou, J., Ai, W., Zheng, X., Zeng, J., Liu, Y., Xiang, X., Guo, R., Li, X. and Wu, X., 2020. Value of swab types and collection time on SARS-COV-2 detection using RT-PCR assay. *Journal of virological methods*, *286*, p. 113974.

22. Hung, D.L.L., Li, X., Chiu, K.H.Y., Yip, C.C.Y., To, K.K.W., Chan, J.F.W., Sridhar, S., Chung, T.W.H., Lung, K.C., Liu, R.W.T. and Kwan, G.S.W., 2020, June. Early-morning vs spot posterior oropharyngeal saliva for diagnosis of SARS-CoV-2 infection: implication of timing of specimen collection for community-wide screening. In *Open Forum Infectious Diseases* (Vol. 7, No. 6, p. ofaa210). US: Oxford University Press.

23. Rao, M., Rashid, F.A., Sabri, F.S., Jamil, N.N., Zain, R., Hashim, R., Amran, F., Kok, H.T., Samad, M.A.A. and Ahmad, N., 2021. Comparing nasopharyngeal swab and early morning saliva for the identification of severe acute respiratory syndrome coronavirus 2 (SARS-CoV-2). *Clinical Infectious Diseases*, *72*(9), pp. e352–e356.

24. Bivins, A., North, D., Wu, Z., Shaffer, M., Ahmed, W. and Bibby, K., 2021. Within-and between-day variability of SARS-CoV-2 RNA in municipal wastewater during periods of varying COVID-19 prevalence and positivity. *Acs Es&T Water*, *1*(9), pp. 2097–2108.

25. Center for Devices and Radiological Health (2019) Pregnancy, U.S. Food and Drug Administration. Available at: https://www.fda.gov/medical-devices/home-use-tests/pregnancy (Accessed: 28 May 2024).

26. Uludag, I.F., Tiftikcioglu, B.I. and Ertekin, C., 2016. Spontaneous swallowing during all-night sleep in patients with Parkinson disease in comparison with healthy control subjects. *Sleep*, *39*(4), pp. 847–854.

27. Dawes, C., 1972. Circadian rhythms in human salivary flow rate and composition. *The Journal of physiology*, *220*(3), pp. 529–545.

28. Mazzoccoli, G., Vinciguerra, M., Carbone, A. and Relógio, A., 2020. The circadian clock, the immune system, and viral infections: the intricate relationship between biological time and host-virus interaction. *Pathogens*, *9*(2), p. 83.

29. Niemeyer, J.E., 2017. Viruses and circadian rhythms. *Lab Animal*, *46*(1), pp. 7–7.

30. Diallo, A.B., Gay, L., Coiffard, B., Leone, M., Mezouar, S. and Mege, J.L., 2021. Daytime variation in SARS-CoV-2 infection and cytokine production. *Microbial pathogenesis*, *158*, p. 105067.

31. Ray, S. and Reddy, A.B., 2020. COVID-19 management in light of the circadian clock. *Nature Reviews Molecular Cell Biology*, *21*(9), pp. 494–495.

32. e Cruz, M.M., Miyazawa, M. and Gozal, D., 2020. Putative contributions of circadian clock and sleep in the context of SARS-CoV-2 infection. *European Respiratory Journal*, *55*(6).

33. Zhuang, X., Tsukuda, S., Wrensch, F., Wing, P.A., Schilling, M., Harris, J.M., Borrmann, H., Morgan, S.B., Cane, J.L., Mailly, L. and Thakur, N., 2021. The circadian clock component BMAL1 regulates SARS-CoV-2 entry and replication in lung epithelial cells. *IScience*, *24*(10).

34. Gallichotte, E.N., Quicke, K.M., Sexton, N.R., Fitzmeyer, E., Young, M.C., Janich, A.J., Dobos, K., Pabilonia, K.L., Gahm, G., Carlton, E.J. and Ebel, G.D., 2020. Longitudinal surveillance for SARS-CoV-2 among staff in six Colorado long-term care facilities: epidemiologic, virologic and sequence analysis. *medRxiv*.

35. Perera, R.A., Tso, E., Tsang, O.T., Tsang, D.N., Fung, K., Leung, Y.W., Chin, A.W., Chu, D.K., Cheng, S.M., Poon, L.L. and Chuang, V.W., 2020. SARS-CoV-2 virus culture and subgenomic RNA for respiratory specimens from patients with mild coronavirus disease. *Emerging infectious diseases*, *26*(11), p.2701.

36. Okeke, I.N. and Ihekweazu, C., 2021. The importance of molecular diagnostics for infectious diseases in low-resource settings. *Nature Reviews Microbiology*, *19*(9), pp.547-548.

37. Sander, A.L., Yadouleton, A., Moreira-Soto, A., Tchibozo, C., Hounkanrin, G., Badou, Y., Fischer, C., Krause, N., Akogbeto, P., F. de Oliveira Filho, E. and Dossou, A., 2021. An observational laboratory-based assessment of SARS-CoV-2 molecular diagnostics in Benin, Western Africa. *MSphere*, *6*(1), pp. 10–1128.

38. Health, T.L.G., 2021. Essential diagnostics: mind the gap. *The Lancet. Global Health*, *9*(11), p. e1474.

39. Terriau, A., Albertini, J., Montassier, E., Poirier, A. and Le Bastard, Q., 2021. Estimating the impact of virus testing strategies on the COVID-19 case fatality rate using fixed-effects models. *Scientific Reports*, *11*(1), p. 21650.

40. Virtanen, P., Gommers, R., Oliphant, T.E., Haberland, M., Reddy, T., Cournapeau, D., Burovski, E., Peterson, P., Weckesser, W., Bright, J. and Van Der Walt, S.J., 2020. SciPy 1.0: fundamental algorithms for scientific computing in Python. *Nature methods*, *17*(3), pp. 261–272.

Supplemental Information

Additional participant and specimen details from Figure 2-1

Viral load was quantified from an average of 32 saliva specimens (SD ±6 specimens) each from the 12 participants in the negative-on-enrollment cohort, while on average 13 saliva specimens (SD ±10 specimens) each were processed from 58 participants positive-on-enrollment (**Figure 2-S2**). For nasal swabs, an average of 35 specimens (SD ±7 specimens) were quantified from seven participants in the negative-on-enrollment cohort, while viral load was quantified in an average of 17 nasal-swab specimens (SD ±9 specimens) from 22 participants who were positive on-enrollment (**Figure 2-S3**).

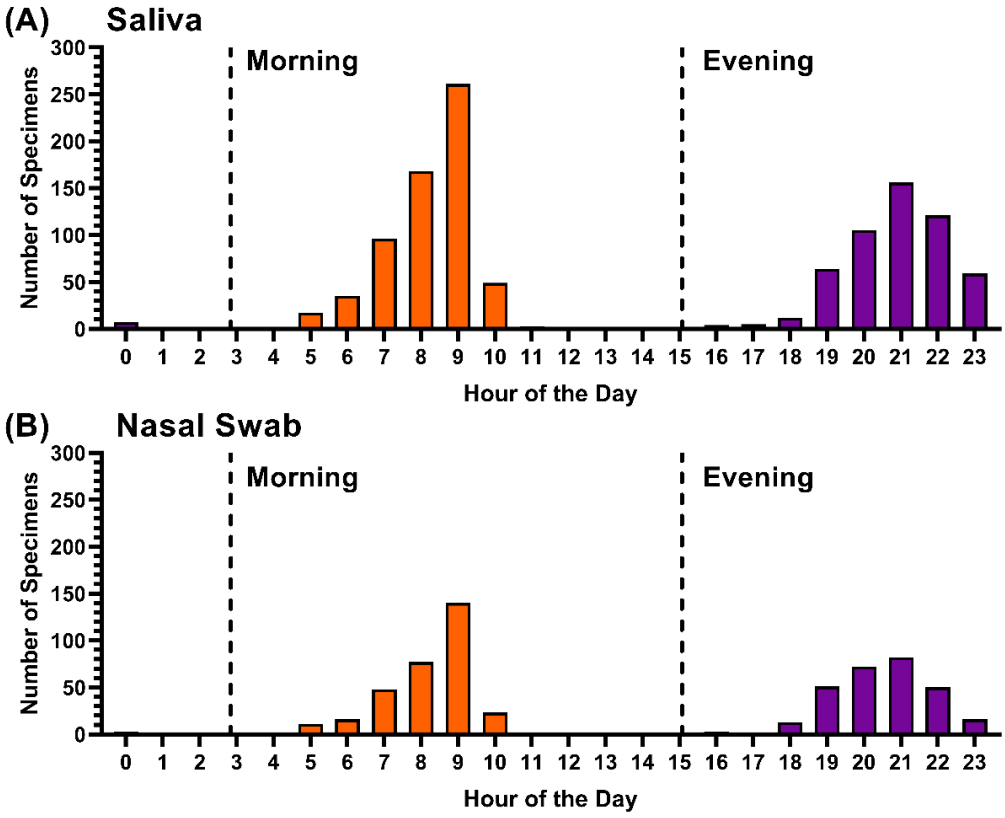

Supplemental Figure 2-1. Frequency of Saliva and Nasal-Swab Specimen Collection Times. Study participants either collected saliva only, or saliva then anterior nasal swab at the same time point, and were instructed to collect specimens immediately after waking up and immediately before bed (see Methods for detailed instructions). The frequency of specimens collected by each hour of the day is plotted for 1,194 saliva specimens (A) and 661 nasal-swab specimens (B). Dashed vertical line indicates cutoff for morning (3 a.m. to 12 p.m.) and evening (3 p.m. to 3 a.m.) collected specimens used in this study.

[Figure On Next Page] **Supplemental Figure 2-2.** Individual salivary RT-PCR Ct measurements, for SARS-CoV-2 N1 gene target (red) and human RNase P control gene target (black), relative to symptom onset. Matching panel labels correspond to the same participant shown in Figure S3. Underlined panel labels indicate that the participant converted from SARS-CoV-2- negative to -positive while enrolled in the study. Gray dashed line indicates Ct threshold for positivity. ND indicates not detected.

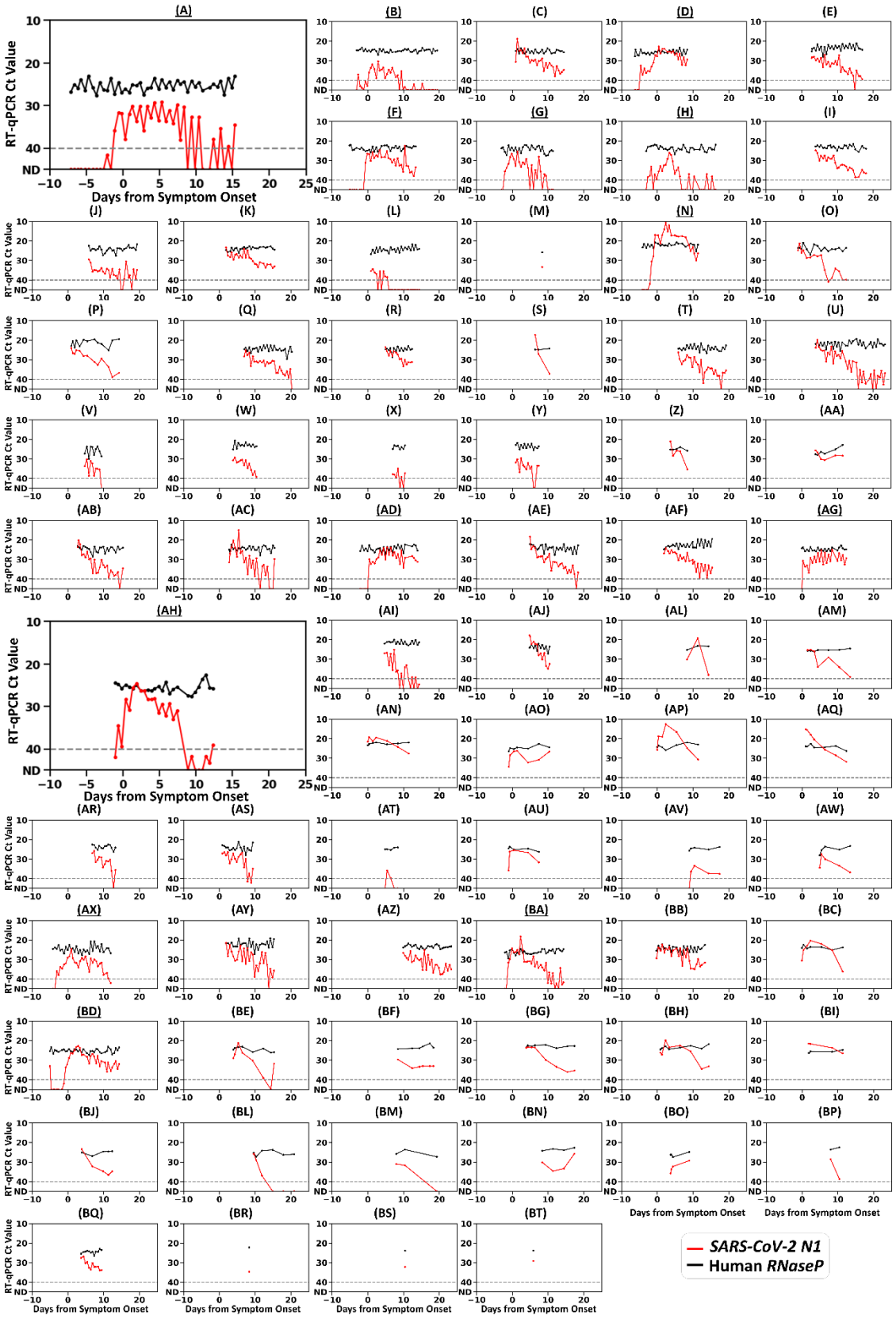
(A)
(B)
(C)
(D)
(E)
(F)
(G)
(H)
(I)
(J)
(K)
(L)
(M)
(N)
(O)
(P)
(Q)
(R)
(S)
(T)
(U)
(V)
(W)
(X)
(Y)
(Z)
(AA)
(AB)
(AC)
(AD)
(AE)
(AF)
(AG)
(AH)
(AI)
(AJ)
(AL)
(AM)
(AN)
(AO)
(AP)
(AQ)
(AR)
(AS)
(AT)
(AU)
(AV)
(AW)
(AX)
(AY)
(AZ)
(BA)
(BB)
(BC)
(BD)
(BE)
(BF)
(BG)
(BH)
(BI)
(BJ)
(BL)
(BM)
(BN)
(BO)
(BP)
(BQ)
(BR)
(BS)
(BT)
RT-qPCR Ct Value
Days from Symptom Onset
ND
SARS-CoV-2 N1
Human RNaseP

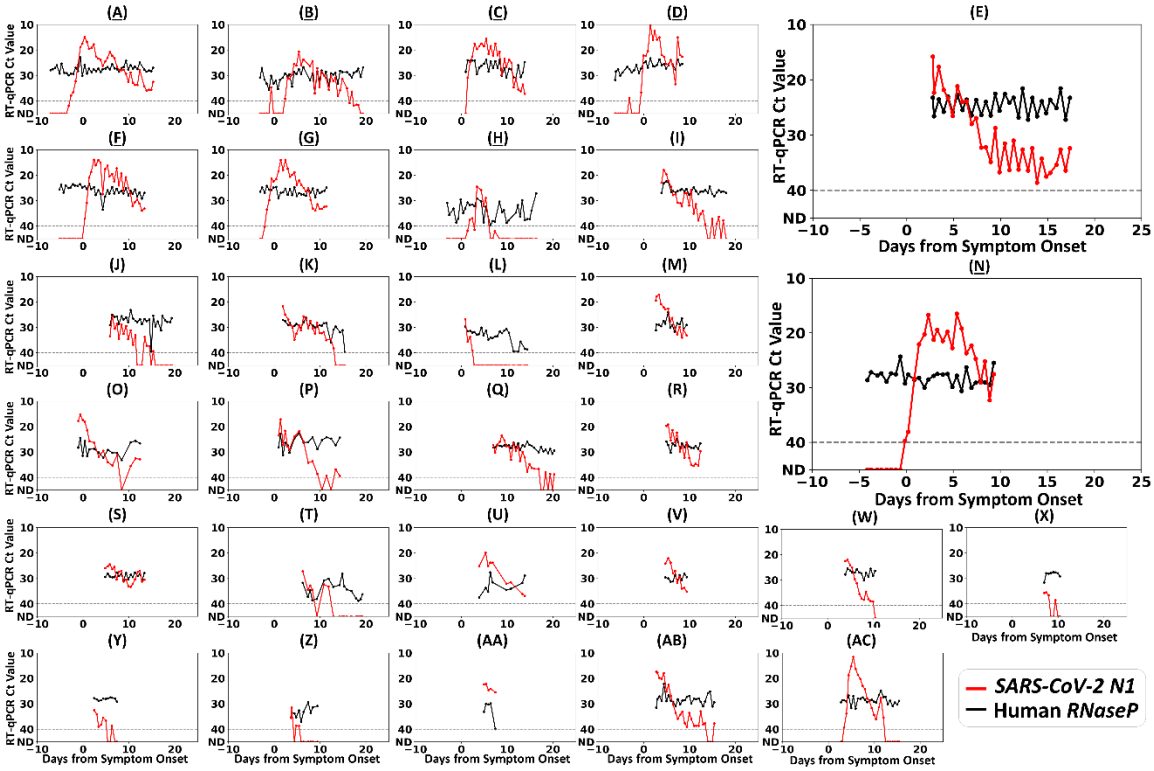

Supplemental Figure 2-3. Individual nasal-swab RT-PCR Ct measurements, for SARS-CoV-2 N1 gene target and human *RNase P* control gene target. Each panel shows the measured SARS-CoV-2 *N1* Ct values (red), and human *RNase P* Ct values (black) for an individual participant, relative to symptom onset. Matching panel labels correspond to the same participant shown in Figure S2. Underlined panel labels indicate that the participant converted from SARS-CoV-2-negative to -positive while enrolled in the study. Gray dashed line indicates Ct threshold for positivity. ND indicates not detected.

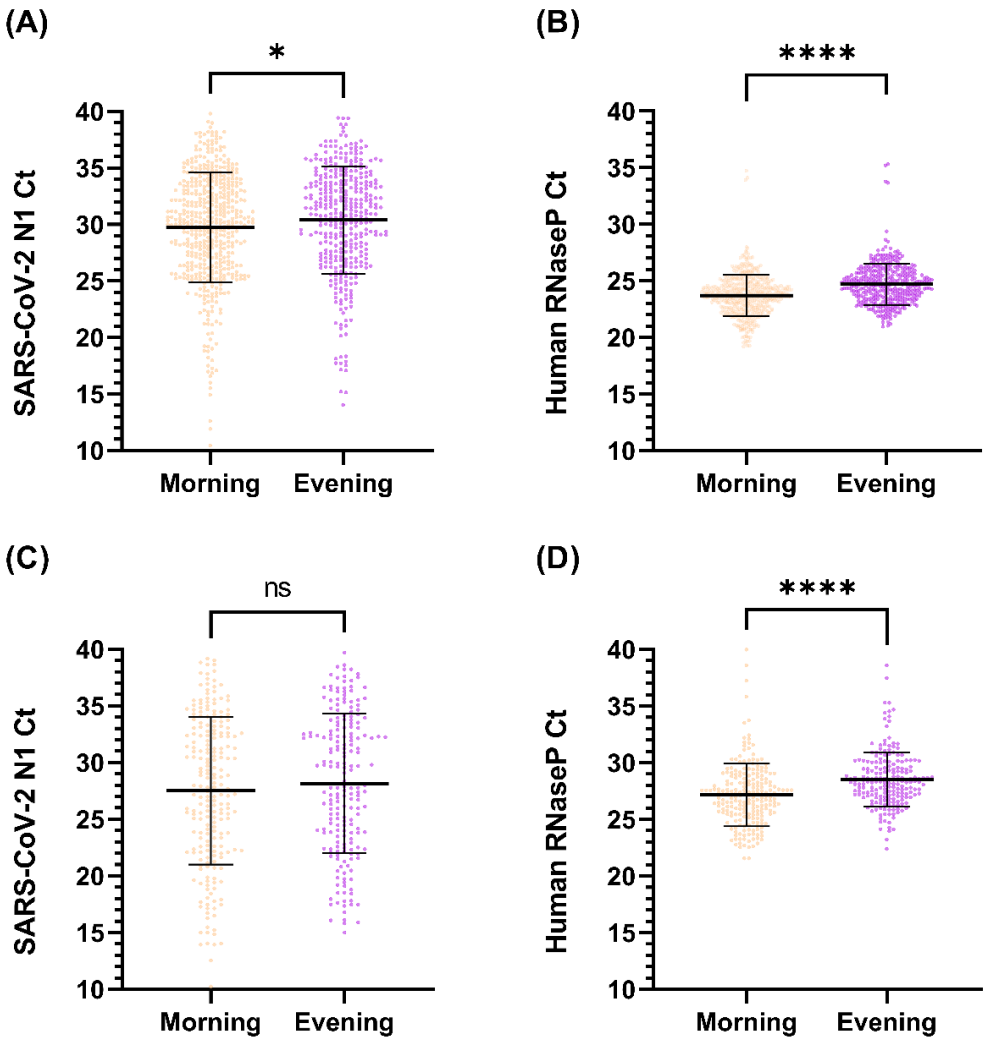

Supplemental Figure 2-4. Aggregated SARS-CoV-2 *N1* and human *RNase P* Ct values grouped by specimens collected in the morning and evening. **(A)** Direct comparison of aggregated Ct values for SARS-CoV-2 *N1* gene target, measured from all SARS-CoV-2 positive saliva specimens from all participants, by either morning or evening collection time. **(B)** Direct comparison of aggregated Ct values for human *RNase P* target from all SARS-CoV-2 positive saliva specimens from all participants, by either morning or evening collection time. **(C)** Direct comparison of aggregated Ct values for SARS-CoV-2 *N1* gene, measured from all SARS-CoV-2 positive nasal-swab specimens from all participants, by either morning or evening collection time. **(D)** Direct comparison of aggregated Ct values for human *RNase P* target from all SARS-CoV-2 positive nasal-swab specimens from all participants, by either morning or evening collection time. Specimens with morning collection times are shown as orange points, while evening are shown as purple points. Black lines indicate mean Ct value, with error bars representing standard deviation. Statistical comparison of Ct values for groups performed by unpaired t-test without correction: ns indicates nonsignificant difference, * indicates P <0.001.

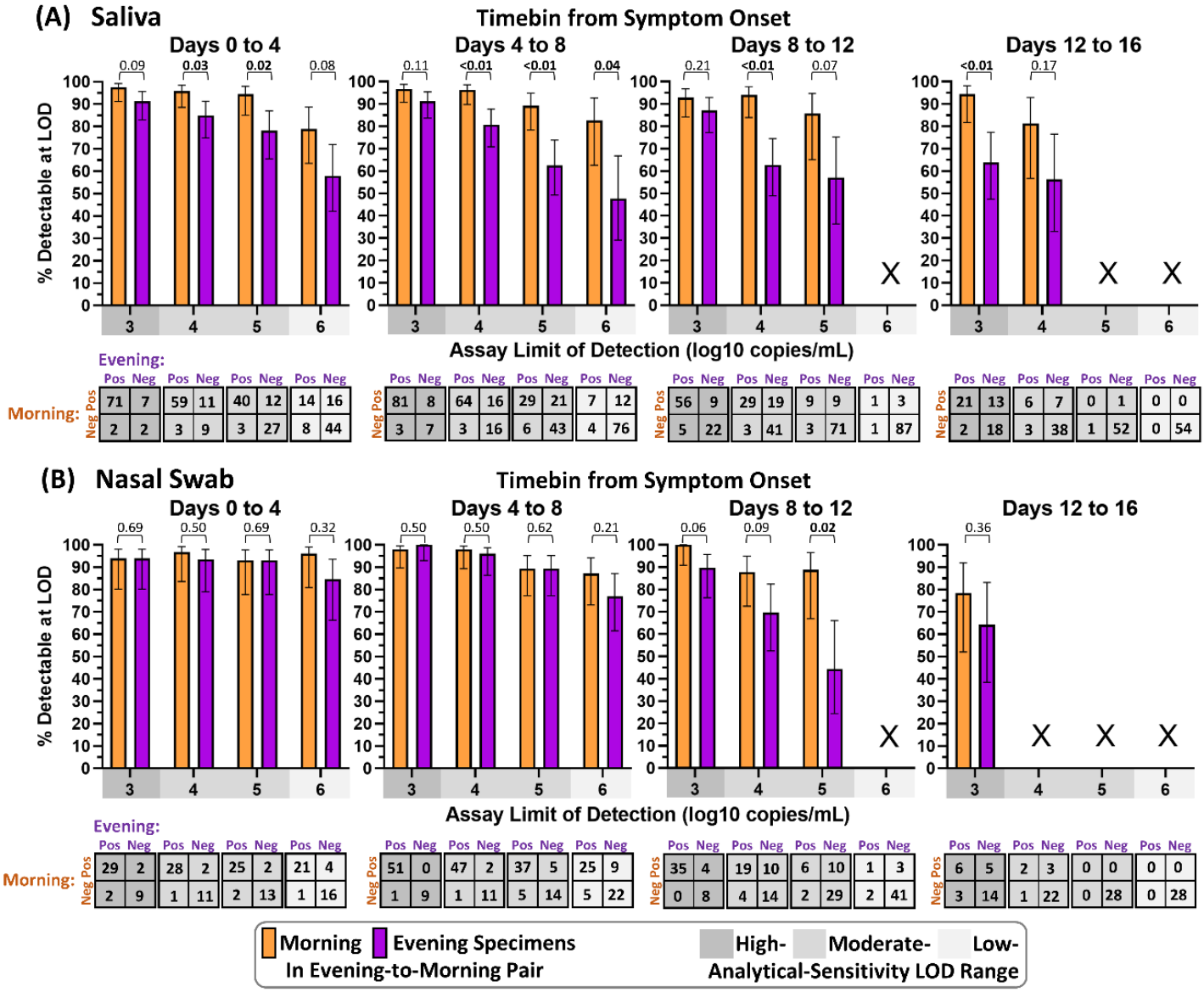

Supplemental Figure 2-5. Morning saliva or nasal-swab specimen collection yields improved detection across infection stages and assay analytical sensitivities. For each four-day time bin relative to symptom onset, pairs of sequentially collected evening-to-morning specimens were assessed. In each pair, the viral load in each specimen was used to predict positivity if tested by an assay with a given LOD. Bar plots show the fraction of pairs with a positive result in either the morning or evening specimen that would be detectable if the morning specimen (orange) or evening specimen (purple) were tested at a given LOD. Error bars indicate the 95% confidence interval. Bars are not shown (X) when fewer than 10 pairs had positive results at the given LOD during the infection time bin. Among LODs and infection time bins with more than 10 positive pairs, the percent detectable for morning versus evening specimens were compared by upper-tailed McNemar Exact Test, applied to the 2 x 2 table shown below each comparison. Resulting P-values are shown above each comparison. Bolded values indicate significantly higher detection with morning sampling over evening sampling. Analysis was performed on **(A)** saliva specimens and **(B)** nasal swab specimens. Equivalent analysis for morning-to-evening pairs is shown in Figure 3.

Author Contributions

Listed alphabetically by last name

Reid Akana (RA): collaborated with AVW in creating digital participant symptom surveys; assisted with data quality control/curation with JJ, NWS, NS; created current laboratory information management system (LIMS) for specimen logging and tracking. Creation of iOS application for specimen logging/tracking. Configured an SQL database for data storage. Created an Apache server and websites to view study data. Configured FTPS server to catalog PCR data. Wrote a Python package to access study data. Worked with ESS, AVW, AER to implement logic that prioritized specimen extraction order.

Jacob T. Barlow (JTB): Created initial specimen tracking database to aid in specimen logging and tracking. Maintenance of database and implementation of corrections.

Alyssa M. Carter (AMC): Received, performed QC on, and logged specimens. Performed nucleic acid extractions and RT-qPCR. Aliquoting and preparing study reagents as needed. Performed preliminary experiments to assess RNA stability in our saliva and nasal swab specimens. Summarizing daily RT-qPCR data of participant time courses to inform participant keep/drop decisions. Provided feedback on early figure drafts.

Matthew M. Cooper (MMC): Collaborated with AVW, MF, NS, YG, RFI, on study design and recruitment strategies. Co-wrote initial IRB protocol and informed consent with AVW and NS; assisted in the writing of the enrollment questionnaire; developed laboratory specimen processing workflow for saliva with AVW and AER; performed specimen processing on subset of specimens; funding acquisition; collaborated with AER to write data processing/visualization code for observing household transmission events for active study participants. Contributor to the design of the calibration curve for saliva LOD experiments. Performed specimen logging and QC.

Matthew Feaster (MF): Co-investigator; collaborated with AVW, MMC, NS, YG, RFI on study design and recruitment strategies; provided guidance and expertise on SARS-CoV-2 epidemiology and local trends.

Ying-Ying Goh (YG): Co-investigator; collaborated with AVW, MMC, NS, MF, RFI on study design and recruitment strategies; provided guidance and expertise on SARS-CoV-2 epidemiology and local trends.

Rustem F. Ismagilov (RFI): Co-investigator; collaborated with AVW, MMC, NS, MF, YYG on study design and recruitment strategies; provided leadership, technical guidance, oversight, and was responsible for obtaining funding for the study.

Jenny Ji (JJ): Researched epidemiological survey structures, performed epidemiological literature review with MMC and AVW, and co-wrote enrollment questionnaire with NS and AVW. Major contributor to curation of participant symptom data. Provided quality control of participant data with RA, NS, NWS.

Michael K. Porter (MKP): Performed specimen logging and QC, RNA extractions, RT-qPCR, data processing. Performed data acquisition and analysis for and made Figure S2 with AVW. Prepared participant specimen collection materials and helped with supplies acquisition. Assisted in literature analysis with ESS, RA, AVW. Performed data analysis and prepared Figure 2-2 with AVW. Assisted in preparation of Figures 2-1, 2-3, 2-S2, 2-S3 with AVW. Verified the underlying data with AVW and NS. Outlined and wrote manuscript with AVW.

Jessica A. Reyes (JAR): Lead study coordinator; collaborated with NS, AVW, NWS, and RFI on recruitment strategies, translated study materials into Spanish, co-wrote informational sheets with AVW and NS; created instructional videos for participants; enrolled and maintained study participants with NS and NWS.

Anna E. Romano (AER): Developed laboratory swab specimen processing workflow with ESS. Optimized extraction protocols working with vendor scientists. Created budgets and managed, planned, and purchased reagents and supplies; developed and validated method for RT-qPCR analysis for saliva and nasal-swab specimens with MMC, and AVW. Performed specimen logging and QC, RNA extractions, RT-qPCR; Design of saliva calibration curve experiment. Managing logistics for the expansion of the BSL-2+ lab space with ESS. Provided feedback on earlier manuscript revision and provided a few references.

Emily S. Savela (ESS): Coordinated laboratory team schedules and division of lab work. Performed initial nasal swab workflow validation experiments with AER. Major contributor to workflow validation, methods, biosafety SOPs. Developed/implemented system for specimen archiving. Performed specimen logging and QC, RNA extractions, RT-qPCR, and data processing. Managing logistics for the expansion of the BSL-2+ lab space with AER and biohazardous waste pickups.

Natasha Shelby (NS): Study administrator; collaborated with AVW, MMC, RFI, YG, MF on initial study design and recruitment strategies; co-wrote IRB protocol and informed consent with AVW and MMC; co-wrote enrollment questionnaire with AVW and JJ; co-wrote participant informational sheets with AVW and JAR; enrolled and maintained study participants with JAR and NWS; study-data quality control, curation, and archiving with RA, JJ,

and NWS; reagents and supplies acquisition; assembled Table 1 with AVW; managed citations and reference library; verified the underlying data with MKP and AVW; edited the manuscript.

Noah W. Schlenker (NWS): Study coordinator; collaborated with NS, AW, JAR, and RFI on recruitment strategies; enrolled and maintained study participants with NS and JAR; study-data quality control, curation and archiving with RA, JJ, and NS. Colten Tognazzini (CT): Coordinated the recruitment efforts at PPHD with case investigators and contact tracers; provided guidance and expertise on SARS-CoV-2 epidemiology and local trends.

Alexander Viloria Winnett (AVW): Collaborated with MMC, NS, RFI, YG, MF on initial study design and recruitment strategies; co-wrote IRB protocol and informed consent with MMC and NS; co-wrote enrollment questionnaire with NS and JJ; co-wrote participant informational sheets with NS and JAR and digital survey; developed and validated methods for saliva and nasal-swab specimen collection; developed and validated methods for RT-qPCR analysis for saliva and swab specimens with AER, ESS, MMC; reagents and supplies acquisition; funding acquisition; developed laboratory specimen processing workflow with AER, ESS, and MMC; performed specimen logging and QC, nucleic acid extraction, RT-qPCR; assembled Table 1 with NS; analyzed viral load time series data to visualize trends (Figure 2-1) with MKP; assisted MKP in the preparation of Figure 2-2; analyzed viral load data to generate Figure 2-3 with MKP; analyzed specimen collection data for Figure 2-S1; generated longitudinal RT-qPCR plot array for Figure 2-S2, Figure 2-S3 with MKP; analyzed data for Figure 2-S4. Verified the underlying data with MKP and NS. Outlined and wrote manuscript with MKP.

Chapter 3

QUANTITATIVE SARS-COV-2 VIRAL-LOAD CURVES IN PAIRED SALIVA SAMPLES AND NASAL SWABS INFORM APPROPRIATE RESPIRATORY SAMPLING SITE AND ANALYTICAL TEST SENSITIVITY REQUIRED FOR EARLIEST VIRAL DETECTION

This chapter was originally published in Savela ES*, Viloria Winnett A*, Romano AE*, Porter MK, Shelby T, Akana R, Ji Jenny, Cooper MM, Schlenker NW, Reyes JA, Carter AM, Barlow JT, Tognazzini C, Feaster M, Goh YY, Ismagilov RF. Quantitative SARS-CoV-2 Viral-Load Curves in Paired Saliva Samples and Nasal Swabs Inform Appropriate Respiratory Sampling Site and Analytical Test Sensitivity Required for Earliest Viral Detection (Feb 2022). Journal of Clinical Microbiology. https://doi.org/10.1128/jcm.01785-21.

Abstract

Early detection of SARS-CoV-2 infection is critical to reduce asymptomatic and presymptomatic transmission, curb the spread of variants, and maximize treatment efficacy. Low-analytical-sensitivity nasal-swab testing is commonly used for surveillance and symptomatic testing, but the ability of these tests to detect the earliest stages of infection has not been established. In this study, conducted between September 2020 and June 2021 in the greater Los Angeles County, California, area, initially SARS-CoV-2 negative household contacts of individuals diagnosed with COVID-19 prospectively self-collected paired anterior-nares nasal-swab and saliva samples twice daily for viral-load quantification by high-sensitivity reverse-transcription quantitative PCR (RT-qPCR) and digital-RT-PCR assays. We captured viral-load profiles from the incidence of infection for seven individuals and compared diagnostic sensitivities between respiratory sites. Among unvaccinated persons, testing saliva with a high-analytical-sensitivity assay detected infection up to 4.5 days before viral loads in nasal swabs reached concentrations detectable by low-analytical-sensitivity nasal-swab tests. For most participants, nasal swabs reached higher peak viral loads than saliva but were undetectable or at lower loads during the first few days of infection. High-analytical-sensitivity saliva testing was most reliable for earliest detection. Our study illustrates the value of acquiring early (within hours after a negative high-sensitivity test) viral-load profiles to guide the appropriate analytical sensitivity and respiratory site for detecting earliest infections. Such data are challenging to acquire but critical to designing optimal testing strategies with emerging variants in the current pandemic and to respond to future viral pandemics.

Introduction

Early detection of SARS-CoV-2 infection is needed to reduce asymptomatic and presymptomatic transmission, including the introduction and spread of new viral variants. More than half of transmission events occur from presymptomatic or asymptomatic persons (1). Early detection enables individuals to isolate sooner, reducing transmission within households and local communities and to vulnerable populations. Rapid antigen or molecular tests performed on nasal swabs are common for both SARS-CoV-2 screening and symptomatic testing (2) but can have low analytical sensitivity compared with lab-based molecular tests. As new variants of concern emerge with increased transmissibility (3–5), high viral loads (4, 6), and breakthrough infections (7), these testing strategies (analytical sensitivity and sample type) need to be assessed and adjusted to ensure detection of early infection. It is still unclear which testing strategy can detect SARS-CoV-2 infection at the earliest stages. Does one need a high-sensitivity test, or would a test with low analytical sensitivity suffice? Which sample site contains detectable virus first?

Tests with high analytical sensitivity can detect low levels of molecular components of the virus (e.g., RNA or proteins) in a sample. Analytical sensitivity is described by the limit of detection (LOD) of a test (defined as the lowest concentration of the viral molecules that produces 95% or better probability of detection). LOD of SARS-CoV-2 diagnostic tests is described in various units, of which the most directly comparable among tests are those that report the number of viruses (viral particles) or viral RNA copies per milliliter of sample. Viral RNA copies/mL are roughly equivalent to genome copy equivalents/mL (GCE/mL) or nucleic-acid detectable units/mL (NDU/mL). These LOD values are tabulated by the FDA and vary by ≥5 orders of magnitude between tests (8). Tests with high analytical sensitivity have LOD values equivalent to ~10^2 to 10^3 copies/mL of sample, whereas tests with low analytical sensitivity have LOD values equivalent to ~10^5 to 10^7 copies/mL (9–12). Importantly, test types (e.g., reverse transcription-quantitative PCR [RT-qPCR], antigen) are often incorrectly equated with a certain analytical sensitivity, despite an FDA analysis (8) demonstrating that the sensitivity of different RT-qPCR tests ranges from highly sensitive (e.g., LOD of 180 NDU/mL for PerkinElmer and 450 NDU/mL for Zymo Research) to substantially less sensitive (e.g., LOD of 180,000 NDU/mL for TaqPath COVID-19 combo kit and 540,000 NDU/mL for Lyra Direct SARS-CoV-2 assay). The low end of this range (corresponding to the higher LOD values) overlaps with the range of low-analytical-sensitivity rapid isothermal nucleic acid tests (e.g., LOD of 180,000 NDU/mL for Atila BioSystems and 300,000 NDU/mL for Abbott ID NOW tests) and approaches the analytical sensitivity range of antigen tests (9, 10). To choose the appropriate test for reliable early detection, one needs to measure viral loads present in samples collected early in the course of infection (13) and then choose a test with an LOD below that viral load. Initial data by us (14) and others (15, 16) show that, at least in some humans, SARS-CoV-2 viral load can be low (in the range of 10^3 to 10^5 copies per mL of saliva sample) early in infection; therefore, only tests with high analytical sensitivity would reliably detect virus in saliva.

Sampling site or specimen type may also be critical to early detection. Other respiratory viruses have been shown to have detection rates that vary by sampling site (17), which have occasionally been linked to viral tropism. For example, the cellular receptor for entry of Middle East respiratory syndrome coronavirus (MERS-CoV) is expressed nearly exclusively in the lower respiratory tract, prompting recommendations for diagnostic testing of specific sample types (bronchoalveolar lavage fluid, sputum, and tracheal aspirates) (18). A previous study on SARS-CoV found high levels of viral RNA in saliva and throat-wash early in the infection course (before the development of lung lesions), suggesting saliva as a promising sample type for early detection (19). Although nasopharyngeal (NP) swab is often considered the gold standard for SARS-CoV-2 detection, it requires collection by a healthcare worker and is not well tolerated. Furthermore, the performance of NP swabs for early detection of current SARS-CoV-2 variants is unknown. Sample types such as anterior-nares or mid-turbinate nasal swabs (20–23) and saliva (24–27) are more practical, especially for repeated sampling in screening.

To understand the required test sensitivity and the optimal sample type for earliest SARS-CoV-2 detection, we designed a case-ascertained study of household transmission with high-frequency sampling of both saliva and anterior-nares nasal swabs. Building on our earlier work (14), we enrolled individuals ages six years and older who had recently tested positive (household index case) and their exposed household contacts at risk of infection. Negative samples preceding the first positive result are needed to confirm that a participant is within the first days of detectable SARS-CoV-2 RNA. All participants self-collected saliva and anterior-nares nasal swabs twice daily, in the morning upon waking and before bed. Importantly, all samples were immediately placed in a guanidinium-based inactivating and RNA-stabilizing solution (see Materials and Methods). Samples were screened for SARS-CoV-2 *N1* and *N2* gene positivity using a high-sensitivity assay. When a transmission event was observed (a previously SARS-CoV-2-negative participant tested positive in at least one sample type), we quantified viral loads in all samples prospectively collected from that participant for at least two weeks from their first positive result. Quantification was performed via quantitative reverse-transcription PCR (RT-qPCR), with a subset of measurements validated by reverse-transcription droplet digital PCR (RT-ddPCR), capturing the early and full course of acute SARS-CoV-2 infection with high sensitivity.

Materials and Methods

Refer to the supplemental material for detailed methods.

Questionnaires and sample collection

Acquisition of participant data was performed as described previously (14). Symptoms (including those listed by the Centers for Disease Control and Prevention [CDC]) were reported by participants twice daily at the time of sample collection (28).

Participants self-collected nasal-swab and saliva samples in the Spectrum SDNA-1000 Saliva Collection Kit (Spectrum Solutions LLC, Draper, UT, USA), which contains 1.5 mL of liquid buffer, at home twice per day (after waking up and before going to bed), per the manufacturer's guidelines. A parent or legal guardian assisted all minors with collection and was instructed to wear a face covering during supervision.

Samples were stored at 4°C and equilibrated to room temperature before being processed with extraction protocols.

RNA extraction and nucleic acid quantification

Participant saliva and anterior-nares swab samples were extracted using the KingFisher Flex 96 instrument (Thermo

Fisher Scientific) with the MagMax Viral Pathogen I Nucleic Acid Isolation Kit (catalog [cat.] no. A42352; Applied Biosystems, Waltham, MA, USA) guided by Thermo Fisher technical notes for SARS-CoV-2 modification and saliva.

RT-qPCR was performed as previously described (14) using the CDC 2019-novel coronavirus (2019-nCoV) real-time RT-PCR diagnostic panel (29), with duplicate reactions. See the supplemental material methods for establishing the extraction to RT-qPCR assay workflow LOD of 1,000 copies/mL (Figures 3.S1A and B in the supplemental material).

For samples defined as positive by assay guidelines from the CDC (29), viral load was quantified by conversion of the mean quantification cycle (C_q) of duplicate RT-qPCRs using the equations obtained from calibration curves of contrived samples—healthy human saliva or nasal fluid spiked with heat-inactivated SARS-CoV-2 particles. See the supplemental material methods for additional details.

Quantification was also performed by reverse-transcription droplet digital PCR (RT-ddPCR) on both the calibration curve samples (**Figure 3-1, Figure 3-S2**) and participant samples (**Figure 3-1)** using the Bio-Rad SARS-CoV-2 droplet digital PCR kit (cat. no. 12013743; Bio-Rad). Droplets were created using the QX200 Droplet Generator (cat. no. 1864002; Bio-Rad); thermocycling was performed on a Bio-Rad C1000 and detected using the QX200 droplet digital PCR system (cat. no. 1864001; Bio-Rad). Samples were analyzed with QuantaSoft analysis Pro 1.0.595 software following Bio-Rad's research-use only (RUO) SARS-CoV-2 guidelines (30).

Viral sequencing

Saliva and nasal-swab samples with an N1 gene C_q of below 26 were sent to Chan Zuckerberg Biohub for SARS-CoV-2 viral genome sequencing, a modification of Deng et al. (31) as described in Gorzynski et al. (32). Sequences were assigned pangolin lineages described by Rambaut et al. (33) using Phylogenetic Assignment of Named Global outbreak LINeages software 2.3.2 (github.com/cov-lineages/pangolin). Chan Zuckerberg Biohub submitted the resulting genomes to GISAID.

Data availability

Data are available on CaltechDATA at https://data.caltech.edu/records/1942.

Results

We first established and validated two independent quantitative assays to measure SARS-CoV-2 viral load, an RT-qPCR based on the assay put forth by the CDC (29) and an RT-ddPCR assay developed by Bio-Rad (30). Both of these assays received an emergency use authorization (EUA) for qualitative, but not quantitative, detection of SARS-CoV-2. We optimized the extraction and each quantitative assay protocol (see supplemental material methods) to obtain more reliable quantification of SARS-CoV-2 viral load. The LOD of the modified assay was determined to be 1,000 copies/mL or better by following FDA guidelines (see Materials and Methods; **Figure 3-S1**). Commercial, heat-inactivated SARS-CoV-2 virus was used to establish calibration curves to convert RT-qPCR quantification cycle values (C_q) to viral load (**Figure 3-1A**; full details in **Figure 3-S2** and supplemental material methods). The linearity of these calibration curves was assessed with 43 participant nasal-swab (**Figure 3-1B**) and 63 participant saliva samples (**Figure 3-1C**) across a wide dynamic range of viral loads.

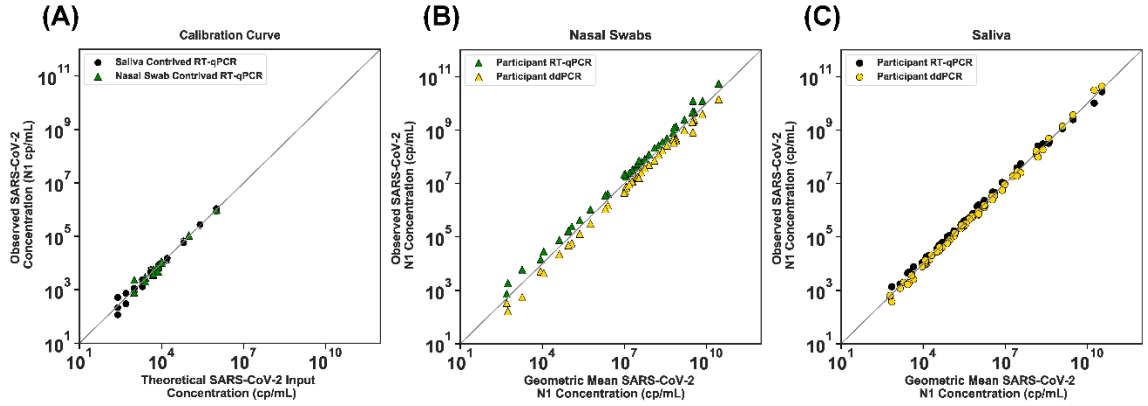

Figure 3-1. SARS-CoV-2 viral-load quantification measured with RT-ddPCR and RT-qPCR. **(A)** Calibration curves were prepared with contrived saliva and nasal-swab samples. The theoretical SARS-CoV-2 concentration was calculated from a dilution series of contrived samples that were prepared using commercial, inactivated SARS-CoV-2 and commercially available SARS-CoV-2-negative saliva (black circles) or nasal fluid (green triangles) and run with the CDC SARS-CoV-2 RT-qPCR assay. Detailed calibration curves are shown in **Figure 3-S2**. **(B)** Participant nasal-swab or **(C)** saliva samples positive for SARS-CoV-2 RNA at a range of viral loads were selected. SARS-CoV-2 *N1* concentrations (copies/mL) by detection method of RT-ddPCR (gold triangles in panel B, gold circles in panel C) and RT-qPCR (green triangles in panel B, black circles in panel C) are plotted against the geometric mean of RT-qPCR and RT-ddPCR viral-load concentrations (the square root of the product of the two viral-load measurements). A total of 42 nasal-swab and 63 saliva samples from study participants were quantified with both methods. The gray line represents $x = y$. See the supplemental material methods for details of contrived samples, calibration curves, and calculations.

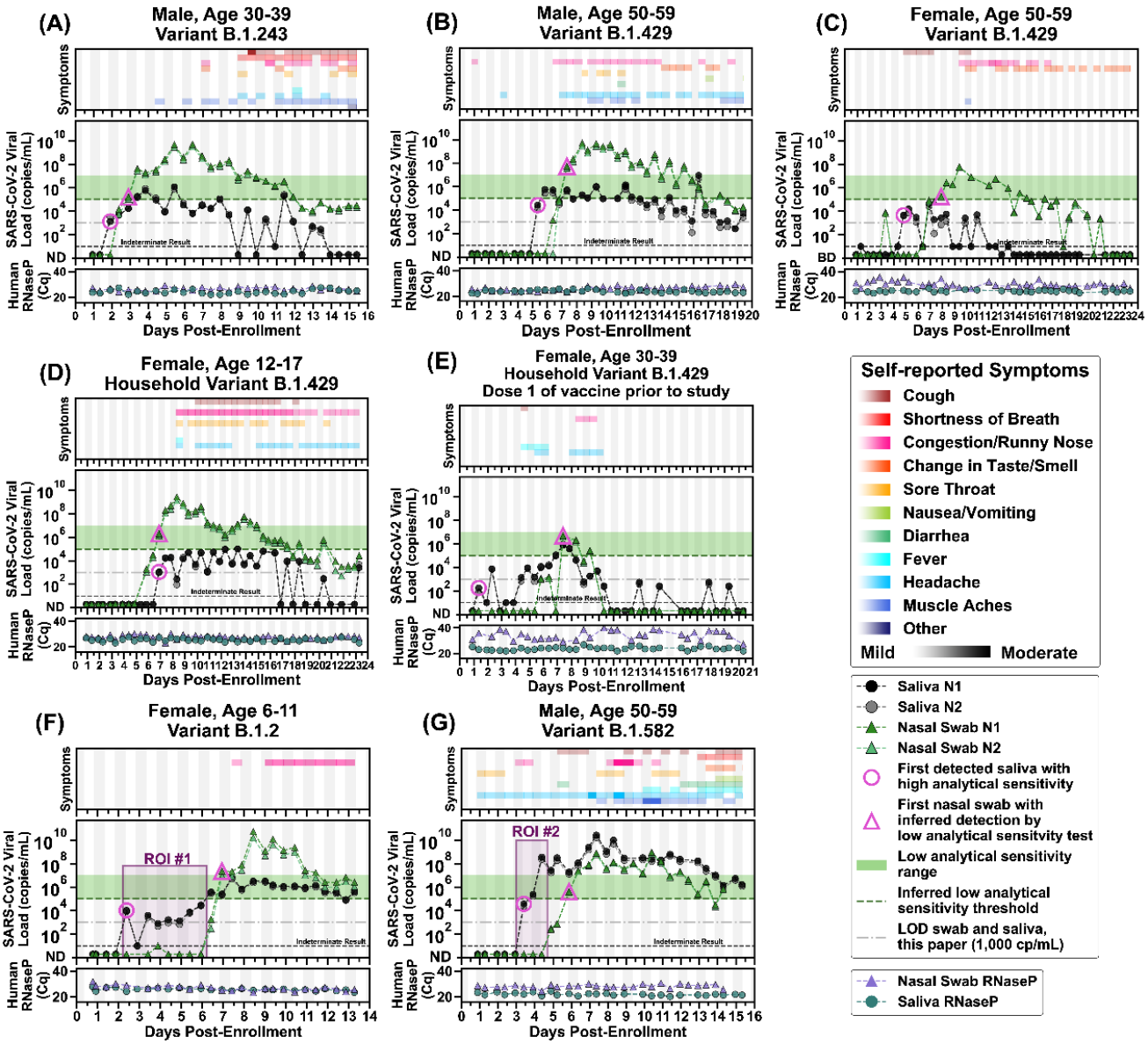

Figure 3-2. Symptoms and SARS-CoV-2 viral loads in paired saliva and nasal-swab samples of seven participants who became SARS-CoV-2 positive during study participation**. (A to G)** Self-reported twice-daily symptom data over the course of enrollment are shown as the top panel for each of the participants (see color-coded legend for symptom categories). Details of symptoms are included in the raw data files. Demographic data including any reported medical conditions are included in Table S1. Viral loads are reported for the *N1* and *N2* genes of SARS-CoV-2 for both saliva (black and gray circles) and nasal-swab samples (dark-green and light-green triangles); ND, not detected for C_qs of ≥40. Samples with an indeterminate result by the CDC RT-qPCR assay are shown along the horizontal black dashed line (see Materials and Methods for details). The limit of detection (LOD) of the assay used for high-analytical-sensitivity measurements is shown with a horizontal gray dashed line. The inferred low-analytical-sensitivity threshold (1.0×10^5 copies/mL) is indicated by the horizontal green dashed line; the low-analytical-sensitivity range (horizontal green bar) is shown. A diagnostic test does not provide reliable detection for samples with viral loads below its LOD. For each participant, the first detected saliva point is emphasized with a pink circle (high analytical sensitivity), and the first nasal-swab point with a viral-load concentration at or above 1.0×10^5 copies/mL (low-analytical-sensitivity threshold) is emphasized with a pink triangle. Vertical shading in gray indicates nighttime (8 p.m. to 8 a.m.). Internal controls of *RNase P* gene C_qs from the CDC primer set are provided for each sample to compare self-sampling consistency and sample integrity (failed samples, where *RNase P* C_q is ≥40, are not plotted). Participant sex, age range, and SARS-CoV-2 variant are given in each panel's title. Two regions of interest (ROI) are indicated by purple-shaded rectangles and discussed in the main text.

Next, to quantify the viral load at the earliest stage of infection, we analyzed the viral loads in the saliva and nasal swabs of participants who were negative in both sample types upon enrollment and became positive during their participation in the study (**Figure 3-2**). We extended each participant's enrollment in our study to acquire 14 days of paired saliva and nasal-swab samples starting from the first positive sample. The data in **Figure 3-2** report the viral-load concentrations as measured on the day of extraction. All samples were stored at 4°C before extraction; time of storage varied between 0 and 27 days. The stability of SARS-CoV-2 RNA and impact on our conclusions is discussed in the supplemental material methods, **Figure 3-S3**, and **Figure 3-S4**.

Here, we report complete viral-load curves in saliva and anterior-nares nasal swabs from seven individuals (**Figure 3-2**). Each participant tested negative (ND, not detected; **Figure 3-2**) in both saliva and nasal swabs upon study enrollment, demonstrating that we captured the earliest days of infection. *RNase P* C_q values remained consistent throughout the collection period for saliva and swabs for most participants **(Figure 3-2A, B, D, F, and G)**, indicating that observed changes in viral loads were likely not a sampling artifact but reflected the underlying biology of the infection. Because nasal swabs are commonly used with tests of low analytical sensitivity, and because such tests are proposed to be utilized for SARS-CoV-2 serial screening testing (34, 35), we wanted to compare whether low-analytical-sensitivity testing with nasal swabs could provide equivalent performance to high-analytical-sensitivity testing with saliva (26, 36, 37). We did not run any tests with low analytical sensitivity; our quantitative viral load measurements were used to infer the performance of a test with an LOD representing low analytical sensitivity. When viral loads in nasal swabs crossed a threshold of 1.0×10^5 copies/mL, entering the low-analytical-sensitivity range, shown as the inferred low-analytical-sensitivity threshold (**Figure 3-2**), we marked the sample with a pink triangle.

In six out of seven participants, high-analytical-sensitivity saliva testing would have been superior for early detection of SARS-CoV-2 infection compared with the predicted performance of nasal-swab tests with low analytical sensitivity. This prediction was made by evaluating when nasal-swab viral loads entered the LOD range of nasal-swab tests with low analytical sensitivity. In the seventh participant, the first positive high-analytical-sensitivity saliva test was detected at the same time point that the first nasal-swab test reached a viral load likely to be detected by a low-analytical-sensitivity nasal-swab test **(Figure 3-2D)**. In the first participant **(Figure 3-2A)**, detection occurred first in saliva at low viral load (1.3×10^3 copies/mL *N1* gene, pink circle), while the nasal swab remained negative, and days before the participant reported any symptoms. As measured, viral load in nasal-swab samples reached the level of LOD of low-analytical-sensitivity tests 1.0 days after the first saliva positive samples (pink triangle). This same pattern of earlier detection in high-sensitivity saliva was observed in five of the other six participants; high-sensitivity saliva was 2.5 days earlier (**Figure 3-2B**), 3.0 days earlier (**Figure 3-2C**), 6.0 days

earlier (**Figure 3-2E**), 4.5 days earlier (**Figure 3-2F**), and 2.5 days earlier (**Figure 3-2G**). The maximum delay in detection between saliva and nasal swab in an unvaccinated person was observed in the youngest participant in our study (see region of interest [ROI] no. 1 of **Figure 3-2F**)**.** This participant had detectable but low viral load (10^3 to 10^4) in saliva for four days, while nasal swabs remained negative by high-sensitivity measurements. Nasal viral loads spiked above 10^{10} copies/mL while the participant's only symptoms were mild congestion/runny nose.

Even with high-analytical-sensitivity nasal-swab testing, only one participant tested positive in nasal swab before saliva (**Figure 3-2D**). In this participant, SARS-CoV-2 RNA was detectable with a high-analytical-sensitivity nasal swab one day before it was detectable in a high-analytical-sensitivity saliva test. Nasal swabs reached the detection range of low-analytical-sensitivity tests (pink triangle) on the same day as the first saliva sample was detected by high-analytical sensitivity testing (pink circle). For all seven participants, high-analytical-sensitivity saliva testing would have detected SARS-CoV-2 RNA either the same day or up to six days before viral loads in nasal swab reached the detection limits of low-sensitivity nasal-swab tests.

Two participants (**Figure 3-2C and E**) had low viral load in both saliva and nasal swabs. Their viral-load measurements were near the LOD of our assay, and therefore, as expected, many samples from these participants had indeterminate results. One participant (**Figure 3-2E**) had received one dose of the Pfizer-BioNTech COVID-19 vaccine (38) 13 days prior to her first sample, though observations here are not powered to make conclusions about viral load due to vaccination.

Remarkably (see ROI no. 2 in **Figure 3-2G**), in one participant, saliva viral load spiked to 3.7×10^8 viral copies/mL (*N1* gene target) while SARS-CoV-2 RNA remained undetectable in nasal swab, even by the high-analytical-sensitivity assay used here.

Compiled data from all seven participants highlight the importance of the interplay among anatomical sampling site, infection stage, and diagnostic test sensitivity (**Figure 3-3**). Participant results were aligned to the first positive result from either sample type (day 0). If a saliva or nasal-swab sample had a SARS-CoV-2 viral load above 1.0×10^5 copies/mL, entering the low-analytical-sensitivity range (39), we inferred that a low-analytical-sensitivity test would have correctly determined that sample to be positive. The percentage of participants with either observed or inferred positive results at each time point (0.5-day intervals) from the first positive sample revealed that high-analytical-sensitivity saliva testing outperformed low-analytical-sensitivity nasal-swab testing for the first 5.5 days of detectable infection (**Figure 3-3A**) and high-analytical-sensitivity nasal-swab testing during the first four days (**Figure 3-3A**). Analytical sensitivity affects the overall test performance in each sample type. Based on early viral

loads in saliva, we inferred that low-sensitivity saliva testing was outperformed by high-sensitivity saliva and both high- and low-sensitivity nasal-swab testing (**Figure 3-3A**).

Next, we plotted paired viral loads in each respiratory site starting from the first positive test (**Figure 3-3B**). From day 0 to day 6, using high-sensitivity testing for both sample types, saliva was more frequently positive than nasal swabs (**Figure 3-3B**). Comparison of paired samples between day 6 and day 12 for both sample types showed highly concordant detection. In a later time interval, between days 12 and 16, nasal swabs were more frequently positive than saliva (**Figure 3-3B**). The median of peak viral loads was higher in nasal swabs than saliva (**Figure 3-3C**), consistent with the literature (21, 23, 40).

Many testing strategies and decisions are based on the presence or absence of symptoms (2, 41). We considered the positivity rate of high- or low-analytical-sensitivity testing methods with each sample type during the first ten days of test-positive infection (to capture the presymptomatic and symptomatic phases of infection for this cohort, not the postsymptomatic phase), separating them into categories of no symptoms or symptomatic if the participant reported at least one COVID-19-like symptom (**Figure 3-3D**). For samples collected while participants were asymptomatic, high-sensitivity saliva testing was more effective (74% positivity) than high- (52%) or low-sensitivity (39%) nasal-swab testing and low-sensitivity saliva testing (20%). In contrast, during symptomatic phases, which are often concurrent with peak nasal viral loads (**Figure 3-2**), high-sensitivity saliva (88%) and high-sensitivity nasal-swab testing (89%) have similar positivity rates (**Figure 3-3D**). Additionally, based on our measured viral loads, low-sensitivity nasal-swab testing is predicted to perform better in symptomatic cohorts (81%) than in asymptomatic persons (39%), consistent with how these tests were originally authorized.

These data reveal a more nuanced view than "saliva is better than swab." Using tests with high analytical sensitivity, SARS-CoV-2 RNA is more detectable in saliva than nasal swab during the early phase of the infection (**Figure 3-3B**). However, because viral loads in saliva generally remained lower than those in nasal swabs (**Figure 3-3C**), we infer that positivity by a low-analytical-sensitivity saliva test would be outperformed by both high- and low-analytical-sensitivity nasal-swab testing (**Figure 3-3A**), independent of symptom status (**Figure 3-3D**). It was the combination of test analytical sensitivity along with sample type that determined the overall test performance.

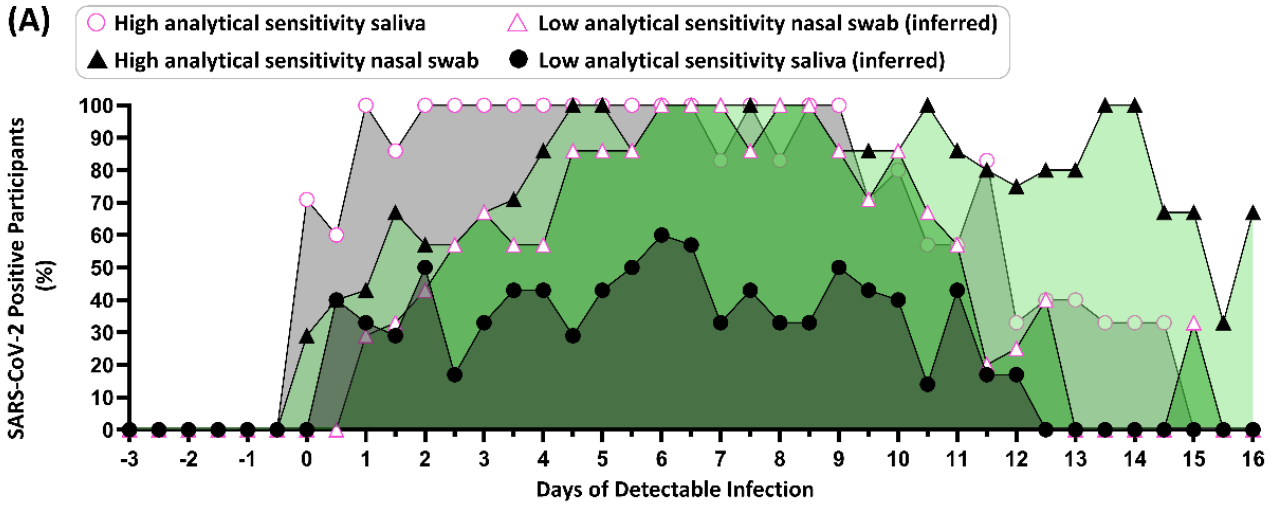

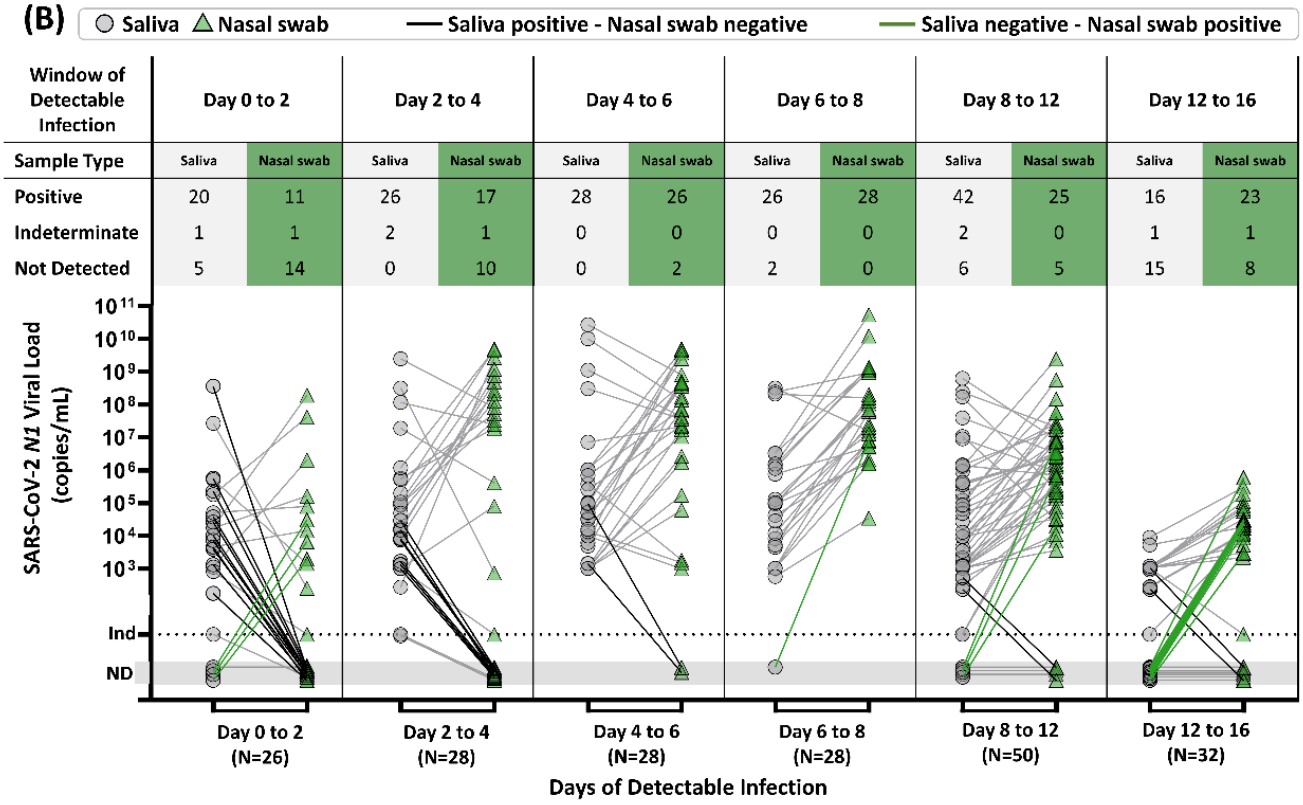

Window of Detectable Infection	Day 0 to 2		Day 2 to 4		Day 4 to 6		Day 6 to 8		Day 8 to 12		Day 12 to 16	
Sample Type	Saliva	Nasal swab	Saliva	Nasal swab	Saliva	Nasal swab	Saliva	Nasal swab	Saliva	Nasal swab	Saliva	Nasal swab
Positive	20	11	26	17	28	26	26	28	42	25	16	23
Indeterminate	1	1	2	1	0	0	0	0	2	0	1	1
Not Detected	5	14	0	10	0	2	2	0	6	5	15	8

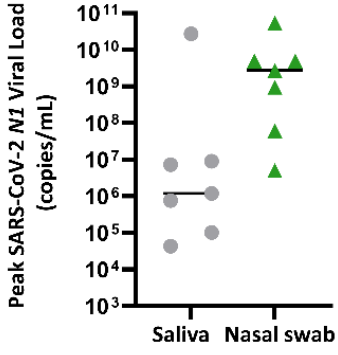

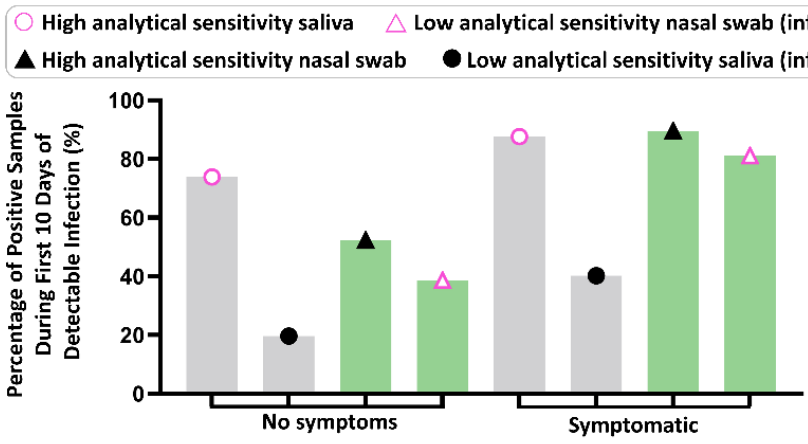

[Figure on previous page] **Figure 3-3.** Summary of diagnostic insights from study participants who became infected with SARS-CoV-2 while enrolled in the study. **(A)** Participant infection time courses were aligned to the first high-sensitivity (LOD of $\leq 1 \times 10^3$ copies/mL) positive result from either saliva or nasal-swab sample type (day 0), and the percentage of positive tests was calculated for each time point (0.5-day intervals) from the first positive sample. The predicted performance of nasal swabs or saliva with low analytical sensitivity was determined using the SARS-CoV-2 *N1* viral-load values for each participant shown in **Figure 3-2**, above a viral-load threshold of 1.0×10^5 copies/mL, entering the low-analytical-sensitivity range. We show the percentage of participants who were detected by our high-analytical-sensitivity saliva test (pink circle), high-analytical-sensitivity nasal-swab test (black triangle), or that could be inferred to be detectable by a low-analytical-sensitivity test nasal-swab (pink triangle) or saliva test (black circle) at a given time point. **(B)** Quantitative SARS-CoV-2 *N1* viral loads of paired samples collected during time windows of the infection (aligned to first positive result by high-sensitivity testing of either sample type) are shown for saliva (gray circles) and nasal swabs (green triangles). Paired samples for a given time point are connected with gray lines, with emphasis on paired samples where only saliva (black connecting line) or nasal swab (green connecting line) was positive. ND, not detected; Ind, indeterminate result. **(C)** Peak SARS-CoV-2 *N1* viral loads measured in saliva (gray circles) and nasal swab (green triangles) for each of the seven participants are shown. Horizontal black line indicates the median. **(D)** Percentage of positive samples (out of all samples of that type and symptom status) are shown for the first ten days of detectable infection for each participant. Saliva (gray bars with circles) and nasal swab (green bars with triangles) are shown. Positivity by a high-analytical-sensitivity test was observed by our assay, while positivity by a low-analytical-sensitivity test was inferred if the sample had a viral load above 1.0×10^5 copies/mL. The symptom status was classified as symptomatic if the participant reported one or more COVID-19-like symptoms at the time of sample collection. Details of the data analysis are included in the supplemental material methods.

Discussion

Limitations

Our study needs to be interpreted in the context of its limitations. First, our results capture viral-load dynamics from a limited number of individuals from one region of one country with limited SARS-CoV-2 diversity. Follow-up studies with a larger sample size, including individuals of diverse ages, genetic backgrounds, medical conditions, COVID-19 severity, and SARS-CoV-2 lineages would be ideal to provide a more nuanced and representative understanding of viral dynamics in saliva and nasal-swab samples. Second, the commercial inactivating buffer used here (Spectrum SDNA-1000) is not authorized (at the time of this writing) for the sample collection of nasal swabs. The solution in the Spectrum SDNA-1000 kits is a guanidinium-based inactivating and stabilizing buffer that preserves viral RNA but eliminated the opportunity to also perform viral culture. Third, we have paired data for saliva and anterior-nares nasal swabs but do not compare nasopharyngeal (NP) swabs, sputum, or other lower-respiratory specimens. We do not know whether other sampling sites, such as NP swabs or oropharyngeal swabs, would have provided earlier or later detection than saliva. Fourth, we are inferring the ability of tests with low analytical sensitivity to detect infections based on the quantified viral load in the participant samples and the LODs reported by the FDA for the diagnostic platforms. Fifth, some degradation may have occurred in some samples (see supplemental material for a complete analysis of RNA stability). Sixth, all samples were self-collected, which may result in lower-quality specimens.

Conclusions

By rapidly enrolling household members at high risk for contracting COVID-19 and having them self-sample twice daily in paired respiratory sites, we observed patterns in SARS-CoV-2 viral load in the earliest days of infection. All seven participants tested negative in saliva and nasal swabs upon enrollment, demonstrating that we captured the earliest detectable SARS-CoV-2 viral load (within 12 h) in both sample types. Our data set helps inform diagnostic testing strategies by showing differences in viral loads in paired nasal swabs and saliva samples at high temporal resolution during the early days and presymptomatic phases of infection.

We made five conclusions from our study.

First, choosing the correct respiratory sampling site is critical for earliest detection of SARS-CoV-2 infection. In our study, alignment of longitudinal data to the first day of positivity clearly shows the superiority of high-sensitivity saliva testing for detection in the first 5.5 days of infection (**Figure 3-3A**). Given our data, early infection viral-load dynamics in multiple sampling sites should be investigated and compared with saliva as new SARS-CoV-2 variants emerge.

Second, our data explain the conflicting results in the literature comparing test performance in paired respiratory sites, with some studies showing that nasal swabs outperform saliva (21, 23, 40) and others showing that saliva (or oral fluid) has detection equivalent to or better than that of nasal swabs (16, 25, 42–50). Through longitudinal rather than cross-sectional sampling, we show that the relative viral loads in each respiratory site are a factor of infection stage (shown in time intervals in **Figure 3-3B**), and the kinetics of viral load may be quite distinct in each sample type for an individual (**Figure 3-2**). Most studies examining paired sample types enrolled participants after a positive test or symptom onset; as our data show, detectable viral loads precede symptoms, in most cases (five of seven participants) by several days (**Figure 3-2**).

Third, peak viral load measured in nasal swabs (**Figure 3-3C**) is not representative of detectable viral load in the earliest days of infection (**Figure 3-3A**) or during the presymptomatic phase (**Figure 3-3D**). Early in an infection, it is inappropriate to assume that a person is "not infectious" or "has low viral load" based on a measurement from a single sample type, such as a nasal swab, given that saliva is known to carry infectious virus (51). In our study, we observed a participant with very high ($>10^7$ to 10^8 copies/mL) viral load in saliva samples while the paired nasal swab was either negative (**Figure 3-2G**, ROI no. 2) or had low ($\sim10^3$ copies/mL) viral load (**Figure 3-2G**, day after ROI no. 2). Quantitative SARS-CoV-2 culture from paired saliva and swab samples is still needed to understand infectiousness during the early stages of SARS-CoV-2 infection.

Fourth, using a diagnostic test with high analytical sensitivity (**Figure 3-3D**), rather than a test of a particular detection method (RT-qPCR, antigen, next-generation sequencing, etc.), is essential to early detection. With many strategies for asymptomatic screening/surveillance testing in use, it is critically important to consider whether the LODs of the tests would be able to detect early infection and to prompt actions that minimize transmission.

Fifth, our data show the utility of combining knowledge of the appropriate respiratory site and the appropriate test of analytical sensitivity for achieving earliest detection. Among our unvaccinated participants, when a high-sensitivity test was combined with saliva as a sample type, SARS-CoV-2 infection was detected up to 4.5 days before viral loads in nasal swabs reached the LODs of low-analytical-sensitivity tests (**Figure 3-2F**). Although high-sensitivity saliva testing was usually able to detect virus earlier than nasal swabs (**Figure 3-3A**), during the peak of the infection viral loads in nasal swabs were usually higher than in saliva (**Figure 3-3C**). Furthermore, SARS-CoV-2 was detected in saliva with high-sensitivity methods, and the viral loads were low (**Figure 3-2, 3-3A and 3-3D**); low-sensitivity saliva tests would likely not have been able to detect these infections early. These observations support the preferred use of nasal swabs in environments where only low-sensitivity testing is available, although the performance of such testing for early detection is poor (**Figure 3-3D**). These observations also show that the optimal respiratory sampling site is nuanced and depends on the phase of the infection being detected (early versus peak) and on the analytical sensitivity of the test being used with each sample type.

Our work suggests four steps to improve the effectiveness of diagnostic tests in early detection and preventing transmission of SARS-CoV-2 as new variants emerge and as infections spread to additional segments of the global population: (i) Additional longitudinal studies are needed that include high-frequency collection from multiple respiratory sites using quantitative assays with high analytical sensitivity; (ii) Policy makers need to use such quantitative data to revise and optimize screening and testing guidelines to ensure early detection of SARS-CoV-2 infections and reduction of transmission; (iii) Innovation is needed to produce rapid point-of-care tests with high analytical sensitivity for a range of sample types (including saliva) at a price point to enable global distribution; (iv) Quantitative studies of the kinetics of early stage viral loads in each respiratory site (collected in parallel with viral culture data) must be updated with the emergence of new SARS-CoV-2 variants.

We hope our data, important work by others in this area (15, 16, 51, 52), and future quantitative studies of early viral-load kinetics will lead to improved testing strategies to combat the current COVID-19 pandemic. The methodology for performing such studies efficiently and quickly will likely be extendable to defining strategies for early detection of causative pathogens in subsequent pandemics.

Acknowledgements

We thank Lauriane Quenee, Junie Hildebrandt, Grace Fisher-Adams, RuthAnne Bevier, Chantal D'Apuzzo, Ralph Adolphs, Victor Rivera, Steve Chapman, Gary Waters, Leonard Edwards, Gaylene Ursua, Cynthia Ramos, and Shannon Yamashita for their assistance and advice on study implementation and/or administration. We thank Jessica Leong, Jessica Slagle, Mika Walton, Angel Navarro, Daniel Brenner, and Ojas Pradhan for volunteering their time to help with this study, Si Hyung Jin for helping with a literature review, and Mary Arrastia for providing biosafety support. We thank Maira Phelps, Lienna Chan, Lucy Li, Dan Lu, and Amy Kistler at the Chan Zuckerberg Biohub for performing SARS-CoV-2 sequencing. We thank Angie Cheng, Susan Magdaleno, Christian Kis, Monica Herrera, and Zaina Lemeir for technical discussions regarding saliva extraction and ddPCR detection. We thank Jennifer Fulcher, Debika Bhattacharya, and Matthew Bidwell Goetz for their ideas on potential study populations and early study design. We thank Omai Garner and David Beenhouwer for providing materials for initial nasal-swab validation. We thank Martin Hill, Alma Sanchez, Scott Kim, Debbie Noble, Nina Paddock, Whitney Harrison, Emily Holman, Isaac Turner, Vivek Desai, Luke Wade, Tom Mayell, Stu Miller, and Jennifer Howes for their support with recruitment. We thank Allison Rhines, Karen Heichman, and Dan Wattendorf for valuable discussions. Finally, we thank all the case investigators and contact tracers at the Pasadena Public Health Department and the City of Long Beach Department of Health & Human Services for their efforts in study recruitment and their work in the pandemic response.

R.F.I. is a cofounder, consultant, and a director and has stock ownership of Talis Biomedical Corp. In addition, R.F.I. is an inventor on a series of patents licensed by the University of Chicago to Bio-Rad Laboratories, Inc., in the context of ddPCR.

This study is based on research funded in part by the Bill & Melinda Gates Foundation (INV-023124). The findings and conclusions contained within are those of the authors and do not necessarily reflect positions or policies of the Bill & Melinda Gates Foundation. This work was also funded by the Ronald and Maxine Linde Center for New Initiatives at the California Institute of Technology and the Jacobs Institute for Molecular Engineering for Medicine at the California Institute of Technology. A.V.W. is supported by a National Institutes of Health NIGMS predoctoral training grant (GM008042) and a UCLA DGSOM Geffen fellowship; M.M.C. is supported by a Caltech graduate student fellowship, and M.K.P. and J.T.B. are each partially supported by a National Institutes of Health Biotechnology Leadership Predoctoral Training Program (BLP) fellowship from Caltech's Donna and Benjamin M. Rosen Bioengineering Center (T32GM112592).

References

1. Johansson, M.A., Quandelacy, T.M., Kada, S., Prasad, P.V., Steele, M., Brooks, J.T., Slayton, R.B., Biggerstaff, M. and Butler, J.C., 2021. SARS-CoV-2 transmission from people without COVID-19 symptoms. *JAMA network open*, *4*(1), pp. e2035057–e2035057.

2. Recommendations for national SARS-CoV-2 testing strategies and diagnostic capacities (2021) WHO. Available at: https://apps.who.int/iris/bitstream/handle/10665/342002/WHO-2019-nCoV-lab-testing-2021.1-eng.pdf (Accessed: 28 May 2024).

3. SPI-M-O: Consensus statement on covid-19, 30 June 2021 (2021) GOV.UK. Available at: https://www.gov.uk/government/publications/spi-m-o-consensus-statement-on-covid-19-30-june-2021 (Accessed: 28 May 2024).

4. Li, B., Deng, A., Li, K., Hu, Y., Li, Z., Shi, Y., Xiong, Q., Liu, Z., Guo, Q., Zou, L. and Zhang, H., 2022. Viral infection and transmission in a large, well-traced outbreak caused by the SARS-CoV-2 Delta variant. *Nature communications*, *13*(1), p. 460.

5. Fisman, D.N. and Tuite, A.R., 2021. Progressive increase in virulence of novel SARS-CoV-2 variants in Ontario, Canada. *MedRxiv*, pp. 2021–07.

6. Yadav, P.D., Mohandas, S., Shete, A.M., Nyayanit, D.A., Gupta, N., Patil, D.Y., Sapkal, G.N., Potdar, V., Kadam, M., Kumar, A. and Kumar, S., 2021. SARS CoV-2 variant B. 1.617. 1 is highly pathogenic in hamsters than B. 1 variant. *BioRxiv*, pp. 2021–05.

7. Brown, C.M., 2021. Outbreak of SARS-CoV-2 infections, including COVID-19 vaccine breakthrough infections, associated with large public gatherings—Barnstable County, Massachusetts, July 2021. *MMWR. Morbidity and mortality weekly report*, *70*.

8. SARS-CoV-2 reference panel comparative data (2020) FDA. Available at: https://www.fda.gov/medical-devices/coronavirus-covid-19-and-medical-devices/sars-cov-2-reference-panel-comparative-data (Accessed: 28 May 2024).

9. Caruana, G., Croxatto, A., Kampouri, E., Kritikos, A., Opota, O., Foerster, M., Brouillet, R., Senn, L., Lienhard, R., Egli, A. and Pantaleo, G., 2021. ImplemeNting SARS-CoV-2 Rapid antigen testing in the Emergency wArd of a Swiss univErsity hospital: the INCREASE study. *Microorganisms*, *9*(4), p. 798.

10. Olearo, F., Nörz, D., Heinrich, F., Sutter, J.P., Roedl, K., Schultze, A., Zur Wiesch, J.S., Braun, P., Oestereich, L., Kreuels, B. and Wichmann, D., 2021. Handling and accuracy of four rapid antigen tests for the diagnosis of SARS-CoV-2 compared to RT-qPCR. *Journal of Clinical Virology*, *137*, p. 104782.

11. Corman, V.M., Haage, V.C., Bleicker, T., Schmidt, M.L., Mühlemann, B., Zuchowski, M., Jo, W.K., Tscheak, P., Möncke-Buchner, E., Müller, M.A. and Krumbholz, A., 2021. Comparison of seven commercial SARS-CoV-2 rapid point-of-care antigen tests: a single-centre laboratory evaluation study. *The Lancet Microbe*, *2*(7), pp. e311–e319.

12. Cubas-Atienzar, A.I., Kontogianni, K., Edwards, T., Wooding, D., Buist, K., Thompson, C.R., Williams, C.T., Patterson, E.I., Hughes, G.L., Baldwin, L. and Escadafal, C., 2021. Limit of detection in different matrices of 19 commercially available rapid antigen tests for the detection of SARS-CoV-2. *Scientific reports*, *11*(1), p. 18313.

13. Suess, T., Remschmidt, C., Schink, S.B., Schweiger, B., Heider, A., Milde, J., Nitsche, A., Schroeder, K., Doellinger, J., Braun, C. and Haas, W., 2012. Comparison of shedding characteristics of seasonal influenza virus (sub) types and influenza A (H1N1) pdm09; Germany, 2007–2011. *PloS one*, *7*(12), p. e51653.

14. Winnett, A., Cooper, M.M., Shelby, N., Romano, A.E., Reyes, J.A., Ji, J., Porter, M.K., Savela, E.S., Barlow, J.T., Akana, R. and Tognazzini, C., 2020. SARS-CoV-2 viral load in saliva rises gradually and to moderate levels in some humans. *medRxiv*.

15. Kissler, S., Fauver, J.R., Mack, C., Tai, C.G., Breban, M.I., Watkins, A.E., Samant, R.M., Anderson, D.J., Ho, D.D., Grubaugh, N.D. and Grad, Y., 2021. Densely sampled viral trajectories suggest longer duration of acute infection with B. 1.1. 7 variant relative to non-B. 1.1. 7 SARS-CoV-2.

16. Kissler, S.M., Fauver, J.R., Mack, C., Olesen, S.W., Tai, C., Shiue, K.Y., Kalinich, C., Jednak, S., Ott, I., Vogels, C. and Wohlgemuth, J., 2020. Viral dynamics of SARS-CoV-2 infection and the predictive value of repeat testing.

17. Kim, Y.G., Yun, S.G., Kim, M.Y., Park, K., Cho, C.H., Yoon, S.Y., Nam, M.H., Lee, C.K., Cho, Y.J. and Lim, C.S., 2017. Comparison between saliva and nasopharyngeal swab specimens for detection of respiratory viruses by multiplex reverse transcription-PCR. *Journal of clinical microbiology*, *55*(1), pp. 226–233.

18. Laboratory Testing for Middle East Respiratory Syndrome Coronavirus (2018) WHO. Available at: https://apps.who.int/iris/bitstream/handle/10665/259952/WHO-MERS-LAB-15.1-Rev1-2018-eng.pdf?sequence=1 (Accessed: 28 May 2024).

19. Wang, W.K., Chen, S.Y., Liu, I.J., Chen, Y.C., Chen, H.L., Yang, C.F., Chen, P.J., Yeh, S.H., Kao, C.L., Huang, L.M. and Hsueh, P.R., 2004. Detection of SARS-associated coronavirus in throat wash and saliva in early diagnosis. *Emerging infectious diseases*, *10*(7), p. 1213.

20. Ku, C.W., Shivani, D., Kwan, J.Q., Loy, S.L., Erwin, C., Ko, K.K., Ng, X.W., Oon, L., Thoon, K.C., Kalimuddin, S. and Chan, J.K., 2021. Validation of self-collected buccal swab and saliva as a diagnostic tool for COVID-19. *International Journal of Infectious Diseases*, *104*, pp. 255–261.

21. Barat, B., Das, S., De Giorgi, V., Henderson, D.K., Kopka, S., Lau, A.F., Miller, T., Moriarty, T., Palmore, T.N., Sawney, S. and Spalding, C., 2021. Pooled saliva specimens for SARS-CoV-2 testing. *Journal of clinical microbiology*, *59*(3), pp. 10–1128.

22. Manabe, Y.C., Reuland, C., Yu, T., Azamfirei, R., Hardick, J.P., Church, T., Brown, D.M., Sewell, T.T., Antar, A., Blair, P.W. and Heaney, C.D., 2021, February. Self-collected oral fluid saliva is insensitive compared with nasal-oropharyngeal swabs in the detection of severe acute respiratory syndrome coronavirus 2 in outpatients. In *Open Forum Infectious Diseases* (Vol. 8, No. 2, p. ofaa648). US: Oxford University Press.

23. Procop, G.W., Shrestha, N.K., Vogel, S., Van Sickle, K., Harrington, S., Rhoads, D.D., Rubin, B.P. and Terpeluk, P., 2020. A direct comparison of enhanced saliva to nasopharyngeal swab for the detection of SARS-CoV-2 in symptomatic patients. *Journal of clinical microbiology*, *58*(11), pp. 10–1128.

24. Al Suwaidi, H., Senok, A., Varghese, R., Deesi, Z., Khansaheb, H., Pokasirakath, S., Chacko, B., Abufara, I., Loney, T. and Alsheikh-Ali, A., 2021. Saliva for molecular detection of SARS-CoV-2 in school-age children. *Clinical Microbiology and Infection*, *27*(9), pp. 1330–1335.

25. Wyllie, A.L., Fournier, J., Casanovas-Massana, A., Campbell, M., Tokuyama, M., Vijayakumar, P., Warren, J.L., Geng, B., Muenker, M.C., Moore, A.J. and Vogels, C.B., 2020. Saliva or nasopharyngeal swab specimens for detection of SARS-CoV-2. *New England Journal of Medicine*, *383*(13), pp. 1283–1286.

26. Allicock, O.M., Petrone, M.E., Yolda-Carr, D., Breban, M., Walsh, H., Watkins, A.E., Rothman, J.E., Farhadian, S.F., Grubaugh, N.D. and Wyllie, A.L., 2022. Evaluation of saliva self-collection devices for SARS-CoV-2 diagnostics. *BMC Infectious Diseases*, *22*(1), p. 284.

27. Tan, S.H., Allicock, O., Armstrong-Hough, M. and Wyllie, A.L., 2021. Saliva as a gold-standard sample for SARS-CoV-2 detection. *The Lancet Respiratory Medicine*, *9*(6), pp. 562–564.

28. Symptoms of COVID-19 (2020) Centers for Disease Control and Prevention. Available at:

https://www.cdc.gov/coronavirus/2019-ncov/symptoms-testing/symptoms.html (Accessed: 28 May 2024).

29. CDC 2019 nCoV real-time RT-PCR diagnostic panel (2020) FDA. Available at: https://www.fda.gov/media/134922/download (Accessed: 28 May 2024).

30. Bio-Rad SARS-COV-2 ddpcr kit instructions for use (2020) Bio-Rad. Available at: https://www.bio-rad.com/webroot/web/pdf/lsr/literature/10000130776.pdf (Accessed: 28 May 2024).

31. Deng, X., Achari, A., Federman, S., Yu, G., Somasekar, S., Bártolo, I., Yagi, S., Mbala-Kingebeni, P., Kapetshi, J., Ahuka-Mundeke, S. and Muyembe-Tamfum, J.J., 2020. Metagenomic sequencing with spiked primer enrichment for viral diagnostics and genomic surveillance. *Nature microbiology*, *5*(3), pp. 443–454.

32. Gorzynski, J.E., De Jong, H.N., Amar, D., Hughes, C., Ioannidis, A., Bierman, R., Liu, D., Tanigawa, Y., Kistler, A.L., Kamm, J. and Kim, J., 2020. High-throughput SARS-CoV-2 and host genome sequencing from single nasopharyngeal swabs. *medRxiv*, pp. 2020–07.

33. Rambaut, A., Holmes, E.C., O'Toole, Á., Hill, V., McCrone, J.T., Ruis, C., du Plessis, L. and Pybus, O.G., 2020. A dynamic nomenclature proposal for SARS-CoV-2 lineages to assist genomic epidemiology. *Nature microbiology*, *5*(11), pp. 1403–1407.

34. Larremore, D.B., Wilder, B., Lester, E., Shehata, S., Burke, J.M., Hay, J.A., Tambe, M., Mina, M.J. and Parker, R., 2021. Test sensitivity is secondary to frequency and turnaround time for COVID-19 screening. *Science advances*, *7*(1), p.eabd5393.

35. Mina, M.J., Parker, R. and Larremore, D.B., 2020. Rethinking Covid-19 test sensitivity—a strategy for containment. *New England Journal of Medicine*, *383*(22), p. e120.

36. Bloom, J.S., Sathe, L., Munugala, C., Jones, E.M., Gasperini, M., Lubock, N.B., Yarza, F., Thompson, E.M., Kovary, K.M., Park, J. and Marquette, D., 2020. Swab-Seq: A high-throughput platform for massively scaled up SARS-CoV-2 testing. *MedRxiv*.

37. Smith, R.L., Gibson, L.L., Martinez, P.P., Ke, R., Mirza, A., Conte, M., Gallagher, N., Conte, A., Wang, L., Fredrickson, R. and Edmonson, D.C., 2021. Longitudinal assessment of diagnostic test performance over the course of acute SARS-CoV-2 infection. *The Journal of infectious diseases*, *224*(6), pp. 976–982.

38. Comirnaty and Pfizer-BioNTech COVID-19 Vaccine (2021) FDA. Available at: https://www.fda.gov/emergency-preparedness-and-response/coronavirus-disease-2019-covid-19/pfizer-

biontech-covid-19-vaccine (Accessed: 28 May 2024).

39. ID now COVID-19 - instructions for use (2021) FDA. Available at: https://www.fda.gov/media/136525/download (Accessed: 28 May 2024).

40. da Costa Fernandes, P.A., da Conceicao Ferreira, F.A., Morais, O.M., Ramos, C.M.T., Fernandes, É.M.R., da Rocha, S.A.A., Rocha, R.J.A., Monteiro, V.J.P., Vilar, P.S.G., Romao, A.M. and Alves, M.R.A., 2021. Performance of saliva as a specimen to detect SARS-CoV-2. *Journal of Clinical Virology*, *142*, p. 104913.

41. Overview of Testing for SARS-CoV-2 (COVID-19) (2021) Centers for Disease Control and Prevention. Available at: https://www.cdc.gov/coronavirus/2019-ncov/hcp/testing-overview.html (Accessed: 28 May 2024).

42. Hanson, K.E., Barker, A.P., Hillyard, D.R., Gilmore, N., Barrett, J.W., Orlandi, R.R. and Shakir, S.M., 2020. Self-collected anterior nasal and saliva specimens versus health care worker-collected nasopharyngeal swabs for the molecular detection of SARS-CoV-2. *Journal of clinical microbiology*, *58*(11), pp. 10–1128.

43. De Santi, C., Jacob, B., Kroich, P., Doyle, S., Ward, R., Li, B., Donnelly, O., Dykes, A., Neelakant, T., Neary, D. and McGuinness, R., 2021. Concordance between PCR-based extraction-free saliva and nasopharyngeal swabs for SARS-CoV-2 testing. *HRB Open Research*, *4*.

44. Sasaki, T., Inoue, O., Ogihara, S., Kubokawa, K., Oishi, S., Shirai, T., Iwabuchi, K. and Suzuki-Inoue, K., 2022. Detection of SARS-CoV-2 RNA using RT-qPCR in saliva samples and nasopharyngeal, lingual, and buccal mucosal swabs. *Japanese Journal of Infectious Diseases*, *75*(1), pp. 102–104.

45. Kojima, N., Turner, F., Slepnev, V., Bacelar, A., Deming, L., Kodeboyina, S. and Klausner, J.D., 2021. Self-collected oral fluid and nasal swabs demonstrate comparable sensitivity to clinician collected nasopharyngeal swabs for coronavirus disease 2019 detection. *Clinical Infectious Diseases*, *73*(9), pp. e3106–e3109.

46. Tu, Y.P., Jennings, R., Hart, B., Cangelosi, G.A., Wood, R.C., Wehber, K., Verma, P., Vojta, D. and Berke, E.M., 2020. Patient-collected tongue, nasal, and mid-turbinate swabs for SARS-CoV-2 yield equivalent sensitivity to health care worker collected nasopharyngeal swabs. *MedRxiv*, pp. 2020–04.

47. Iwasaki, S., Fujisawa, S., Nakakubo, S., Kamada, K., Yamashita, Y., Fukumoto, T., Sato, K., Oguri, S., Taki, K., Senjo, H. and Sugita, J., 2020. Comparison of SARS-CoV-2 detection in nasopharyngeal swab and saliva. *Journal of Infection*, *81*(2), pp. e145–e147.

48. To, K.K.W., Tsang, O.T.Y., Yip, C.C.Y., Chan, K.H., Wu, T.C., Chan, J.M.C., Leung, W.S., Chik, T.S.H., Choi, C.Y.C., Kandamby, D.H. and Lung, D.C., 2020. Consistent detection of 2019 novel coronavirus in saliva. *Clinical Infectious Diseases*, *71*(15), pp. 841–843.

49. Kernéis, S., Elie, C., Fourgeaud, J., Choupeaux, L., Delarue, S.M., Alby, M.L., Quentin, P., Pavie, J., Brazille, P., Néré, M.L. and Minier, M., 2021. Accuracy of antigen and nucleic acid amplification testing on saliva and naopharyngeal samples for detection of SARS-CoV-2 in ambulatory care. *MedRxiv*, pp. 2021–04.

50. Callahan, C., Ditelberg, S., Dutta, S., Littlehale, N., Cheng, A., Kupczewski, K., McVay, D., Riedel, S., Kirby, J.E. and Arnaout, R., 2021. Saliva is comparable to nasopharyngeal swabs for molecular detection of SARS-CoV-2. *Microbiology spectrum*, *9*(1), pp. 10–1128.

51. Huang, N., Pérez, P., Kato, T., Mikami, Y., Okuda, K., Gilmore, R.C., Conde, C.D., Gasmi, B., Stein, S., Beach, M. and Pelayo, E., 2021. SARS-CoV-2 infection of the oral cavity and saliva. *Nature medicine*, *27*(5), pp. 892–903.

52. Ke, R., Martinez, P.P., Smith, R.L., Gibson, L.L., Mirza, A., Conte, M., Gallagher, N., Luo, C.H., Jarrett, J., Conte, A. and Liu, T., 2021. Daily sampling of early SARS-CoV-2 infection reveals substantial heterogeneity in infectiousness. *medRxiv*, pp. 2021–07.

Supplementary Information

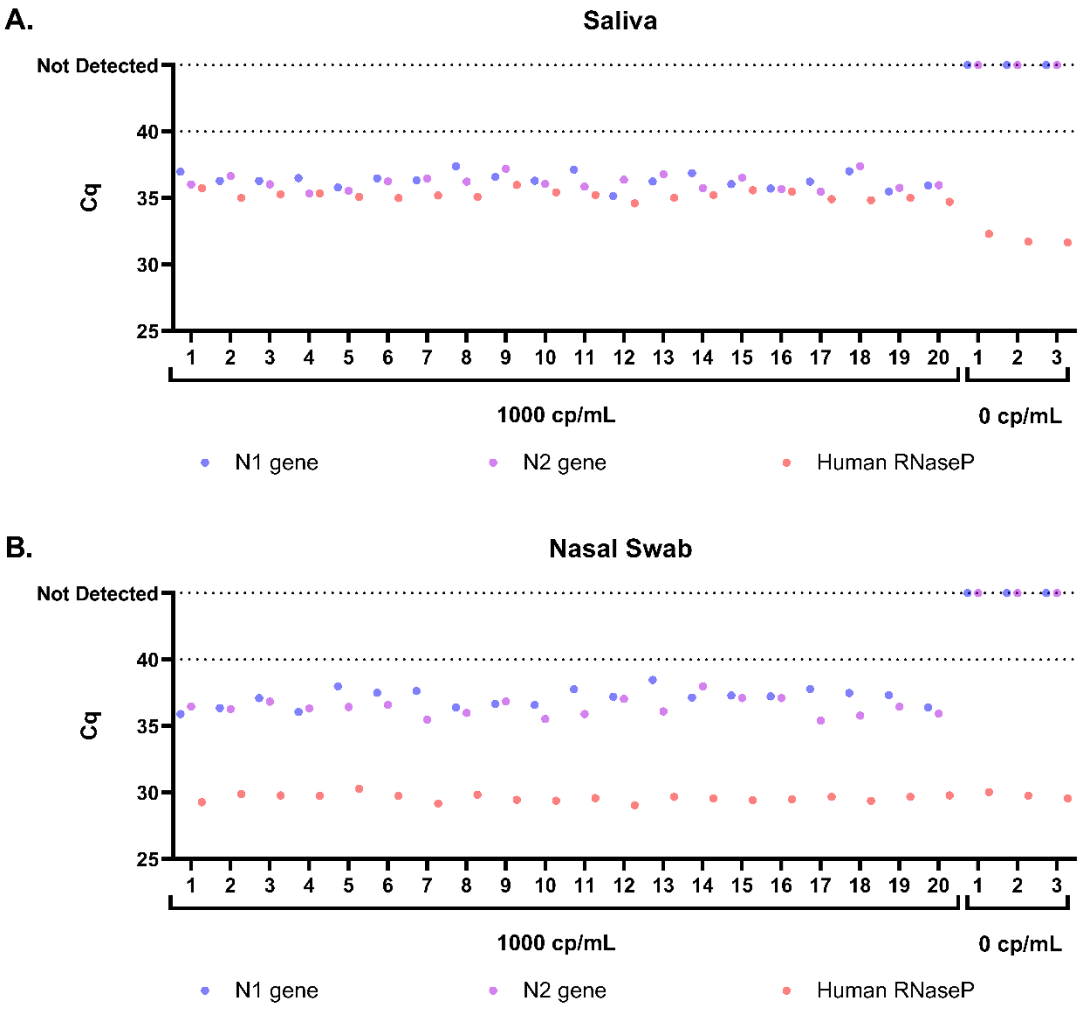

Supplemental Figure 3-1. Limit of detection of saliva and nasal-swab RT-qPCR assays used in this study. RT-qPCR quantification cycle (Cq) for SARS-CoV-2 *N1* gene (blue circle), *N2* gene (purple circle), and human *RNase P* gene (orange circle) in 20 replicates of pooled matrix spiked with 1,000 copies/mL (cp/mL) heat-inactivated SARS-CoV-2 RNA and three replicates of pooled matrix spiked with a buffer blank for saliva **(A)** and nasal-swab **(B)** samples. Duplicate RT-qPCR reactions were performed for each extraction replicate and the averages are shown, with the following three exceptions: replicate 9 (saliva), in which the *N1* gene only amplified in one of the duplicate runs (*N2* in this run was positive, so per CDC EUA guidelines1 this run was interpreted as inconclusive), replicate 10 (nasal swab) in which the *N2* gene only amplified in one of the duplicate runs (*N1* in this run was positive, so this run was interpreted as inconclusive), and replicate 18 (nasal swab) in which the *N1* gene only amplified in one of the duplicate runs (*N2* in this run was positive, so this run was also interpreted as inconclusive). None of the samples spiked at 1,000 copies/mL gave a negative detection result.

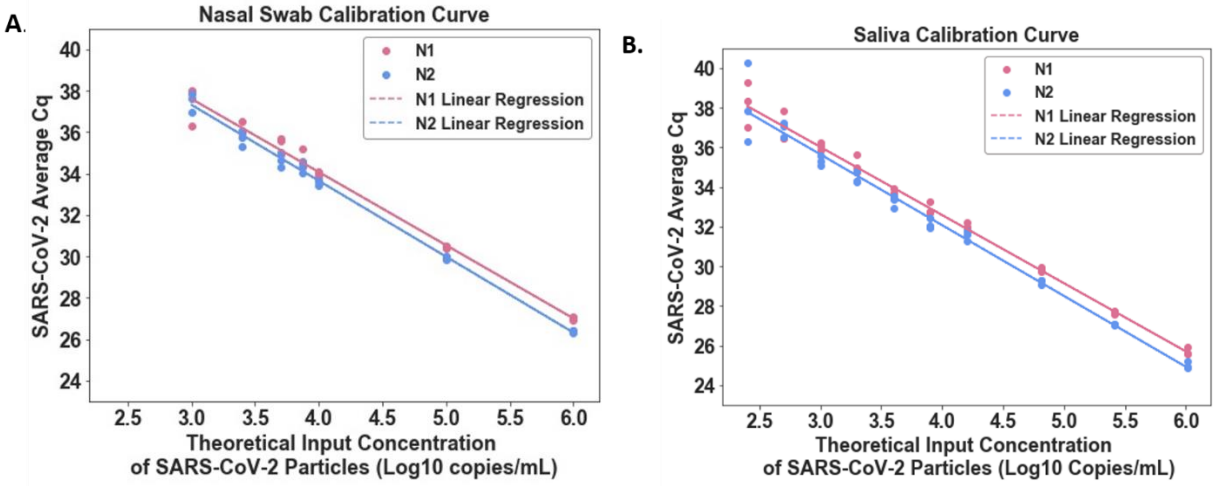

Supplemental Figure 3-2. Calibration curve of SARS-CoV-2 inactivated particles to establish viral-load conversion equations. Linear regression of RT-qPCR quantification cycle (Cq) for *N1* (red circle) and *N2* (blue circles) genes at known concentrations of inactivated SARS-CoV-2 particles for saliva **(A)** or nasal swab **(B)** using this study's collection and laboratory workflows. Triplicate replicates per concentration were performed. Linear regression for N1 represented by red line and *N2* represented by blue line. Linear regression R^2 values are 0.986 for *N1* in nasal swabs, 0.994 for *N2* in nasal swabs, 0.989 for *N1* in saliva, and 0.979 for *N2* in saliva.

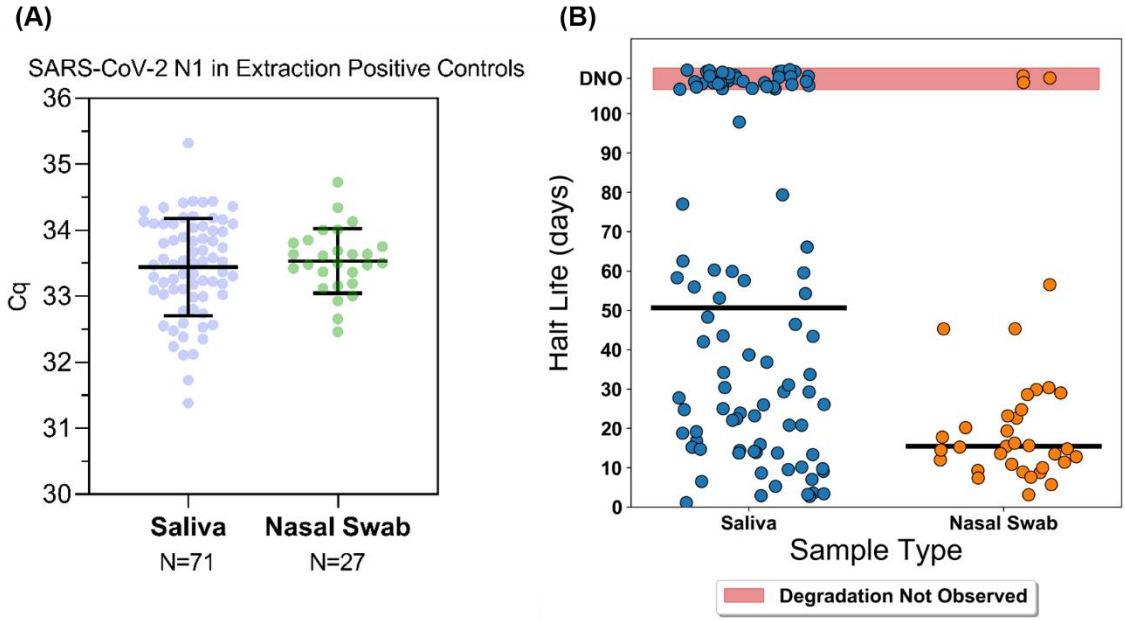

Supplemental Figure 3-3. SARS-CoV-2 RNA stability over time in Spectrum SDNA-1000 buffer at 4 °C. **(A)** Positive extraction control samples from 71 saliva extraction runs and 27 nasal-swab extraction runs are included to show the measurement noise in the quantification workflow. The standard deviation for the positive control measurements was 0.74 Cq for saliva and 0.49 for nasal swab. **(B)** The observed half-life (days) of participant saliva (blue circles) and nasal-swab (orange circles) samples in Spectrum SDNA-1000 buffer stored at 4 °C. Individual samples were extracted at multiple time points. Half-life in this context refers to the time required to observe a 1 Cq increase (representing a two-fold decrease) in RNA detected by RT-qPCR. The median point is identified for each sample type (black bars), at 15.0 days for nasal swabs (red circle) and 51.0 days for saliva (green circle). Of the 110 total participant saliva samples plotted in panel B, 36 samples had no evidence of degradation (DNO) under the time frame measured. Only three of the 36 total participant nasal-swab samples plotted in panel B had no evidence of degradation under the timeframe measured. DNO = degradation not observed, meaning that the difference in extraction Cq values of the same sample at multiple time points was within 1 standard deviation observed in replicate extraction positive controls for the respective sample type, as shown in panel A.

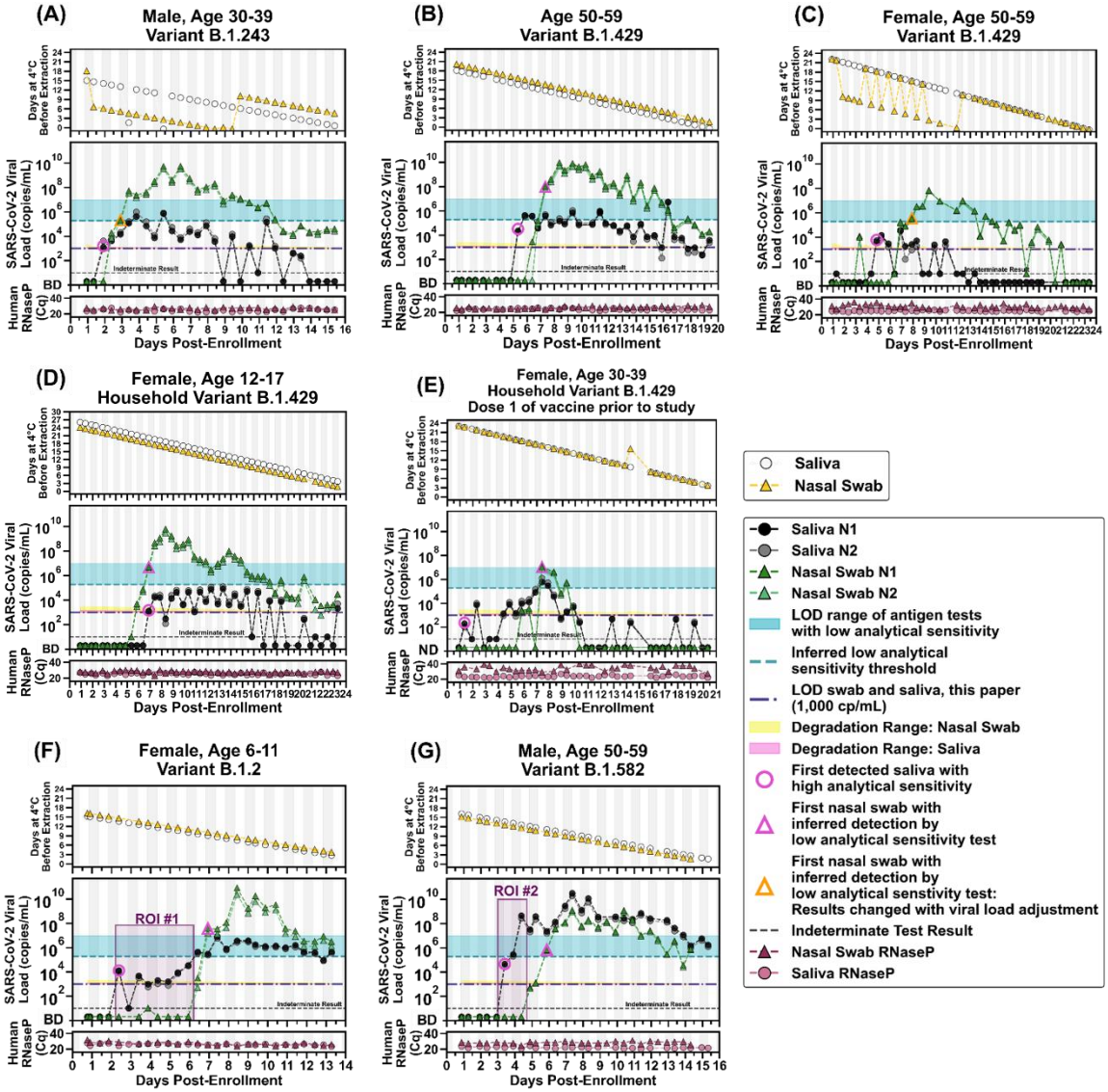

Supplemental Figure 3-4. Predicted impact of SARS-CoV-2 RNA stability on quantitative viral loads shown in **Figure 3-2**. **(A–G)** The time [days] of sample storage at 4 °C between sample collection and RNA extraction is shown in the topmost panels. Open circles represent saliva samples and yellow triangles represent the nasal swabs. Viral-load calculations are corrected for the median half-life (1 Cq decrease in RNA detected by RT-qPCR) of each sample type and the duration of storage at 4 °C before quantification (15 days for two-fold decrease in detected RNA in nasal swabs and 51 days for two-fold decreased in detected RNA in saliva). The degradation ranges, represented by a shaded yellow (nasal swab) or pink (saliva) region to represent how a measured value of 1,000 copies/mL may have degraded from concentrations in this range. As in Figure 3-2, ND = not detected for Cqs ≥40 (see Methods for details). The LOD of the saliva and nasal-swab assays used here (1,000 cp/mL) is indicated with the purple dashed line; low-analytical-sensitivity threshold Supplemental Information page 6 is indicated by the horizontal green dashed line; the low-analytical-sensitivity range (horizontal blue bar) is shown for reference. A diagnostic test does not provide reliable detection for samples with viral loads below its LOD. For each participant, the first detected saliva point is emphasized with a pink circle and their first nasal-swab point above the LOD of the ID NOW is emphasized with a pink triangle. Vertical shading in gray indicates nighttime (8 p.m.–8 a.m.). Internal control of *RNase P* gene Cqs from the CDC primer set are provided for each sample to compare self-sampling consistency and sample integrity (failed samples, where *RNase P* Cq ≥40, are not plotted). Samples with an indeterminate result by the CDC RT-qPCR assay are shown along the horizontal black dashed line. Participant gender, age range, and SARS-CoV-2 variant is given in each panel's title. Two regions of interest (ROI) are indicated by purple-shaded rectangles and discussed in the main text. For the two points that change interpretation with the viral-load adjustment, orange triangles show which new data points become the first nasal-swab point in range of low-analytical-sensitivity tests.

Supplemental Table 3-1. Study participant demographic data. Figure 3-2 shows viral loads and symptoms data for the seven participants for whom we observed transmission during their enrollment in the study.

	Age Range (Years)	**Sex**	**Race; Ethnicity**	**Reported Medical Conditions Associated with Increased Risk of Severe COVID-19**[88]
Figure. 2A, Figure. S4A	30–39	Male	Other; Mexican/Mexican-American/Chicano (Salvadoran)	Diabetes
Figure. 2B, Figure. S4B	50–59	Male	Do not wish to respond; Mexican/Mexican-American/Chicano	None
Figure. 2C, Figure. S4C	50–59	Female	White; Mexican/Mexican-American/Chicano (Spanish-American from Spain)	None
Figure. 2D, Figure. S4D	12–17	Female	White; Mexican/Mexican-American/Chicano	None
Figure. 2E, Figure. S4E	30–39	Female	White; Mexican/Mexican-American/Chicano	None
Figure. 2F, Figure. S4F	6–11	Female	White; Non-Hispanic	None
Figure. 2G, Figure. S4G	50–59	Male	American Indian or Alaskan Native, White; Other Hispanic, Latinx or Spanish origin	Obesity

Supplementary Methods

Participant population

This study is an extension of our previous study examining viral load in saliva (3). Both studies were reviewed and approved by the Institutional Review Board of the California Institute of Technology, protocol #20-1026. All participants provided either written informed consent (or for minors ages 6–17, assent accompanied by parental permission), prior to enrollment. Household index cases were eligible for participation if they had recently (within seven days) been diagnosed with COVID-19 by a CLIA laboratory test. Individuals were ineligible if they were hospitalized or if they were not fluent in either Spanish or English. All participant data were collected and managed using REDCap (Research Electronic Data Capture) on a server hosted at the California Institute of Technology. Demographic and health information for the seven participants can be found in Table 3.S1.

Questionnaires and symptom monitoring

Acquisition of participant data was performed as described previously (3). Briefly, upon enrollment each participant completed an online questionnaire regarding demographics, health factors, prior COVID-19 tests, COVID-19-like symptoms since February 2020, household infection-control practices, and perceptions of COVID-19 risk. Participants also filled out a post-study questionnaire in which they documented medications taken and their interactions with each household member during their enrollment.

Information on symptoms was collected twice daily in parallel with sample collection. Participants recorded any COVID-19-like symptoms (as defined by the CDC) they were experiencing at the time of sample donation on a symptom-tracking card or on a custom app run on REDCap (4). Whenever possible, participants indicated the self-reported severity of each symptom. Participants were also given the opportunity to write-in additional symptoms or symptom details not otherwise listed.

Collection of respiratory specimens

Participants self-collected both their nasal-swab and saliva samples using the Spectrum SDNA-1000 Saliva Collection Kit (Spectrum Solutions LLC, Draper, UT, USA), which contains 1.5 mL of liquid buffer, at home twice per day (after waking up and before going to bed), per manufacturer guidelines. Of note, at the time of this writing, Spectrum devices are not approved for the collection of nasal-swab samples. Participants self-collected nasal-swab (1 swab) and saliva (~1.5 mL) samples in the Spectrum SDNA-1000 Saliva Collection Kit (Spectrum Solutions LLC, Draper, UT, USA), which contains 1.5 mL of liquid buffer, at home twice per day (after waking up and before going to bed), per manufacturer's guidelines. Of note, at the time of this writing, Spectrum devices are not approved for the collection of nasal-swab samples.

Participants were instructed not to eat, drink, smoke, brush their teeth, use mouthwash, or chew gum for at least 30 min prior to donating. Prior to nasal-swab donation, participants were asked to gently blow their noses to remove debris. Participants were provided with one of the following types of sterile flocked swabs: Nest Oropharyngeal Specimen Collection Swabs (Cat. NST-202003, Stellar Scientific, Baltimore, MD, USA) Puritan HydraFlock Swab (Cat. 25-3000-H E30, Puritan, Guilford, ME, USA), or Copan USA FLOQSwab (Cat. 520CS01, VWR International, Radnor, PA, USA). Participants were instructed to swab each nostril for four complete rotations using the same swab while applying gentle pressure, then to break the tip of the swab into the Spectrum tube and securely screw on the cap. A parent or legal guardian assisted all minors with swab collection, and they were instructed to wear a face covering during supervision. Tubes were labeled and packaged by the participants and transported at room temperature by a touch-free medical courier to the California Institute of Technology daily for analysis.

Upon receipt of the samples in the California Institute of Technology laboratory, each sample was inspected for quality. A sample failed quality control if the preservation buffer was not released from the Spectrum SDNA1000 cap, or if sample tubes were leaking or otherwise unsafe to handle. Samples that failed quality control were not processed. Inactivated samples were stored at 4 °C and were equilibrated to room temperature before being processed with extraction protocols.

RNA extraction protocols

In initial testing, when combined with standard KingFisher MagMax sample-preparation protocols, these assays performed well to quantify heat-inactivated SARS-CoV-2 viral particles spiked into commercially available SARS-CoV-2 negative saliva and nasal fluid from pooled donors. However, the assay did not provide reliable quantification from freshly collected individual saliva samples with varying viscosity from positive participants in this study. Carryover of materials from some of the mucus-rich samples was inhibitory, as determined by RTddPCR analysis of dilutions of eluted RNA (data not shown). Following recommendations from ThermoFisher, the protocol was adjusted and described below. Briefly, we added a centrifugation step after proteinase K treatment to pellet the mucus-rich cell debris. We also include a third wash to improve RNA quality for viral genome sequencing. These steps reduced bead carryover into the eluate, as well as ddPCR inhibition.

Participant saliva and anterior-nares swab samples were extracted using the KingFisher Flex 96 instrument (ThermoFisher Scientific) with the MagMax Viral Pathogen I Nucleic Acid Isolation kit (Cat. A42352, Applied Biosystems, Waltham, MA, USA) guided by ThermoFisher technical notes for SARS-CoV-2 modification and saliva. Each extraction batch, depending on the sample type being extracted, contained a contrived SARS-CoV-2

negative control sample containing either 225 µL of Spectrum buffer mixed with 225 µL of commercial pooled human saliva (Lee Bio 991-05-P-PreC) or 240 µL of Spectrum buffer with 10 µL of pooled commercial nasal fluid (Lee Bio 991-13-P-PreC); a contrived SARS-CoV-2 positive control sample was also included in each extraction batch, with the formulations above, but with the Spectrum buffer spiked with 7,500 genomic copy equivalents/mL of heat-inactivated SARS-CoV-2 particles (BEI NR-52286).

Saliva and anterior-nares swab samples were prepared for purification by transferring 550 µl (for saliva) or 250 µl (for nasal swab) of each sample from its corresponding Spectrum buffer tube into a 1.5 mL lo-bind Eppendorf tube containing 10 µl (for saliva) or 5 µl (for nasal swab) of proteinase K. To maximize recovery of RNA off swabs, prior to transfer, pipet mixing was performed 5–7 times near the swab in the Spectrum tube before aliquoting into an Eppendorf tube. Saliva samples were vortexed for 30 sec in the Eppendorf tube. Samples were incubated at 65 °C for 10 min, then centrifuged at 13,000 x g for 1 min. Aliquots of 400 µl (for saliva) or 200 µl (for nasal swab) were transferred into a KingFisher 96 deep well plate (Cat. 95040450, ThermoFisher Scientific) and processed following KingFisher protocols MVP_400ul_3washes.bdz (for saliva) or MVP_200ul_2washes.bdz (for nasal swab). Ethanol washes were performed with 80% ethanol. Both sample types were eluted into 100 µl of MagMax viral pathogen elution buffer.

RT-qPCR

Quantification of SARS-CoV-2 was performed as previously described.(3) Briefly, the CDC5 SARS-CoV-2 *N1* and *N2* gene primers and probes with an internal control targeting *RNase P* gene primer and probe were run in a multiplex RT-qPCR reaction using TaqPath 1-Step Rt-qPCR Mastermix (Cat. A15299, ThermoFisher Scientific). Reactions were run in duplicate on a CFX96 Real-Time Instrument (Bio-Rad Laboratories, Hercules, CA, USA).

RT-ddPCR

Reverse-transcription droplet digital PCR (RT-ddPCR) was performed using the Bio-Rad SARS-CoV-2 Droplet Digital PCR kit (Cat. 12013743, Bio-Rad). Swab samples were processed following the manufacturer's RUO protocol with 5.5 µl template per 22 µl reaction. A total of 42 participant nasal-swab samples were characterized by RT-ddPCR. Modifications were made for saliva samples by reducing the template addition to 2.75 µl per 22 µl reaction. A total of 63 participant saliva samples were characterized by RT-ddPCR. Prior to adding template, samples were diluted into digital range using nuclease-free water. Droplets were created using the QX200 Droplet Generator (Cat #1864002, Bio-Rad), thermocycling performed on Bio-Rad C1000 and detected using the QX200 Droplet Digital PCR system (Cat. 1864001, Bio-Rad). Samples were analyzed with QuantaSoft analysis Pro 1.0.595 software following Bio-Rad's RUO SARS-CoV-2 guidelines (6).

Viral-load calibration curves

A calibration curve was prepared for both the saliva and nasal-swab protocols. Contrived samples were prepared with known concentrations (based on the certificate of analysis, COA) of heat-inactivated SARS-CoV-2 virus ($3.75x10^8$ GE/mL, Batch 70034991, Cat. NR-52286, BEI Resources, Manassas, VA, USA) in the inactivating buffer from the Spectrum SDNA-1000 Saliva Collection Kit (Spectrum Solutions LLC, Draper, UT, USA) and commercial, healthy human fluids were used as healthy human samples. Commercial pooled human saliva collected prior to November 2019 (Cat, 991-05-P, Lee Biosolutions, Maryland Heights, MO, USA) for the contrived saliva samples or commercial human nasal fluid collected prior to November 2019 (Cat No 991-13-PPreC, Lee Biosolutions) for the contrived nasal-swab samples. Details of reagent volumes are described in the following two paragraphs for how the samples were prepared for both nasal swab and saliva calibration curves.

To establish the nasal-swab calibration curve (**Figure 3-S2A**), contrived samples were prepared by creating a dilution series of commercial heat-inactivated SARS-CoV-2 virus from BEI ($3.75x10^8$ GE/mL) in a 10-fold dilution series from $1x10^6$ to $1x10^4$ copies/mL with finer resolution down to our LOD at $1x10^3$ copies/mL. Dilutions were prepared in Spectrum device inactivation buffer, to a volume of 768 µL, at concentrations of 0 copies/mL, 1,000 copies/mL, 2,500 copies/mL, 5,000 copies/mL, 7,500 copies/mL, 10,000 copies/mL, 100,000 copies/mL, and 1,000,000 copies/mL. To bring the volume to 800 µL total, 32 µL of healthy human nasal fluid collected prior to November 2019 (Cat No 991-13-P-PreC, Lee Biosolutions) was added. Triplicate extractions, 250 µL each, were performed according to the nasal-swab RNA extraction protocol (described above). Each extraction was run in triplicate RT-qPCR reactions.

To establish the saliva calibration curve (**Figure 3-S2B**), contrived samples were prepared by creating a dilution series of commercial BEI heat-inactivated SARS-CoV-2 virus in Spectrum device inactivation buffer at concentrations of 0 copies/mL, 1,000 copies/mL, 2,000 copies/mL, 4,000 copies/mL, 8,000 copies/mL, 16,000 copies/mL, 64,000 copies/mL, 256,000 copies/mL, and 1,020,000 copies/mL. Contrived samples were made by mixing 620 µL of each concentration of the dilution series with 620 µL of healthy pooled human saliva (Cat, 991-05-P, Lee Biosolutions). Triplicate extractions, 550 µL each, were performed according to the saliva RNA extraction protocol. Each extraction was run in triplicate RT-qPCR reactions.

Equations, calculated from the linear regression of the calibration curves, are shown below as **Equations 3.1 – 3.4**. These calibration curves are used to convert the Cq values obtained by RT-qPCR to viral load in each participant sample. For saliva, viral load is a calculation of viral copies/mL in the saliva corrected for dilution with the Spectrum

buffer. We assumed that participants donate saliva to the fill line, matching the 1:1 dilution in Spectrum buffer recreated when preparing contrived samples for the saliva calibration curve. For nasal swabs, viral load is a calculation of the concentration of viral copies/mL released from the swab into the 1.5 mL of inactivating buffer (which is a similar volume as the 1–3 mL of viral transport media typically used for sample collection). Concentrations higher than 1,000,000 copies/mL could not be characterized due to a limitation of the available stock concentration of commercial inactivated SARS-CoV-2. To validate linear conversion was acceptable at concentrations higher than 1,000,000 copies/mL, we compared RT-ddPCR and RT-qPCR quantification on some participant samples (**Figure 3-1**) as described in the next section "Viral-load Quantification between qPCR and ddPCR assays."

$$Saliva\ N1\ gene\ viral\ load\ \left[\frac{copies}{mL}\right] = 2^{((Cq-46.349)/-1.0357)}$$

(**Equation 3.1**)

$$Saliva\ N2\ gene\ viral\ load\ \left[\frac{copies}{mL}\right] = 2^{((Cq-46.374)/-1.0759)}$$

(**Equation 3.2**)

$$Nasal\ Swab\ N1\ gene\ viral\ load\ \left[\frac{copies}{mL}\right] = 2^{((Cq-48.221)/-1.0643)}$$

(**Equation 3.3**)

$$Nasal\ Swan\ N2\ gene\ viral\ load\ \left[\frac{copies}{mL}\right] = 2^{((Cq-48.330)/-1.1044)}$$

(**Equations 3.4**)

Viral-load quantification between qPCR and ddPCR assays

Contrived saliva and nasal-swab calibration curve RT-qPCR data was converted into viral load (*N1* copies/mL) using **Equations 3.1 and 3.3** listed in the above section. Calculated viral load was plotted against the theoretical input of heat-inactivated SARS-CoV-2.

Extending quantification capabilities above $1x10^6$ *N1* copies/mL was achieved using SARS-CoV-2-positive participant samples. Due to the limitation of the commercial SARS-CoV-2 standard concentration, we were not able to prepare contrived samples with SARS-CoV-2 input concentrations greater than $1x10^6$ copies/mL. To capture a

range of participant samples over seven orders of magnitude ($1x10^3$ to $1x10^{10}$ copies/mL SARS-CoV-2 *N1* gene), 63 saliva and 42 nasal-swab samples from SARS-CoV-2-positive participants were selected based on RTqPCR data to quantify using RT-ddPCR. Using the geometric mean of the viral load computed from RT-qPCR and the calibration curves and the concentration measured by RT-ddPCR, we were able to evaluate the linearity of the calibration curve across the seven orders of magnitude viral load seen in the participant samples (**Figure 3-1B–C**). Samples were selected to capture the range of viral concentrations within our calibration curve and to the highest viral loads recorded for each sample type (nasal and saliva). The geometric means of RT-qPCR and RT-qPCR viral concentrations were calculated by taking the square root of RT-qPCR *N1* concentrations × RT-ddPCR *N1* concentration.

We observed excellent concordance between the calibration curve (**Figure 3-1A**, complete data in **Figure 3-S2**), RT-qPCR and RT-ddPCR assays over the entire dynamic range of input concentrations (**Figure 3-1B–C**), even though RT-qPCR eluents were run as-is and RT-ddPCR eluents from high-concentration samples were significantly diluted. For nasal-swab samples, RT-ddPCR values were slightly below the RT-qPCR values, however this difference was consistent across the entire dynamic range, indicating no concentration-dependent biases like enzymatic inhibition. We chose not to adjust the calibration curve to fit RT-ddPCR values; we reported the concentrations based on the calibration curves derived from the certificate of analysis from the BEI Resources reference material. For saliva samples, all points tightly clustered around the x=y line (**Figure 3-1A–C**).

Establishment of Limit of Detection

Results of the calibration curve (**Figure 3-S2A, B**) demonstrated three of three replicates detected at 1,000 copies/mL saliva (for saliva) and 1,000 copies/mL buffer (for nasal swabs). For each sample type (saliva, nasal swab), 20 contrived samples with the equivalent of 1,000 copies/mL were prepared as described above, individually extracted as described above, and subjected to RT-qPCR as described above. The LOD for each sample type through the workflow was considered established if a positive result for detection (as defined in the EUA for the CDC RT-qPCR assay) was obtained for ≥ 19 of 20 (≥95% as required by FDA EUA guidelines for determining LOD) of replicates at the input concentration (**Figure 3-S1A, B**).

Three of three replicate sample extractions included in the calibration curves for both contrived nasal-swab samples and contrived saliva samples spiked with heat-inactivated SARS-CoV-2 particles at a concentration of 1,000 copies/mL were detected by RT-qPCR, prompting testing of additional 20 replicates of each sample type spiked at that concentration, individually extracted, and tested by RT-qPCR to establishment of the LOD for our RT-qPCR assay. For both sample types (saliva and nasal swabs), 20 of 20 replicates were positive for SARSCoV-2 (**Figure**

3-S1A, B), establishing 1,000 copies/mL of saliva and 1,000 copies/mL of swab buffer as the high-sensitivity LOD for our RT-qPCR assays.

Threshold to infer Performance of tests with low analytical sensitivity

The threshold of $1.0x10^5$ copies/mL is applied generally to both saliva and nasal swabs viral loads (copies/mL) to infer detection by a test with low analytical sensitivity. The rationale to use this threshold is to demonstrate a best-case scenario performance of tests with low-analytical-sensitivity (from the low-analytical-sensitivity range $1.0x10^5$–$1.0x10^7$ copies/mL used in this paper). The comparisons in the paper would be more dramatic if a low analytical-sensitivity threshold greater than this number was selected.

Data analysis

Before we converted Cq values to viral load, we used Cq cutoffs based on the CDC guidelines (5) to define samples as positive, negative, indeterminate, or invalid (fail), and then excluded from the viral-load plots any points that failed, and any samples whose RNase P Cq values ≥40. Because we ran duplicate RT-qPCR reactions, the mean Cq of positive reactions was used for conversion to viral load.

Figure 3-3A percentages are calculated by **Equation 3.5**, where the percentage positive by a test of a given analytical sensitivity (high-analytical-sensitivity results are all measured values, by our internal test with an LOD ≤ 1000 cp/mL; low-analytical-sensitivity results are measured values at or above a threshold of $1.0x10^5$ cp/mL):

$$Percent\ Positive_{as} = \frac{n}{N} \times 100$$

(**Equation 3.5**)

Where "as" refers to the analytical sensitivity. In **Equation 3.5**, "N" is defined as the total number of participants with saliva samples passing quality-control evaluations (see Methods) for safety and human *RNaseP* gene Cq threshold at the corresponding aligned time point in column "Days from First Positive Results in Either Sample Type." Maximum denominator of number of 7, corresponding to the number of participants in the study and each participant has a maximum of one sample per time point. Numbers may vary before day 0 as each participant had a variable number of negative test results before first detected SARS-CoV-2 RNA. In **Equation 3.5**, "n" represents the number of participants, at a given time point, with detectable SARS-CoV-2 RNA (see RT-qPCR methods) in the sample type (saliva or nasal swab) using a high-analytical-sensitivity assay. For predicting performance of each sample type (saliva or nasal swab) with a test of low analytical sensitivity, "n" is defined as the number of participants with a SARS-CoV-2 *N1* gene viral load of SARS-CoV-2 greater than $1.0x10^5$ copies/mL (cp/mL) in samples, which would indicate an inferred positive result using a low-sensitivity assay with an LOD of SARSCoV-

2 *N1* gene viral load of $1.0x10^5$ copies/mL. Details of the calculations are included in the Data_Annotation file on CaltechDATA.

Figure 3-3D considers only samples collected within 10 days after the assigned first positive result were analyzed to consider symptoms relevant to an early infection. The first date of positive result observed using our high analytical-sensitivity assay (either sample type) was assigned for each participant shown in the panels of **Figure 3-2** and days 0–10 were analyzed for panel D.

Samples were designated as being collected while symptomatic if the participant reported experiencing one or more COVID-19-like symptoms at the time of sample collection; if no COVID-19 like symptoms were reported, the sample was designated as "No Symptoms Reported." Samples were defined as either positive, negative, or indeterminate by our high-analytical-sensitivity assay, based on the criteria from the manufacturer of the RT-qPCR assay, detailed above. Samples were inferred as either positive or negative by a low-analytical-sensitivity assay if the viral load measured in the sample was greater than our inferred low-analytical-sensitivity threshold, $1.0x10^5$ copies/mL.

Figure 3-3D utilizes **Equation 3.5**, where "N" is defined as the number of participant samples positive for SARSCoV-2 RNA within the symptomatic categories defined in the first 10 days of detectable infection (criteria above). There were 97 saliva and 95 nasal-swab samples collected while symptomatic, and 46 saliva and 44 nasal-swab samples collected with the participant reporting no symptoms. The value of "n" corresponds to the percent positive by either observed positivity by our high-analytical-sensitivity assay or inferred positive by a low analytical-sensitivity assay as the numerator over the denominator corresponding to that sample type and symptom status, multiplied by 100%.

RNAseq

Saliva and nasal-swab samples below *N1* Cq of 26 were sent to Chan Zuckerberg Biohub for SARS-CoV-2 viral genome sequencing, a modification of Deng et al. (2020)[7] as described in Gorzynski et al. (2020).[8] Sequences were assigned pangolin lineages described by Rambaut et al. (2020)[9] using Phylogenetic Assignment of Named Global outbreak LINeages software v2.3.2 (github.com/cov-lineages/pangolin). Consequences viral genomes were submitted to GISAID by Chan Zuckerberg Biohub, see data availability section for accession id details.

SARS-CoV-2 RNA stability at 4 ˚C

As described above, each extraction batch included a contrived sample spiked with SARS-CoV-2 heat-inactivated particles. For all available saliva or nasal-swab extraction batches, the Cq value of the SARS-CoV-2 *N1* gene in the contrived SARS-CoV-2 positive extraction control was collected. The standard deviation of these measurements was calculated and used to establish a threshold for expected noise between repeat extractions of the same sample. To assess samples for evidence of SARS-CoV-2 RNA degradation, any participant sample that had more than one extraction replicate performed were analyzed. Samples where the difference in Cq values between the extractions was less than the threshold of expected noise between replicate extractions were defined as degradation not observed, (DNO). For samples where the difference was above this threshold, the time for 1 Cq increase (2-fold decrease) in RNA detected by RT-qPCR is described by the term half-life, which was calculated according to **Equation 3.6**, below:

$$t_{1/2} = \frac{-\ln 2}{k}$$

(**Equation 3.6**)

Where "k" is defined as the slope of the linear regression of the natural logarithm of the viral load versus extraction date (relative to sample collection date). The median over the entire dataset (saliva or swab) was used as a point estimate of RNA half-life. The median point was determined to be 15.0 days for nasal swabs and 51.0 days for saliva.

Calculations that predict the impact of storage time at 4 °C and RNA stability on viral load are calculated according to **Equation 3.7**, below.

$$y_{adj} = y_{deg} 2^{\frac{\Delta t}{t_{1/2}}}$$

(**Equation 3.7**)

Where y_{adj} is defined as the adjusted viral load, y_{deg} is defined as the viral load before adjustment for degradation (as calculated by **Equations 3.1–3.4**), and $t_{1/2}$ is defined as the RNA half-life, shown in **Equation 3.5**.

All samples were stored at 4 °C before extraction; time of storage varied between 0–27 days. The stability of SARS-CoV-2 RNA in nasal-swab samples was slightly lower (1 Cq loss of RNA detected after a median of 15 days) than the stability of SARS-CoV-2 RNA in saliva samples (1 Cq loss of RNA detected after a median of 51 days) (**Figure 3-S3**). An assessment of how viral-load measurements in **Figure 3-2** may have been affected by time between sample collection and quantification is included in **Figure 3-S4**. Given the large dynamic range of the viral loads in

these samples (~24 Cq or about 10,000,000 fold), we considered stability corresponding to a 1 Cq (2 fold) loss to be adequate.

The predicted impact of RNA degradation on the comparisons of high-analytical-sensitivity saliva to inferred low-analytical-sensitivity nasal testing is shown in **Figure 3-S4**. Accounting for potential decreases of viral RNA in the nasal swab resulting from delays between sample collection and quantification only impact the interpretation of two points, conservatively decreasing the delay from 2.0 to 1.5 day for the first participant (**Figure 3-2B and Figure 3-S4B**) and from 3.0 to 2.0 days for the third participant (**Figure 3-2C and Figure 3-S4C**).

Supplementary Discussion

Three participants (**Figure 3-1C–E**) were infected with the same variant, B.1.429 (CAL20), classified as a variant of concern at the time of this study. The SARS-CoV-2 variant for the participants in **Figure 3-1D and Figure 3-1E** were inferred from the sequenced sample of the household's presumed index case. Saliva viral loads for each of these participants (**Figure 3-2C–E**) were low. Of note, the participants in **Figure 3-2C and 3-2E** showed high *RNase* P Cq values (indicating low concentration of the human control target); and variability of *RNase* P Cq values across the nasal swab samples suggests that inconsistent swab-sampling quality could have impacted these participants' viral-load data and should be taken into account when interpreting those data.

Beyond outbreak prevention and control, early detection of COVID-19 may also be useful for individual patient care, as high-risk patients who are identified early can be monitored and have treatment initiated swiftly if it becomes appropriate. Several treatments show exclusive or increased efficacy only when given early in the infection. The advantage of earlier treatment initiation is likely due to reduction of viral replication either directly or by promotion of an early effective immune response, which prevents a later exaggerated inflammatory response (10). Results of the ACTT-1 trial demonstrated a survival benefit in patients for whom Remdesivir was initiated in the early stages of treatment (supplemental oxygen only), but that benefit was lost once disease progressed, and advanced respiratory support was needed (10–12). More recently, the MOVe-OUT clinical trial demonstrated the efficacy of molnupiravir when (per trial inclusion criteria) initiated among outpatients within the first five days from symptom onset, whereas the inpatient study (MOVe-IN) did not proceed to a Phase 3 Clinical Trial, as clinical benefit was not observed for hospitalized patients with a longer duration of symptoms prior to initiation of the treatment (10). Other therapies, such as plasma and monoclonal antibody therapies (bamlanivimab or casirivimab plus imdevimab) show similar clinical benefits in early initiation of treatment (11–16).

Although national vaccination efforts are reducing severe COVID-19 outcomes in the U.S., a sizable portion of the

world's population is likely to remain unvaccinated due to limited vaccine availability, medical ineligibility (in the U.S., children under five years of age are not yet eligible), or personal preference. Thus, testing remains an important tool for preventing outbreaks among children in schools and daycare facilities (where children under age two generally do not wear masks), which may spread to the community and increase rates of infection among high-risk and unvaccinated individuals. Tests that detect early infections are also important to prevent viral transmission in congregate settings with high-risk or unvaccinated populations, such as hospitals, college dormitories, homeless shelters, correctional facilities, summer camps for children, elementary schools, and long-term care facilities.

As new SARS-CoV-2 variants emerge, quantitative studies of the kinetics of early-stage viral loads must be continually updated in follow-up studies. Importantly, such studies should be undertaken in people of a wide range of ethnicities, races, health conditions, vaccination status, and ages. Breakthrough cases are often asymptomatic (17) and recent evidence suggests that vaccinated individuals may transmit infections from the new variants, including Delta (18). Another reason for continued monitoring of early viral kinetics is that viral evolution, including of host tropism, can markedly diminish the effectiveness of a diagnostic strategy. In one study, decreased clinical sensitivity of NP swabs was observed in SARS-CoV-2 variant B.1.616 (19) which may indicate a tropism shift of the virus into lower-respiratory compartments. Finally, quantitative data must be acquired in parallel with viral-culture data to understand the viral loads and phases of infection that are most relevant to transmission.

Early detection of infection clearly reduces community transmission, however, for most of the COVID-19 pandemic, policy makers have had to develop testing strategies in the absence of quantitative data on viral kinetics from the earliest stage of infection. Lacking such data-based guidance, diagnostic tests have been used incorrectly (with false-negative results due to using tests with insufficient sensitivity) in several scenarios, resulting in outbreaks that could have been prevented with an appropriate testing strategy (20–26).

One barrier to implementing such more advanced testing strategies is availability of appropriate tests. Because the optimal sample type for early detection might be different for different populations, or might change as new variants emerge, tests with robust high analytical sensitivity across multiple sample types are needed. Developing such tests is challenging because it requires incorporating robust sample-preparation technology to purify and concentrate pathogen nucleic acids from diverse human matrices, from upper respiratory (e.g., fluids from the nasal, nasopharyngeal, oral, and oropharyngeal compartments, captured in swabs or saliva) to lower respiratory samples (e.g., sputum, tracheal aspirate, bronchoalveolar lavage). It is even more challenging to incorporate such sample-preparation technology into tests that can be broadly deployed—at very low cost—at the point of care in limited-

resource settings (such as schools, homes, and businesses, and especially in the developing countries). Development of such highly sensitive, rapid, and inexpensive tests with broad sample-type compatibility is urgently needed.

Supplemental references

1. Centers for Disease Control and Prevention, 2020. Real-time RT-PCR panel for detection 2019-Novel Coronavirus. 2020.
2. Centers for Disease Control and Prevention, 2021. COVID-19: People with certain medical conditions. *Centers for Disease Control and Prevention, Atlanta, GA. https://www. cdc. gov/coronavirus/2019-ncov/need-extra-precautions/people-with-medical-conditions.html*.
3. Winnett, A., Cooper, M.M., Shelby, N., Romano, A.E., Reyes, J.A., Ji, J., Porter, M.K., Savela, E.S., Barlow, J.T., Akana, R. and Tognazzini, C., 2020. SARS-CoV-2 viral load in saliva rises gradually and to moderate levels in some humans. *medRxiv*.
4. Symptoms of COVID-19 (2020) Centers for Disease Control and Prevention. Available at: https://www.cdc.gov/coronavirus/2019-ncov/symptoms-testing/symptoms.html (Accessed: 28 May 2024).
5. CDC 2019 nCoV real-time RT-PCR diagnostic panel (2020) FDA. Available at: https://www.fda.gov/media/134922/download (Accessed: 28 May 2024).
6. Bio-Rad SARS-COV-2 ddpcr kit instructions for use (2020) Bio-Rad. Available at: https://www.bio-rad.com/webroot/web/pdf/lsr/literature/10000130776.pdf (Accessed: 28 May 2024).
7. Deng, X., Achari, A., Federman, S., Yu, G., Somasekar, S., Bártolo, I., Yagi, S., Mbala-Kingebeni, P., Kapetshi, J., Ahuka-Mundeke, S. and Muyembe-Tamfum, J.J., 2020. Metagenomic sequencing with spiked primer enrichment for viral diagnostics and genomic surveillance. *Nature microbiology*, *5*(3), pp. 443–454.
8. Gorzynski, J.E., De Jong, H.N., Amar, D., Hughes, C., Ioannidis, A., Bierman, R., Liu, D., Tanigawa, Y., Kistler, A.L., Kamm, J. and Kim, J., 2020. High-throughput SARS-CoV-2 and host genome sequencing from single nasopharyngeal swabs. *medRxiv*, pp. 2020–07.
9. Rambaut, A., Holmes, E.C., O'Toole, Á., Hill, V., McCrone, J.T., Ruis, C., du Plessis, L. and Pybus, O.G., 2020. A dynamic nomenclature proposal for SARS-CoV-2 lineages to assist genomic epidemiology. *Nature microbiology*, *5*(11), pp. 1403–1407.

10. Merck, M., 2021. Merck and Ridgeback Biotherapeutics Provide Update on Progress of Clinical Development Program for Molnupiravir, an Investigational Oral Therapeutic for the Treatment of Mild-to-Moderate COVID-19.

11. Simonovich, V.A., Burgos Pratx, L.D., Scibona, P., Beruto, M.V., Vallone, M.G., Vázquez, C., Savoy, N., Giunta, D.H., Pérez, L.G., Sánchez, M.D.L. and Gamarnik, A.V., 2021. A randomized trial of convalescent plasma in Covid-19 severe pneumonia. *New England Journal of Medicine*, *384*(7), pp. 619–629.

12. Libster, R., Marc, G.P., Wappner, D., Coviello, S., Bianchi, A., Braem, V., Esteban, I., Caballero, M.T., Wood, C., Berrueta, M. and Rondan, A., 2020. Prevention of severe COVID-19 in the elderly by early high-titer plasma. *MedRxiv*, pp. 2020–11.

13. Activ-3/Tico Ly-CoV555 Study Group, 2021. A neutralizing monoclonal antibody for hospitalized patients with Covid-19. *New England Journal of Medicine*, *384*(10), pp. 905–914.

14. Chen, P., Nirula, A., Heller, B., Gottlieb, R.L., Boscia, J., Morris, J., Huhn, G., Cardona, J., Mocherla, B., Stosor, V. and Shawa, I., 2021. SARS-CoV-2 neutralizing antibody LY-CoV555 in outpatients with Covid-19. *New England Journal of Medicine*, *384*(3), pp. 229–237.

15. Weinreich, D.M., Sivapalasingam, S., Norton, T., Ali, S., Gao, H., Bhore, R., Musser, B.J., Soo, Y., Rofail, D., Im, J. and Perry, C., 2021. REGN-COV2, a neutralizing antibody cocktail, in outpatients with Covid-19. *New England Journal of Medicine*, *384*(3), pp. 238–251.

16. Food and Drug Administration, 2020. Fact sheet for health care providers; Emergency Use Authorization (EUA) of casirivimab and imdevimab. *Available at: Fact Sheet For Health Care Providers Emergency Use Authorization (Eua) Of Bamlanivimab And Etesevimab (fda.gov)*.

17. Covid, C.D.C., Team, V.B.C.I., Birhane, M., Bressler, S., Chang, G., Clark, T., Dorough, L., Fischer, M., Watkins, L.F., Goldstein, J.M. and Kugeler, K., 2021. COVID-19 vaccine breakthrough infections reported to CDC—United States, January 1–April 30, 2021. *Morbidity and Mortality Weekly Report*, *70*(21), p. 792.

18. Brown, C.M., 2021. Outbreak of SARS-CoV-2 infections, including COVID-19 vaccine breakthrough infections, associated with large public gatherings—Barnstable County, Massachusetts, July 2021. *MMWR. Morbidity and mortality weekly report*, *70*.

19. Fillâtre, P., Dufour, M.J., Behillil, S., Vatan, R., Reusse, P., Gabellec, A., Velmans, N., Montagne, C., Du Coudret, S.G., Droumaguet, E. and Merour, V., 2022. A new SARS-CoV-2 variant with high lethality

poorly detected by RT-PCR on nasopharyngeal samples: an observational study. *Clinical Microbiology and Infection*, *28*(2), pp. 298–e9.

20. Pray, I.W., 2020. COVID-19 outbreak at an overnight summer school retreat—Wisconsin, July–August 2020. *MMWR. Morbidity and mortality weekly report*, *69*.

21. Moreno, G.K., Braun, K.M., Pray, I.W., Segaloff, H.E., Lim, A., Poulsen, K., Meiman, J., Borcher, J., Westergaard, R.P., Moll, M.K. and Friedrich, T.C., 2021. Severe acute respiratory syndrome coronavirus 2 transmission in intercollegiate athletics not fully mitigated with daily antigen testing. *Clinical Infectious Diseases*, *73*(Supplement_1), pp. S45–S53.

22. Winichakoon, P., Chaiwarith, R., Liwsrisakun, C., Salee, P., Goonna, A., Limsukon, A. and Kaewpoowat, Q., 2020. Negative nasopharyngeal and oropharyngeal swabs do not rule out COVID-19. *Journal of clinical microbiology*, *58*(5), pp. 10–1128.

23. Schwartz, N.G., 2020. Adolescent with COVID-19 as the source of an outbreak at a 3-week family gathering—Four states, June–July 2020. *MMWR. Morbidity and mortality weekly report*, *69*.

24. Cao, G., Tang, S., Yang, D., Shi, W., Wang, X., Wang, H., Li, C., Wei, J. and Ma, L., 2020. The potential transmission of SARS-CoV-2 from patients with negative RT-PCR swab tests to others: two related clusters of COVID-19 outbreak. *Japanese Journal of Infectious Diseases*, pp. JJID–2020.

25. Hagan, L.M., 2020. Mass testing for SARS-CoV-2 in 16 prisons and jails—six jurisdictions, United States, April–May 2020. *MMWR. Morbidity and mortality weekly report*, *69*.

26. Szablewski, C.M., 2020. SARS-CoV-2 transmission and infection among attendees of an overnight camp—Georgia, June 2020. *MMWR. Morbidity and mortality weekly report*, *69*.

Author Contributions

Listed alphabetically by name

Reid Akana (RA): Assisted in literature analysis with ES, MKP, AVW, MC; collaborated with AVW in creating digital participant symptom surveys; assisted with data quality control/curation with JJ, NWS, NS; collaborated with ES, JJ to write data analysis/visualization code; created current laboratory information management system (LIMS) for specimen logging and tracking. Creation of iOS application for sample logging/tracking. Configured a SQL database for data storage. Created an Apache server and websites to view study data. Configured FTPS server to catalog PCR data. Wrote a Python package to access study data. Worked with ES, AVW, AR to implement logic that prioritized specimen extraction order. Collaborated with ES, MKP, AVW, AR in analyzing RNA stability. Created supplementary Figures 3-3B and 3-3C.

Jacob T. Barlow (JTB): Created initial specimen tracking database to aid in specimen logging and tracking. Maintenance of database and implementation of corrections. Feedback on manuscript draft.

Alyssa M. Carter (AMC): Received and logged specimens, and performed sample QC. Prepared reagents for and assisted with RNA extractions. Performed RT-qPCR and analyzed RT-qPCR data for both time series and screening experiments. Performed some of the initial experiments that assessed RNA stability in nasal swab samples.

Matthew M. Cooper (MMC): Collaborated with AVW, MF, NS, YG, RFI, on study design and recruitment strategies. Co-wrote initial IRB protocol and informed consent with AVW and NS; assisted in the writing of the enrollment questionnaire; developed laboratory sample processing workflow for saliva with AVW and AER; performed sample processing on subset of samples; funding acquisition; collaborated with AR to write data processing/visualization code for observing household transmission events for active study participants. Contributor to the design of the calibration curve for saliva LOD experiments.

Matthew Feaster (MF): Co-investigator; collaborated with AVW, MMC, NS, YG, RFI on study design and recruitment strategies; provided guidance and expertise on SARS-CoV-2 epidemiology and local trends.

Ying-Ying Goh (YYG): Co-investigator; collaborated with AVW, MMC, NS, MF, RFI on study design and recruitment strategies; provided guidance and expertise on SARS-CoV-2 epidemiology and local trends.

Rustem F. Ismagilov (RFI): Co-investigator; collaborated with AVW, MMC, NS, MF, YYG on study design and recruitment strategies; provided leadership, technical guidance, oversight, and was responsible for obtaining funding for the study.

Jenny Ji (JJ): Contributed to study design and study organization and implementation with NS and JAR; co-wrote enrollment questionnaire with NS and AVW. Major contributor to curation of participant symptom data. Provided quality control of participant data with RA, NS, NWS. Major contributor to the symptom data analysis and visualization shown in Figure 3-2.

Michael K. Porter (MKP): Performed specimen logging and QC, RNA extractions, RT-qPCR, data processing. Performed data acquisition and analysis for and made Figure 3-S1 with AVW. Prepared participant sample collection materials and helped with supplies acquisition. Assisted in literature analysis with ES, RA, AVW.

Jessica A. Reyes (JAR): Study coordinator; collaborated with NS, AVW, NWS, and RFI on recruitment strategies, translated study materials into Spanish, co-wrote informational sheets with AVW and NS; created instructional videos for participants; enrolled and maintained study participants with NS and NWS.

Anna E. Romano (AER): Developed laboratory swab sample processing workflow with ES. Optimized extraction and ddPCR protocols working with vendor scientists. Created budgets and managed, planned, and purchased reagents and supplies; developed and validated method for RT-qPCR and RT-digital droplet PCR analysis for saliva and swab samples with MMC, and AVW. Performed specimen logging and QC, RNA extractions, RT-qPCR and RT-digital droplet PCR; Design of saliva calibration curve experiment. Analyzed ddPCR data for participant and calibration curve data included in Figure 3-1. Interpretation of sequence data with AVW. Prepared Figure 3-1 and Figure 3-S2 with ES and AVW; Collaborated with ES and RA to generate and curate data for RNA stability analysis. Managing logistics for the expansion of the BSL-2+ lab space with ESS. Edited manuscript.

Emily S. Savela (ESS): Coordinated the laboratory team and division of lab work, coordinated lab schedules to ensure completion of time-sensitive analyses of participant samples while complying with COVID-19 lab occupancy restrictions and biosafety requirements. Performed initial nasal-swab workflow validation experiments with AER. Major contributor to workflow validation, methods, biosafety SOPs, and sample storage. Developed a plan for, and executed, the long-term sample storage for efficient, safe, storage. Performed specimen logging and QC, RNA extractions, RT-qPCR, data processing, and conducted biosafety training. Performed the data curation and data analysis for Figure 3-2. Made Figure 3-2. Minor contributor to symptoms data analysis and visualization

with JJ and RA for Figure 3-2. Experimental design and RNA extractions of the samples, to Figure 3-1A and minor contributor to Figure 3-S2A with AER. Managing logistics for the expansion of the BSL-2+ lab space with AER and biohazardous waste pickups. Collaborated with ES, RA, and AVW to generate data for and curated data set to assess viral RNA stability (Figure 3-S3). Prepared Figure 3-S4. Co-wrote the manuscript. Verified the underlying data with AVW.

Noah W. Schlenker (NWS): Study coordinator; collaborated with NS, AVW, JAR, and RFI on recruitment strategies; enrolled and maintained study participants with NS and JAR; study-data quality control, curation, and archiving with RA, JJ, and NS.

Natasha Shelby (NS): Study administrator; collaborated with AVW, MMC, RFI, YG, MF on initial study design and recruitment strategies; co-wrote IRB protocol and informed consent with AVW and MMC; co-wrote enrollment questionnaire with AVW and JJ; co-wrote participant informational sheets with AVW and JAR; enrolled and maintained study participants with JAR and NWS; study-data quality control, curation, and archiving with RA, JJ, and NWS; reagents and supplies acquisition; assembled Table 3-S1; managed citations and reference library; co-wrote and edited the manuscript.

Colten Tognazzini (CT): Coordinated the recruitment efforts at PPHD with case investigators and contact tracers; provided guidance and expertise on SARS-CoV-2 epidemiology and local trends.

Alexander Viloria Winnett (AVW): Collaborated with MMC, NS, RFI, YG, MF on initial study design and recruitment strategies; co-wrote IRB protocol and informed consent with MMC and NS; co-wrote enrollment questionnaire with NS and JJ; co-wrote participant informational sheets with NS and JAR and digital survey; developed and validated methods for saliva and nasal-swab sample collection; developed and validated methods for RT-qPCR and RT-digital droplet PCR analysis for saliva and swab samples with AER, ESS, MMC; reagents and supplies acquisition; funding acquisition; developed laboratory sample processing workflow with AER, ESS, and MMC; performed specimen logging and QC, nucleic acid extraction, RT-qPCR, data processing – including experimental data generation for saliva calibration curve (Figure 3-1, Figure 3-S2) designed with MMC and AER, establishment of nasal swab limit of detection (Figure 3-S1), and viral load timeseries data (Figure 3-2) with ESS, AER, MKP, and AMC; interpreted sequencing data with AER; analyzed viral load timeseries data to visualize trends (Figure 3-3) with ESS; generated, analyzed, and visualized data to assess degradation of viral RNA in saliva and nasal swab samples (Figure 3-S3) with RA, ESS, and AER; literature analysis with RA, ESS, and MKP; co-wrote sections of the manuscript outlined by ESS and RFI, edited the manuscript. Verified the underlying data with ESS.

Chapter 4

SARS-COV-2 OMICRON VARIANT EXHIBITS EXTREME DIFFERENCES IN EARLY VIRAL LOADS AMONG RESPIRATORY SPECIMEN TYPES RESULTING IN HIGHER SENSITIVITY BY NASAL-OROPHARYNGEAL COMBINATION SPECIMENS

This chapter was originally published in Viloria Winnett A*, Akana R*, Shelby N*, Romano AE, Davich H, Caldera S, Kim MK, Carter AM, Yamada T, Reyna JR, Ji J, Reyes JA, Cooper MM, Thomson M, Tognazzini C, Feaster M, Goh YY, Ismagilov. SARS-CoV-2 Omicron variant exhibits extreme differences in early viral loads among respiratory specimen types resulting in higher sensitivity by nasal-oropharyngeal combination specimens (March 2023). PNAS Nexus. https://doi.org/10.1093/pnasnexus/pgad033.

Abstract

SARS-CoV-2 viral-load measurements from a single specimen type are used to establish diagnostic strategies, interpret clinical-trial results for vaccines and therapeutics, model viral transmission, and understand virus-host interactions. However, measurements from a single specimen type are implicitly assumed to be representative of other specimen types. We quantified viral-load timecourses from individuals who began daily self-sampling of saliva, anterior-nares (nasal), and oropharyngeal (throat) swabs before or at the incidence of infection with the Omicron variant. Viral loads in different specimen types from the same person at the same timepoint exhibited extreme differences, up to 10^9 copies/mL. These differences were not due to variation in sample self-collection, which was consistent. For most individuals, longitudinal viral-load timecourses in different specimen types did not correlate. Throat-swab and saliva viral loads began to rise as many as seven days earlier than nasal-swab viral loads in most individuals, leading to very low clinical sensitivity of nasal swabs during the first days of infection. Individuals frequently exhibited presumably infectious viral loads in one specimen type while viral loads were low or undetectable in other specimen types. Therefore, defining an individual as infectious based on assessment of a single specimen type underestimates the infectious period, and overestimates the ability of that specimen type to detect infectious individuals. For diagnostic COVID-19 testing, these three single specimen types have low clinical sensitivity, whereas a combined throat–nasal swab, and assays with high analytical sensitivity, were inferred to have significantly better clinical sensitivity to detect presumed pre-infectious and infectious individuals.

Significance Statement

In a longitudinal study of SARS-CoV-2 Omicron viral loads in three paired specimen types (saliva, anterior-nares swabs, and oropharyngeal swabs), we found extreme differences among paired specimen types collected from a person at the same timepoint, and that viral loads in different specimen types from the same person often do not correlate throughout infection. Individuals often exhibited high, presumably infectious viral loads in oral specimen types before nasal viral loads remained low or even undetectable. Combination nasal–throat swabs were inferred to have superior clinical sensitivity to detect infected and infectious individuals. This demonstrates that single specimen type reference standard tests for SARS-CoV-2, such as in clinical trials or diagnostics evaluations, may miss infected and even infectious individuals.

Introduction

Measurements of viral load in respiratory infections are used to establish diagnostic strategies, interpret results of clinical trials of vaccines and therapeutics, model viral transmission, and understand virus-host interactions. But how viral loads change across multiple specimen types early in SARS-CoV-2 infection is not well understood. Specifically in the context of diagnostics, as new SARS-CoV-2 variants-of-concern (and new respiratory viruses) emerge with different viral kinetics(1), it is imperative to continually re-evaluate testing strategies (including specimen type and test analytical sensitivity) for detecting pre-infectious and infectious individuals. Early detection can reduce transmission within communities(2, 3) and the global spread of new variants, and enable earlier initiation of treatment resulting in better outcomes(4–6).

Selecting testing strategies to achieve detection in the pre-infectious and infectious periods requires filling two critical knowledge gaps: 1. Which respiratory specimen type accumulates virus first? 2. What is the appropriate test analytical sensitivity to detect accumulation of virus in the pre-infectious and infectious stages? These two gaps must be filled in parallel. Commonly, an individual's infection is described by the viral load sampled from a single specimen type, which is appropriate when there is one principal specimen type (e.g., HIV in blood plasma). However, some respiratory pathogens, including SARS-CoV-2, can infect multiple respiratory sampling sites(7–9).

Nasopharyngeal swabs have been the gold standard for SARS-CoV-2 detection but are poorly tolerated and challenging for serial sampling and self-collection. Many alternate specimen types are now widely used. Some of these are suitable for routine testing and are approved for self-collection (e.g., saliva, anterior-nares (nasal) swabs, and oropharyngeal (throat) swabs) in some countries. Cross-sectional studies comparing paired specimen types from the same person have shown that cycle threshold (Ct, a semi-quantitative proxy for viral load) values can differ substantially between specimen types(10), and the clinical sensitivity of different specimen types is not equivalent(11). Sometimes, viral loads in one specimen type are low or even absent while viral loads in another type are high(12–14). Nasal swabs (including those used for rapid antigen testing) are the dominant specimen type used in the USA for workplace screenings and at-home testing. However, several studies(15–18), news media(19), and social-media posts have speculated that in Omicron infections, viral load accumulates in oral specimens before the nasal cavity. Formal investigations of specimen types from single timepoints and cross-sectional studies have been contradictory, potentially due to when individuals were sampled; viral loads from individuals sampled after symptom onset may not reflect viral loads from earlier in the infection. Rigorous, longitudinal comparisons of paired specimen types starting from the incidence of infection are needed to fill this gap.

The second knowledge gap is the analytical sensitivity needed for reliable detection of pre-infectious and infectious individuals. The assay analytical sensitivity is described by the LOD; generally, the LOD of an assay describes its ability to detect and quantify target at or above a certain concentration in that specimen type with >95% probability(20). Assays with high LODs (low analytical sensitivity) require a high concentration of virus to reliably yield positive results, whereas assays with low LODs (high analytical sensitivity) can reliably detect much lower concentrations of virus. For example, in early SARS-CoV-2 variants, some studies showed that saliva accumulated virus earlier than nasal swabs, but at low levels(14, 21, 22), thus saliva required a high-analytical-sensitivity (low LOD) assay(14, 23). However, low-analytical-sensitivity tests (including rapid antigen tests) are increasingly authorized and used globally(24, 25). Which of these tests can detect pre-infectious and infectious individuals requires quantitative, longitudinal measurements of viral concentration in multiple specimen types starting from the incidence of infection.

Early detection, in the pre-infectious period, is ideal to prompt infection-control practices (e.g., isolation) before transmission occurs, and detection during the infectious period is critical to minimize outbreaks. Replication-competent (i.e., infectious) virus has been recovered from saliva(9), oropharyngeal swabs(26), and nasal swabs(27), but it is impractical and infeasible to perform viral culture on each positive specimen to determine if a person is infectious. However, studies that performed both culture and RT-qPCR found that low Ct values (high viral loads) are associated with infectious virus. Specific viral loads likely to be infectious for each specimen type have not been established(28), partly because Ct values are not comparable across assays(29, 30), and culture methods differ. However, as a general reference, viral loads of $>10^4$–10^7 RNA copies/mL are associated with the presence of replication-competent virus(17, 31–41), and these values have been used in outbreak simulations(35, 39, 42–44). The enormous range (>four orders of magnitude) in observed viral loads that correspond with infectiousness emphasizes why quantitative measurements of loads in different specimen types are needed to make robust predictions about tests that will detect the pre-infectious and infectious periods.

The assumption made early in the COVID-19 pandemic that viral load always rises rapidly from undetectable to likely infectious(45), has been challenged by numerous longitudinal studies of viral load in different specimen types that show early SARS-CoV-2 viral loads can rise slowly over days(14, 17, 18, 21, 27, 41, 46–49), not hours. These findings are encouraging because a longer window provides more time to identify and isolate pre-infectious individuals. However, making use of this opportunity by selecting an optimal diagnostic test requires a thorough understanding of how viral load changes in each specimen type early in infection. Moreover, to reliably detect an infectious person, the infectious specimen must be tested with an assay that has an LOD below the infectious viral load for that specimen type. However, many authorized COVID-19 tests (including rapid antigen tests) have LODs well above the range of reported infectious viral loads(50, 51).

Filling the two critical and inter-related knowledge gaps about specimen type and assay LOD requires high-frequency quantification of viral loads, rather than semi-quantitative Ct values, in multiple specimen types starting from the incidence of infection, not after a positive test or after symptom onset, as is commonly done. Moreover, quantification must be performed with a high-analytical-sensitivity assay to capture low viral loads in the first days of detectable infection. It is challenging to acquire such data. Individuals at high risk of infection must be prospectively enrolled prior to detectable infection and tested longitudinally with high frequency in multiple paired specimen types.

To our knowledge, four studies have reported longitudinal viral-load timecourses in multiple, paired specimen types from early infection. A university study(27) captured daily saliva and nasal-swab samples for two weeks from 60 individuals, only three of whom were negative for SARS-CoV-2 upon enrollment. In our prior study, we captured twice-daily viral-load timecourses from 72 individuals for two weeks(52), seven of whom were negative upon enrollment(14). In six of seven individuals, we inferred from viral-load quantifications that a high-analytical-sensitivity saliva assay would detect infections earlier than a low-analytical-sensitivity nasal-swab test. In a SARS-CoV-2 human challenge study(17), 10 of 18 infected participants had detectable virus by PCR in throat swabs at least one day prior to nasal swabs, and replication-competent virus was recovered from throat swabs before nasal swabs in at least 12 of 18 participants. Participants in these three studies were infected with pre-Omicron variants. One longitudinal study(15) analyzed viral loads in saliva, nasal swabs, and throat swabs in Omicron, however, daily measurements in all three specimen types were captured for only two individuals, both of whom were already positive upon enrollment. A separate case-ascertained household-transmission study with prospective daily sampling also captured viral-load measurements from the incidence of infection using a combination nasal–throat swab specimen type(41). In the U.K., where this study was performed, a combination nasal–throat swab specimen type is regularly used for diagnostic testing(53, 54). However, the rise and fall of Omicron viral loads in multiple paired single specimen types from the incidence of infection has not been characterized, despite these data being necessary to define the appropriate test analytical sensitivity and specimen type to best detect pre-infectious and infectious individuals.

Here, we measured and analyzed the viral-load timecourses of the Omicron variant in three specimen types appropriate for self-sampling (saliva, nasal swabs, and throat swabs) by individuals starting at or before the incidence of infection as part of a household-transmission study in Southern California. We then utilized these data to determine which specimen type and analytical sensitivity would yield the most reliable detection of pre-infectious and infectious individuals**.** A separate paper reports the results of daily rapid antigen testing in this study(55).

Materials and Methods

Study Design

This case-ascertained study of household transmission (approved under Caltech IRB #20-1026) was conducted in the greater Los Angeles County area between November 23, 2021, and March 1, 2022. All adult participants provided written informed consent; all minor participants provided verbal assent accompanied by written permission from a legal guardian. Children ages 8–17 years old additionally provided written assent. See Supplemental Information for details.

A total of 228 participants from 56 households were enrolled; 90 of whom tested positive for SARS-CoV-2 infection during enrollment (**Figure 4–1**). We limited our analyses to 14 individuals (**Table S4–1, Table S4–5, Figure 4–2**) who enrolled in the study at or before the incidence of acute SARS-CoV-2 infection. To be included in the cohort, a participant must have had at least one specimen type with viral loads below quantification upon enrollment, followed by positivity and quantifiable viral loads in all three specimen types.

Each day, participants reported symptoms, then self-collected saliva, anterior-nares (nasal) swab, and posterior oropharyngeal (hereafter throat) swab specimens for RT-qPCR testing in Zymo Research SafeCollect devices (CE-marked for EU use), following manufacturer's instructions(56, 57). Participants collected specimens immediately upon enrollment, then daily upon waking, as morning sample collection has been shown to yield higher viral loads than evening collection(52).

RT-qPCR Testing for SARS-CoV-2

Extraction and RT-qPCR were performed at Pangea Laboratories (Tustin, CA, USA) using the FDA-authorized *Quick* SARS-CoV-2 RT-qPCR Kit, with results assigned per manufacturer criteria(58). Additional details in Supplemental Information. This assay has a reported LOD of 250 copies/mL of sample.

Quantification of Viral Load from RT-qPCR Result

To quantify viral load in RT-qPCR specimens, contrived specimens across a 13-point standard curve (dynamic range from 250 copies/mL to 4.50×10^8 copies/mL) for each specimen type were generated at Caltech and underwent extraction and RT-qPCR as described above. All three replicates at 250 copies/mL of specimen were detected, independently validating the reported LOD for the assay. For each specimen type, the standard curve generated an equation to convert from SARS-CoV-2 *N* gene Ct values to viral loads in genomic copy equivalents (hereafter copies) per mL of each specimen type. See Supplemental Information for additional details and equations. Positive specimens with viral loads that would be quantified below the assay LOD were considered not quantifiable.

Viral Sequencing and Lineage/Variant Determination

Viral sequencing of at least one specimen for each participant with incident infection was performed on nasal or throat specimens with moderate to high viral loads by Zymo Research at Pangea Lab. See Supplemental Information for details.

Defining pre-infectious and infectious periods

The pre-infectious period is all SARS-CoV-2-positive timepoints prior to the first timepoint in which any specimen type contains viral load greater than the indicated infectious viral-load threshold. There are three main methods for defining the infectious period for an individual based on viral loads. First, the infectious period may be defined as the continuous period between the first specimen (of any type) with an infectious viral load until the first timepoint after which no specimen has an infectious viral load(59, 60). Or, to account for viral-load fluctuations, one may instead define an instantaneous infectious period (i.e., an individual is presumed infectious only when at least one specimen type has a viral load above the infectious viral load threshold). Both methods neglect the role of the neutralizing immune response, and the impact of infection stage on viral-culture positivity(32, 61, 62). To account for these factors, the infectious period may be limited to a number of days following symptoms or the first infectious timepoint. Our analyses (**Table S4–3, Figure 4–7**), include all three common definitions. First, we used a "continuous infectious period" whereby a participant is presumed infectious for all timepoints between the first specimen with an infectious viral load and the first timepoint after which no specimens had infectious viral loads. Second, we used an "instantaneous infectious period," which presumes that a participant is infectious only at timepoints when viral load in at least one specimen type is above the infectious viral load threshold. Third, we presumed that a participant is infectious only for the first five days from their first timepoint when viral load in at least one specimen type rose above the infectious viral-load threshold.

Statistical Analyses

Comparison of Viral-Load Timecourses Across Specimen Types

To quantify the difference between viral-load timecourses, we first aligned each timecourse to the time of collection of the first SARS-CoV-2-positive specimen (of any type) for each participant. Differences between viral loads from the same infection timepoint were quantified (**Figure 4–3A–B**). We compared both intra- and interparticipant viral-load timecourses: when the lengths of two participant timecourses differed, the longer timecourse was truncated. We then hypothesized that if the viral load timecourses followed the same time-dependent distribution, then the observed noise between these viral load measurements would be attributable to expected sampling noise.

Expected sampling noise was estimated as a zero-centered normal distribution fitted on human *RNase P* control target measurements (**Figure S4–4B**, Supplemental Information). The distribution of observed noise was obtained by performing maximum likelihood estimation on each pair of viral-load timecourses being compared (**Figure 4-3C**). We then tested whether observed differences in viral load across pairs of viral-load timecourses could be explained by expected sampling noise alone. *P*-values were obtained from upper-tailed Kolmogorov–Smirnov tests of the differences between the distributions of the observed noise across viral-load timecourses and expected sampling noise. Two-stage Benjamini–Hochberg correction was used to limit the false-discovery rate to 5%; viral-load timecourse comparisons with adjusted *P*-values <0.05 were considered statistically significantly different (**Figure 4–3D**). See Supplemental Information. Analyses were performed in Python 3.8 using the scipy package(63).

Inferred Clinical Sensitivity by Viral-Load Quantification

Inferred clinical sensitivity of each specimen type and analytical sensitivity were calculated for each timebin as the number of specimens of a given type with viral load above a given LOD divided by all participants considered infected (**Figure 4–4**) or infectious (**Figures 4–6** and **4–7**) at that timepoint. Confidence intervals were calculated as recommended by CLSI(64). Statistical testing for differences in inferred clinical sensitivity were performed for paired data (comparing performance at two LODs for one specimen type, or at one LOD for two paired specimen types collected by a participant at a timepoint) using McNemar exact tests, and for unpaired data (comparing the performance of one specimen type at one LOD between infection stages) using Fisher exact tests. Analyses were performed in Python v3.8.8.

Participants were considered infected from the time of collection of the first SARS-CoV-2-positive specimen (any type) until negative in all three specimen types by RT-qPCR. Individuals were presumed infectious when viral load in any specimen type was above an IVLT (10^4, 10^5, 10^6, or 10^7 copies/mL).

Combination specimen types were computationally-contrived to have either the maximum (**Figure 4–5** to **4–8**) or average (**Figure S7**) viral loads from the specimen types included in the combination that were collected by a participant at that timepoint.

Results

Among the 228 participants, incident SARS-CoV-2 infection was observed in 14 participants (**Figure 4–1**), all of whom were enrolled before or at the start of acute SARS-CoV-2 infection with the Omicron variant of concern. All 14 had received at least one vaccine dose more than two weeks prior to enrollment (**Table 4–S1**). From this cohort, 260 saliva, 260 oropharyngeal (throat) swab, and 260 anterior-nares (nasal) swab specimens were collected for viral-load quantification and plotted relative to enrollment in the study (**Figure 4–2**). All participants additionally took daily rapid antigen tests; analyzed in a separate manuscript(55).

Viral-load timecourses in the earliest stage of acute SARS-CoV-2 infection differed substantially among specimen types and participants (**Figure 4–2**). In only two (**Figure 4–2A,I**) of the 14 participants, viral loads became quantifiable in all three specimen types at the same timepoint; in most (11 out of 14) participants (**Figure 4–2B-H,J-M**), saliva or throat swabs were positive first, while nasal swabs remained negative or at low, inconsistently detectable viral loads for up to the first 6–7 days of infection. However, later in the infection, peak viral loads in nasal swabs were significantly higher than in saliva or throat swabs (**Figure 4–S1**).

Surprisingly, several participants reported zero symptoms on the day of their peak viral loads (**Figure 4–2A,C,G,N**), all of which were $>10^6$ copies/mL. Overall, we found only a weak relationship between viral load and symptoms (**Figure 4–S1–D**). Importantly, individuals had infectious viral loads in 42% of timepoints at which no symptoms were reported (**Figure 4–S1E**).

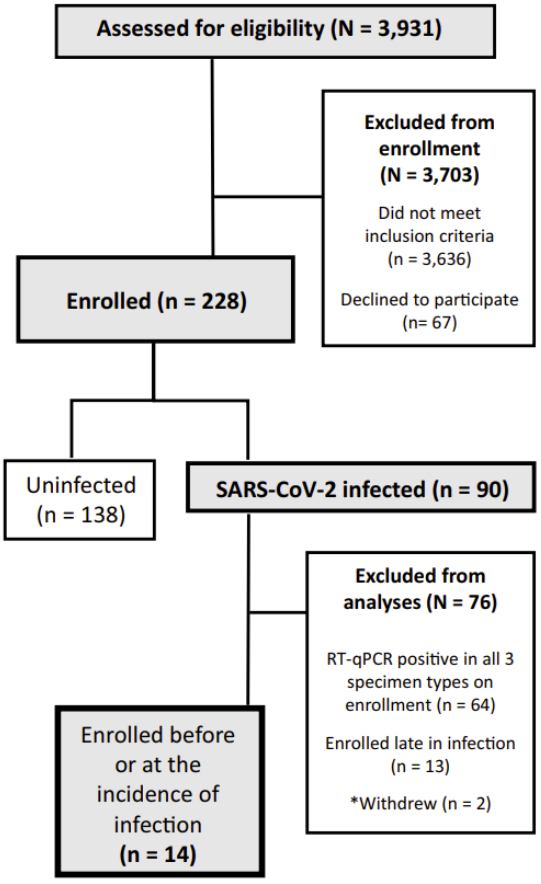

Figure 4-1. A CONSORT diagram shows participant recruitment, eligibility, enrollment, and selection for inclusion in the study cohort.

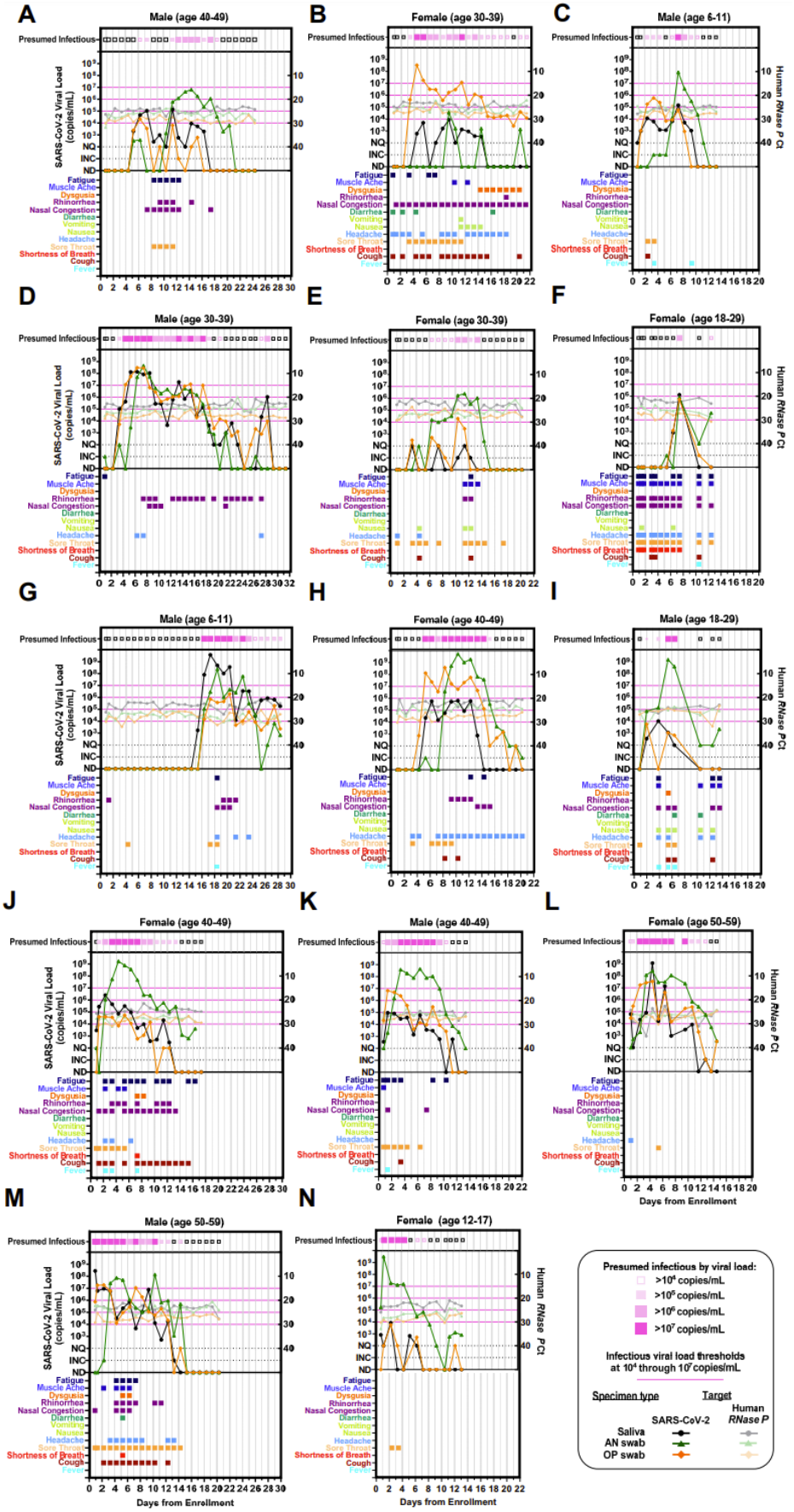
A
Male (age 40-49)
B
Female (age 30-39)
C
Male (age 6-11)
D
Male (age 30-39)
E
Female (age 30-39)
F
Female (age 18-29)
G
Male (age 6-11)
H
Female (age 40-49)
I
Male (age 18-29)
J
Female (age 40-49)
K
Male (age 40-49)
L
Female (age 50-59)
M
Male (age 50-59)
N
Female (age 12-17)
Presumed Infectious
SARS-CoV-2 Viral Load (copies/mL)
Human RNase P Ct
Fatigue
Muscle Ache
Dysgusia
Rhinorrhea
Nasal Congestion
Diarrhea
Vomiting
Nausea
Headache
Sore Throat
Shortness of Breath
Cough
Fever
Days from Enrollment
Presumed infectious by viral load:
>10⁴ copies/mL
>10⁵ copies/mL
>10⁶ copies/mL
>10⁷ copies/mL
Infectious viral load thresholds at 10⁴ through 10⁷ copies/mL
Specimen type
Target
SARS-CoV-2
Human RNase P
Saliva
AN swab
OP swab

[Figure on Previous Page] **Figure 4-2.** Individual Viral-load Timecourse Measurements from 14 Participants Enrolled at or Before the Incidence of Acute SARS-CoV-2 Infection. Each panel (A–N) represents a single participant throughout the course of enrollment. Each panel plots SARS-CoV-2 viral-load measurements (left y-axis) and human RNase P Ct values (right y-axis). Line colors indicate specimen type: black/grey are saliva, green are anterior-nares (AN) swabs, and orange are oropharyngeal (OP) swabs. Timepoints at which at least one specimen type had presumably infectious viral load (>104-107 copies/mL) are indicated at the top of each plot. Colored boxes below each plot indicate the symptoms reported at each sample-collection timepoint. Each of the 14 participants collected three specimen types throughout the course of acute infection, resulting in 42 viral-load timecourses. Participants collected an average of 15 (±5 S.D.) daily timepoints. ND, not detected; INC, inconclusive result; NQ, virus detected however viral loads below the test LOD (250 copies/mL) and thus not reliably quantifiable for RT-qPCR measurements.

SARS-CoV-2 viral loads differ significantly between specimen types during the early period of infection

We next sought to quantify the magnitude of differences in viral load across paired specimens, to answer three questions: (i) Are differences in viral loads between specimen types large enough to impact detectability by assays with varying analytical sensitivity? (ii) Are differences in viral loads attributable to variability in participant sampling behavior? (iii) Are viral-load timecourses in different specimen types within a person correlated with each other?

First, we calculated the absolute (**Figure 4–3A**) and relative (fold) differences (**Figure 4–S3**) in viral loads between paired specimens of different types collected by the same participant at the same timepoint. Large differences in absolute viral loads were observed between paired specimen types for both the first four days from the incidence of infection **(Figure 4–3A)** and all timepoints **(Figure 4–3B).** We observed absolute differences of more than nine orders of magnitude, and all specimen type comparisons had median absolute differences greater than 10^4 copies/mL, a scale of difference likely to impact the detection of SARS-CoV-2.

If the observed differences in viral loads between specimen types were the result of variability in sample collection during self-sampling, we would expect the fold differences to be similar to the variability of the human *RNase P* control marker. However, *RNase P* Ct measurements were relatively stable for each specimen type collected by participants across their timecourse (**Figure 4–2, Figure 4–S4**). For some participants, *RNase P* Ct values decreased slightly after the first sample collection, but the average standard deviation in *RNase P* Ct across all participants was <1.5 in all specimen types (saliva: 1.37, nasal: 1.42, throat: 1.46) over enrollment (**Figure 4–S4B**), which corresponds to, at most, a 2.8-fold change in target abundance. In contrast, most (84%) comparisons between specimen types had a >2.8-fold difference in viral load (**Figure 4–S2B**), demonstrating the extreme differences in load were not due to variability in self-sampling.

Although the differences in viral loads across paired specimens of different types were extreme, we recognized the possibility that the longitudinal timecourse (the rise and fall of viral loads) from different specimen types in a person might still be synchronized. For example, viral loads in one specimen type (e.g., saliva) might be

consistently lower than those in another (e.g., nasal), but follow the same pattern throughout acute infection. If this were the case, viral load measured in one specimen type would still be associated with the viral load in another specimen type despite extreme absolute differences. To test whether timecourses from different specimen types were synchronized, we quantified the correlation between viral-load timecourses for each specimen type collected from a single participant, and across different participants. These intra- and interparticipant correlations are represented as a matrix for the 42 viral-load timecourses (14 participants with three specimen types each (**Figure 4–3C,D**). The strength of each correlation (**Figure 4–3C**) was quantified by estimating the standard deviation of pairwise differences in viral load across the two timecourses. The statistical significance of the correlations between viral-load timecourses **(Figure 4–3D)** was then calculated by comparing the distribution of pairwise differences in viral-load timecourses to a distribution of expected sampling noise.

We found that viral-load timecourses in different specimen types collected by the same individual often do not correlate. In nearly all participants (13 of 14), at least two specimen types from the same participant had significantly different timecourses. In 38% of comparisons (16 of 42), we observed significantly different timecourses for each of the three specimen types from the same individual (**Figure 4–3D**). In some instances, the timecourses of specimen types from the same participant were less correlated with each other than with other participants. For example (see white circles in **Figure 4–3D**), the saliva viral-load timecourse for individual A was not significantly different from the saliva timecourses for participants D, F, G, H, J, K, L, or M, however Individual A's saliva timecourse was significantly different from the participant's own throat timecourse.

Within the same individual, throat-swab and nasal-swab viral-load timecourses were most commonly different (64%, 9 of 14 individuals). Additionally, in 29% (4 of 14) of individuals, saliva and nasal-swab viral-load timecourses differed significantly. Finally, despite the proximity of the two oral sampling locations in 21% (three of 14) of individuals, their own saliva and throat viral-load timecourses were significantly different (**Figure 4–3D**).

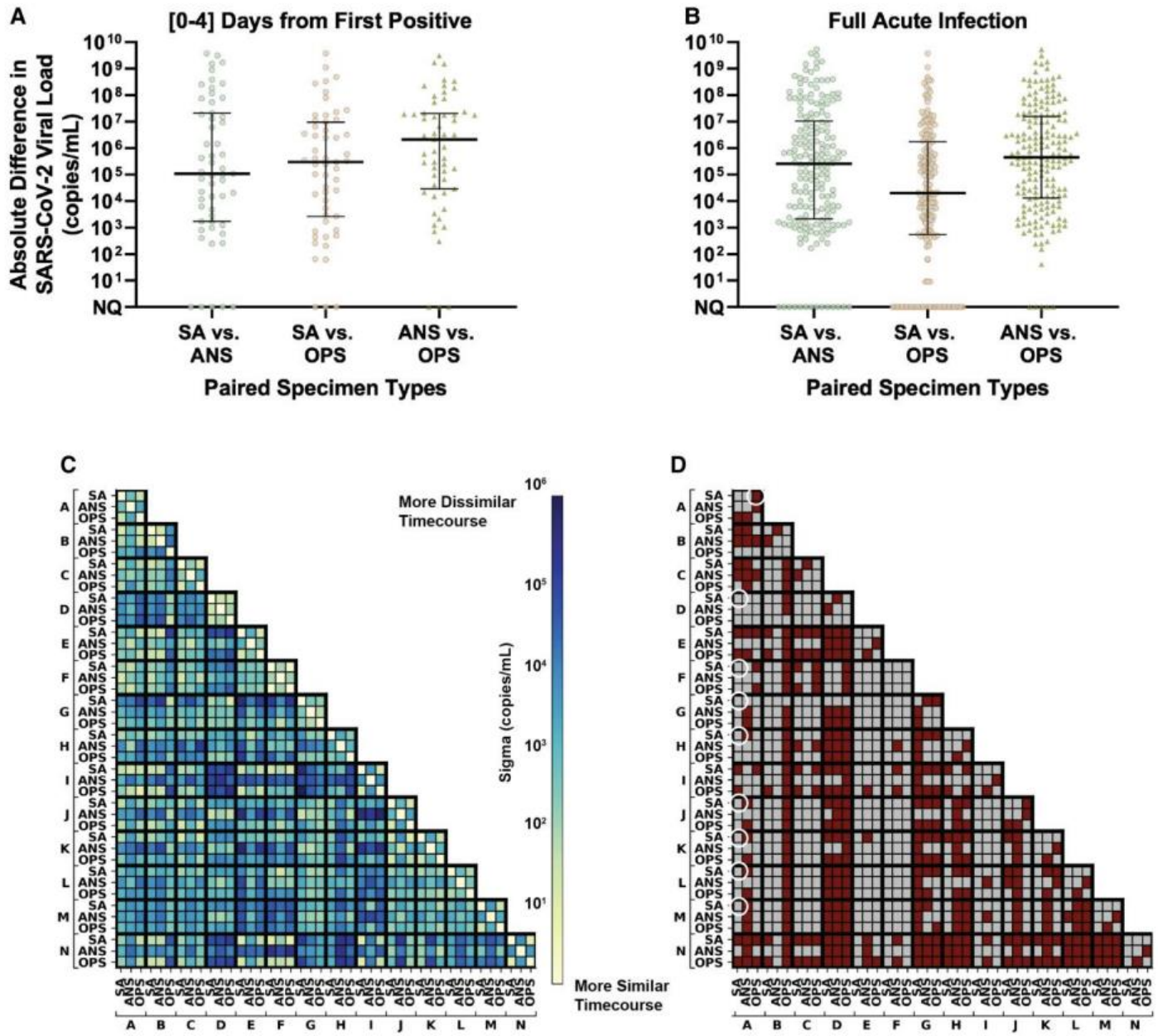

Figure 4-3. Extreme differences in viral loads across specimen types collected from the same person at the same timepoint for the 14 participants enrolled before or at the incidence of acute SARS-CoV-2 infection. (A–B) Absolute differences in viral loads across paired specimen types were calculated as the absolute value of viral load in one specimen type minus another from the same participant at the same specimen-collection timepoint. Black lines indicate median, with interquartile range. Differences are shown for: **(A)** 55 timepoints collected in the first four days from the incidence of infection (first positive specimen of any type) in each participant and **(B)** 186 timepoints collected throughout the entirety of acute infection (at least one specimen type from the participant at the timepoint was positive and had quantifiable SARS-CoV-2 viral load; 11 timepoints were positive but not quantifiable). **(C)** Correlation of viral-load timecourses, measured as the standard deviation across paired viral-load timecourses, assuming Gaussian-distributed noise (see Methods, "Comparison of Viral-Load Timecourses Across Specimen Types"). **(D)** Statistical significance of the difference in viral-load timecourses between specimens and between participants. Statistically significantly different timecourses are represented as red cells and non-significant comparisons are grey. White circles are called out as examples in the text. Expected sampling noise was estimated by analyzing *RNase P* Ct data from our study (**Supplementary Figure 4-4**) and from reference (65). P-values were obtained by comparing residuals from observed data and expected sampling noise. Additional method details are shown in **Figure 4-S5**. SA, saliva, ANS, anterior-nares nasal swab, OPS, oropharyngeal swab. Participant labels match **Figure 4-2 panels (A–N)**.

Clinical sensitivity to detect SARS-CoV-2 infection strongly depends on infection stage, specimen type, and assay analytical sensitivity

Because viral load determines whether an assay with a given analytical sensitivity will reliably yield a positive result, we hypothesized that the extreme differences in viral loads among different specimen types would significantly impact the clinical sensitivity of COVID-19 tests performed on different specimen types during different stages of the infection. To examine the inferred clinical sensitivity to detect SARS-CoV-2 infections as a factor of both specimen type and test LOD, viral-load timecourses were aligned to first detectable viral load and divided into four-day timebins. We assumed that only viral loads above a given assay's LOD would reliably yield a positive result. The inferred clinical sensitivity of detecting infected persons by each specimen type and assay LOD during each timebin was calculated as the proportion of specimens with viral loads greater than the assay LOD, divided by all timepoints collected by infected participants in that same timebin (**Figure 4–4**).

For all specimen types and timebins, testing with a high-analytical-sensitivity assay (LOD of 10^3 copies/mL) yielded significantly better inferred clinical sensitivity to detect infected persons than testing with a low-analytical-sensitivity assay (LOD of 10^6 copies/mL) (**Table 4–S4A–I**). During the first four days of infection, when individuals are often pre-symptomatic, no single specimen type achieved >90% inferred clinical sensitivity with any LOD (**Figure 4–4A–C**), suggesting that no single specimen type will reliably provide early detection of infection with the Omicron variant.

In the first four days, nasal swabs generally had the poorest inferred clinical sensitivity of all three specimen types. Even with a high-analytical-sensitivity assay (LOD of 10^3 copies/mL), nasal swabs were predicted to miss more than half (54%) of timepoints from infected persons. Saliva and throat-swab specimens had significantly better inferred clinical sensitivity than nasal swabs when a high-analytical-sensitivity assay was used, and worse (but not significantly) when a low-analytical-sensitivity assay (LOD of 10^6 copies/mL) was used (**Table 4–S4J–Z)**.

As infection progresses to days 4–8, individuals are more likely to become symptomatic. Inferred nasal-swab performance improved significantly during days 4–8 (**Table 4–S4AH–AN**) and became significantly better than saliva and throat swabs at LODs of 10^3 copies/mL and above (**Table S4–4AO–BB**). This improvement can be attributed to the rise to high viral loads in nasal swabs during this period: SARS-CoV-2 was not detected in almost half of nasal swabs in days 0–4, but in days 4–8, more than half of nasal swabs had high viral loads (>10^6 copies/mL) (**Figure 4–S1I,J**). In contrast, during both timebins, more than half of all saliva or throat-swab specimens had viral loads below 10^6 copies/mL, and thus detection using saliva or throat swabs was more dependent on assay LOD (**Figure 4–S1I,J**).

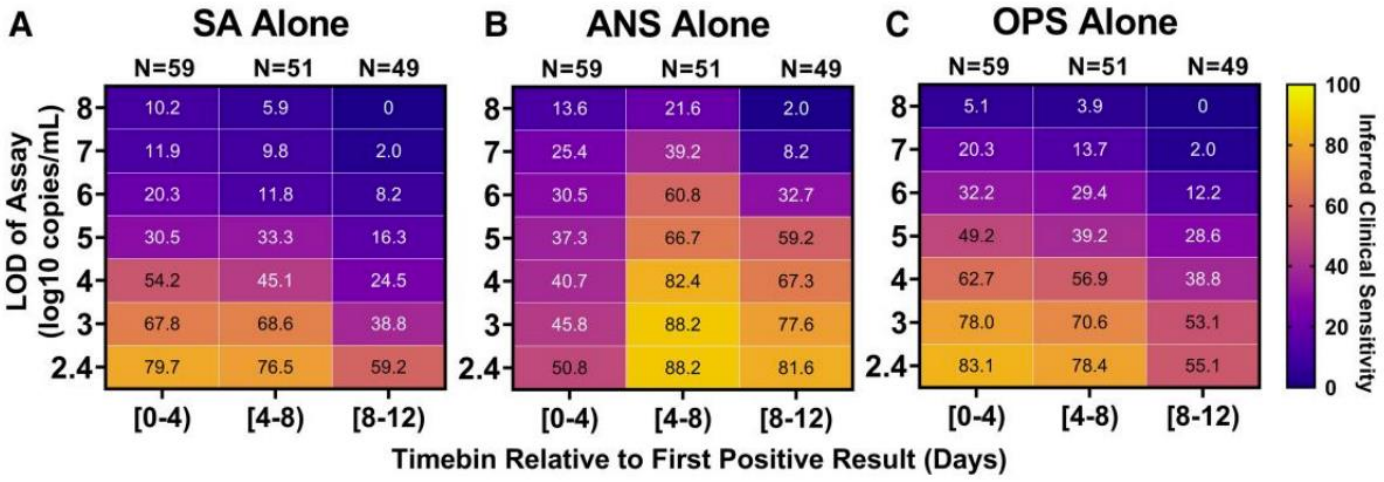

Figure 4-4. Inferred clinical sensitivity of assays with different LODs to detect infected persons by any single specimen type **(A–C)**. Heatmaps show the inferred clinical sensitivity as a function of test LOD throughout the course of the infection (in four-day timebins relative to the first positive specimen of any type) for **(A)** SA specimens alone, **(B)** nasal-swab specimens alone, and **(C)** throat-swab specimens alone. Inferred clinical sensitivity was calculated as the number of specimens of the given type with viral loads greater than the given LOD divided by the total number of specimens collected within that timebin. N indicates the number of timepoints. Only timepoints where at least one specimen type had a quantifiable viral load (≥250 copies/mL) were included. Two-day timebins shown in **Supplementary Figure 4–6**. The performances of computationally-contrived combination specimen types are shown in **Supplementary Figure 4–6** and **Supplementary Figure 4–7**.

Differences in viral loads among specimen types hinders detection of presumably infectious individuals when tests utilize single specimen types

Prompt identification of individuals who are or will become infectious can prevent further transmission. We next compared the ability of each specimen type and assay analytical sensitivity to detect presumably infectious individuals. An individual was presumed to be infectious if the viral load in any specimen type collected from that participant at a given timepoint was above an infectious viral load threshold. We performed separate analyses for four well-accepted infectious viral-load thresholds (log values of 10^4 to 10^7 copies/mL) to test the robustness of our conclusions.

We found that because of the extreme differences in viral-load timecourses, a presumed non-infectious viral load in one specimen type did not reliably indicate that a participant would have presumed non-infectious viral loads in all specimen types. At the highest infectious viral-load threshold (10^7 copies/mL), a presumed non-infectious viral load in one specimen type (**Figure 4–5A**) correctly inferred the participant did not have an infectious viral load in any specimen type collected at that timepoint 70% of the time (138 of 197 timepoints). In contrast, at the lowest infectious viral-load threshold (10^4 copies/mL), a presumed non-infectious viral load in one specimen type correctly inferred a non-infectious participant only about 24% of the time (47 of 197 timepoints).

Across infectious viral-load thresholds, we saw a pattern that suggested combination specimen types might capture more presumably infectious timepoints than single specimen types (**Figure 4–5B–C**), as 90–95% of timepoints with a presumed infectious viral load in any specimen type had infectious viral loads in either nasal swab or throat swab. This complementarity suggested that a nasal–throat combination swab could be superior for detecting nearly all infectious timepoints.

We interrogated this complementarity between nasal and throat swabs by comparing the viral loads of the three specimen types at each of the 150 timepoints in which at least one specimen had viral loads above a 10^4 copies/mL infectious viral-load threshold (**Figure 4–5C**). We found that 52% of individuals with presumed non-infectious viral loads in saliva, 38% of individuals with presumed non-infectious viral loads in throat swabs, and 30% of individuals with presumed non-infectious viral loads in nasal swabs actually had presumably infectious viral loads in another specimen type at the same timepoint. In some cases, high-analytical-sensitivity testing could capture individuals with infectious viral loads in specimen types other than the one tested. However, 19% of saliva, 20% of nasal swab, and 13% of throat swab specimens had either undetectable or unquantifiable viral loads while another specimen type in the same individual had presumably infectious viral load (**Figure 4–5C**). In such cases, testing a single specimen type even with a very-high-analytical-sensitivity assay (e.g., LOD of 250 copies/mL) would not reliably detect a presumably infectious person.

Given that the infectious periods for different specimen types were often asynchronous, considering infectiousness in all three specimen types yielded a significantly longer infectious period than if only nasal viral loads were considered (**Figure 4–5D**) across all infectious viral load thresholds. We also found that the infectious period in nasal swabs and throat swabs together was longer than any other combination of two specimen types, and similar to that of all three specimen types. These results suggest that testing only single specimen types (such as nasal-swab) may fail to detect individuals with infectious viral loads in untested specimen types.

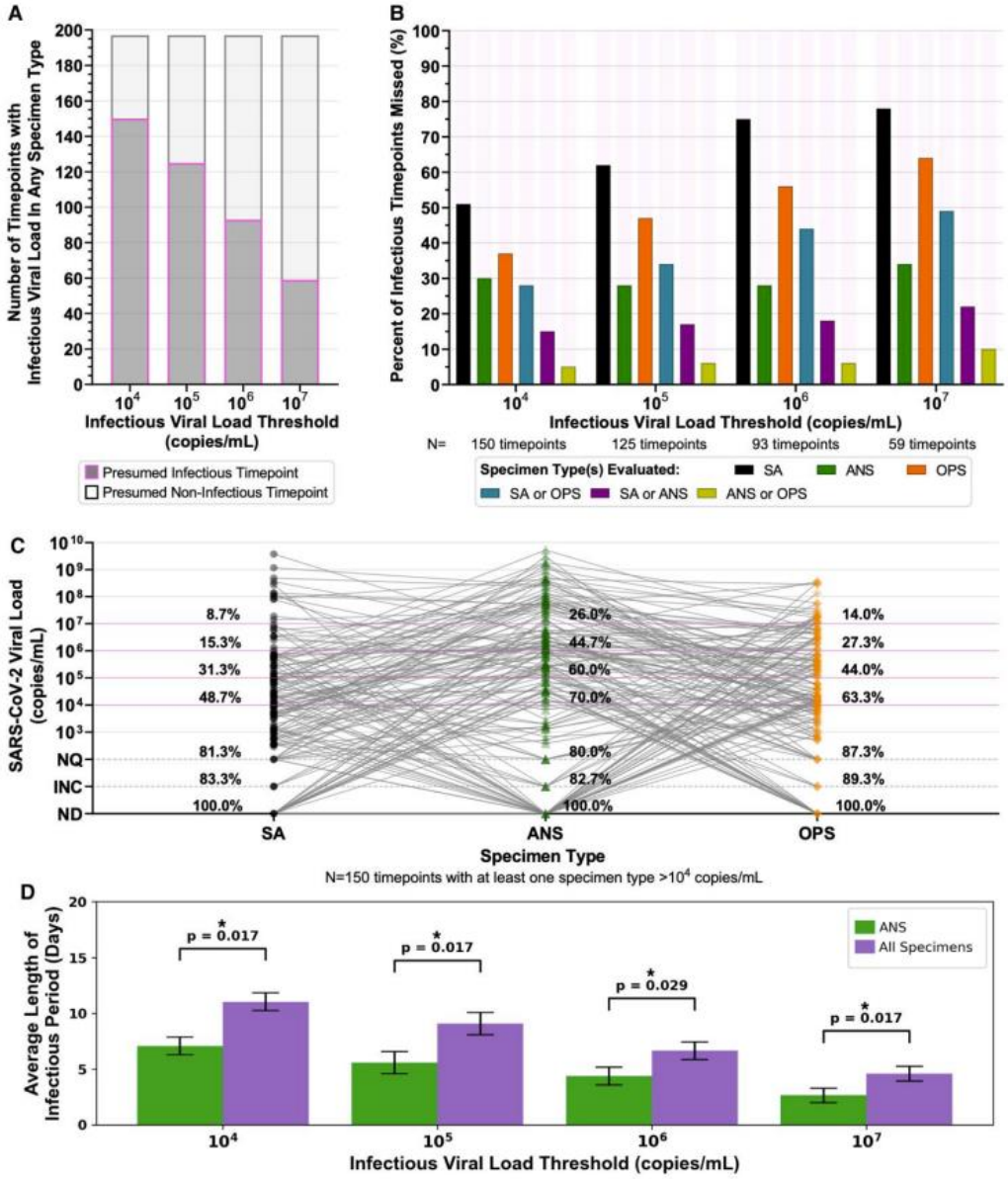

Figure 4-5. Analyses of Presumed Infectious Viral Loads in Each Specimen Type Using Different Infectious Thresholds. **(A)** Stacked bar plots of the number of timepoints with at least one specimen type above the indicated infectious viral-load threshold (dark grey with magenta outline), and where all paired specimen types collected at a timepoint had viral loads below the infectious viral-load threshold (light grey with black outline). **(B)** Each bar represents the proportion of all infectious timepoints (i.e., saliva or nasal swab or throat swab had a viral load above the infectious viral-load threshold), where the given specimen type or combination of specimen types did not have an infectious viral load. For example, with an infectious viral-load threshold of 10^4 copies/mL, 150 timepoints had an infectious viral load in at least one specimen type: in 105 of those 150 timepoints (70%), the nasal-swab (ANS) specimen had an infectious viral-load. Therefore, 30% of infectious timepoints would be missed if only the ANS specimen type were evaluated for infectious viral load. Each group of bars provides values for alternate infectious viral-load thresholds, 10^5, 10^6, and 10^7 copies/mL. **(C)** Viral loads of all three specimen types collected by each participant at the same timepoint where at least one specimen type had a viral load above 10^4 copies/mL (N=150 timepoints). Percentages above each specimen type provide the cumulative proportion of specimens with viral loads at or above each line. Magenta lines indicate possible infectious viral-load thresholds based on literature. **(D)** Average length of the infectious period when considering only presumably infectious loads in ANS (green) or when considering all specimen types (purple). Error bars are S.E.M. *P*-values were obtained by performing related-sample t-tests for each IVLT. *P*-values were adjusted using two-stage Benjamini–Hochberg correction to account for multiple hypotheses being tested. ANS, anterior-nares swab; SA, saliva; OPS, oropharyngeal swab; ND, not detected by RT-qPCR; INC, inconclusive result by RT-qPCR; NQ, not quantifiable by RT-qPCR.

Inferring detection of infectious individuals by specimen type and assay analytical sensitivity across infectious viral-load thresholds

Having observed that a person can have low viral loads in one specimen type while having high and infectious loads in another type prompted us to question how well each specimen type and assay LOD would impact the detection of infectious individuals at different stages of the infection. We binned timepoints into four-day bins and assessed the ability of each specimen type to detect presumably infectious individuals using assays with either high- (LOD 10^3 copies/mL) or low- (LOD 10^6 copies/mL) analytical sensitivity in each bin (**Figure 4–6**).

Regardless of specimen type, the inferred clinical sensitivity of both high and low-analytical-sensitivity assays to detect presumed infectious individuals typically increased as the infectious viral-load threshold increased. Improved clinical sensitivity at higher infectious viral-load thresholds was most pronounced for assays with LODs of $\geq 10^6$ copies/mL. This pattern is intuitive; specimens with viral loads above the infectious viral-load threshold but below the LOD are presumed infectious but missed by the assay, resulting in poor inferred clinical sensitivity. Increasing the infectious viral-load threshold would exclude those specimens from being presumed infectious, thereby resulting in better inferred clinical sensitivity (**Figure 4–5**).

Three major patterns in the specimen types were consistent regardless of the infectious viral-load threshold, so for simplicity, the rest of this section describes inferred clinical performances and statistical comparisons using only an infectious viral-load threshold of 10^5 copies/mL. First, even when tested with a high-analytical-sensitivity assay, no single specimen type achieved >95% inferred clinical sensitivity to detect presumed infectious individuals (**Figure 4–6A–C**). Second, because the rise in nasal-swab viral load was delayed relative to saliva or throat swab in most participants (**Figure 4–2**), nasal swabs had significantly worse performance than saliva and throat swabs during days 0-4 (**Table 4–S4BS–BU**). At an assay LOD of 10^3 copies/mL, the inferred clinical sensitivity of nasal swabs was only 57% (**Figure 4–6C**). This suggests that nasal-swab testing, even with high analytical sensitivity, would miss approximately 43% of presumed infectious individuals the first four days of infection. Third, from days 4–8 of infection, when nasal-swab viral loads increased rapidly in many participants (**Figure 4–2, Figure 4–4**), nasal swabs had significantly higher inferred clinical sensitivity regardless of LOD (**Figure 4–6C,H–J; Table 4–S4BU,BV)** across LODs **(Table 4–S4BW–BZ)**.

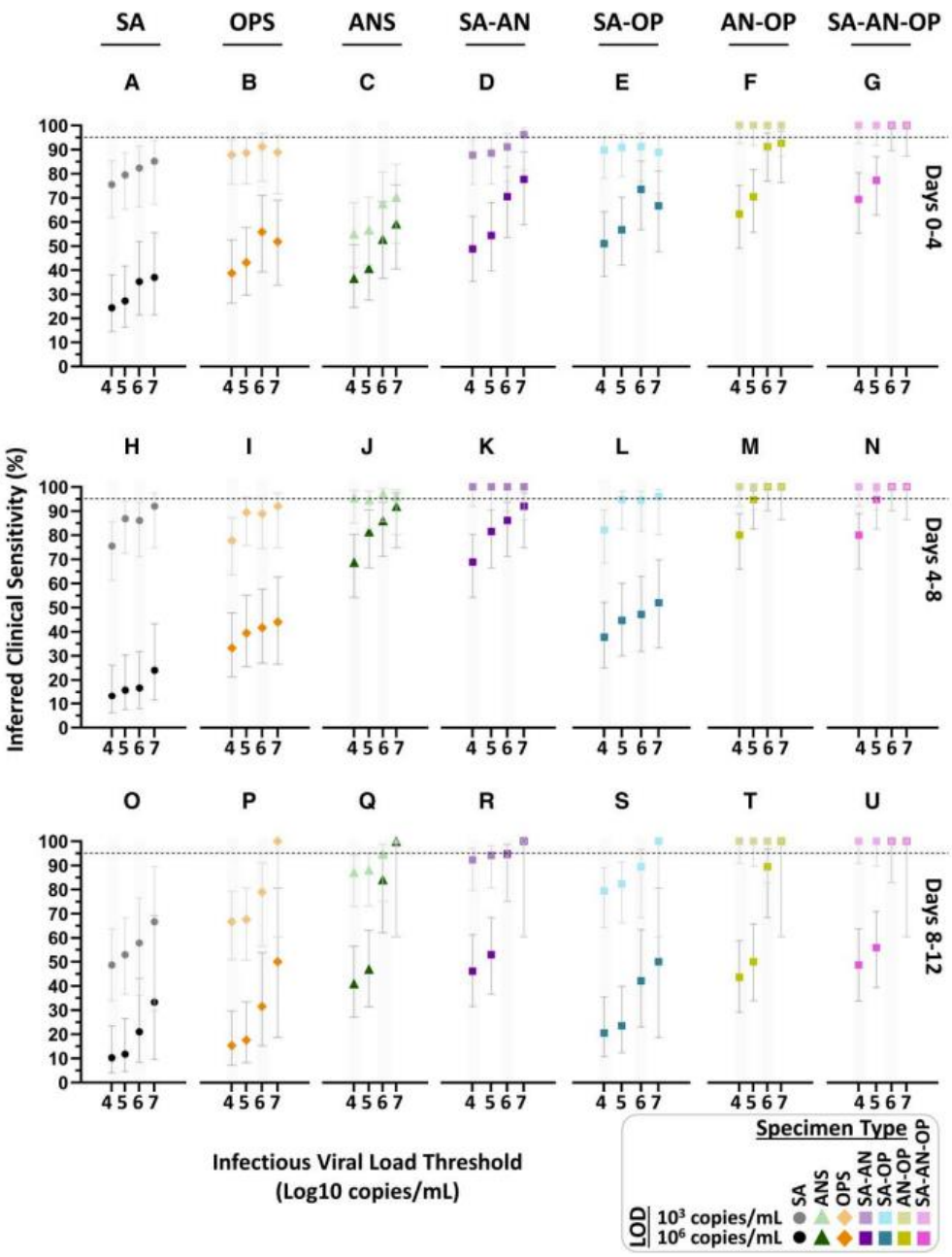

Figure 4-6. Inferred clinical sensitivity of high- and low-analytical-sensitivity assays to detect presumed infectious individuals by testing single and combination specimen types throughout acute, incident infection. For each four-day timebin relative to the first SARS-CoV-2 positive specimen (of any type), participants were classified as being presumed infectious if viral load in any specimen type collected at a given timepoint was above an infectious viral load threshold. For a high-analytical-sensitivity assay with an LOD of 103 copies/mL and low-analytical-sensitivity assay with an LOD of 106 copies/mL, the inferred clinical sensitivity was calculated as the number of specimens of that specimen type with a measured viral load at or above the LOD divided by the total specimen-collection timepoints included in that timebin. Error bars indicate the 95% C.I. The viral load of computationally-contrived combination specimen types was taken as the higher viral load of the specimen types included in the combination collected by a participant at a given timepoint. SA, saliva; ANS, anterior-nares swab; OPS, oropharyngeal (throat) swab; SA–AN, saliva-anterior-nares swab combination; SA-OP, saliva–oropharyngeal combination swab; AN–OPS, anterior-nares–oropharyngeal combination swab; SA–AN–OP, saliva-anterior-nares–oropharyngeal combination swab. Inferred clinical sensitivity for LODs from 102.4 to 108 copies/mL shown in **Supplementary Figure 4-8**; 2-day timebins are shown in **Supplementary Figure 4-9**.

Combination specimen types inferred to significantly improve clinical sensitivity to detect infected and infectious individuals

The extreme differences and lack of correlation in viral loads among specimen types as well as the poor performance of all three specimen types in all timebins and all test LODs led us to hypothesize that combination specimen types might achieve better clinical sensitivity. We generated computationally-contrived specimen types representing combinations of specimen types. For each timepoint, the viral load of a combination specimen type was the highest viral load of any single specimen type included in the combination. We then inferred the clinical sensitivity of these combination specimen types to detect infectious individuals with assays of different analytical sensitivities for each timebin (**Figure 4–4D-G**). The high clinical sensitivity of throat swabs days 0–4, and of nasal swabs at days 4–8, suggested complementarity. Complementarity was further supported by nasal and throat swabs having the most extreme differences in viral load (**Figure 4–3A,B**), and that many individuals had significantly different nasal-swab and throat-swab viral-load timecourses (**Figure 4–3D**). Moreover, rarely did individuals have infectious viral loads in saliva alone (**Figure 4–5, Table 4–S2**).

Indeed, the nasal–throat combination swab had higher clinical sensitivity to detect infected individuals than any single specimen type, at most LODs (**Figure 4–S6**). This nasal–throat combination specimen type (**Figure 4–6F**) was also inferred to perform significantly better than all single specimen types (**Figure 4–6A–C**) at detecting presumed infectious individuals during the first four days of infection, and significantly better than saliva (**Figure 4–6H,O**) and throat swab (**Figure 4–6I,P**) during later stages of infection (**Figure 4–6M,T, Table 4–S4CA–CJ**). In addition, the nasal–throat combination swab had significantly better inferred performance than nasal swabs when tested with a low-analytical-sensitivity assay during days 4–8 (**Figure 4–6J,M**). The combination of all three specimen types (**Figure 4–6G,N,U**) would by definition capture all presumed infectious individuals. However, this combination type never had a significantly higher inferred clinical sensitivity than nasal–throat combination swab (**Table 4–S4CM-CR**).

Performance of Specimen Types and Analytical Sensitivities in the Pre-infectious and Infectious Periods

For public health purposes, understanding assay performance during the pre-infectious and infectious periods, rather than in timebins relative to the rarely-captured incidence of infection, is more informative and actionable. Therefore, we next evaluated the performance of each single specimen type and the nasal–throat combination swab for each assay LOD during the presumed pre-infectious and infectious periods (**Figure 4–7**). To ensure our conclusions were robust, we compared the results of our analysis across three definitions of the infectious period: a “continuous” infectious period, an “instantaneous” infectious period), and a “day [0–5]” infectious period (only the first five days after an initial presumed infectious specimen (see Methods).

At all infectious viral-load thresholds above 10^5 copies/mL, the nasal–throat combination swab had the highest inferred clinical sensitivity of any specimen type to detect pre-infectious individuals (**Figure 4–7E,I,M**). In all cases where the assay LOD was at least two orders of magnitude lower than the infectious viral-load threshold, there were more than 10 detectable specimens available for comparison of inferred clinical sensitivity, and nasal–throat combination swab was inferred to perform significantly better than nasal swab alone (**Table 4–S4CS-DT**). With an infectious viral load threshold of 10^4 copies/mL, fewer pre-infectious timepoints were available for analysis. In this case, we see that nasal swabs had very low performance, but no specimen type emerged as optimal (**Figure 4–7A**).

Three additional trends held across all infectious viral-load thresholds and all definitions of the infectious period. First, nasal swabs had similar performance to saliva and throat swabs when testing with high-analytical-sensitivity assays (LODs at or below 10^3 copies/mL), except when infectious period is defined as the five days following the first infectious specimen. This definition selects earlier timepoints, prior to the rise in nasal swab viral loads (**Figure 4–2**, **Figure 4–5C**) so nasal swab testing had lower inferred clinical sensitivity to detect both infected (**Figure 4–4B**) and infectious (**Figure 4–6C**) individuals. Second, as noted previously (**Figure 4–4**), nasal swab performance for the detection of infectious individuals was more robust to differences in assay LOD than saliva and throat swabs because nasal-swab loads tended to be either very low or very high ($>10^6$ copies/mL), whereas saliva and throat swabs tended to fluctuate between 10^4 to 10^7 copies/mL (**Figure 4–S1D,E**). Furthermore, in all but one comparison (**Figure 4–7D**) nasal swabs were inferred to have higher performance than saliva or throat swab alone when tested with lower analytical sensitivity assays (LODs at and above 10^5 copies/mL). Third, a nasal–throat combination swab always had the highest inferred clinical sensitivity at all LODs.

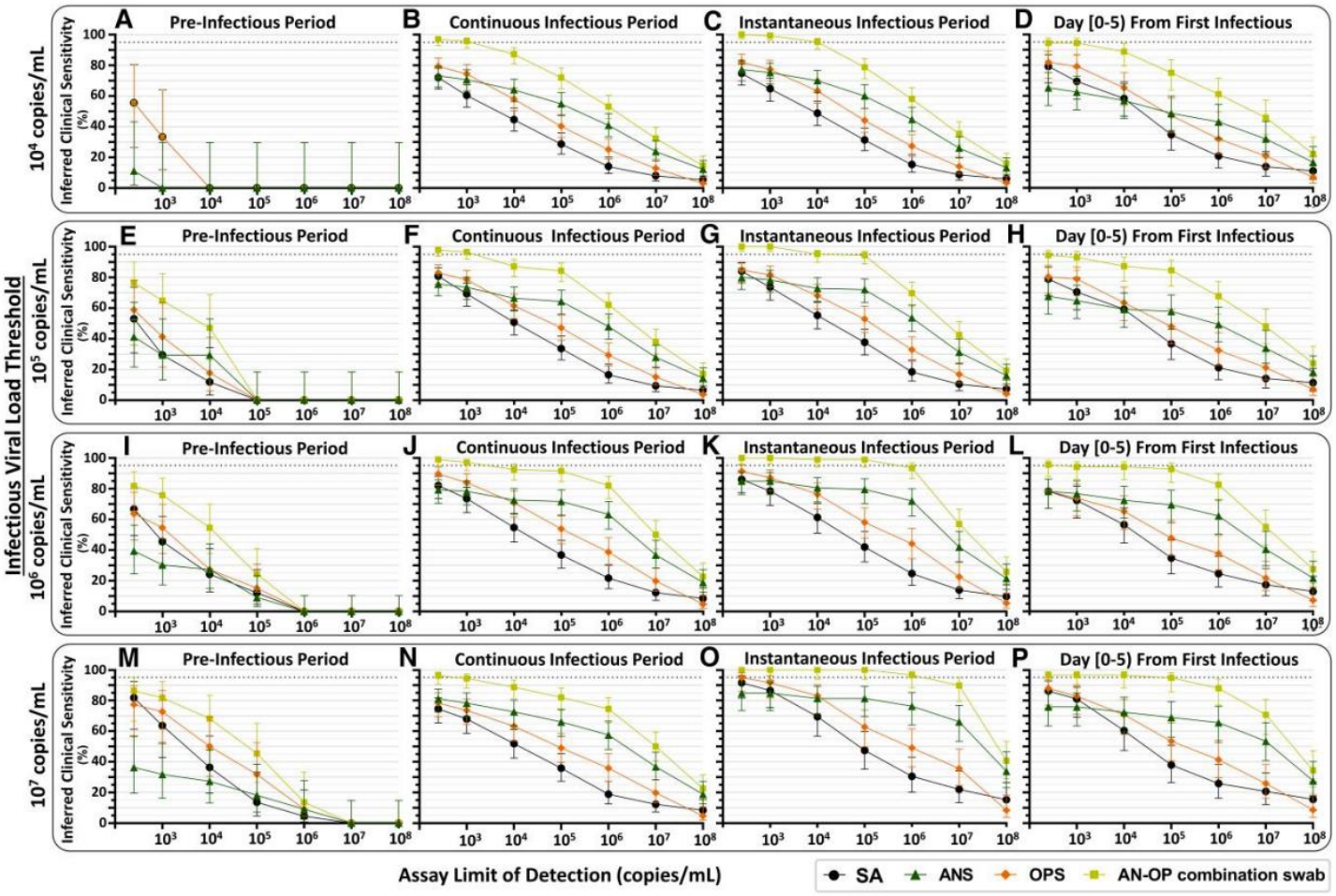

Figure 4-7. Inferred detection of presumed pre-infectious and infectious individuals at a range of test LODs and with single-specimen tests or AN–OP combination swab specimen type. For each participant, the pre-infectious period was defined as all timepoints with quantifiable SARS-CoV-2 viral load before the first timepoint when at least one specimen type had a viral load above the indicated infectious viral load threshold. We then used three different, common definitions for the infectious period, to assess the robustness of our conclusions. First, we used a "continuous infectious period" whereby a participant is presumed infectious for all timepoints between the first specimen with an infectious viral load and the first timepoint after which no specimens had infectious viral loads. Second, we used an "instantaneous infectious period," which presumes that a participant is infectious only at timepoints when viral load in at least one specimen type is above the infectious viral load threshold. Third, we presumed that a participant is infectious only for the first five days from their first timepoint when at least one specimen type had a viral load above the infectious viral load threshold. These three types of infectious periods were determined for each infectious viral-load threshold: 10^4, 10^5, 10^6, and 10^7 copies/mL. Each panel provides the inferred clinical performance to detect pre-infectious or infectious individuals, using a given specimen type, for a given assay LOD. Inferred clinical sensitivity was calculated as the number of specimens of each type with a viral load above the assay LOD, divided by the total number of specimens of that type in that period of infection. N indicates the total number of specimens of each type included in the inferred clinical sensitivity calculation. Dotted line indicates 95% inferred clinical sensitivity. SA, saliva; ANS, anterior-nares swab; OPS, oropharyngeal swab; AN–OP combination swab, predicted combined anterior-nares–oropharyngeal swab specimen type.

Discussion

In 14 individuals enrolled before or at the incidence of acute infection, we observed extreme and statistically significant differences in SARS-CoV-2 viral loads among three common respiratory specimen types (saliva, anterior-nares [nasal] swab, and oropharyngeal [throat] swab) collected at the same timepoint from the same individual. In all 14 individuals we also observed that the viral-load measurements in different specimen types followed significantly different longitudinal timecourses. These intra-participant differences were as extreme as those observed between participants (**Figure 4–3C-D**). The differences in viral load resulted in significantly different inferred clinical sensitivities to detect both infected and infectious individuals depending on the infection stage, specimen type, and analytical sensitivity (LOD) of the assay. We conclude that unlike infections where a single specimen type is typically sampled to test for virus (e.g., HIV in blood), SARS-CoV-2 viral load only describes the state of the specimen type tested, not the general state of the individual's infection. A person can have high and presumably infectious viral loads in one specimen type but low or even undetectable loads in another specimen type at the same time point. Thus, defining infectiousness based on assessment of only one specimen type(32, 33, 35, 37, 38, 66–71) likely underestimates the full infectious period, particularly if only nasal swabs (which typically exhibit infectious viral loads days after oral specimen types) are used. Relatedly, policies guiding isolation time that are based on estimates of the infectious period from a single specimen type may result in premature release of infectious individuals from isolation. Our results also suggest that field evaluations of diagnostics to detect infectious individuals that use a single specimen type as the comparator assay(67, 72–78) are likely to overestimate the clinical sensitivity of the test being evaluated. Additionally, consideration of infectiousness in multiple specimen types may further elucidate the mechanism behind interpersonal heterogeneity in SARS-CoV-2 transmission to contacts (including super-spreader events)(79).

Because of the extreme differences in viral-load patterns in the early and pre-infectious periods of infection, of the three specimen types considered here, none is optimal for detecting Omicron. However, nasal swab was the poorest specimen type for detection in the first four days of infection. In most participants, we observed a delay in nasal-swab viral loads relative to oral specimens similar to what has been observed previously(14, 22, 80) with earlier SARS-CoV-2 variants. In our study, 12 of 14 participants (86%) were either negative in nasal-swab specimens or had nasal-swab viral loads below 250 copies/mL at the incidence of infection (the first day viral RNA was detected in any specimen type). In three of these 12 participants (25%), nasal-swab viral loads were either undetectable or inconclusive for more than five days (**Figure 4–1B,C,H**). Because of the delay in nasal-swab viral loads in the first days of infection, the inferred clinical sensitivity of nasal swabs at the beginning of infection was low (<60%), even with high-analytical-sensitivity assays. Although clinical sensitivity of nasal swabs improves later in the infection, which likely coincides with the period after symptom onset in some individuals, the resulting poor clinical sensitivity of nasal swabs raises concerns about the performance of

diagnostic tests that use nasal specimens as well as diagnostic assays that have been validated against reference tests that use only nasal specimens.

Furthermore, we found that low-analytical-sensitivity testing was inferred to have poor performance for early detection of infected individuals, regardless of the specimen type used. High-analytical-sensitivity assays (LODs $\leq 10^3$ copies/mL) were inferred to improve clinical sensitivity in all specimen types and at all stages of infection. We also found that even with high-analytical-sensitivity testing, none of the three specimen types considered here were optimal for detection of presumed infectious individuals (based on viral-load thresholds of 10^4 to 10^7 copies/mL or greater in any specimen type). Of the three single specimen types, nasal-swab testing was inferred to miss the lowest proportion of presumed infectious individuals overall; yet nasal swabs still missed at least a quarter of all presumably infectious timepoints because of high viral loads in oral specimen types (**Figure 4–5–4–7**). The failure to detect presumed infectious individuals was inferred to be even worse when using tests of low analytical sensitivity. To assess this point directly, daily rapid antigen testing results for a broader cohort from this study population are reported separately(55).

Testing with combination specimen types (e.g., sampling from both the throat and nose) was inferred to yield significantly improved clinical sensitivity to detect both infected (**Figure 4–S6, 4–S7**) and presumed infectious individuals (**Figure 4–6–4–7**) than any single specimen type, regardless of whether the combination specimen type was assumed to have the maximum or the average viral load of constituent specimen types (**Figure 4–S7**). Combination swabs have high acceptability(81), and are already common in many regions of the world. In the U.K., the National Health Service website even states that PCR tests that rely only on nasal swabbing will be "less accurate" than those with a combined nose and tonsil swab(53, 54). The U.K. also uses a combination nasal–throat swab for rapid antigen testing. However, despite hundreds of emergency use authorizations (EUAs) that the U.S. FDA has issued for diagnostics that detect SARS-CoV-2(82), including 280 molecular tests and 51 antigen rapid diagnostic tests, none use a combination specimen type.

Our results explain why studies comparing single and oral-nasal combination specimen types have generally shown that combination specimens are either equivalent(26, 83–87) or superior(88–93) to single specimens. Importantly, in nearly all studies evaluating the use of combination swabs, or evaluating combination swab antigen rapid diagnostic tests using a combination swab RT-PCR as reference(33, 51), sample collection began *after* the onset of COVID-like symptoms and/or *after* an initial positive test (usually by nasal swab); thus, they likely did not sample the earliest days of infection, which is the period when we found the greatest benefit of sampling with saliva or a throat swab. One prospective cohort study that did begin testing early (using pre-symptomatic and asymptomatic close contacts) and used combination oropharyngeal–nasal swabs with an RT-qPCR assay as reference to evaluate two antigen rapid diagnostic tests(40) found a similar clinical sensitivity to

detect presumed infectious individuals (~85–90%) with this combination swab specimen type as what we inferred for a combination swab specimen type based on the viral loads in each specimen type individually tested with a moderate- or low-analytical-sensitivity assay. Additionally, longitudinal viral-load timecourses from the incidence of infection in combination nasal–throat specimens have been obtained for participants in a studied that utilized a similar design(41). This combination swab specimen type likely detected infected individuals, despite the heterogeneity that our data suggest would exist between viral loads in each individual specimen type. Infectious virus was also present in this combination swab specimen type early in the course of the infection, which our data suggest would have been missed if only the nose had been sampled.

We note four main study limitations. First, although this is the most comprehensive study of complete viral loads in multiple specimen types to date, data are from a limited number of individuals and demographics. Obtaining early viral-load timecourses from these 14 individuals required enrollment and daily testing of 228 participants for a total of 6,825 RT-qPCR tests. Future studies for new SARS-CoV-2 variants and new respiratory viruses should ideally involve multi-institution partnerships to enroll a diverse cohort from a broad geographic range. Second, we presumed infectiousness based on viral-load thresholds in three specimen types; we did not perform viral culture on these specimens (and acknowledge that specimen types not collected here could have contained infectious viral loads(94)). Third, other specimen types, such as nasopharyngeal swabs, may exhibit different viral-load timecourses and correlate with other specimen types(10). Finally, Omicron remains a relevant variant more than a year after its emergence, but additional variants will continue to develop and may exhibit different patterns in their viral-load timecourses by specimen type. Similar studies will be needed to identify optimal testing methods for new variants (and emerging respiratory viruses).

Viral loads are used in many clinical and basic-science contexts, including diagnostics, epidemiological models, clinical trials, and studies of human immune response. Our results show that early in SARS-CoV-2 infection, viral load cannot be defined for a person, only for a specific specimen type within a person. Thus, when viral-load studies or viral-detection studies are performed with only single specimen type, the results should be interpreted while considering the heterogeneity of viral loads across specimen types. Additional quantitative longitudinal studies of differences in viral loads in multiple specimen types starting immediately at the incidence of infection are needed for new emerging variants and new respiratory viruses. In the absence of such studies, combination specimen types and tests with high analytical sensitivity are likely to be the most robust approaches for earliest detection and for the design of studies seeking to assess infection status or presence of infectious virus.

Acknowledgments

This work was funded in part by a grant from the Ronald and Maxine Linde Center for New Initiatives at the California Institute of Technology (to RFI), a grant from the Jacobs Institute for Molecular Engineering for Medicine at the California Institute of Technology (to RFI), and a DGSOM Geffen Fellowship at the University of California, Los Angeles (to AVW). We sincerely thank the study participants for making this work possible. We thank Lauriane Quenee, Grace Fisher-Adams, Junie Hildebrandt, Megan Hayashi, RuthAnne Bevier, Chantal D'Apuzzo, Ralph Adolphs, Victor Rivera, Steve Chapman, Gary Waters, Leonard Edwards, Gaylene Ursua, Cynthia Ramos, and Shannon Yamashita for their assistance and advice on study implementation and/or administration. We thank Jessica Leong, Ojas Pradhan, Si Hyung Jin, Emily Savela, Bridget Yang, Ekta Patel, Hsiuchen Chen , Paresh Samantaray, Zeynep Turan, Cindy Kim, Trinity Lee, Vanessa Mechan, Katherine Stiefel, Rosie Zedan, Rahulijeet Chadha, Minkyo Lee, and Jenny Ji for volunteering their time to help with this study. We thank Prabhu Gounder, Tony Chang, Jennifer Howes, and Nari Shin for their support with recruitment. Finally, we thank all the case investigators and contact tracers at the Pasadena Public Health Department and Caltech Student Wellness Services for their efforts in study recruitment and their work in the pandemic response. This manuscript was posted on the preprint server medRxiv at https://www.medrxiv.org/content/10.1101/2022.07.13.22277113v2.

Data and materials availability

The data underlying the results presented in the study can be accessed at CaltechDATA:

https://data.caltech.edu/records/20223.

References

1. Elie B, *et al.* (2022) Variant-specific SARS-CoV-2 within-host kinetics. *J. Med. Virol.* 94(8):3625-3633.

2. Laajaj R, *et al.* (2022) Understanding how socioeconomic inequalities drive inequalities in COVID-19 infections. *Sci. Rep.* 12(1):8269.

3. Hart WS, Maini PK, & Thompson RN (2021) High infectiousness immediately before COVID-19 symptom onset highlights the importance of continued contact tracing. *eLife* 10:e65534.

4. NIH (2021) Therapeutic Management of Adults With COVID-19. https://www.covid19treatmentguidelines.nih.gov/therapeutic-management/.

5. Beigel JH, *et al.* (2020) Remdesivir for the Treatment of Covid-19 — Final Report. *N. Engl. J. Med.* 383(19):1813-1826.

6. Libster R, *et al.* (2020) Prevention of severe COVID-19 in the elderly by early high-titer plasma. *medRxiv*:2020.2011.2020.20234013.

7. Kim Y-g, *et al.* (2017) Comparison between Saliva and Nasopharyngeal Swab Specimens for Detection of Respiratory Viruses by Multiplex Reverse Transcription-PCR. *J. Clin. Microbiol.* 55(1):226.

8. Liu J, *et al.* (2021) SARS-CoV-2 cell tropism and multiorgan infection. *Cell Discovery* 7(1):17.

9. Huang N, *et al.* (2021) SARS-CoV-2 infection of the oral cavity and saliva. *Nat. Med.* 27(5):892-903.

10. Huber M, *et al.* (2021) High Efficacy of Saliva in Detecting SARS-CoV-2 by RT-PCR in Adults and Children. *Microorganisms.* 9(3). 10.3390/microorganisms9030642.

11. Hayden MK, *et al.* (2022) The Infectious Diseases Society of America Guidelines on the Diagnosis of COVID-19: Antigen Testing. *IDSA* v.2 updated 12/20/2022.

12. Marais G, *et al.* (2021) Saliva swabs are the preferred sample for Omicron detection. *medRxiv*:2021.2012.2022.21268246.

13. Chu CY, *et al.* (2021) Performance of saliva and mid-turbinate swabs for detection of the beta variant in South Africa. *The Lancet Infectious Diseases* 21(10):1354.

14. Savela ES, *et al.* (2021) Quantitative SARS-CoV-2 viral-load curves in paired saliva and nasal swabs inform appropriate respiratory sampling site and analytical test sensitivity required for earliest viral detection. *J. Clin. Microbiol.* 0(ja):JCM.01785-01721.

15. Lin J, *et al.* (2022) Where is Omicron? Comparison of SARS-CoV-2 RT-PCR and Antigen Test Sensitivity at Commonly Sampled Anatomic Sites Over the Course of Disease. *medRxiv*:2022.2002.2008.22270685.

16. Galliez Rafael M, *et al.* (Evaluation of the Panbio COVID-19 Antigen Rapid Diagnostic Test in Subjects Infected with Omicron Using Different Specimens. *Microbiology Spectrum* 0(0):e01250-01222.

17. Killingley B, *et al.* (2022) Safety, tolerability and viral kinetics during SARS-CoV-2 human challenge in young adults. *Nat. Med.* 28(5):1031-1041.

18. Adamson B, Sikka R, Wyllie AL, & Premsrirut P (2022) Discordant SARS-CoV-2 PCR and Rapid Antigen Test Results When Infectious: A December 2021 Occupational Case Series. *medRxiv*:2022.2001.2004.22268770.

19. Binnicker MJ (2022) Should I Use a Throat Swab for My At-Home COVID-19 Antigen Test? in *Forbes*.

20. Arnaout R, *et al.* (2021) The Limit of Detection Matters: The Case for Benchmarking Severe Acute Respiratory Syndrome Coronavirus 2 Testing. *Clin. Infect. Dis.* 73(9):e3042-e3046.

21. Winnett A, *et al.* (2020) SARS-CoV-2 Viral Load in Saliva Rises Gradually and to Moderate Levels in Some Humans. *medRxiv*:2020.2012.2009.20239467.

22. Lai J, *et al.* (2022) Comparison of Saliva and Mid-Turbinate Swabs for Detection of COVID-19. *medRxiv*:2021.2012.2001.21267147.

23. European Centre for Disease Prevention and Control (2022) Diagnostic Testing and Screening for SARS-CoV-2.

24. Drain PK (2022) Rapid Diagnostic Testing for SARS-CoV-2. *N. Engl. J. Med.* 386(3):264-272.

25. Rader B, *et al.* (2022) Use of At-Home COVID-19 Tests - United States, August 23, 2021-March 12, 2022. *MMWR Morb. Mortal. Wkly. Rep.* 71(13):489-494.

26. Wölfel R, *et al.* (2020) Virological assessment of hospitalized patients with COVID-2019. *Nature* 581(7809):465-469.

27. Ke R, *et al.* (2022) Daily longitudinal sampling of SARS-CoV-2 infection reveals substantial heterogeneity in infectiousness. *Nature Microbiology* 7(5):640-652.

28. Walsh KA, *et al.* (2020) SARS-CoV-2 detection, viral load and infectivity over the course of an infection. *The Journal of infection* 81(3):357-371.

29. Rhoads DD & Pinsky BA (2021) The Truth about SARS-CoV-2 Cycle Threshold Values Is Rarely Pure and Never Simple. *Clin. Chem.* 68(1):16-18.

30. Poon KS & Wen-Sim Tee N (2021) Caveats of Reporting Cycle Threshold Values from Severe Acute Respiratory Syndrome Coronavirus 2 (SARS-CoV-2) Qualitative Polymerase Chain Reaction Assays: A Molecular Diagnostic Laboratory Perspective. *Clin. Infect. Dis.* 73(9):e2851-e2852.

31. van Kampen JJA, *et al.* (2021) Duration and key determinants of infectious virus shedding in hospitalized patients with coronavirus disease-2019 (COVID-19). *Nature communications* 12(1):267.

32. Perera R, *et al.* (2020) SARS-CoV-2 Virus Culture and Subgenomic RNA for Respiratory Specimens from Patients with Mild Coronavirus Disease. *Emerg. Infect. Dis.* 26(11):2701-2704.

33. Pickering S, *et al.* (2021) Comparative performance of SARS-CoV-2 lateral flow antigen tests and association with detection of infectious virus in clinical specimens: a single-centre laboratory evaluation study. *Lancet Microbe* 2(9):e461-e471.

34. L'Huillier AG, Torriani G, Pigny F, Kaiser L, & Eckerle I (2020) Culture-Competent SARS-CoV-2 in Nasopharynx of Symptomatic Neonates, Children, and Adolescents. *Emerg Infect Dis.* 26(10).

35. Jones Terry C, *et al.* (2021) Estimating infectiousness throughout SARS-CoV-2 infection course. *Science* 373(6551):eabi5273.

36. Quicke K, *et al.* (2020) Longitudinal Surveillance for SARS-CoV-2 RNA Among Asymptomatic Staff in Five Colorado Skilled Nursing Facilities: Epidemiologic, Virologic and Sequence Analysis. *medRxiv*:2020.2006.2008.20125989.

37. Puhach O, *et al.* (2022) Infectious viral load in unvaccinated and vaccinated patients infected with SARS-CoV-2 WT, Delta and Omicron. *medRxiv*:2022.2001.2010.22269010.

38. Bal A, *et al.* (2020) Clinical and microbiological assessments of COVID-19 in healthcare workers: a prospective longitudinal study. *medRxiv*:2020.2011.2004.20225862.

39. Holmdahl I, Kahn R, Hay J, Buckee CO, & Mina M (2021) Estimation of Transmission of COVID-19 in Simulated Nursing Homes With Frequent Testing and Immunity-Based Staffing. *JAMA Network Open* 4(5):e2110071.

40. Schuit E, *et al.* (2021) Diagnostic accuracy of rapid antigen tests in asymptomatic and presymptomatic close contacts of individuals with confirmed SARS-CoV-2 infection: cross sectional study. *BMJ* 374:n1676.

41. Hakki S, *et al.* (2022) Onset and window of SARS-CoV-2 infectiousness and temporal correlation with symptom onset: a prospective, longitudinal, community cohort study. *Lancet Respir Med* 10(11):1061-1073.

42. Lin Y, *et al.* (2022) Incorporating temporal distribution of population-level viral load enables real-time estimation of COVID-19 transmission. *Nat Commun* 13(1):1155.

43. Goyal A, Reeves DB, Cardozo-Ojeda EF, Schiffer JT, & Mayer BT (2021) Viral load and contact heterogeneity predict SARS-CoV-2 transmission and super-spreading events. *Elife* 10.

44. Gomez J, Prieto J, Leon E, & Rodríguez A (2021) INFEKTA—An agent-based model for transmission of infectious diseases: The COVID-19 case in Bogotá, Colombia. *PLoS One* 16(2):e0245787.

45. Mina MJ, Parker R, & Larremore DB (2020) Rethinking Covid-19 Test Sensitivity — A Strategy for Containment. *N. Engl. J. Med.*

46. Ke R, *et al.* (2022) Longitudinal analysis of SARS-CoV-2 vaccine breakthrough infections reveal limited infectious virus shedding and restricted tissue distribution. *Open Forum Infectious Diseases*:ofac192.

47. Kissler SM, *et al.* (2021) Viral dynamics of acute SARS-CoV-2 infection and applications to diagnostic and public health strategies. *PLoS Biol.* 19(7):e3001333-e3001333.

48. Kissler SM, *et al.* (2021) Viral Dynamics of SARS-CoV-2 Variants in Vaccinated and Unvaccinated Persons. *N. Engl. J. Med.* 385(26):2489-2491.

49. Stankiewicz Karita HC, *et al.* (2022) Trajectory of Viral RNA Load Among Persons With Incident SARS-CoV-2 G614 Infection (Wuhan Strain) in Association With COVID-19 Symptom Onset and Severity. *JAMA Network Open* 5(1):e2142796-e2142796.

50. Deerain J, *et al.* (2022) Assessment of the Analytical Sensitivity of 10 Lateral Flow Devices against the SARS-CoV-2 Omicron Variant. *J. Clin. Microbiol.* 60(2):e0247921-e0247921.

51. Corman VM, *et al.* (2021) Comparison of seven commercial SARS-CoV-2 rapid point-of-care antigen tests: a single-centre laboratory evaluation study. *The Lancet Microbe* 2(7):e311-e319.

52. Winnett AV, *et al.* (2022) Morning SARS-CoV-2 testing yields better detection of infection due to higher viral loads in saliva and nasal swabs upon waking. *Microbiology Spectrum*.

53. National Health Service (2021) How to use an NHS rapid lateral flow test for coronavirus (COVID-19). https://www.nhs.uk/conditions/coronavirus-covid-19/testing/how-to-do-a-test-at-home-or-at-a-test-site/how-to-do-a-rapid-lateral-flow-test/.

54. National Health Service (2021) How to use an NHS PCR test for coronavirus (COVID-19). https://www.nhs.uk/conditions/coronavirus-covid-19/testing/how-to-do-a-test-at-home-or-at-a-test-site/how-to-do-a-pcr-test/.

55. Viloria Winnett A, *et al.* (2022) Why Daily SARS-CoV-2 Nasal Rapid Antigen Testing Poorly Detects Infected and Infectious Individuals. *medRxiv*. doi: 10.1101/2022.1107.1113.22277513.

56. Zymo Research (2021) SafeCollect Saliva Collection Kit User Instruction Manual. https://files.zymoresearch.com/protocols/r1211e-dna_rna_shield_safecollect_saliva_collection_kit_user_instructions.pdf.

57. Zymo Research (2021) SafeCollect Swab Collection Kit User Instruction Manual. https://files.zymoresearch.com/protocols/r1160_r1161-dna_rna_shield_safecollect_swab_collection_kit_user_Instructions.pdf.

58. Zymo Research (2021) Quick SARS-CoV-2 rRT-PCR Kit. https://www.zymoresearch.com/products/quick-sars-cov-2-rrt-pcr-kit.

59. Cheng H-Y, *et al.* (2020) Contact Tracing Assessment of COVID-19 Transmission Dynamics in Taiwan and Risk at Different Exposure Periods Before and After Symptom Onset. *JAMA Internal Medicine* 180(9):1156-1163.

60. Rhee C, Kanjilal S, Baker M, & Klompas M (2021) Duration of Severe Acute Respiratory Syndrome Coronavirus 2 (SARS-CoV-2) Infectivity: When Is It Safe to Discontinue Isolation? *Clin. Infect. Dis.* 72(8):1467-1474.

61. CDC (2022) What We Know About Quarantine and Isolation. ed Centers for Disease C, and Prevention.

62. Bouton TC, *et al.* (2022) Viral Dynamics of Omicron and Delta Severe Acute Respiratory Syndrome Coronavirus 2 (SARS-CoV-2) Variants With Implications for Timing of Release from Isolation: A Longitudinal Cohort Study. *Clin. Infect. Dis.*:ciac510.

63. Virtanen P, *et al.* (2020) SciPy 1.0: fundamental algorithms for scientific computing in Python. *Nat. Methods* 17(3):261-272.

64. CLSI (2008) *EP12-A2 User Protocol for Evaluation of Qualitative Test Performance, 2nd edition*.

65. Levy JM, *et al.* (2021) Impact of repeated nasal sampling on detection and quantification of SARS-CoV-2. *Sci. Rep.* 11(1):14903.

66. Boucau J, *et al.* (2022) Duration of Shedding of Culturable Virus in SARS-CoV-2 Omicron (BA.1) Infection. *N. Engl. J. Med.*

67. Pray IW, *et al.* (2021) Performance of an Antigen-Based Test for Asymptomatic and Symptomatic SARS-CoV-2 Testing at Two University Campuses - Wisconsin, September-October 2020. *MMWR Morb. Mortal. Wkly. Rep.* 69(5152):1642-1647.

68. Cosimi LA, *et al.* (2022) Duration of Symptoms and Association With Positive Home Rapid Antigen Test Results After Infection With SARS-CoV-2. *JAMA Network Open* 5(8):e2225331-e2225331.

69. Bullard J, *et al.* (2020) Predicting Infectious Severe Acute Respiratory Syndrome Coronavirus 2 From Diagnostic Samples. *Clin. Infect. Dis.* 71(10):2663-2666.

70. Tom MR & Mina MJ (2020) To Interpret the SARS-CoV-2 Test, Consider the Cycle Threshold Value. *Clin. Infect. Dis.* 71(16):2252-2254.

71. Chu VT, *et al.* (2022) Comparison of Home Antigen Testing With RT-PCR and Viral Culture During the Course of SARS-CoV-2 Infection. *JAMA Internal Medicine* 182(7):701-709.

72. Bays D, *et al.* (2021) Mitigating isolation: The use of rapid antigen testing to reduce the impact of self-isolation periods. *medRxiv*:2021.2012.2023.21268326.

73. Pekosz A, *et al.* (2021) Antigen-Based Testing but Not Real-Time Polymerase Chain Reaction Correlates With Severe Acute Respiratory Syndrome Coronavirus 2 Viral Culture. *Clin. Infect. Dis.* 73(9):e2861-e2866.

74. Prince-Guerra JL, *et al.* (2021) Evaluation of Abbott BinaxNOW Rapid Antigen Test for SARS-CoV-2 Infection at Two Community-Based Testing Sites - Pima County, Arizona, November 3-17, 2020. *MMWR Morb. Mortal. Wkly. Rep.* 70(3):100-105.

75. Kirby JE, *et al.* (2023) SARS-CoV-2 antigen tests predict infectivity based on viral culture: comparison of antigen, PCR viral load, and viral culture testing on a large sample cohort. *Clin. Microbiol. Infect.* 29(1):94-100.

76. Smith RL, *et al.* (2021) Longitudinal Assessment of Diagnostic Test Performance Over the Course of Acute SARS-CoV-2 Infection. *The Journal of Infectious Diseases* 224(6):976-982.

77. Connor BA, *et al.* (2022) Comparative Effectiveness of Single vs Repeated Rapid SARS-CoV-2 Antigen Testing Among Asymptomatic Individuals in a Workplace Setting. *JAMA Network Open* 5(3):e223073-e223073.

78. Korenkov M, *et al.* (2021) Evaluation of a Rapid Antigen Test To Detect SARS-CoV-2 Infection and Identify Potentially Infectious Individuals. *J. Clin. Microbiol.* 59(9):e00896-00821.

79. Frieden TR & Lee CT (2020) Identifying and Interrupting Superspreading Events-Implications for Control of Severe Acute Respiratory Syndrome Coronavirus 2. *Emerg. Infect. Dis.* 26(6):1059-1066.

80. Wyllie AL, *et al.* (2020) Saliva is more sensitive for SARS-CoV-2 detection in COVID-19 patients than nasopharyngeal swabs. *medRxiv*:2020.2004.2016.20067835.

81. Thomas HM, *et al.* (2022) Acceptability of OP/Na swabbing for SARS-CoV-2: a prospective observational cohort surveillance study in Western Australian schools. *BMJ Open* 12(1):e055217.

82. FDA (2022) In Vitro Diagnostic EUAs - Other Tests for SARS-CoV-2.

83. LeBlanc JJ, *et al.* (2020) A combined oropharyngeal/nares swab is a suitable alternative to nasopharyngeal swabs for the detection of SARS-CoV-2. *J. Clin. Virol.* 128:104442.

84. Vlek ALM, Wesselius TS, Achterberg R, & Thijsen SFT (2021) Combined throat/nasal swab sampling for SARS-CoV-2 is equivalent to nasopharyngeal sampling. *European journal of clinical microbiology & infectious diseases : official publication of the European Society of Clinical Microbiology* 40(1):193-195.

85. Lee Rose A, *et al.* (Performance of Saliva, Oropharyngeal Swabs, and Nasal Swabs for SARS-CoV-2 Molecular Detection: a Systematic Review and Meta-analysis. *J. Clin. Microbiol.* 59(5):e02881-02820.

86. Shakir SM, *et al.* (2020) Combined Self-Collected Anterior Nasal and Oropharyngeal Specimens versus Provider-Collected Nasopharyngeal Swabs for the Detection of SARS-CoV-2. *J. Clin. Microbiol.* 59(1).

87. Desmet T, *et al.* (2021) Combined oropharyngeal/nasal swab is equivalent to nasopharyngeal sampling for SARS-CoV-2 diagnostic PCR. *BMC Microbiol.* 21(1):31.

88. Pan Y, Zhang D, Yang P, Poon LLM, & Wang Q (2020) Viral load of SARS-CoV-2 in clinical samples. *The Lancet Infectious Diseases* 20(4):411-412.

89. Yan Y, Chang L, & Wang L (2020) Laboratory testing of SARS-CoV, MERS-CoV, and SARS-CoV-2 (2019-nCoV): Current status, challenges, and countermeasures. *Rev. Med. Virol.* 30(3):e2106.

90. Mawaddah A, Gendeh HS, Lum SG, & Marina MB (2020) Upper respiratory tract sampling in COVID-19. *Malays. J. Pathol.* 42(1):23-35.

91. Manabe YC, *et al.* (2021) Self-Collected Oral Fluid Saliva Is Insensitive Compared With Nasal-Oropharyngeal Swabs in the Detection of Severe Acute Respiratory Syndrome Coronavirus 2 in Outpatients. *Open Forum Infectious Diseases* 8(2).

92. Sharma K, *et al.* (2021) Comparative analysis of various clinical specimens in detection of SARS-CoV-2 using rRT-PCR in new and follow up cases of COVID-19 infection: Quest for the best choice. *PLoS One* 16(4):e0249408.

93. Michel W, *et al.* (2021) A combined oro-nasopharyngeal swab is more sensitive than mouthwash in detecting SARS-CoV-2 by a high-throughput PCR assay. *Infection* 49(3):527-531.

94. Jeong HW, *et al.* (2020) Viable SARS-CoV-2 in various specimens from COVID-19 patients. *Clin. Microbiol. Infect.* 26(11):1520-1524.

Supplemental Materials and Methods

Study Participants

All adult participants provided written informed consent, and minors provided assent with legal guardian providing written permission. Individuals were eligible for enrollment if someone in their home had recently (within five days) become positive for SARS-CoV-2, or if they had a recent known exposure to a person suspected to be SARS-CoV-2-positive. All participants had to be six years of age or older and fluent in English.

Extraction and RT-qPCR

Participants packaged their specimens each morning for transport by medical courier to Pangea Laboratories in Tustin, CA, USA. Most specimens were received at the facility within 10 hours of collection; some specimens were received at the facility ~24–48 hours after donation due to transport delays. Most specimens were extracted and run in RT-qPCR within a few hours of arrival to the facility. Extraction and RT-qPCR operators and supervisors (at Pangea Laboratory) were blinded to which participant a specimen originated from, as well as the infection status and test results of participants.

Extraction and RT-qPCR were performed using the FDA-authorized Quick SARS-CoV-2 RT-qPCR Kit,[58] which extracts nucleic acids using the Quick-DNA/RNA Viral MagBead Kit (Zymo Research, Catalog #R2141) followed by amplification of three target regions within the SARS-CoV-2 N gene.

A specimen was considered inconclusive if the human *RNase P* Ct value was >40 or not detected. If *RNase P* had a Ct < 40, then for a SARS-CoV-2 *N* gene target Ct value <40 the sample was considered positive. If the SARS-CoV-2 target Ct value was 40-45 it was considered inconclusive, and if >45 or not detected it was considered negative.

Quantification of viral load from RT-qPCR result

To quantify viral load in RT-qPCR specimens, a nine-point standard curve was generated at Caltech using dilutions from a commercial heat-inactivated SARS-CoV-2 particles (BEI Cat. N4-52286 Lot 70034991). To achieve higher concentrations and greater dynamic range in the standard curve, volume from a participant saliva specimen previously quantified to have a viral load of 6.44×10^9 copies/mL[53] was used to generate four additional points. Diluted particles or volume from the participant specimen was spiked into pooled matrix from freshly collected SA, ANS, or OPS specimens from SARS-CoV-2 negative donors, collected as described above. Specimens were then shipped to Pangea Laboratories (concentrations blinded) for extraction and RT-qPCR testing. Three of three replicates at 250 copies/mL of specimen were detected, independently validating the reported LOD for the assay.

From the dynamic range of the standard curve (250 copies/mL to $4.50x10^8$ copies/mL), the following equations were used to convert RT-qPCR SARS-CoV-2 *N* gene Ct value to viral load in genomic copy equivalents (copies) per mL of each specimen type:

- Viral Load in copies/mL saliva = $2^{(\mathbf{Ct} - 42.374)/-0.8973}$
- Viral Load in copies/mL buffer for nasal swabs = $2^{(\mathbf{Ct} - 43.050)/-0.9282}$
- Viral Load in copies/mL buffer for oropharyngeal swabs = $2^{(\mathbf{Ct} - 43.903)/-0.9653}$

Positive specimens with viral loads that would be quantified below the assay LOD (250 copies/mL) were considered not quantifiable, as amplification and resulting Ct values become noisy at these very low viral loads.

Viral sequencing and lineage/variant determination

Whenever possible, we sequenced the putative index case's highest viral load nasal-swab specimens. When this was not possible (e.g., if the index case was not enrolled, or the index case's highest viral load nasal-swab specimen was insufficient for sequencing, or limitations in available specimen volume), we chose an alternate high viral load (viral load $<2x10^4$ copies/mL) nasal or oropharyngeal swab specimen from the index case or a secondary case in the household.

All sequencing was performed by Zymo Research at Pangea Lab using a variant ID detection workflow that closely resembles the Illumina COVDISeq™ NGS Test (EUA).[59,60] In brief, RNA extracted from samples underwent cDNA synthesis using random hexamers according to the manufacturer's recommendation (Illumina, Catalog #20043675).

The SARS-CoV-2 virus genome was amplified using primers designed to tile across the full sequence length as originally described by the ARTICnetwork (https://artic.network/ncov-2019). Amplicons containing the SARS-CoV-2 viral genome fragments were then pooled and subjected to tagmentation to further fragment and tag amplicons with adapter sequences. Adapter-tagged amplicons then underwent a second round of PCR amplification using a PCR master mix and unique index adapters. The indexed libraries were then pooled and cleaned up for downstream sequencing.

Finished libraries were sequenced on an Illumina MiniSeq using a PE 100 bp read configuration to a depth of approximately 100,000 reads per library. Illumina sequence reads were converted from bcl to fastq files, adaptor trimmed, then quality filtered using standard parameters. Variant calls as described by Phylogenetic Assignment of Named Global outbreak LINeages software 2.3.2 (github.com/cov-lineages/pangolin) were made using a custom bioinformatics data analysis pipeline developed by Zymo Research.

Shuffled viral-load timecourses and data validations

In addition to controls built into the study design (e.g., specimen have barcodes specific to each specimen type, barcodes are confirmed to be the expected specimen type when packaging specimen-collection materials prior to delivery to participants, participants take and package specimen types in a specific order during each timepoint, and the receiving laboratory assessed arriving specimen for the presence of a swab), we assessed mathematically whether the observed viral loads were likely to come from viral-load timecourses of their designated specimen type, or whether they could have been switched between specimen types. We assessed the correlation between the viral load for a given specimen at a timepoint and either the viral load in the same specimen type or the viral load from a different, randomly selected specimen type at the following timepoint (**Figure 4–S3**), for all measurements. The correlation between viral-load measurements from randomly selected specimen types is significantly different ($P<0.001$) from the correlations between viral-load measurements from the same specimen type (**Figure 4–S3C**). Erroneously assigned specimen types would yield similar ($P>0.01$) correlations for both randomized and non-randomized viral-load timecourses. The analysis showed greater standard deviation for shuffled compared with unshuffled viral-load timecourses, suggesting that all specimens were correctly assigned to specimen type by participants.

Estimations of sample noise with RNase P

To estimate expected sampling noise that would affect viral-load measurements in each specimen type, we examined RT-qPCR Ct measurements of the human *RNase P* control target in the same specimen type from each of the 14 participants in this cohort (**Figure 4–2**; **Figure 4–S4B**). The standard deviation of the *RNase P* Ct was calculated for each timecourse and then averaged over all 14 participants: the average standard deviation of *RNase P* Ct for saliva specimens was 1.37, nasal-swab specimens was 1.42, and oropharyngeal swab specimens was 1.46 (**Figure 4–S4B**). We then used the average standard deviation of *RNase P* Ct across all three specimen types (1.42 Ct) as the overall estimate of sampling noise in all viral-load measurements, which is consistent with the standard deviation (1.7 Ct) of SARS-CoV-2 *N2* gene Ct values in two MT nasal-swab specimens collected immediately in sequence in a separate study.[66]

Alternate viral load calculation for computationally contrived combination specimens

We recognize that specimen-collection and processing factors (e.g., buffer volumes, type, and carrying capacity of swabs), may cause dilution effects that would impact the viral load for combination specimen types. To account for this, we also performed an analysis where the viral load of a computationally-contrived combination specimen was calculated as the average (rather than maximum) viral load of paired single specimen types in each combination (**Figure 4–S7**). Using the average introduced at most a two- or three-fold correction for the two- or three-specimen combinations, respectively, because viral loads differed by orders of magnitude (**Figure 4–3**).

Clinical sensitivities of combination specimen types remained similar (**Figure 4–S7I-J**) to those calculated in **Figure 4–4** and the nasal–throat combination swab remained superior with this alternate calculation (**Figure 4–S7F**).

Supplemental Analyses

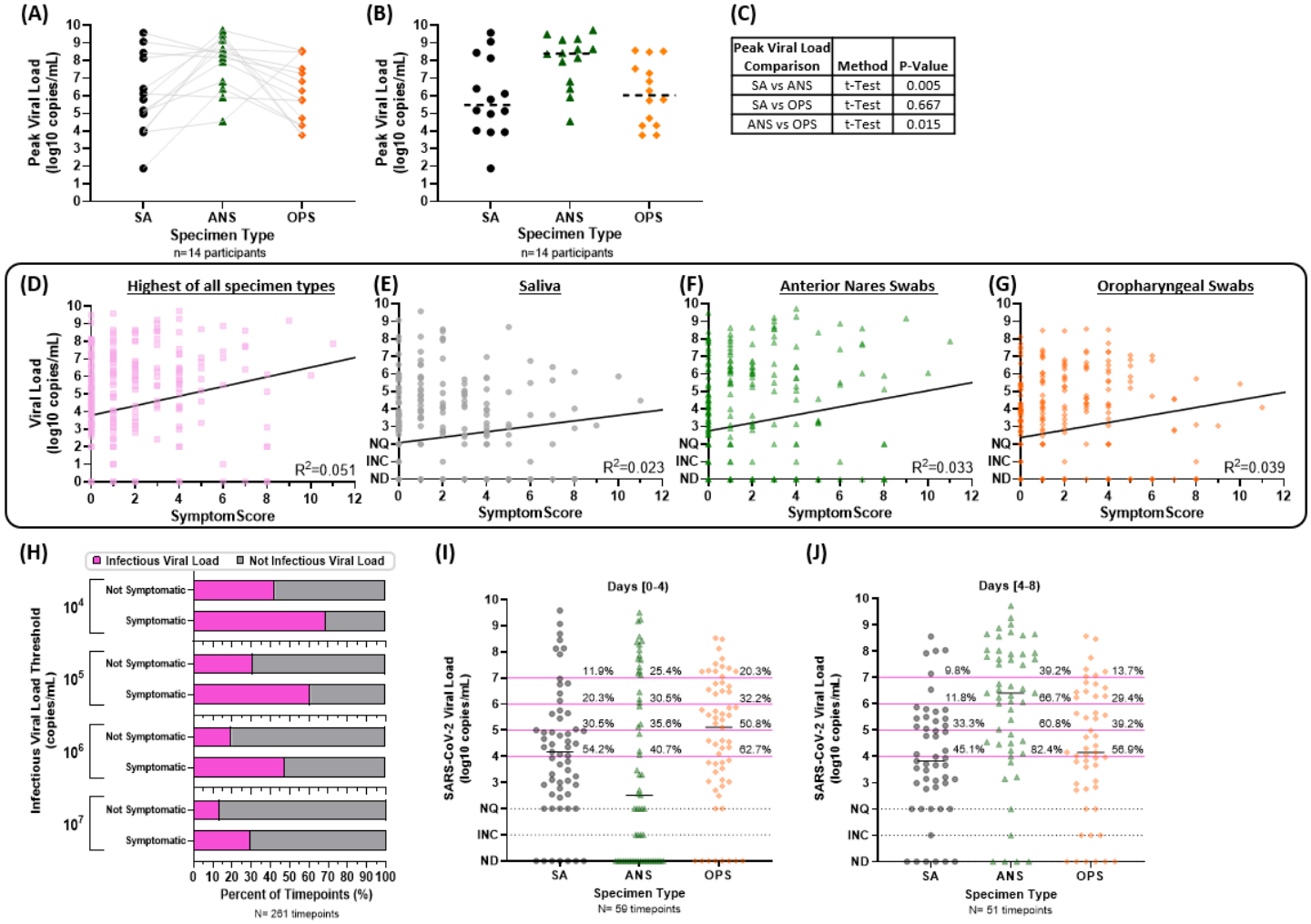

Supplemental Figure 4-1. Peak and distribution of viral loads from the 14 participants enrolled before or at the incidence of acute SARS-CoV-2 infection. **(A)** The peak viral load for each participant is plotted with lines connecting to the viral loads of the other two specimen types at the same timepoint. **(B)** The distribution of peak viral loads for each specimen type is plotted; dashed horizontal bars indicate the medians. **(C)** Table showing statistical test results for comparisons of peak viral load in each specimen type, including the test method, performed in Graphpad Prism 9.2.0. For the cohort of 14 participants enrolled before or at the incidence of infection, the total number of symptoms reported at each timepoint was considered the Symptom Score. The Symptom Score was then plotted against the **(D)** highest viral load in all specimen types, the **(E)** viral load in SA specimens **(F)** ANS specimens and **(G)** OPS specimens. The text on each plot provides the Pearson correlation R squared value, and black lines indicate the line of best fit from linear regression. **(H)** For each symptomatic (Symptom Score >0) or asymptomatic timepoint, viral loads in any specimen type above the given IVLTs were considered infectious (magenta) and those below were considered not infectious (grey). The percentage of infectious and not infectious timepoints, for either symptomatic or not symptomatic timepoints is shown as a horizontal stacked bar graph. **(I)** The distribution of viral loads measured from a positive specimen of each specimen type during the first four days and **(J)** days 4 to 8 from the incidence of infection. N indicates the number of positive specimens of each type (by our high-analytical-sensitivity assay). Percentages above magenta lines to the right of each distribution indicate the fraction of all positive specimen of that type with a viral load at or above that infectious threshold. Black horizontal lines indicate the median viral load for each specimen type. SA, saliva; ANS, anterior-nares swab; OPS, oropharyngeal swab; NQ, below quantifiable; INC, inconclusive; ND, not detected.

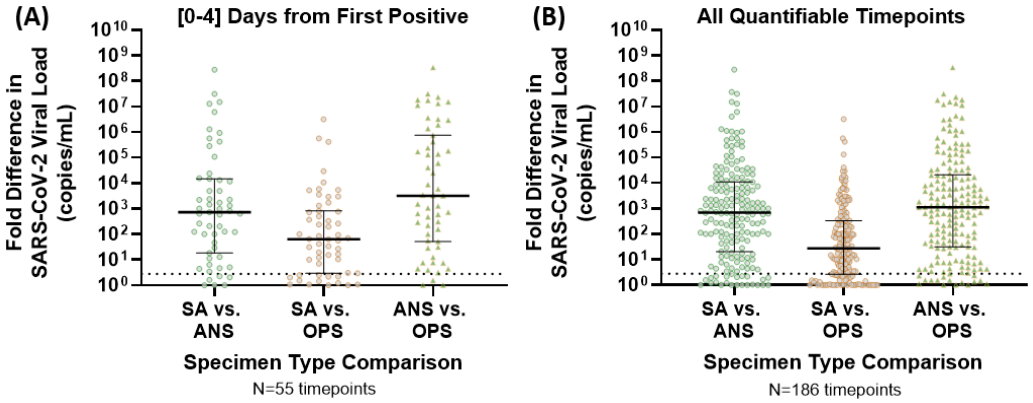

Supplemental Figure 4-2. Relative (fold) differences in viral loads from paired specimen types. The fold difference (ratio of higher viral-load specimen of one type over a lower viral-load specimen of another type from the same participant at the same specimen-collection timepoint) are shown for **(A)** the first four days of infection (relative to first positive specimen of any type) and **(B)** for specimens collected at all timepoints when at least one specimen from the participant was positive for SARS-CoV-2. Specimens negative for SARS-CoV-2 or with viral loads below quantification had a viral load of 1 copy/mL imputed for calculations. Black bar indicates median. Dashed line indicates 2.8 fold difference, the level of *RNase P* sampling noise (**Supplementary Figure 4-4**). SA, saliva; ANS, nasal anterior-nares swab; OPS. oropharyngeal swab, NQ indicates that both specimens being compared had unquantifiable viral loads so an absolute difference could not be calculated.

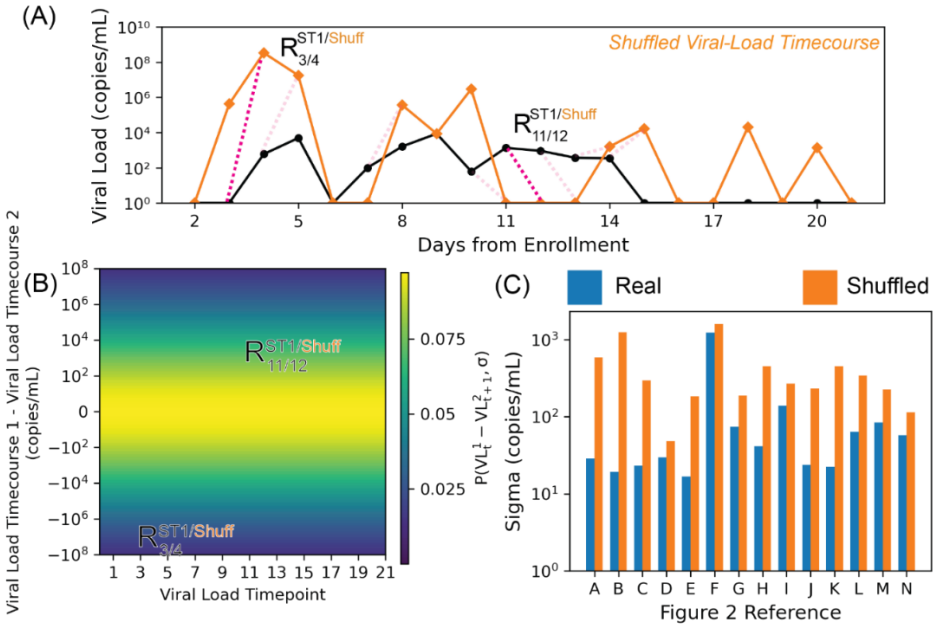

Supplemental Figure 4-3. Increased Standard Deviation for Shuffled Viral-Load Timecourses Suggests Correct Sample Assignment by Participant and Specimen Type. **(A)** Viral-load timecourses for SA specimens collected from participant B (black). A "shuffled" timecourse (orange), obtained by randomizing specimen types at every timepoint, is shown in orange. This "shuffled" timecourse represents data that would be collected if an individual collected the incorrect specimen type when submitting samples. As in Figure S2, differences between timepoints for both "shuffled" and saliva timecourses were calculated. However, the timepoint after the one used for SA is selected for the "shuffled" timecourse. **(B)** Comparisons between pairwise differences between timepoints were visualized on a heatmap. Background coloring represents the probability of observing pairwise residuals between the shuffled timecourse and the data from the saliva timecourse. Probabilities were generated from a normal distribution centered on 0 with a standard deviation (sigma) generated from the two timecourses. **(C)** Noise obtained from comparison of timecourses against themselves (blue) and shuffled equivalents (orange). Noise was estimated for each of the three specimen types for each individual. Estimates of noise from self-comparisons are statistically significantly from those obtained from comparisons with "shuffled timecourses" (P<0.001).

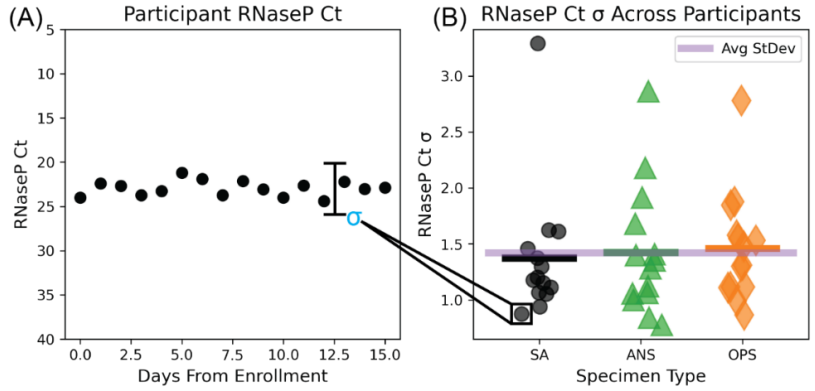

Supplemental Figure 4-4. *RNase P* as a Measure of Sampling Variation for 14 Individuals Enrolled At or Before the Incidence of Infection. **(A)** Example longitudinal *RNase P* Ct measurements from a single individual. σ represents the standard deviation of the *RNase P* timecourse for a single individual in a single specimen type. (B) *RNase P* Ct standard deviations aggregated across specimen types and over all individuals. Horizontal black, green, and orange bars denote average standard deviations for each specimen type (saliva, SA; anterior-nares swab, ANS; oropharyngeal swab, OPS) across participants; the purple horizontal bar represents the average standard deviation over all participants and all specimen types.

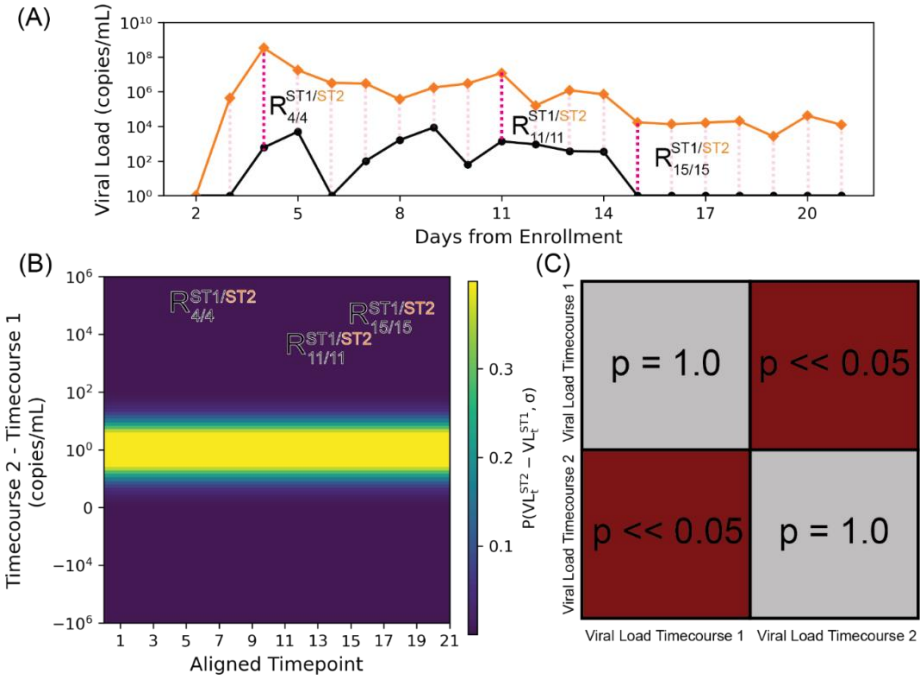

Supplemental Figure 4-5. Pairwise Comparison of Viral-Load Timecourses. **(A)** As an example, the viral-load timecourses for saliva and oropharyngeal swab specimens collected from Z144 are shown. To compare two timecourses, first, the magnitude of the differences between the two timecourses at the same timepoint were calculated. Subscripts refer to time indices and superscripts refer to specimen types. **(B)** These differences were visualized on a graph with the x-axis representing the viral loads of the first timecourse and the y-axis representing the viral loads from the second timecourse. The line y=x, representing perfect agreement between the two timecourses, is plotted in red and background coloring represents probability of observing data given the null hypothesis that the two timecourses are equal. Such probabilities are either estimated from the timecourses themselves (**Figure 4–3A**) or from noise contained in *RNase P* data (**Figure 4–3B**). **(C)** Statistical significance of differences between viral-load timecourses. Absolute differences between timecourses were compared with the magnitude of bootstrapped noise samples and statistical significance was determined via an upper-tailed hypothesis test. Statistically significant timecourses are depicted in maroon and timecourses that are not significantly different are depicted in gray.

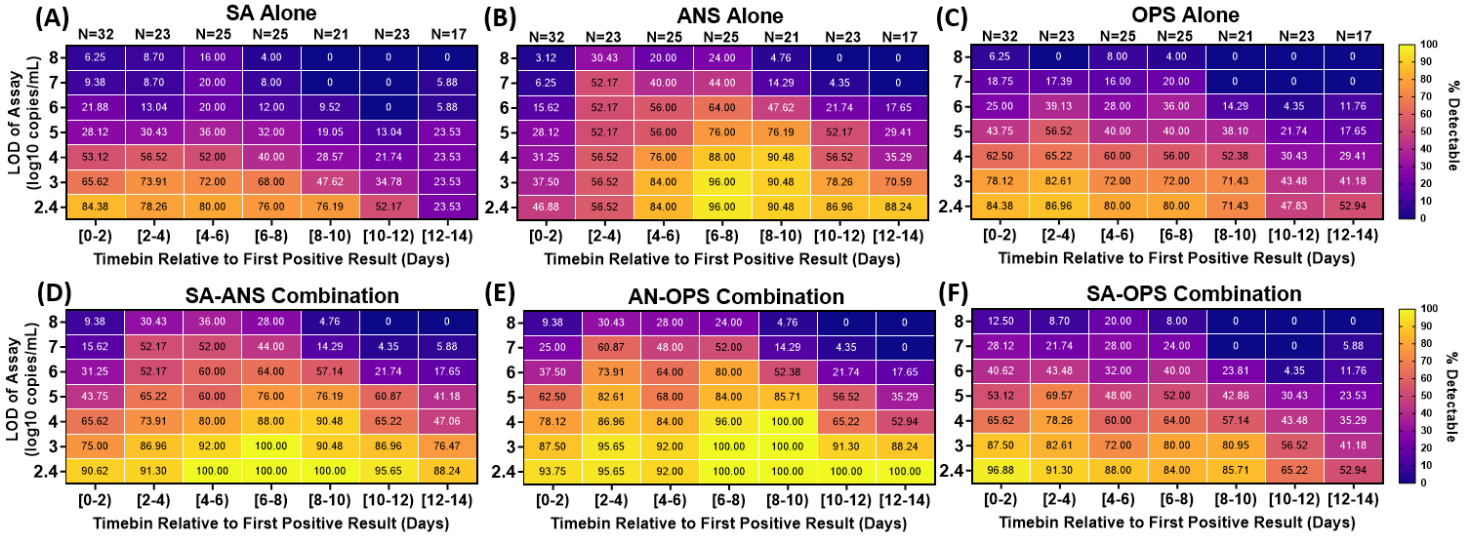

Supplemental Figure 4-6. Extreme differences in viral load between specimen types result in low clinical sensitivity to detect infected persons by any single specimen type (A–C) but improved by combination specimen types (D–G). Heatmaps show the inferred clinical sensitivity for (**A**) saliva (SA) specimens alone (**B**) anterior-nares swab (ANS) specimens alone and (**C**) oropharyngeal swab (OPS) specimens alone, throughout the course of the infection (in two-day timebins relative to the first positive specimen of any type) for varying test LODs. Inferred clinical sensitivity was calculated as the number of specimens of the given type with viral loads greater than the given LOD, divided by the total number of specimens collected within that timebin. N indicates the number of specimens for each timebin. Only timepoints where at least one specimen had a quantifiable viral load (250 copies/mL) are included. (**D**) Inferred clinical sensitivity of a computationally-contrived specimen that combines saliva and anterior-nares swab (SA–ANS), **(E)** anterior-nares–oropharyngeal swab (AN–OPS) combination, **(F)** saliva and oropharyngeal swab (SA–OPS) combination, and (**G**) all three specimen types measured. The viral load for these contrived combination specimen types is the higher viral load from the specimen types included in the combination collected by a participant at a given timepoint. SA, saliva; ANS, anterior-nares swab; OPS, oropharyngeal swab. Four-day timebins are shown in **Figure 4-4**.

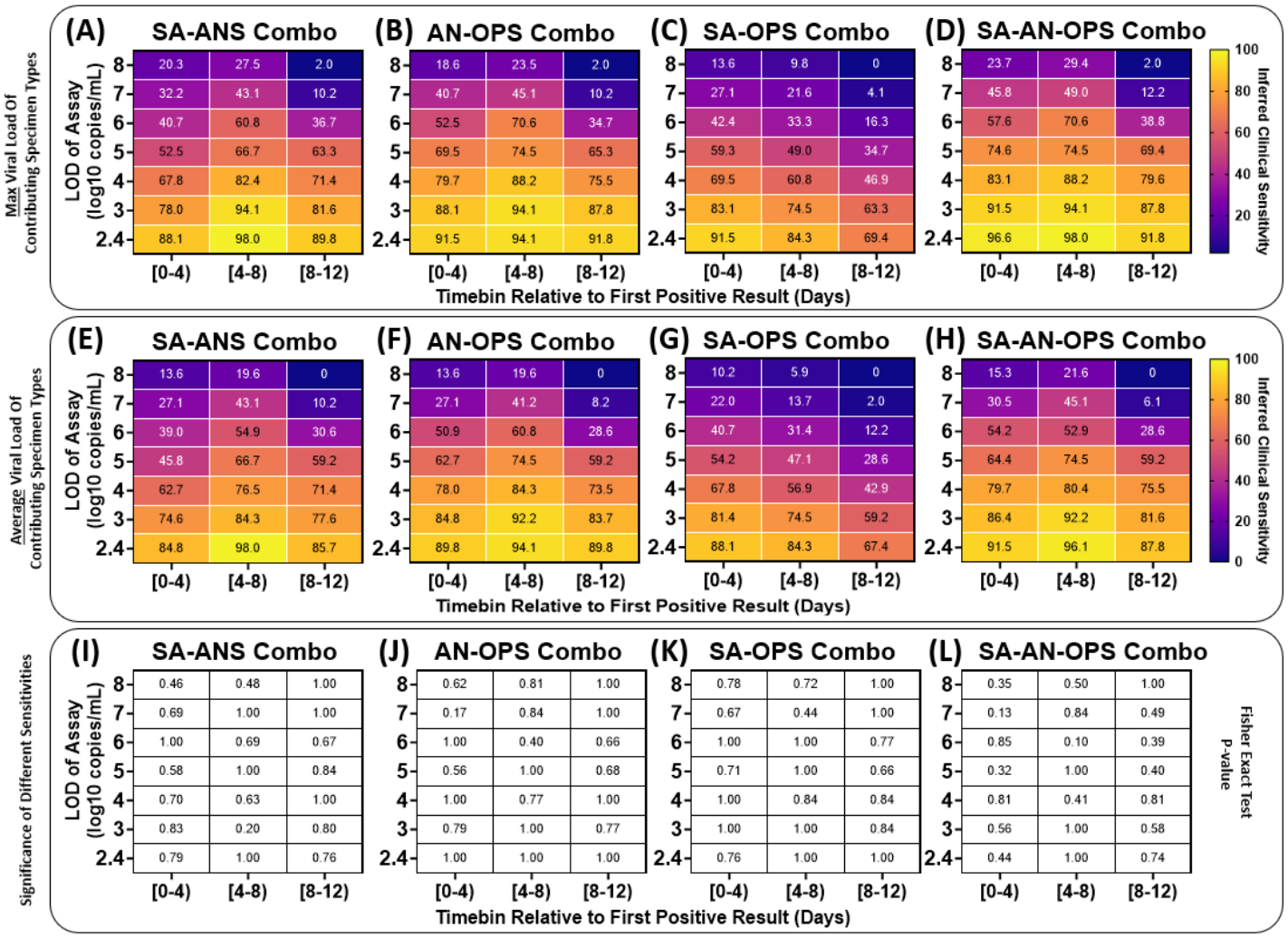

Supplemental Figure 4-7. Inferred performance of computationally-contrived combination specimen types by averaging paired single specimen viral loads is similar to taking the maximum viral load of paired single specimen viral loads. Computationally-contrived combination specimen types were generated by taking a function of the viral loads from paired single specimen types collected by a participant at a timepoint. Detection of an infected person was inferred if the viral load in the computationally-contrived specimen type was above the LOD of the assay being used for testing (y-axis). The inferred clinical sensitivity of a given combination specimen type was calculated as the proportion of specimens inferred to be detectable at a given LOD over all positive specimen during each phase of the infection relative to the incidence of infection (x-axis), Each panel provides a heatmap colored by inferred clinical sensitivity when the viral load of computationally-contrived combination specimen types is calculated as the (**A–D**) maximum or (**E–H**) average viral load of paired single specimen types included in the combination, collected by a participant at a given timepoint. The binomial proportions using each function were compared with each other for each cell in each heatmap using the one-sided Fisher Exact Test with the alternative hypothesis that the maximum function would result in greater clinical sensitivity; resulting *P*-values are provided for respective cells in (**I–L**). SA–ANS, saliva–anterior-nares swab combination specimen: AN–OPS, anterior-nares–oropharyngeal swab combination specimen; SA–OPS, saliva–oropharyngeal swab combination specimen; SA–AN–OPS, saliva–anterior-nares–oropharyngeal swab combination specimen.

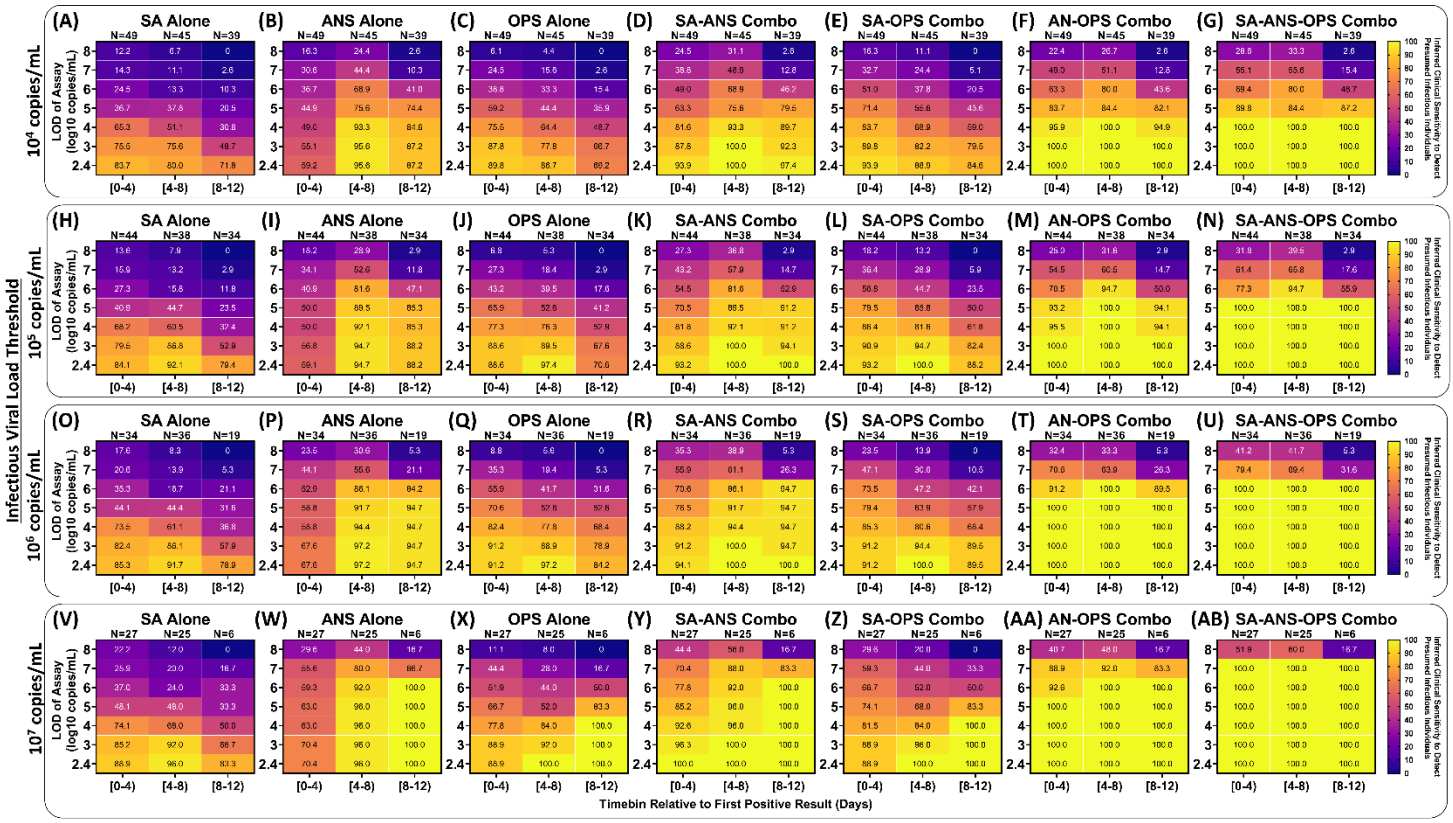

Supplemental Figure 4-8. Inferred clinical sensitivity to detect presumed infectious individuals by testing single and combination specimen types using a range of test analytical sensitivities throughout acute, incident infection. For each four-day timebin relative to the first SARS-CoV-2 positive specimen (of any type), participants were classified as being presumed infectious if viral load in any specimen type collected at a given timepoint was above an infectious viral load threshold (shown on the left side for each group of panels). The inferred clinical sensitivity of each specimen type to detect presumed infectious participants was calculated for each LOD as the number of specimens of that specimen type with a measured viral load at or above the LOD divided by the total specimen-collection timepoints included that timebin. The value inside each cell is the inferred clinical sensitivity to detect a presumed infectious person with that specimen type using an assay with the given LOD during that period of infection. The viral load of computationally- contrived combination specimen types was taken as the higher viral load of the specimen types included in the combination collected by a participant at a given timepoint. SA, saliva; ANS, anterior-nares swab; OPS, oropharyngeal swab. Two-day timebins are shown in **Supplementary Figure 4-9**.

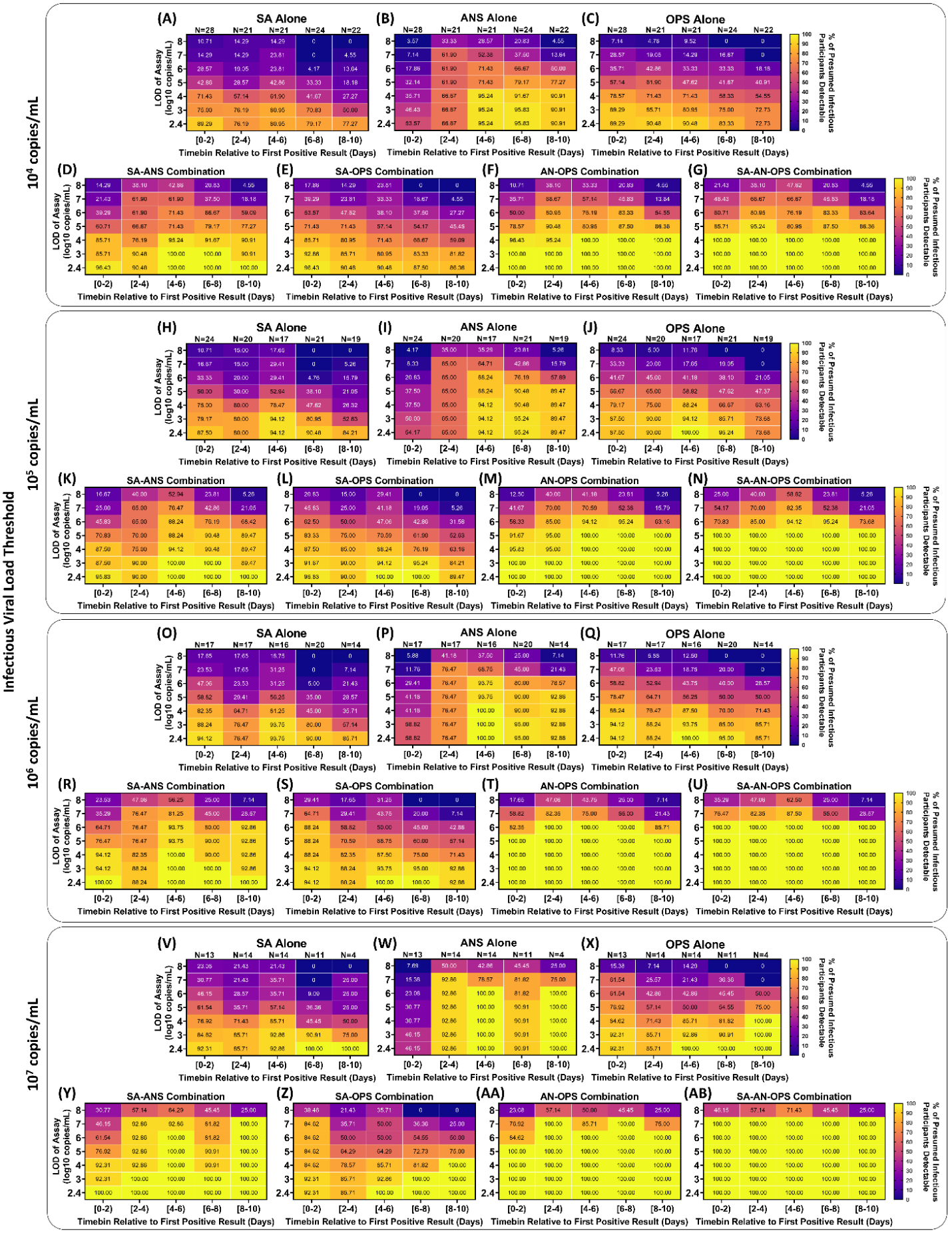
Infectious Viral Load Threshold
10⁴ copies/mL
10⁵ copies/mL
10⁶ copies/mL
10⁷ copies/mL
(A) SA Alone
(B) ANS Alone
(C) OPS Alone
(D) SA-ANS Combination
(E) SA-OPS Combination
(F) AN-OPS Combination
(G) SA-AN-OPS Combination
(H) SA Alone
(I) ANS Alone
(J) OPS Alone
(K) SA-ANS Combination
(L) SA-OPS Combination
(M) AN-OPS Combination
(N) SA-AN-OPS Combination
(O) SA Alone
(P) ANS Alone
(Q) OPS Alone
(R) SA-ANS Combination
(S) SA-OPS Combination
(T) AN-OPS Combination
(U) SA-AN-OPS Combination
(V) SA Alone
(W) ANS Alone
(X) OPS Alone
(Y) SA-ANS Combination
(Z) SA-OPS Combination
(AA) AN-OPS Combination
(AB) SA-AN-OPS Combination
LOD of Assay (log10 copies/mL)
Timebin Relative to First Positive Result (Days)
% of Presumed Infectious Participants Detectable

[Figure on prior page] **Supplemental Figure 4-9.** Inferred detection of presumed infectious individuals by single and combination specimen types and varying test analytical sensitivity throughout acute infection. For each two-day timebin relative to the first SARS-CoV-2 positive specimen (of any type), participants were classified as being presumed infectious based on whether the viral load in any specimen type collected at a given timepoint was above an infectious viral-load threshold (shown on the left side for each group of panels). The inferred clinical sensitivity of each specimen type to detect presumed infectious participants was calculated for each LOD as the number of specimens of that specimen type with a measured viral load at or above the LOD. The viral load of computationally-contrived combination specimen types was taken as the higher viral load of the specimen types included in the combination collected by a participant at a given timepoint. SA, saliva; ANS, anterior-nares swab; OPS, oropharyngeal swab. Four-day timebins are shown in **Supplementary Figure 4-8**.

Supplemental Table 4-1. Summary of the demographics, medical information, and vaccine history for the 14-participant cohort. Detailed information by participant can be found in Supp. Table 4-5.

Sex*		
Male	7	50.0%
Female	7	50.0%
Age		
6-11	2	14.3%
12-17	1	7.1%
18-29	2	14.3%
30-39	3	21.4%
40-49	4	28.6%
50-59	2	14.3%
Race		
White	11	78.6%
Asian or Pacific Islander	1	7.1%
Multiple Races	2	14.3%
Ethnicity		
Hispanic	2	14.3%
Non-Hispanic	12	85.7%
Tobacco Smoker or Vape User History		
Current	0	0.0%
Former	2	14.3%
Never	12	85.7%
Active Medications and Supplements		
Vitamins/Supplements	6	42.9%
Acetaminophen/NSAIDs	3	21.4%
Allergy medications/Antihistamines	2	14.3%
Antibiotics/Antivirals	1	7.1%
Medical Comorbidities		
Asthma	1	7.1%
Anxiety or Depression	2	14.3%
Diabetes	1	7.1%
Overweight/Obesity	6	42.9%
GI condition	2	14.3%
SARS-CoV-2 Vaccination Status		
Partially Vaccinated	1	7.1%
Completed Vaccination	5	35.7%
Fully vaccinated and boosted	8	57.1%
No SARS-CoV-2 vaccines reported	0	0.0%

*Participants were asked to report both sex at birth and current gender identity; all participants in this cohort responded cis-gender identities to sex at birth

Supplemental Table 4-2. The Number of Presumed Infectious Specimens as a Factor of Specimen Type and Infectious Viral-Load Threshold.

Specimen Type(s)	**No. Presumed Infectious Specimens (%) by Infectious Viral Load**							
	10^4 copies/mL		**10^5 copies/mL**		**10^6 copies/mL**		**10^7 copies/mL**	
SA Only	7	(4.4%)	7	(5.3%)	6	(6.5%)	6	(11%)
SA & **NS**	6	(3.9%)	8	(6%)	5	(5.4%)	3	(4.3%)
SA & **OPS**	15	(8.8%)	8	(6%)	3	(3.2%)	1	(2.9%)
SA & **NS** & **OPS**	45	(32%)	24	(20.7%)	9	(9.7%)	3	(4.3%)
NS & **OPS**	12	(11%)	14	(15%)	12	(12.9%)	4	(7.1%)
NS Only	42	(27%)	43	(31.3%)	41	(44.1%)	29	(51%)
OPS Only	23	(13%)	21	(16%)	17	(18.3%)	13	(19%)
Total		(100%)	150	(100%)	**93**	**(100%)**	70	(100%)

Supplemental Table 4-3. Times from First Positive by Any Specimen Type to First Viral Load Above Infectious Viral-Load Thresholds (IVLT) of 10^4, 10^5, 10^6, 10^7 copies/mL, and to First Timepoint with All Specimen Types Below IVLT.

Figure 2 Reference IVLT = 10^7 copies/mL	Time First Detected from Enrollment (Days)	Time to First Infectious from Enrollment (Days)	Time to Non-Infectious from Enrollment (Days)	Time to Infectious from First Positive (Days)	Time to Non-Infectious from First Positive (Days)
A	5.25	No Samples Above IVLT	No Samples Above IVLT	No Samples Above IVLT	No Samples Above IVLT
B	3.36	4.41	12.4	1.05	9.00
C	0.84	7.31	8.30	6.47	7.46
D	0.92	4.36	18.4	3.45	17.5
E	3.33	No Samples Above IVLT	No Samples Above IVLT	No Samples Above IVLT	No Samples Above IVLT
F	5.41	No Samples Above IVLT	No Samples Above IVLT	No Samples Above IVLT	No Samples Above IVLT
G	15.3	16.4	23.4	1.03	8.07
H	4.27	5.30	15.2	1.02	11.0
I	2.00	5.41	10.5	3.41	8.51
J	0.88	3.36	8.29	2.48	7.41
K	0.77	3.39	9.38	2.62	8.60
L	1.01	2.49	10.7	1.48	9.64
M	0.90	0.90	11.3	0.00	10.4
N	0.86	1.30	5.32	0.44	4.47
Figure 2 Reference IVLT = 10^6 copies/mL	Time First Detected from Enrollment (Days)	Time to First Infectious from Enrollment (Days)	Time to Non-Infectious from Enrollment (Days)	Time to Infectious from First Positive (Days)	Time to Non-Infectious from First Positive (Days)
A	5.25	12.3	18.4	7.07	13.2
B	3.36	4.41	14.3	1.05	11.0
C	0.84	7.31	9.37	6.47	8.53
D	0.92	4.36	29.2	3.45	28.3
E	3.33	10.4	14.4	7.05	11.1
F	5.41	7.42	10.5	2.01	5.11
G	15.3	16.4	24.4	1.03	9.06
H	4.27	5.30	15.2	1.02	11.0
I	2.00	5.41	10.5	3.41	8.51
J	0.88	2.28	10.4	1.41	9.47
K	0.77	1.41	10.4	0.63	9.60
L	1.01	2.49	10.7	1.48	9.64
M	0.90	0.90	11.3	0.00	10.4
N	0.86	1.30	5.32	0.44	4.47

Figure 2 Reference IVLT = 10^5 copies/mL	Time First Detected from Enrollment (Days)	Time to First Infectious from Enrollment (Days)	Time to Non-Infectious from Enrollment (Days)	Time to Infectious from First Positive (Days)	Time to Non-Infectious from First Positive (Days)
A	5.25	7.36	18.4	2.11	13.2
B	3.36	3.36	15.4	0.00	12.0
C	0.84	2.40	10.4	1.56	9.55
D	0.92	3.34	29.2	2.42	28.3
E	3.33	10.4	14.4	7.05	11.1
F	5.41	7.42	10.5	2.01	5.11
G	15.3	16.4	28.3	1.03	13.0
H	4.27	5.30	16.3	1.02	12.0
I	2.00	3.87	10.5	1.87	8.51
J	0.88	1.30	14.3	0.42	13.4
K	0.77	1.41	10.4	0.63	9.60
L	1.01	1.37	12.8	0.37	11.8
M	0.90	0.90	15.3	0.00	14.4
N	0.86	0.86	5.32	0.00	4.47
Figure 2 Reference IVLT = 10^4 copies/mL	Time First Detected from Enrollment (Days)	Time to First Infectious from Enrollment (Days)	Time to Non-Infectious from Enrollment (Days)	Time to Infectious from First Positive (Days)	Time to Non-Infectious from First Positive (Days)
A	5.25	6.29	19.4	1.04	14.1
B	3.36	3.36	21.4	0.00	18.0
C	0.84	2.4	11.3	1.56	10.5
D	0.92	3.34	29.2	2.42	28.3
E	3.33	6.38	14.4	3.04	11.1
F	5.41	7.42	12.5	2.01	7.04
G	15.3	16.4	28.3	1.03	13.0
H	4.27	5.30	16.3	1.02	12.0
I	2.00	2.00	10.5	0.00	8.51
J	0.88	1.30	14.3	0.42	13.4
K	0.77	0.77	11.4	0.00	10.6
L	1.01	1.01	13.7	0.00	12.7
M	0.9	0.90	15.3	0.00	14.4
N	0.86	0.86	8.4	0.00	7.53

Supplemental Table 4-4. Statistical comparisons of inferred clinical sensitivity drawn from **Figure 4–7**. For select comparisons (across specimen types, assay LODs, infection stages/timebins, or IVLTs), the comparison is stated, along with the inferred clinical sensitivity (with 95% Confidence Intervals), statistical method, and significance of the difference. Index is referenced in the main text. Bolded cells in each row indicate the groups being compared. Values under Contingency Table indicate number of specimens. "Infectious" indicates timepoints from individuals with a viral load in any specimen type above the infectious viral-load threshold listed in parentheses. Test Methods: A- Lower-Tailed McNemar Exact Test, B- Upper-Tailed McNemar Exact Test, C- Two-Tailed McNemar Exact Test, D- Lower-Tailed Fisher Exact Test. SA, saliva; ANS, anterior-nares swab; OPS, oropharyngeal swab; AN–OP, anterior-nares–oropharyngeal combination swab; SA–ANS, saliva–anterior-nares combination specimen; SA–OPS, saliva–oropharyngeal swab combination specimen; SA–ANS–OPS, saliva–anterior-nares–oropharyngeal swab combination specimen.

Supplemental Table 4-5. Demographic and Medical Information for the Participants Shown in Figure 4-3. SARS-CoV-2 variant was determined by ANS swab in all cases except individual (B) who had low ANS viral loads so viral load was sequenced from a throat swab. The variant for participant (I) is inferred from the household index case.

Fig 3 panel	Status on enrollment			Months* since vaccine #			Active Medications	Comorbidities/ medical conditions	Gender**	Age range (in years)	Race	Ethnicity	SARS-CoV-2 Variant
	Saliva PCR	Throat PCR	Nasal PCR	1st dose	2nd dose	3rd dose							
(A)	**neg**	**neg**	**neg**	9 [M]	8 [M]	<2 [M]	n/a	n/a	male	40-49	White	not Hispanic	Omicron BA.1.1
(B)	**neg**	**neg**	**neg**	11 [JJ]	3 [P]	none	PPI, vitamin/ supplement	obesity, GI condition, anxiety or depression	female	30-39	White	not Hispanic	Omicron BA.1.1
(C)	**inc**	**neg**	**neg**	<1 [P]	none	none	acetaminophen	n/a	male	6-11	Multiple Races	not Hispanic	Omicron BA.1.1
(D)	**neg**	**neg**	**neg**	10 [M]	9 [M]	2 [M]	none	obesity	male	30-39	Asian or Pacific Islander	not Hispanic	Omicron BA.1.1
(E)	**neg**	**neg**	**neg**	>11 [P]	<10 [P]	<3 [P]	allergy medication; acetaminophen, antihistamine, dextromethorphan, phenylephrine HCl, doxylamine	obesity	female	30-39	White	Hispanic	Omicron BA.1
(F)	**neg**	**neg**	**neg**	10 [P]	9 [P]	none	vitamin/ supplement	n/a	female	18-29	White	not Hispanic	Omicron BA.1.1
(G)	**neg**	**neg**	**neg**	<2 [P]	<1 [P]	none	vitamin/ supplement	n/a	male	6-11	White	not Hispanic	Omicron BA.1.1
(H)	**neg**	**neg**	**neg**	10 [M]	9 [M]	2 [M]	vitamin/ supplement	n/a	female	40-49	White	not Hispanic	Omicron BA.1.1
(I)	**neg**	**neg**	**neg**	10 [P]	9 [P]	none	antibiotic, vitamin/ supplement	obesity	male	18-29	White	Hispanic	Omicron BA.1.1 (index case)
(J)	*pos*	*pos*	**inc**	9 [M]	8 [M]	<2 [M]	vitamin/ supplement	anxiety or depression	female	40-49	White	not Hispanic	Omicron BA.1.1
(K)	*pos*	*pos*	**inc**	9.5 [M]	8.5 [M]	0.5 [P]	NSAID	n/a	male	40-49	White	not Hispanic	Omicron BA.1.1
(L)	*pos*	*pos*	*pos*	11 [P]	10 [P]	2 [P]	allergy medication, diabetes medication, cholesterol medication	diabetes, high blood pressure, obesity, asthma, sleep apnea, GI condition	female	50-59	Multiple Races	not Hispanic	Omicron BA.1.1
(M)	*pos*	*pos*	**neg**	10 [M]	9 [M]	2 [M]	SSRI	oveweight, anxiety or depression	male	50-59	White	not Hispanic	Omicron BA.1.1
(N)	*pos*	**neg**	*pos*	5 [P]	4[P]	none	none	n/a	female	12-17	White	not Hispanic	Omicron BA.1.1

* Months from vaccine date are given relative to enrollment date

Vaccine abbreviations: [P], Pfizer-BioNTech COVID-19 Vaccine (COMIRNATY); [M], Moderna COVID-19 Vaccine (Spikevax); [JJ], Johnson & Johnson

NQ, not quantifiable; viral load was below the test LOD (250 SARS-CoV-2 RNA copies/mL)

** Participants were asked to report both sex at birth and current gender identity; all participants in this cohort responded cis-gender identities to sex at birth

Author Contributions (listed alphabetically by last name):

Reid Akana (RA): Collaborated with AVW in creating digital participant symptom surveys; assisted with data quality control/curation with NS, HD, SC; created current laboratory information management system (LIMS) for specimen logging and tracking. Creation of iOS application for sample logging/tracking. Configured an SQL database for data storage. Created an Apache server and websites to view study data. Configured FTPS server to catalog PCR data. Wrote a Python package to access study data. Trained study coordinators on SQL. Troubleshooting and QC of LIMS. Made Figure 3(C-D) and 5D, and SI Figs S3, S4, S5, Table S2, S3, S4, S5, S6. Wrote and edited the manuscript with AVW and NS.

Alyssa M. Carter (AMC): Assisted with the inventory and archiving of >6,000 samples at Caltech; coordinated shipment of samples to Caltech with AER and JRBR; assisted with procurement of antigen tests; assisted with organizing volunteers and making participant kits; assisted AER in developing and implementing QC for participant kits. Provided feedback and edited the manuscript.

Yap Ching Chew (YCC): Primary liaison with Caltech team. Prepared and provided Zymo SafeCollect kits and related materials to Caltech team. Supervised the extraction, PCR, and QC teams at Pangea Laboratory. Sent PCR results daily to Caltech team. Arranged for Pangea team to perform viral-variant sequencing on selected samples; reported results and provided sequencing files.

Saharai Caldera (SC): Study coordinator; recruited, enrolled and maintained study participants with NS and HD; study-data quality control, curation and archiving with RA, NS, HD and MKK; supplies acquisition with AER, NS, HD and MKK.

Hannah Davich (HD): Lead study coordinator; co-wrote participant informational sheets with NS; developed recruitment strategies and did outreach with NS; participant kit creation and co-coordinated kit-making by volunteers with AER; recruited, enrolled and maintained study participants with NS and SC; managed the study-coordinator inventory; study-data quality control, curation and archiving with RA, NS, SC and MKK; supplies acquisition with AER, NS, SC and MKK.

Matthew Feaster (MF): Co-investigator; collaborated with AVW, MMC, NS, YG, RFI on study design and recruitment strategies; provided guidance and expertise on SARS-CoV-2 epidemiology and local trends.

Ying-Ying Goh (Y-YG): Co-investigator; collaborated with AVW, MMC, NS, MF, RFI on study design and recruitment strategies; provided guidance and expertise on SARS-CoV-2 epidemiology and local trends.

Rustem F. Ismagilov (RFI): Principal investigator; collaborated with AVW, MMC, NS, MF, YYG on study design and recruitment strategies; provided leadership, technical guidance, oversight of all analyses, and was responsible for obtaining the primary funding for the study.

Mi Kyung Kim (MKK): Study coordinator (part-time); maintained participants with NS, HD, and SC; study-data quality control, curation and archiving with RA, NS, SC and HD; supplies acquisition with AER, NS, SC and HD; collected contact info for local university/college student health centers for recruitment; assembled Table S5 with NS.

John Raymond B. Reyna (JRBR): Organized sample labeling and short-term storage of all samples at Pangea Laboratories. Arranged shipment of all samples to Caltech team. Assisted with processing of the specimens.

Anna E. Romano (AER): Co-coordinated kit-making by volunteers with HD; implemented QC process for kit-making; participated in kit-making; managed logistics for the inventory and archiving of >6,000 samples at Caltech; supplies acquisition with HD, NS, SC and MKK; assisted with securing funding; compiled Table S3; organized and performed QC on sequencing data. Provided feedback and edited the manuscript.

Natasha Shelby (NS): Study administrator; collaborated with AVW, RFI, YG, MF on initial study design and recruitment strategies; co-wrote IRB protocol and informed consent with AVW; co-wrote enrollment questionnaire and post-study questionnaire with AVW; initiated the collaboration with Zymo and served as primary liaison throughout study; reviewed pilot sampling data and amended instructional sheets/graphics for specimen collections in collaboration with Zymo; co-wrote participant informational sheets with HD; hired, trained, and supervised the study-coordinator team; developed recruitment strategies and did outreach with HD; recruited, enrolled and maintained study participants with HD and SC; co-developed participant keep/drop criteria with AVW; performed the daily upload, review, and QC of PCR data received from Zymo; made the daily keep/drop decisions based on viral-load trajectories in each household; made all phone calls to alert presumptive positives of their status and provide resources; study-data quality control, curation and archiving with RA, HD, SC and MKK; organized archiving of all participant data and antigen-test photographs; supplies acquisition with AER, HD, SC and MKK; assisted with securing funding; managed the overall study budget; assembled Figs 1-2 with AVW; assembled Table S2; assembled Table S5 with MKK; managed citations and reference library; verified the underlying data with AVW and RA; co-wrote and edited the manuscript with AVW and RA.

Matt Thomson (MT): Assisted with statistical approach and analyses.

Colten Tognazzini (CT): Coordinated the recruitment efforts at PPHD with case investigators and contact tracers; provided guidance and expertise on SARS-CoV-2 epidemiology and local trends.

Alexander Viloria Winnett (AVW): Collaborated with NS, RFI, YG, MF on initial study design and recruitment strategies; co-wrote IRB protocol and informed consent with NS; co-wrote enrollment questionnaire and post-study questionnaire with NS; co-developed participant keep/drop criteria with NS; funding acquisition; designed and coordinated LOD validation experiments; selected and prepared specimen for viral-variant

sequencing with NS, YC, and AER; assisted with the inventory and archiving of >6,000 specimen at Caltech with AER and AMC; minor role supporting outreach by HD and NS; minor role supporting kit-making by AER, HD and AMC; verified the underlying data with NS and RA; assembled Figs 1-2 with NS; performed analysis and prepared Figs 4-7, Table S1, Figure S1, S2, S6, S7, S8, S9. Major contributor to the selection of references. Co-wrote and edited the manuscript with NS and RA.

Taikun Yamada (TY): Performed the RT-qPCR COVID-19 testing at Pangea Laboratory.

Chapter 5

THE RATIO BETWEEN SARS-COV-2 RNA VIRAL LOAD AND CULTURABLE VIRAL TITER DIFFERS DEPENDING ON STAGE OF INFECTION

This chapter was originally published in Porter MK, Viloria Winnett A, Hao L, Shelby N, Reyes JA, Schlenker NW, Romano AE, Tognazzini C, Feaster M, Goh YY, Gale M, Ismagilov RF. The ratio between SARS-CoV-2 RNA viral load and culturable viral titer differs depending on stage of infection (Nov 2023). Access Microbiology. https://doi.org/10.1099/acmi.0.000732.v1.

Abstract

Analysis of incident, longitudinal RNA viral loads in saliva and nasal swabs and culturable viral titers in nasal swabs collected twice-daily by a tricenarian male infected with SARS-CoV-2 revealed the ratio between viral load and viral titer can be five orders of magnitude higher during early infection than late infection.

Introduction

Throughout the COVID-19 pandemic, the relationship between the detection of viral RNA and replication-competent virus has been used as guiding evidence for infection-control strategies. For example, studies suggesting that low viral load specimens are unlikely to have observable replication-competent virus (1) were used to argue that low-analytical-sensitivity antigen tests (which only detect high viral loads (2)) would more specifically identify infectious individuals (3, 4). Additionally, the lack of replication-competent virus in specimens collected more than a week after symptom onset (5–10) was used as evidence to release individuals from isolation despite persistently detectable viral RNA (11).

Assessment of replication-competent virus in clinical specimens is technically challenging (12) and therefore not routinely performed to determine whether an individual is infectious. Rather, the studies which have generated viral-culture data are often applied broadly to guide infection-control strategies (13). However, the design of such studies influences the data, conclusions, and resulting policies.

Many studies that assess presence of replication-competent virus in specimens from individuals with SARS-CoV-2 infection are primarily cross-sectional, include data from only one specimen type, and are biased toward specimens collected late in the course of infection (e.g., after symptom onset) (4, 14–18). However, during the earliest phase of infection, detection of infected individuals can help reduce subsequent transmission (19, 20) and improve clinical outcomes (21). Few studies report viral loads starting from the incidence of acute SARS-CoV-2 infection (13, 22–29), and of these, few report both viral-load and viral-culture data (25, 27). If studies of replication-competent virus during SARS-CoV-2 infection are insufficiently representative of early infection, resulting infection control policies may not be optimally effective.

As part of the Caltech COVID-19 Study (23, 24, 30), we attempted to fill this gap by capturing both viral load and viral titer measurements longitudinally from the incidence of acute SARS-CoV-2 infection in a subset of participants at risk of becoming infected. Within this subset, one individual was found to have incident infection with the B.1.243 lineage of SARS-CoV-2 while enrolled and collecting twice-daily specimens, from which we measured both

anterior-nares (nasal) swab viral load and viral titer. This participant also collected saliva specimens for viral-load measurements. SARS-CoV-2 *N* gene viral loads and human *RNaseP* marker Cq values in saliva and nasal swab specimens from this individual (Participant AC) have previously been reported (30). Here, we provide additional quantifications of SARS-CoV-2 *E* and *RdRp* gene viral loads and viral-titer measurements from this participant's nasal-swab specimens to investigate the relationship of RNA viral load and infectious virus longitudinally from the incidence of naturally acquired infection.

Results

We report the case (**Figure 5-1A**) of a 30–39-year-old male (Participant AC), who does not smoke/vape and is otherwise healthy (no chronic medical conditions and self-reported health as "very good"). The participant did not report evidence of prior SARS-CoV-2 infection nor receipt of any SARS-CoV-2 vaccine doses. The participant reported taking Vitamin C and fish oil supplements, and no other medications. In late-January 2021, six days prior to enrollment in this study, the participant reported exposure to SARS-CoV-2. Three days prior to enrollment, the participant began experiencing a sore throat, but two days prior to enrollment tested negative on an outpatient, non-rapid nasopharyngeal test. At this time, a household contact of Participant AC (Participant AB, **Figure 5-S1**) tested positive, prompting eligibility of Participant AB and AC for enrollment in this study.

Upon enrollment, Participant AC had detectable and rising salivary viral loads, but was negative in anterior-nares nasal-swab specimens collected over the next day. During this time, the participant remained symptomatic with only a sore throat. In the subsequent day the participant developed shortness of breath and low ($<10^5$copies/mL) nasal viral loads without replication-competent virus detected by culture. After this point, the participant's nasal swab specimens achieved high ($>10^7$ copies/mL) viral loads and high ($>10^6$ TCID50/mL) viral titers for approximately three days before gradually declining. Throughout this time, headaches, cough, congestion, change in taste/smell, muscle aches, and one event of severe nausea were reported, all of which resolved before completion of enrollment.

Cross-sectional SARS-CoV-2 viral loads from different gene targets in nasal swab specimens correlated closely with each other (**Figure 5-1A, Figure 5-S2A**) and the relationship between viral loads from different gene targets remained proportional throughout the course of infection (**Figure 5-S2B**). Cross-sectional analysis of viral load and viral titer revealed that only high viral load nasal swab specimens ($>10^8$ *N* cp/mL) would contain replication competent virus (**Figure 5-1B**). Additionally, saliva viral load is less distinguishable between samples with and without replication competent virus in nasal swab specimens (**Figure 5-1B**). However, longitudinal analysis revealed that the ratio of nasal swab viral load and viral titer changed by over five orders of magnitude throughout the course of acute infection (**Figure 5-1C**). This relationship indicates that RNA viral load alone, without

considering infection stage, may not represent whether a specimen or a person is likely to be infectious or not.

Discussion

High-frequency nasal swab and saliva sampling from the incidence of infection, and paired measurements of viral load and viral titer in nasal swab specimens revealed four key findings uniquely enabled by this study design.

First, saliva exhibited higher *N* gene viral loads than in nasal swabs for approximately the first two days of incident infection, after which nasal swab viral loads rose and remained subsequently higher than saliva viral loads. This supports previous observations that SARS-CoV-2 often presents first in oral specimen types before anterior nares swabs (23, 24), and that testing a single specimen type (e.g., nasal swabs) may yield false negative results during early infection.

Second, replication-competent virus was observed in nasal swabs at many timepoints when saliva viral loads were low. This suggests that the low viral load of one specimen type is not necessarily indicative of the absence of replication-competent virus in another specimen type.

Third, nasal-swab viral-load measurements from different gene targets (*N*, *E*, and *RdRP* genes) correlated strongly with each other longitudinally, such that measurement of any one viral RNA target was indicative of other viral RNA targets (31).

Fourth, we note that the ratio between RNA viral load and culturable viral titer in nasal swabs decreased substantially (greater than five orders of magnitude) through the first week of infection. Cross-sectional analyses of data from Participant AC and in other studies (4, 15, 18, 25, 32) have suggested a correlation between viral load and the presence of infectious virus. However, these cross-sectional analyses overlook that the relationship between viral load and infectious virus is dynamic, and that early viral loads are more indicative of viral titer than viral loads later in the infection. Therefore, earlier in the infection, individuals with lower viral loads could actually be more infectious than expected based on cross-sectional data.

Data from a SARS-CoV-2 human challenge study (25) supported these conclusions (**Figure 5-S3**). In that study, 36 human participants were inoculated intranasally with 10 $TCID_{50}$ virus, and 18 participants had subsequent sustained detectable infection. We reanalyzed longitudinal nasal swab viral load and viral culture data graciously provided by the study authors to compare to what was observed in Participant AC's naturally acquired infection. Indeed, among specimens with replication-competent virus, the average ratio between viral titer and viral load at each timepoint

after inoculation decreased by nearly four orders of magnitude in the five days following inoculation.

Taken together, these results caution against conclusions about infectiousness that assume a constant ratio of RNA viral load and culturable viral titer, commonly inferred based on cross-sectional data or from single specimen types (4, 33–35). Assuming a constant ratio of RNA viral load and culturable viral titer may not reflect early infection or all anatomical sites from which transmissible virus can be shed, and therefore may be suboptimal evidence for public health policies that seek to reduce transmission.

We acknowledge three main limitations. First, data are from a single unvaccinated person with acute SARS-CoV-2 B.1.243 infection, prior to the availability of COVID-19 vaccines and the emergence of currently circulating variants. Infection characteristics may exhibit substantial person-to-person variation, and vaccination status and/or viral variant may affect the relationship between viral load and viral titer (36). Second, Participant AC collected saliva specimens in a preservation buffer that precluded the ability to perform viral culture, thereby prohibiting inferences on the relationship between saliva viral load and viral titer, or saliva viral titer and nasal viral titer. Third, the lack of detection of replication-competent virus by viral culture may not reflect a true absence of replication-competent virus in the specimen or shedding of infectious virus by the individual as specimen collection, handling, and storage affect virion viability (37, 38). Moreover, both the methods of attempted viral culture and viral characteristics can affect the analytical sensitivity to detect replication-competent virus (39). Therefore, it is possible that replication-competent virus was present in the first two nasal-swab specimens with detectable viral RNA collected by this participant, but at a concentration below the LOD by viral culture.

The data presented here is rare and challenging to obtain. We hope that similar datasets of viral load and viral titer in paired specimen types collected longitudinally starting from early infection can be made accessible for meta-analysis and guide optimized public health strategies that reduce the burden of SARS-CoV-2 or other pathogens.

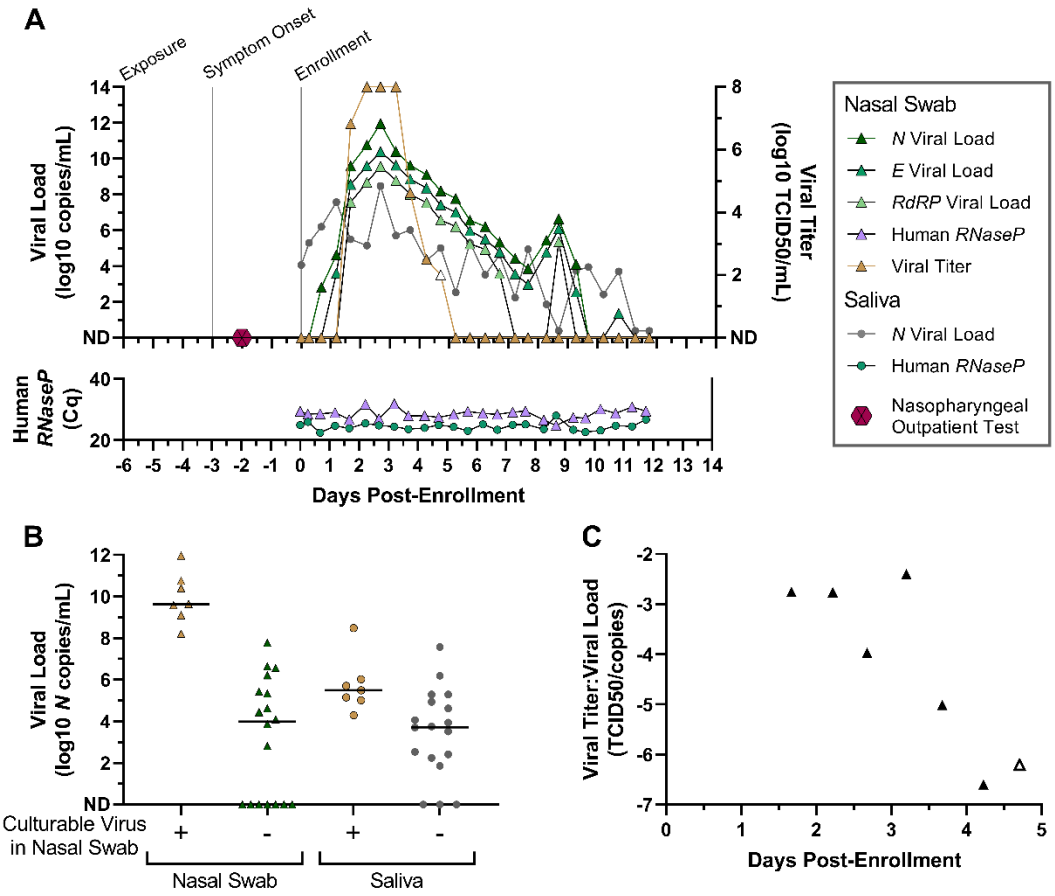

Figure 5-1. The viral load and viral titer trajectories from a single study participant from the incidence of infection. **(A)** A timeline of Participant AC's infection is shown with notable case events (exposure, symptom onset, study enrollment), as well as SARS-CoV-2 viral loads in saliva (circles) and anterior-nares nasal swabs (triangles) on the left y-axis, and SARS-CoV-2 viral titer (log_{10} $TCID_{50}$/mL) on the right y-axis. Human *RNaseP* Cq values are shown as a measure of sampling consistency and specimen RNA integrity. **(B)** Cross-sectional relationship of SARS-CoV-2 viral load (log_{10} *N* copies/mL, y axis) in nasal swab specimens (triangles) or saliva specimens (circles) based on whether viral culture positivity (yellow) of the nasal swab from the same timepoint. Black horizontal bars indicate median viral load. **(C)** For specimens with detectable viral titer and viral load, the ratio of viral titer ($TCID_{50}$/mL) over *N* gene viral load (copies/mL) in nasal swab specimens collected by the participant is plotted through days of enrollment. The open symbol indicates a specimen with detectable but not quantifiable viral titer, for which 100 $TCID_{50}$/mL was imputed. ND, not detected.

Methods

Participant consent statement

This COVID-19 household transmission study was approved under California Institute of Technology Institutional Review Board under protocol #20-1026, as previously described (23, 30).

Study design and specimen collection

Enrolled participants began self-collecting saliva and nasal swab specimens immediately upon receipt of specimen collection materials at enrollment, and then each subsequent morning (immediately after waking), and evening (prior to bed). Participants self-collected anterior-nares nasal swabs in Nest VTM (catalog no. NST-NST-202117; Stellar Scientific, Baltimore, MD) and saliva specimens in the Spectrum SDNA-1000 Saliva Collection Kit (Spectrum Solutions LLC, Draper, UT). Study participants were instructed not to eat, smoke, chew gum, or brush their teeth for at least 30 min prior to collection and were asked to gently blow their noses before nasal swabbing (four complete rotations with gentle pressure in each nostril) with sterile flocked swabs. Specimens were transported daily by medical courier to the Caltech laboratory for analysis. Additional reagent information is tabulated in Table S1.

Nucleic acid extraction, quantification of viral load by RT-qPCR, and viral variant determination

Nucleic-acid extraction was performed as previously described (23). Conversion from RT-qPCR Cq to viral load (in copies/mL) was determined via calibration curves, reported for *N* gene previously (23), and built for *E* and *RdRP* gene using standard positive controls (IDT 10006896, IDT 10006897):

$$E\left[\frac{cp}{uL}\right] = 2^{\frac{38.241-Cq}{0.9841}}$$

$$RdRP\left[\frac{cp}{uL}\right] = 2^{\frac{39.085-Cq}{0.8981}}$$

Nucleic acids extracted from the seventh saliva and nasal swab specimens collected by the participant underwent viral sequencing and variant determination as previously described (23).

Measurement of viral titer

Tissue culture infection dose to infect 50% of test cultures ($TCID_{50}$) assay was performed to measure the viral titer in VTM samples. Briefly, 500 µl VTM sample was filter-cleaned with a spin column (CLS-8160, Corning). VeroE6 cells ectopically expressing human ACE2 and TMPRSS2 (VeroE6-AT cells; a gift from Dr. Barney Graham, National Institutes of Health, Bethesda MD) were seeded confluent in a 96-well plate, after replacing the seeding

medium with 90 µL of assay medium (Dulbecco's Modified Eagle Media (DMEM) + 2% heat inactivated Fetal Bovine Serum (FBS) + 10 mM HEPES + 1% Penicillin/Streptomycin), 10 µL of filtered VTM sample was added to the first row of the plate as the starting inoculation. Then, 10-fold serial dilutions were performed in the second through seventh rows, leaving the eighth row as the negative control. Each sample was tested with five replicates. Cells were fixed with 10% formaldehyde and stained with 1% crystal violet three days post infection. Digital photographs were taken, and cell death indicated by clear areas in a well, were scored to calculate $TCID_{50}$.

Acknowledgements

We wish to thank the participant who contributed these specimens for analysis, the contact tracers at the Pasadena Public Health Department, as well as Dr. Matthew Bidwell Goetz and Dr. David Beehouwer for their thoughts on this data. We thank Maira Phelps, Lienna Chan, Lucy Li, Dan Lu, and Amy Kistler at the Chan Zuckerberg Biohub for performing SARS-CoV-2 sequencing.

Funding Information

This study is based on research funded in part by the Bill & Melinda Gates Foundation (INV-023124). The findings and conclusions contained within are those of the authors and do not necessarily reflect positions or policies of the Bill & Melinda Gates Foundation. This work was also funded by the Ronald and Maxine Linde Center for New Initiatives at the California Institute of Technology and the Jacobs Institute for Molecular Engineering for Medicine at the California Institute of Technology. A.V.W. is supported by a UCLA DGSOM Geffen Fellowship. MG and LH were supported by National Institutes of Health grant AI151698 for the United World Antiviral Research Network (UWARN) component of the Centers for Research in Emerging Infectious Disease (CREID).

Data Availability

The data underlying the results presented in the study are available at CaltechDATA at https://data.caltech.edu/records/cgf4q-byr92.

Statements and Declarations

R.F.I. is a cofounder, consultant, and a director and has stock ownership of Talis Biomedical Corp. All other co-authors report no competing interests.

Consent to publish

The two adult participants in this report provided written informed consent.

References

1. Walsh, K.A., Jordan, K., Clyne, B., Rohde, D., Drummond, L., Byrne, P., Ahern, S., Carty, P.G., O'Brien, K.K., O'Murchu, E. and O'Neill, M., 2020. SARS-CoV-2 detection, viral load and infectivity over the course of an infection. *Journal of Infection*, *81*(3), pp. 357–371.

2. Drain, P.K., 2022. Rapid diagnostic testing for SARS-CoV-2. *New England journal of medicine*, *386*(3), pp. 264–272.

3. Mina, M.J., Parker, R. and Larremore, D.B., 2020. Rethinking Covid-19 test sensitivity—a strategy for containment. *New England Journal of Medicine*, *383*(22), p.e120.

4. Pickering, S., Batra, R., Merrick, B., Snell, L.B., Nebbia, G., Douthwaite, S., Reid, F., Patel, A., Ik, M.T.K., Patel, B. and Charalampous, T., 2021. Comparative performance of SARS-CoV-2 lateral flow antigen tests and association with detection of infectious virus in clinical specimens: a single-centre laboratory evaluation study. *The Lancet Microbe*, *2*(9), pp. e461–e471.

5. Perera, R.A., Tso, E., Tsang, O.T., Tsang, D.N., Fung, K., Leung, Y.W., Chin, A.W., Chu, D.K., Cheng, S.M., Poon, L.L. and Chuang, V.W., 2020. SARS-CoV-2 virus culture and subgenomic RNA for respiratory specimens from patients with mild coronavirus disease. *Emerging infectious diseases*, *26*(11), p. 2701.

6. Wölfel, R., Corman, V.M., Guggemos, W., Seilmaier, M., Zange, S., Müller, M.A., Niemeyer, D., Jones, T.C., Vollmar, P., Rothe, C. and Hoelscher, M., 2020. Virological assessment of hospitalized patients with COVID-2019. *Nature*, *581*(7809), pp. 465–469.

7. Siedner, M.J., Boucau, J., Gilbert, R.F., Uddin, R., Luu, J., Haneuse, S., Vyas, T., Reynolds, Z., Iyer, S., Chamberlin, G.C. and Goldstein, R.H., 2022. Duration of viral shedding and culture positivity with postvaccination SARS-CoV-2 delta variant infections. *JCI insight*, *7*(2).

8. Murata, T., Sakurai, A., Suzuki, M., Komoto, S., Ide, T., Ishihara, T. and Doi, Y., 2021. Shedding of viable virus in asymptomatic SARS-CoV-2 carriers. *MSphere*, *6*(3), pp. 10–1128.

9. Jefferson, T., Spencer, E.A., Brassey, J. and Heneghan, C., 2021. Viral cultures for coronavirus disease 2019 infectivity assessment: a systematic review. *Clinical Infectious Diseases*, *73*(11), pp. e3884–e3899.

10. van Kampen, J.J., van de Vijver, D.A., Fraaij, P.L., Haagmans, B.L., Lamers, M.M., Okba, N., van den Akker, J.P., Endeman, H., Gommers, D.A., Cornelissen, J.J. and Hoek, R.A., 2021. Duration and key determinants of infectious virus shedding in hospitalized patients with coronavirus disease-2019 (COVID-19). *Nature communications*, *12*(1), p. 267.

11. *Centers for Disease Control and Prevention. "Ending isolation and precautions for people with COVID-19: interim guidance." URL: https://www.cdc.gov/coronavirus/2019-ncov/hcp/duration-isolation.html [accessed 2022-05-01]© Nicole Zahradka, Juliana Pugmire, Jessie Lever Taylor, Adam Wolfberg, Matt Wilkes. Originally published in JMIR Formative Research (https://formative.jmir.org) 29 (2022).*

12. Santos Bravo, M., Berengua, C., Marín, P., Esteban, M., Rodriguez, C., Del Cuerpo, M., Miró, E., Cuesta, G., Mosquera, M., Sánchez-Palomino, S. and Vila, J., 2022. Viral culture confirmed SARS-CoV-2 subgenomic RNA value as a good surrogate marker of infectivity. *Journal of clinical microbiology*, *60*(1), pp. e01609–21.

13. Ke, R., Martinez, P.P., Smith, R.L., Gibson, L.L., Achenbach, C.J., McFall, S., Qi, C., Jacob, J., Dembele, E., Bundy, C. and Simons, L.M., 2022, July. Longitudinal analysis of SARS-CoV-2 vaccine breakthrough infections reveals limited infectious virus shedding and restricted tissue distribution. In *Open Forum Infectious Diseases* (Vol. 9, No. 7, p. ofac192). Oxford University Press.

14. Pekosz, A., Parvu, V., Li, M., Andrews, J.C., Manabe, Y.C., Kodsi, S., Gary, D.S., Roger-Dalbert, C., Leitch, J. and Cooper, C.K., 2021. Antigen-based testing but not real-time polymerase chain reaction correlates with severe acute respiratory syndrome coronavirus 2 viral culture. *Clinical Infectious Diseases*, *73*(9), pp. e2861–e2866.

15. Kirby, J.E., Riedel, S., Dutta, S., Arnaout, R., Cheng, A., Ditelberg, S., Hamel, D.J., Chang, C.A. and Kanki, P.J., 2023. SARS-CoV-2 antigen tests predict infectivity based on viral culture: comparison of antigen, PCR viral load, and viral culture testing on a large sample cohort. *Clinical Microbiology and Infection*, *29*(1), pp. 94–100.

16. Korenkov, M., Poopalasingam, N., Madler, M., Vanshylla, K., Eggeling, R., Wirtz, M., Fish, I., Dewald, F., Gieselmann, L., Lehmann, C. and Fätkenheuer, G., 2021. Evaluation of a rapid antigen test to detect SARS-CoV-2 infection and identify potentially infectious individuals. *Journal of clinical microbiology*, *59*(9), pp. 10–1128.

17. Kohmer, N., Toptan, T., Pallas, C., Karaca, O., Pfeiffer, A., Westhaus, S., Widera, M., Berger, A., Hoehl, S., Kammel, M. and Ciesek, S., 2021. The comparative clinical performance of four SARS-CoV-2 rapid antigen tests and their correlation to infectivity in vitro. *Journal of clinical medicine*, *10*(2), p. 328.

18. Bullard, J., Dust, K., Funk, D., Strong, J.E., Alexander, D., Garnett, L., Boodman, C., Bello, A., Hedley, A., Schiffman, Z. and Doan, K., 2020. Predicting infectious severe acute respiratory syndrome coronavirus 2 from diagnostic samples. *Clinical infectious diseases*, *71*(10), pp. 2663–2666.

19. Ji, J., Viloria Winnett, A., Shelby, N., Reyes, J.A., Schlenker, N.W., Davich, H., Caldera, S., Tognazzini, C., Goh, Y.Y., Feaster, M. and Ismagilov, R.F., 2023. Index cases first identified by nasal-swab rapid COVID-19 tests had more transmission to household contacts than cases identified by other test types. *Plos one*, *18*(10), p. e0292389.

20. McGarry, B.E., Gandhi, A.D. and Barnett, M.L., 2023. Covid-19 surveillance testing and resident outcomes in nursing homes. *New England Journal of Medicine*, *388*(12), pp. 1101–1110.

21. COVID-19 Treatments and Medications. (2023) CDC.

22. Kissler, S.M., Fauver, J.R., Mack, C., Olesen, S.W., Tai, C., Shiue, K.Y., Kalinich, C.C., Jednak, S., Ott, I.M., Vogels, C.B. and Wohlgemuth, J., 2021. Viral dynamics of acute SARS-CoV-2 infection and applications to diagnostic and public health strategies. *PLoS biology*, *19*(7), p. e3001333.

23. Savela, E.S., Viloria Winnett, A., Romano, A.E., Porter, M.K., Shelby, N., Akana, R., Ji, J., Cooper, M.M., Schlenker, N.W., Reyes, J.A. and Carter, A.M., 2022. Quantitative SARS-CoV-2 viral-load curves in paired saliva samples and nasal swabs inform appropriate respiratory sampling site and analytical test sensitivity required for earliest viral detection. *Journal of Clinical Microbiology*, *60*(2), pp. e01785–21.

24. Viloria Winnett, A., Akana, R., Shelby, N., Davich, H., Caldera, S., Yamada, T., Reyna, J.R.B., Romano, A.E., Carter, A.M., Kim, M.K. and Thomson, M., 2023. Extreme differences in SARS-CoV-2 viral loads among respiratory specimen types during presumed pre-infectious and infectious periods. *PNAS nexus*, *2*(3), p.pgad033.

25. Killingley, B., Mann, A.J., Kalinova, M., Boyers, A., Goonawardane, N., Zhou, J., Lindsell, K., Hare, S.S., Brown, J., Frise, R. and Smith, E., 2022. Safety, tolerability and viral kinetics during SARS-CoV-2 human challenge in young adults. *Nature Medicine*, *28*(5), pp. 1031–1041.

26. Kissler, S.M., Fauver, J.R., Mack, C., Tai, C.G., Breban, M.I., Watkins, A.E., Samant, R.M., Anderson, D.J., Metti, J., Khullar, G. and Baits, R., 2021. Viral dynamics of SARS-CoV-2 variants in vaccinated and unvaccinated persons. *New England Journal of Medicine*, *385*(26), pp. 2489–2491.

27. Ke, R., Martinez, P.P., Smith, R.L., Gibson, L.L., Mirza, A., Conte, M., Gallagher, N., Luo, C.H., Jarrett, J., Zhou, R. and Conte, A., 2022. Daily longitudinal sampling of SARS-CoV-2 infection reveals substantial heterogeneity in infectiousness. *Nature microbiology*, *7*(5), pp. 640–652.

28. Karita, H.C.S., Dong, T.Q., Johnston, C., Neuzil, K.M., Paasche-Orlow, M.K., Kissinger, P.J., Bershteyn, A., Thorpe, L.E., Deming, M., Kottkamp, A. and Laufer, M., 2022. Trajectory of viral RNA load among persons with incident SARS-CoV-2 G614 infection (Wuhan strain) in association with COVID-19 symptom onset and severity. *JAMA Network Open*, *5*(1), pp. e2142796–e2142796.

29. Hakki, S., Zhou, J., Jonnerby, J., Singanayagam, A., Barnett, J.L., Madon, K.J., Koycheva, A., Kelly, C., Houston, H., Nevin, S. and Fenn, J., 2022. Onset and window of SARS-CoV-2 infectiousness and temporal correlation with symptom onset: a prospective, longitudinal, community cohort study. *The Lancet Respiratory Medicine*, *10*(11), pp. 1061–1073.

30. Viloria Winnett, A., Porter, M.K., Romano, A.E., Savela, E.S., Akana, R., Shelby, N., Reyes, J.A., Schlenker, N.W., Cooper, M.M., Carter, A.M. and Ji, J., 2022. Morning SARS-CoV-2 testing yields better detection of infection due to higher viral loads in saliva and nasal swabs upon waking. *Microbiology Spectrum*, *10*(6), pp. e03873–22.

31. Dimcheff, D.E., Valesano, A.L., Rumfelt, K.E., Fitzsimmons, W.J., Blair, C., Mirabelli, C., Petrie, J.G., Martin, E.T., Bhambhani, C., Tewari, M. and Lauring, A.S., 2021. Severe acute respiratory syndrome coronavirus 2 total and subgenomic RNA viral load in hospitalized patients. *The Journal of infectious diseases*, *224*(8), pp. 1287–1293.

32. Stanley, S., Hamel, D.J., Wolf, I.D., Riedel, S., Dutta, S., Contreras, E., Callahan, C.J., Cheng, A., Arnaout, R., Kirby, J.E. and Kanki, P.J., 2022. Limit of detection for rapid antigen testing of the SARS-CoV-2 Omicron and Delta variants of concern using live-virus culture. *Journal of Clinical Microbiology*, *60*(5), pp. e00140–22.

33. Babady, N.E., Cohen, B., McClure, T., Chow, K., Caldararo, M., Jani, K., McMillen, T., Taur, Y., Shah, M., Robilotti, E. and Aslam, A., 2022. Variable duration of viral shedding in cancer patients with coronavirus disease 2019 (COVID-19). *Infection Control & Hospital Epidemiology*, *43*(10), pp. 1413–1415.

34. Puhach, O., Adea, K., Hulo, N., Sattonnet, P., Genecand, C., Iten, A., Jacquérioz, F., Kaiser, L., Vetter, P., Eckerle, I. and Meyer, B., 2022. Infectious viral load in unvaccinated and vaccinated individuals infected with ancestral, Delta or Omicron SARS-CoV-2. *Nature medicine*, *28*(7), pp. 1491–1500.

35. Smith, R.L., Gibson, L.L., Martinez, P.P., Ke, R., Mirza, A., Conte, M., Gallagher, N., Conte, A., Wang, L., Fredrickson, R. and Edmonson, D.C., 2021. Longitudinal assessment of diagnostic test performance over the course of acute SARS-CoV-2 infection. *The Journal of infectious diseases*, *224*(6), pp. 976–982.

36. Tassetto, M., 2022. Detection of higher cycle threshold values in culturable SARS-CoV-2 Omicron BA. 1 sublineage compared with pre-omicron variant specimens—San Francisco Bay Area, California, July 2021—March 2022. *MMWR. Morbidity and Mortality Weekly Report*, *71*.

37. Chin, A.W., Chu, J.T., Perera, M.R., Hui, K.P., Yen, H.L., Chan, M.C., Peiris, M. and Poon, L.L., 2020. Stability of SARS-CoV-2 in different environmental conditions. *The Lancet Microbe*, *1*(1), p. e10.

38. McAuley, J., Fraser, C., Paraskeva, E., Trajcevska, E., Sait, M., Wang, N., Bert, E., Purcell, D. and Strugnell, R., 2021. Optimal preparation of SARS-CoV-2 viral transport medium for culture. *Virology Journal*, *18*, pp. 1–6.

39. Mautner, L., Hoyos, M., Dangel, A., Berger, C., Ehrhardt, A. and Baiker, A., 2022. Replication kinetics and infectivity of SARS-CoV-2 variants of concern in common cell culture models. *Virology journal*, *19*(1), p. 76.

Supplementary Information

Supplemental Table 5-1. Reagent list. Table includes all reagents utilized in this study.

Step	ReagentName	Description	Manufacturer	Catalogue Number
Specimen Collection	Spectrum SDNA1000 Saliva Collection Device	For at-home collection of spit saliva into a guandinium-thiocyanate based preservation buffer	Spectrum Solutions LLC	SDNA1000
Specimen Collection	NEST Scientific 10mL Sterile Screw-Cap Transport Tube with 3mL VTM	For at-home collection of nasal swab specimens into media that maintains live virions	Stellar Scientific	NST-NST-202117
Nucleic Acid Extraction	MagMAX™ Viral/Pathogen Nucleic Acid Isolation Kit	For extraction of nucleic acids from clinical upper respiratory specimens	ThermoFisher Scientitif	A42352
Viral Load Quantification	TaqPath™ COVID-19 Combo Kit	For RT-qPCR measurement of human RNaseP and SARS-CoV-2 N gene	ThermoFisher Scientific	A47814
Viral Load Quantification	Heat-inactivated SARS-CoV-2 2019-nCoV/USA-WA1/2020	Extraction control and standard for RT-qPCR quantification	BEI	NR-52286
Viral Load Quantification	2019-nCoV_E Positive Control	Standard for RT-qPCR quantification	IDT	10006896
Viral Load Quantification	2019-nCoV_RdRp (ORF1ab) Positive Control	Standard for RT-qPCR quantification	IDT	10006897
Viral Load Quantification	E_Sarbeco_F1 Forward Primer, 50 nmol	Forward primer for RT-qPCR measurement of SARS-CoV-2 E gene	IDT	10006888
Viral Load Quantification	E_Sarbeco_R2 Reverse Primer, 50 nmol	Reverse primer for RT-qPCR measurement of SARS-CoV-2 E gene	IDT	10006890
Viral Load Quantification	E_Sarbeco_P1 (FAM) Probe, 25 nmol	Probe for RT-qPCR measurement of SARS-CoV-2 E gene	IDT	10006892
Viral Load Quantification	RdRP_SARSr_F2 Forward Primer, 50 nmol	Forward primer for RT-qPCR measurement of SARS-CoV-2 RdRp gene	IDT	10006860
Viral Load Quantification	RdRP_SARSr_R1 Reverse Primer, 50 nmol	Reverse primer for RT-qPCR measurement of SARS-CoV-2 RdRp gene	IDT	10006881
Viral Load Quantification	RdRP_SARSr_P2 (SUN) Probe, 25 nmol	Probe for RT-qPCR measurement of SARS-CoV-2 RdRp gene	IDT	10007063
Viral Culture	Culture Media	DMEM 2%FBS (heat inactivated) 1% Penicillin-Streptomycin 1% HEPES (1M)	Fisher Scientific Fisher Scientific	MT10013CV SH30071.03 MT30002CI MT25060CI
Viral Culture	Cell Line	VeroE6-AT	A gift from Dr. Barney Graham (NIH)	
Viral Culture	Stain for Readout	1% crystal violet 20% Ethanol	Sigma_Aldrich Fisher	C-6158 4355222

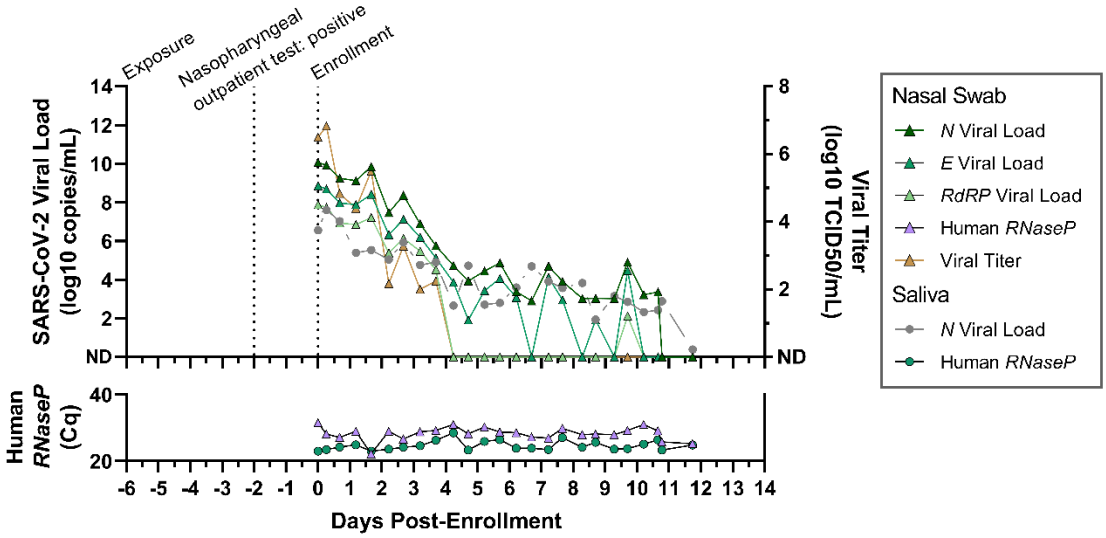

Supplemental Figure 5-1. The viral load and viral titer trajectories from a single study participant from the incidence of infection. A timeline of this participant's infection is shown with notable case events (e.g., exposure, positive nasopharyngeal outpatient test, study enrollment), as well as SARS-CoV-2 viral loads (log10 copies/mL) in saliva (circles) and anterior nares nasal swab (triangles) on the left y-axis, and SARS-CoV-2 viral titer (log10 TCID50/mL) on the right y-axis. Human *RNaseP* Cq values are shown as a measure of sampling consistency and specimen RNA integrity. ND, not detected.

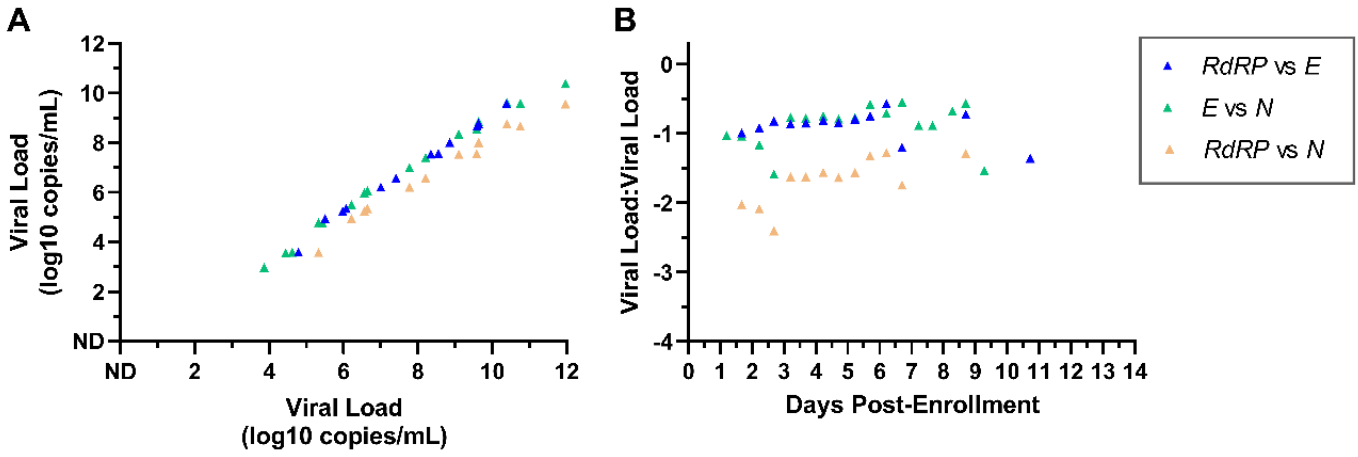

Supplemental Figure 5-2. Swab viral loads measured from *N*, *E*, and *RdRP* genes remain constant with respect to each other through the course of infection. **(A)** The viral load from one gene is plotted on the y axis with respect to another gene comparing *RdRP* and *E* genes (blue triangle), *E* and *N* genes (green triangles), and *RdRP* and *N* genes (tan triangles). **(B)** The ratios of viral loads are plotted over days post-enrollment for RdRP and *E* genes (blue triangle), *E* and *N* genes (green triangles), and *RdRP* and *N* genes (tan triangles). Viral loads that were not detected were omitted from analysis. ND, not detected.

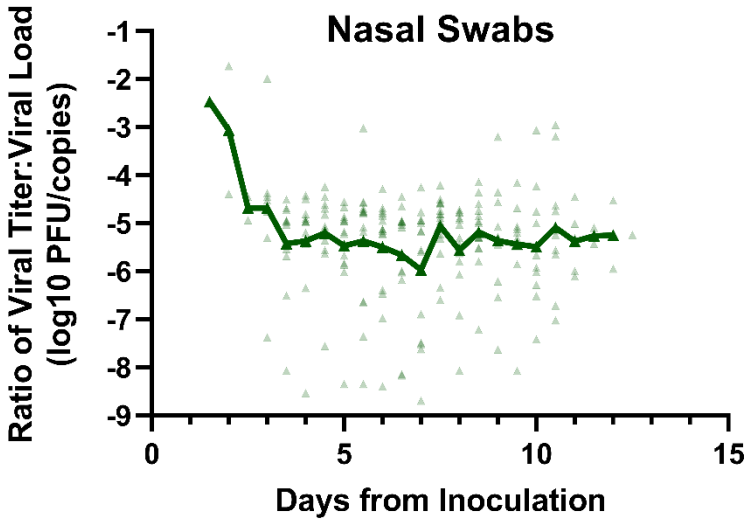

Supplemental Figure 5-3. Longitudinal ratio of viral titer to viral load from participants in SARS-CoV-2 human challenge study. As part of a SARS-CoV-2 human challenge study performed in (1), participants were inoculated intranasally with 10 $TCID_{50}$ virus. Eighteen participants had subsequent sustained detectable infection in nasal swab and throat swab specimens collected daily after inoculation. Viral load and viral culture data from these specimens was graciously provided by the authors of this study. We plotted the log10 transformed ratio of viral titer to viral load in nasal swabs, for all specimens with replication competent virus, by the time from inoculation (green triangles). Green line represents the average log10 transformed ratio of viral titer to viral load among culture-positive nasal swab specimen, for each day following inoculation.

Supplemental References

1. Killingley, B., Mann, A.J., Kalinova, M., Boyers, A., Goonawardane, N., Zhou, J., Lindsell, K., Hare, S.S., Brown, J., Frise, R. and Smith, E., 2022. Safety, tolerability and viral kinetics during SARS-CoV-2 human challenge in young adults. *Nature Medicine*, *28*(5), pp.1031-1041.

Author Contribution Statements

Michael K. Porter (MKP) – Conceptualization of nested study with AVW and RFI. Literature review with AVW. Co-wrote biosafety protocols for receipt and processing of live specimens with AVW. Reagent and supply acquisition. Determined and validated live specimen collection methods with AVW. Received, logged and aliquoted live specimens with AVW. Established academic collaboration with colleagues at University of Washington. Performed nucleic acid extractions and RNaseP, N, E, and RdRP gene RT-qPCR. Coordinated and prepared shipments of live specimens to collaborators. Interpreted paired viral load and culture data with AVW and LH. Outlined and co-wrote manuscript with AVW. Prepared Figures 1, S1, S2, and S3. Validated underlying data with AVW. Managed author citations and references.

Alexander Viloria Winnett (AVW) – Conceptualization of nested study with MKP and RFI. Literature review with MKP. Co-wrote biosafety protocols for receipt and processing of live specimens with MKP. Reagent and supply acquisition. Determined and validated live specimen collection methods with MKP. Received, logged and aliquoted live specimens with MKP. Performed nucleic acid extractions and RNaseP and N gene RT-qPCR. Coordinated and prepared shipments of nucleic acids for viral sequencing. Coordinated and prepared shipments of live specimens to collaborators for viral culture. Interpreted paired viral load and culture data with MKP and LH. Outlined and co-wrote manuscript with MKP. Provided feedback on the design of Figures 1, S1, and S2. Validated underlying data with MKP.

Linhui Hao (LH) – Received live specimens for viral culture. Performed viral culture at BSL3 and analyzed viral culture data. Interpreted paired viral load and culture data with AVW and MKP. Wrote viral culture methods section. Edited the manuscript.

Natasha Shelby (NS) – Study Administrator; collaborated on study design and recruitment strategies; created instructions for live viral-load sampling with JAR; enrolled and maintained study participants with JAR and NS. Edited the manuscript.

Jessica A. Reyes (JAR) – Lead Study Coordinator; created instructions for live viral-load sampling with NS; enrolled and maintained study participants with NS and NWS.

Noah W. Schlenker (NWS) – Study Coordinator; enrolled and maintained study participants with NS and JAR.

Anna E. Romano (AER) – Analyzed and summarized viral sequencing data.

Colton Tognazzini (CT) – Coordinated the recruitment efforts at PPHD with case investigators and contact tracers and provided guidance and expertise on SARS-CoV-2 epidemiology and local trends.

Matthew Feaster (MF) – Co-investigator; collaborated on study design and recruitment strategies; provided guidance and expertise on SARS-CoV-2 epidemiology and local trends.

Ying-Ying Goh (YYG) – Co-investigator; collaborated on study design and recruitment strategies; provided guidance and expertise on SARS-CoV-2 epidemiology and local trends.

Michael Gale (MG) – Co-investigator; coordinated and oversaw viral culture method development and execution. Edited the manuscript.

Rustem F. Ismagilov (RFI) – Co-investigator; collaborated on study design and recruitment strategies; provided leadership, technical guidance, oversight, and was responsible for obtaining funding for the study.

Chapter 6

DAILY SARS-COV-2 NASAL ANTIGEN TESTS MISS INFECTED AND PRESUMABLY INFECTIOUS PEOPLE DUE TO VIRAL-LOAD DIFFERENCES AMONG SPECIMEN TYPES

This chapter was originally published in Viloria Winnett A*, Akana R*, Shelby N*, Romano AE, Davich H, Caldera S, Kim MK, Carter AM, Yamada T, Reyna JR, Ji J, Reyes JA, Cooper MM, Thomson M, Tognazzini C, Feaster M, Goh YY, Ismagilov. Daily SARS-CoV-2 Nasal Rapid Antigen Testing Poorly Detects Infected and Infectious Individuals (March 2023). Microbiology Spectrum. https://doi.org/10.1128/spectrum.01295-23.

Abstract

In a recent household-transmission study of SARS-CoV-2, we found extreme differences in SARS-CoV-2 viral loads among paired saliva, anterior-nares swab (ANS) and oropharyngeal swab specimens collected from the same timepoint. We hypothesized these differences may hinder low-analytical-sensitivity assays (including antigen rapid diagnostic tests, Ag-RDTs) using a single specimen type (e.g., ANS) from reliably detecting infected and infectious individuals. We evaluated a daily at-home ANS Ag-RDT (Quidel QuickVue) in a cross-sectional analysis of 228 individuals and in a longitudinal analysis (throughout infection) of 17 individuals enrolled early in the course of infection. Ag-RDT results were compared to RT-qPCR results and high, presumably infectious viral loads (in each, or any, specimen type). The ANS Ag-RDT correctly detected only 44% of timepoints from infected individuals on cross-sectional analysis, and in this population had an inferred limit of detection of $7.6x10^6$ copies/mL. From the longitudinal cohort, daily Ag-RDT clinical sensitivity was very low (<3%) during the early, pre-infectious period of the infection. Further, the Ag-RDT detected ≤63% of presumably infectious timepoints. The poor observed clinical sensitivity of the Ag-RDT was similar to what was predicted based on quantitative ANS viral loads and the inferred limit of detection of the ANS Ag-RDT being evaluated, indicating high-quality self-sampling. Nasal Ag-RDTs, even when used daily, can miss individuals infected with the Omicron variant and even those presumably infectious. Evaluations of Ag-RDTs for detection of infected or infectious individuals should be compared with a composite (multi-specimen) infection status to correctly assess performance.

Importance

We reveal three findings from a longitudinal study of daily nasal antigen rapid-diagnostic test (Ag-RDT) evaluated against SARS-CoV-2 viral-load quantification in three specimen types (saliva, nasal-swab, throat-swab) in participants enrolled at the incidence of infection. First, the evaluated Ag-RDT showed low (44%) clinical sensitivity for detecting infected persons at all infection stages. Second, the Ag-RDT poorly detected (≤63%) timepoints that participants had high and presumably infectious viral loads in at least one specimen type. This poor clinical sensitivity to detect infectious individuals is inconsistent with the commonly held view that daily Ag-RDTs have near-perfect detection of infectious individuals. Third, use of a combination nasal-throat specimen type was inferred by viral loads to significantly improve Ag-RDT performance to detect infectious individuals.

Introduction

Antigen rapid diagnostic tests (Ag-RDTs) with nasal swabs are increasingly used for SARS-CoV-2 screening and diagnosis globally.[1-3] Ag-RDTs are powerful tools given their low cost (compared with molecular tests), speed, and portability—making them appropriate for low-resource settings and at-home use.[2,4,5] However, Ag-RDTs and some rapid molecular tests have lower analytical sensitivity than most gold-standard reverse-transcription quantitative PCR (RT-qPCR) tests and therefore require high viral loads (typically $>10^5$ copies/mL) to reliably yield positive results.[4,6-11] Some contend that Ag-RDTs may miss some infected individuals, but will result positive when individuals are infectious with high viral loads.[12-14] Such concordance would allow high-frequency Ag-RDTs (with immediate results) to more effectively prompt isolation of infectious individuals than a high-analytical-sensitivity test (with delayed results).[12,15]

Investigating Ag-RDT performance for detecting the infectious period by viral culture is challenging and infrequently performed. Instead, because replication-competent virus is associated with viral loads $\geq 10^4$ copies/mL in studies that have performed SARS-CoV-2 viral culture (**Supplemental Table 6-1**), viral load is often used as a surrogate for infectiousness. Longitudinal studies that captured viral-load measurements from early in infection[16-30] show that for some individuals, several days can pass between when viral loads reach potentially infectious levels and when viral loads rise to the limits of detection (LODs) of Ag-RDTs ($\sim 10^5$–10^7 copies/mL).[4,6-10,20,21,31] During this window, false-negative Ag-RDT results may occur, emboldening social contact and increasing transmission.[32,33]

In our household-transmission study analyzing viral loads from daily sampling of anterior-nares nasal swabs (ANS), oropharyngeal swabs (OPS) and saliva (SA) beginning from the incidence of SARS-CoV-2 Omicron infection, two findings suggested Ag-RDTs may miss many infected and infectious individuals.[26] First, viral loads for an individual often differed significantly (>9 orders of magnitude) among specimen types at the same timepoint, and did not correlate with each other over time. Individuals often had high, presumably infectious viral loads in one type (e.g., OPS), yet low loads in another (e.g., ANS). Because all at-home Ag-RDTs authorized by the U.S. Food and Drug Administration (FDA) are for nasal swabs,[7] this lack of correlation among specimen types could hinder the ability of Ag-RDTs to detect infectious individuals with high loads in non-nasal specimen types. Second, we observed that most individuals exhibit a delay in the rise of ANS viral loads relative to the oral cavity[26]; this finding is consistent with previous reports by us[21] for ancestral SARS-CoV-2 variants and other studies[17,18,20,25] that included the early period of infection in multiple specimen types. A delayed rise in ANS viral loads could delay nasal Ag-RDT detection of infected and infectious individuals.

These underlying viral-load patterns impact interpretation of Ag-RDT field evaluations. Although many Ag-RDT evaluations report concordance with infectiousness (by viral culture[16-19,34-44] or presumed by quantitative viral

loads or semi-quantitative Ct values[45-48]), in several studies[16,34,36,37,41,43,45,47,48] most participants were already symptomatic so results may not generalize to early infection. Among longitudinal nasal Ag-RDT studies that accounted for infection stage,[17-19,35,38,39,43] some[17-19,35,38] used prospective sampling to capture early infections, but none tested for infectious virus in multiple specimen types. To our knowledge, only one nasal Ag-RDT evaluation examined infectiousness in oral specimens; the Ag-RDT was often negative while individuals had infectious loads in saliva.[20] There is a paucity of data on Ag-RDT performance in early infection, and compared to infectiousness in multiple upper-respiratory specimen types.

Here, we report a field evaluation of an ANS Ag-RDT (QuickVue At-Home OTC COVID-19 Test), with cross-sectional and longitudinal analyses. A daily ANS Ag-RDT was taken prospectively by participants with a recently infected or exposed household contact. Participants also collected daily SA, ANS, and OPS specimens for SARS-CoV-2 testing and viral-load quantification.[26] From these viral-load measurements we assessed Ag-RDT performance to identify individuals with detectable or presumably infectious viral loads in any of the three specimen types. This design allowed us to probe the performance of this Ag-RDT for early detection, and identify underlying reasons why Ag-RDTs may exhibit poor performance to detect infected and infectious individuals.

Methods

Study Design

We performed a case-ascertained study in the greater Los Angeles County area November 2021 to March 2022 in which participants prospectively self-collected SA, then ANS, and OPS specimens for high-analytical-sensitivity RT-qPCR testing. RT-qPCR testing was performed using the FDA-authorized Zymo *Quick* SARS-CoV-2 rRT-PCR Kit,[49] which targets regions of the SARS-CoV-2 *N* gene and human *RNase P* gene. RT-qPCR N gene Ct values were used to quantify viral load in the starting specimen, based on a conversion equation generated via a standard curve of known inputs of commercial heat-inactivated SARS-CoV-2 viral particles. Additional details of RT-qPCR testing are provided separately.[26] After self-collecting specimens, participants immediately performed an at-home ANS Ag-RDT (Quidel QuickVue At-Home OTC COVID-19 Test[50]) per manufacturer's instructions. Antigen test results were interpreted by the participant immediately upon completion of the test, and they reported the result and submitted a photograph of the test strip to the research team via a secure REDCap link. Repeat testing of the nasal cavity has been previously shown to maintain diagnostic test performance.[51]

RT-qPCR results and viral-load quantifications were compared with Ag-RDT results for cross-sectional and longitudinal analyses of Ag-RDT performance. The 228 participants provided 2,107 (ANS), 2,108 (OPS), and 2,114 (SA) timepoints with valid ANS Ag-RDT and RT-qPCR results for cross-sectional analysis (see

Supplemental Methods). A composite RT-qPCR result was generated for each timepoint: a participant was considered infected if any of their three specimen types resulted positive by RT-qPCR and uninfected if all specimen types resulted negative by RT-qPCR. Results were inconclusive if at least one specimen type resulted inconclusive while all others resulted negative by RT-qPCR. In total, 2,104 timepoints had valid, paired ANS Ag-RDT and composite RT-qPCR results. For analyses oriented to early infection, we analyzed longitudinal data from 17 participants who began sampling early in infection (negative in at least one test, RT-qPCR or Ag-RDT, upon enrollment).

All households were infected with either the Delta or Omicron variants (see Supplementary Methods).

Statistical Analyses

Positive and negative percent agreement for each specimen type was calculated as the number of specimens with concordant results by RT-qPCR and ANS Ag-RDT over the total number of specimens with positive or negative results, respectively, by RT-qPCR for the given specimen type as reference test.

Quantitative viral loads were used to predict expected results for a specimen tested by a hypothetical assay with a given limit of detection (LOD). Results were also predicted fora computationally-contrived AN–OP combination swab, using the higher viral load of the ANS or OPS specimens from a participant at a timepoint.[26] Results were used to calculate inferred positive percent agreement and inferred clinical sensitivity.

Clinical sensitivity was calculated as the number of specimens with either observed or predicted positive results over the total number of infected or infectious timepoints. We denoted clinical sensitivity as inferred when predicted based on viral load. Error bars indicate 95% confidence intervals calculated as recommended by CLSI.[52]

We also presumed that individuals were infectious if viral loads were above the specified infectious viral-load threshold (IVLT) of 10^4, 10^5, 10^6, or 10^7 copies/mL (based on viral culture literature, **Supplemental Table 6-S1**) in at least one specimen type. Differences in the inferred or observed clinical sensitivity from paired RT-qPCR and Ag-RDT data were analyzed using the McNemar exact test using the statsmodels package in Python v3.8.8, with Benjamini–Yekutieli correction.

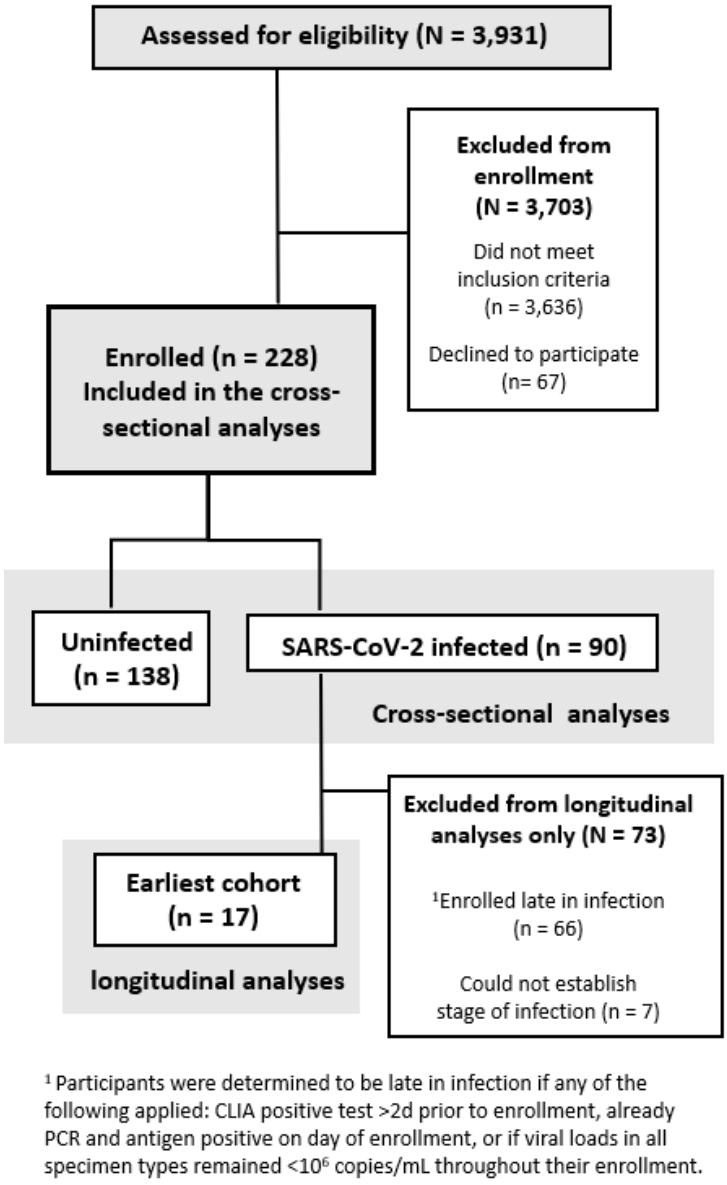

Figure 6-1. A CONSORT diagram of participant recruitment, eligibility, and enrollment for the cross-sectional and longitudinal analyses. Demographic and medical information can be found in **Supplementary Tables 1-2**. Cross-sectional analyses are presented in **Figures 6-2** and **6-3**; longitudinal analyses are presented in **Figures 6-4** through **6-6**.

Results

Ag-RDT Detects <50% of Infected Individuals

We first performed a cross-sectional analysis to estimate the LOD of the ANS Ag-RDT, then compared the positive percent agreement (PPA) of the ANS Ag-RDT against ANS RT-qPCR or composite infection status (based on RT-qPCR results from ANS, OPS and SA). Of 680 ANS specimens with quantifiable viral loads and valid, paired ANS Ag-RDT results, 95% PPA was observed when ANS specimens had viral loads $\geq 7.6 \times 10^6$ copies/mL (**Figure 6–2A**), suggesting this value as an inferred estimate of the assay LOD[16,31,50] We observed

48% (347 of 731) PPA between the ANS Ag-RDT and ANS RT-qPCR (**Figure 6–2B**). However, the observed clinical sensitivity of the ANS Ag-RDT (**Figure 6–2H**) when compared to composite infection status was 44% (357 of 812 infected timepoints), significantly lower (P<0.001, upper-tailed McNemar exact test) than the PPA against ANS RT-qPCR alone (**Figure 6–2B**). Although low PPA and clinical sensitivity to detect infection were expected due to the low analytical sensitivity of the Ag-RDT, the Ag-RDT resulted negative at many timepoints participants had high, presumably infectious, viral loads in ANS, SA, or OPS specimens (**Figure 6–2E–G**). Approximately 50% of timepoints at which the ANS Ag-RDT resulted negative had viral loads above 10^4 copies/mL in ANS (**Figure 6–2E**) or OPS (**Figure 6–2F**) or any specimen type (**Figure 6–2I**).

Analytical Sensitivity, IVLT, and Specimen Type Strongly Impact the Ability to Detect Infectious Individuals

We next assessed how well presumably infectious individuals would be detected by low-analytical-sensitivity assays. Infectious viral load thresholds (IVLTs) were used to classify individuals as infectious. To examine differences resulting from IVLT selection, we created a matrix of IVLTs (10^4, 10^5, 10^6 or 10^7 copies/mL) and low-analytical-sensitivity assay LODs (10^5–10^7 copies/mL), for each specimen type. In each cell, we calculated inferred clinical sensitivity for each hypothetical assay to detect presumed infectious timepoints. We calculated inferred clinical sensitivity against timepoints with viral loads above the IVLT only in one specimen type (**Figure 6–3A-C**), and against timepoints with a viral load above the IVLT in any of the three specimen types (**Figure 6–3D-F**).

When considering viral loads only in the specimen type tested, clinical sensitivity increased as IVLT increased, and decreased as LOD increased. Setting an IVLT at or above the LOD of the assay artificially increased the inferred clinical sensitivity to detect presumed infectious individuals. We highlight three instances (red boxes in **Figure 6–3A–C**) where inferred clinical sensitivities increased by up to 74% as a result of IVLT selection. Perfect performance was observed where IVLT was at or above the assay LOD (lower-right cells, **Figure 6–3A-C**). This analysis demonstrates how selection of an IVLT similar to the assay LOD will overestimate clinical sensitivity to detect infectious individuals.

Importantly, when considering viral loads above the IVLT in any of the three specimen types tested (**Figure 6-3D-F**), inferred clinical sensitivities was lower for all specimen types, regardless of IVLT or assay LOD. Because extreme differences in viral load among specimen types from the same individual at a given timepoint,[26] individuals often had high, presumably infectious viral loads in one but not all specimen types. Thus, inferred clinical sensitivity decreased drastically when infectiousness in multiple specimen types, rather than just one, is considered.

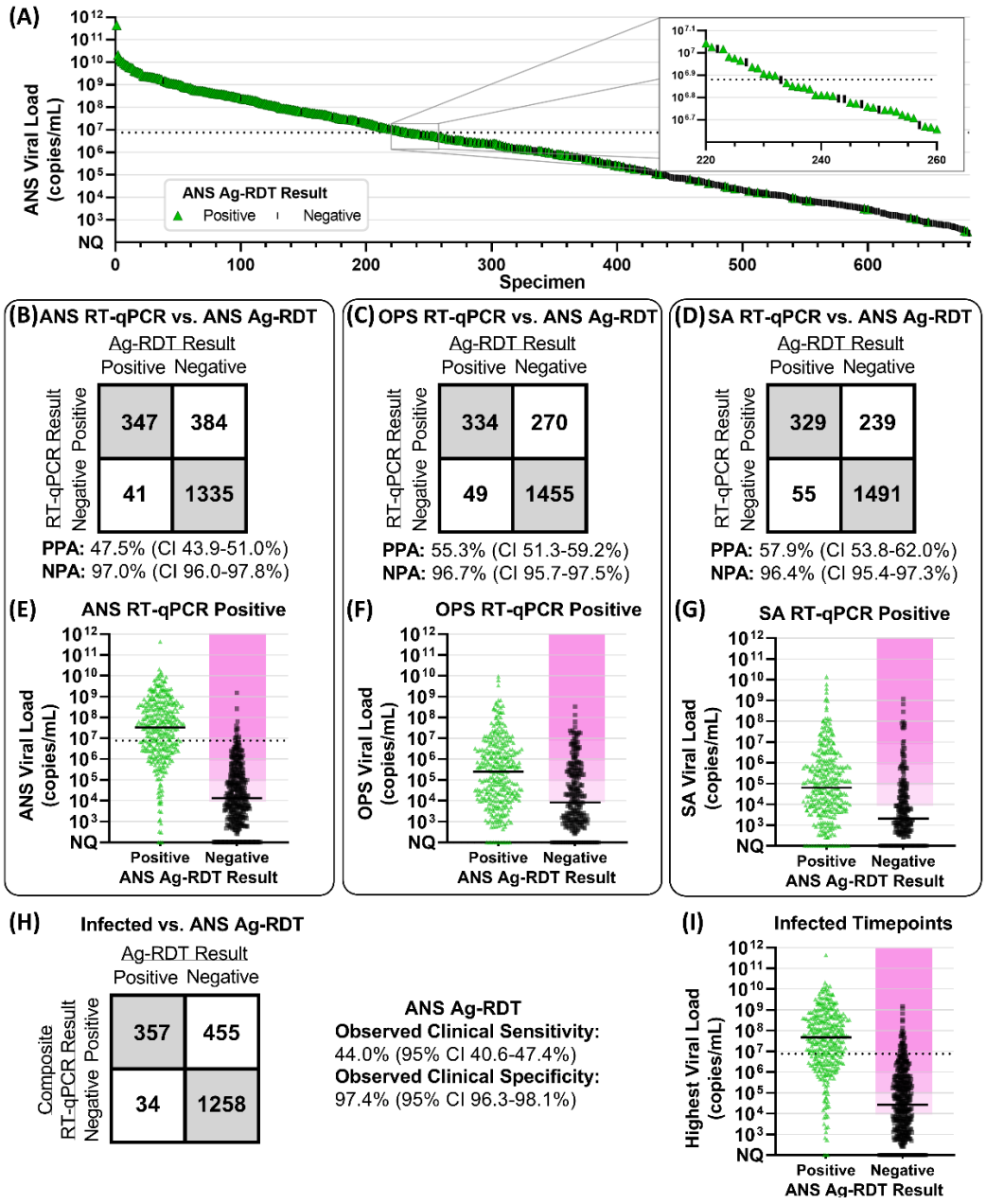

Figure 6-2. Comparison of Anterior-Nares Swab Antigen Rapid Diagnostic Test (Ag-RDT) Results to RT-qPCR Results and Viral Loads. **(A)** 680 ANS specimens with quantifiable SARS-CoV-2 viral loads are ordered by viral load and colored by Ag-RDT results (green for positive antigen test result, black for antigen negative). Inset shows higher resolution for results with viral loads around $7.6x10^6$ copies/mL (black dashed line), above which 95% of ANS specimen resulted Ag-RDT positive. 2x2 matrices of concordance between ANS Ag-RDT results and valid, conclusive RT-qPCR results for **(B)** 2107 ANS specimens, **(C)** 2108 OPS specimens and **(D)** 2114 SA specimens. PPA, positive percent agreement; NPA, negative percent agreement. CI indicates 95% confidence interval. Distribution of viral loads from **(E)** 731 RT-qPCR positive ANS specimens, **(F)** 604 RT-qPCR positive OPS specimens and **(G)** 568 RT-qPCR positive SA specimens, with either positive or negative Ag-RDT results. Solid horizontal black lines indicate medians. **(H)** A 2x2 matrix of observed concordance between Ag-RDT results, and infected status, based on composite RT-qPCR results from all three specimen types, at 2104 timepoints with valid, conclusive results for all specimen types by RT-qPCR and valid ANS Ag-RDT results. **(I)** Distribution of the highest viral load among ANS, OPS, and SA specimens collected by any participant at 812 composite RT-qPCR positive (infected) timepoints, with either positive or negative Ag-RDT results. Magenta shading in panels E, F, G, and I indicates infectious viral loads (above 10^4, 10^5, 10^6 or 10^7 copies/mL). ANS, anterior-nares swab; OPS, oropharyngeal swab; SA, saliva; Ag-RDT, antigen rapid diagnostic test. Detailed tabulation including inconclusive and invalid results shown in **Supplemental Table 6-2**.

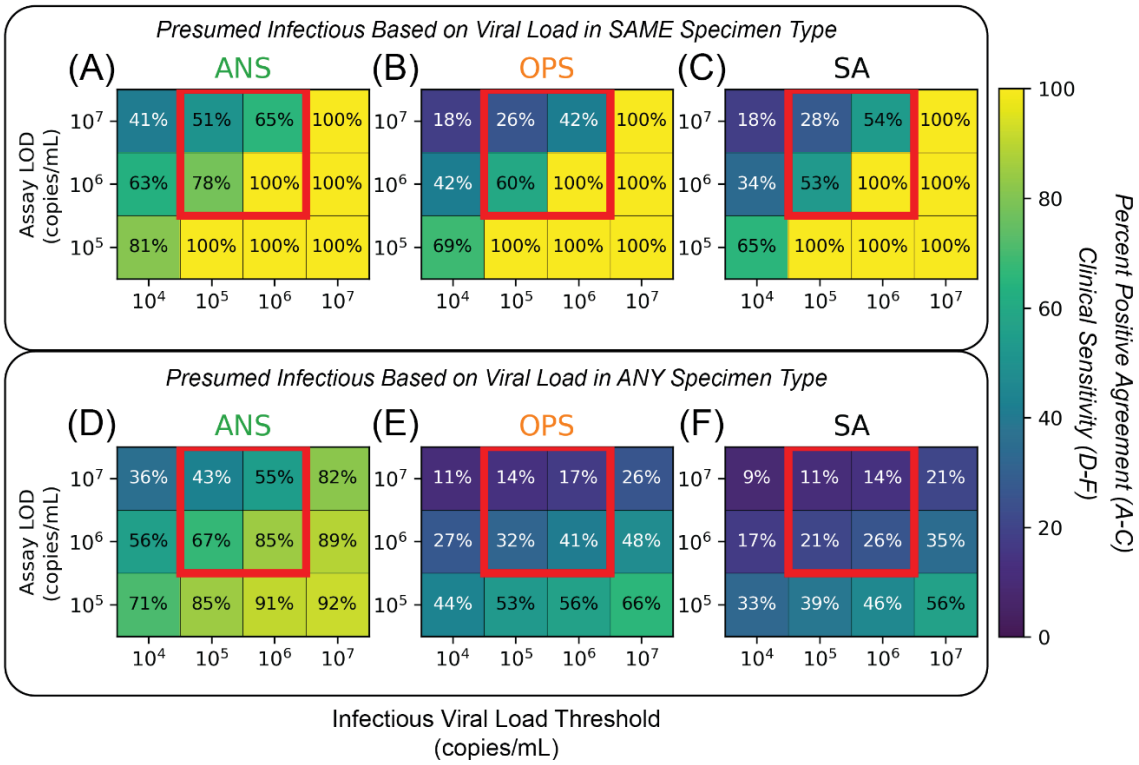

Figure 6-3. Effects of Low-Analytical-Sensitivity Assay LOD, Infectious Viral-Load Threshold (IVLT), and Inclusion of Multiple Specimen Types on Inferred Clinical Sensitivity to Detect Presumed Infectious Individuals. **(A-C)** Heatmaps visualizing positive percent agreement (A-C) for each specimen type, **(A)** saliva (SA), **(B)** anterior-nares swab (ANS), and **(C)** oropharyngeal swab (OPS), tested with assays of different LODs in the range of low-analytical-sensitivity tests (such as Ag-RDTs) to detect individuals presumed infectious only if the viral load in the tested specimen type was at or above a given IVLT. Red boxes highlight an important interaction between assay LOD and IVLT that is elaborated in the text. **(D-F)** Heatmaps visualizing the inferred clinical sensitivity for each specimen type, **(D)** SA, **(E)** ANS, **(F)** OPS, tested with assays of different LODs to detect individuals presumed to be infectious if the viral load in any specimen type was at or above a given IVLT. Heatmaps for computationally contrived combination specimen types are shown in **Supplemental Figure 6-2**.

Longitudinal Ag-RDT Performance

We next assessed the performance of the ANS Ag-RDT longitudinally through acute infection. We identified a cohort of 17 individuals who began sampling early in the course of infection (**Figure 6-1**). We compiled participants' daily viral-load measurements for each specimen type (SA, ANS, OPS),[26] with paired ANS Ag-RDT results, and classified timepoints as presumably infectious when viral load in any of the three specimen types was above a given IVLT (**Figure 6-4**).

All but two of the 17 participants (**Figure 6-4D,F**) reached presumed infectious viral loads at least 1 day before their first positive Ag-RDT result: Of these 15 participants, six had a delay of one to two days (**Figure 6-4G,J,N,O,P,Q**), five had a delay of three days (**Figure 6-4H,I,K,L,M**), one had a delay of five days (**Figure 6-**

4C), and one had a delay of eight days (**Figure 6-4A**). Two participants (**Figure 6-4B,E**) had infectious viral loads for more than eight days each, but neither ever reported a positive ANS Ag-RDT result. The participant in **Figure 6-4B** had high (>10^5 copies/mL) OPS viral loads for 12 days while ANS specimens remained low (rising just above 10^4 copies/mL only once). The participant in **Figure 6-4E** had ANS viral loads >10^6 copies/mL on three days, but never yielded a positive Ag-RDT result, likely because these viral loads were near the Ag-RDT LOD.

In this cohort, the overall observed clinical sensitivity of the ANS Ag-RDT to detect infected individuals was significantly higher when participants were symptomatic (**Supplemental Figure 6-1**), but low (<50%) at both symptomatic and asymptomatic timepoints.

Nasal Ag-RDT Misses Infectious Viral Loads in Other Specimen Types

Given that many individuals had high, presumably infectious viral loads before their first ANS Ag-RDT positive result (**Figure 6-4**), we next assessed how periods of infectiousness in each of the three specimen types overlapped, and which timepoints were detected by the ANS Ag-RDT. We aligned each participant's timecourse to their first RT-qPCR positive result in any specimen type then plotted the period each specimen type had viral loads above the IVLT. Periods when viral loads were above the IVLT in any specimen type were indicated in magenta. Positive ANS Ag-RDT results were overlaid (**Figure 6-5**).

For IVLTs below 10^7 copies/mL (**Figure 6-5A-C**), all 17 individuals were presumably infectious for at least one day. As IVLT increased, the length of the infectious period for each participant decreased. At an IVLT of 10^7 copies/mL (**Figure 6-5D**), three participants (**Figure 6-5D[A,E,F])** would not be considered infectious.

If infectious periods in OPS and SA overlapped perfectly with infectious period in ANS, then OPS and SA viral loads would not affect the performance of the ANS Ag-RDT to detect infectious individuals. But this was not the case. The presumed infectious periods for different specimen types were often asynchronous (non-overlapping). For many individuals, OPS or SA specimens reached infectious viral loads prior to ANS. Thus, the Ag-RDT often resulted negative during the infectious period (pink-shaded days lacking green triangles in **Figure 6-5**), particularly in the first days of the infectious period.

Performance of Ag-RDT in Pre-Infectious and Infectious Periods

We next investigated the performance of the daily ANS Ag-RDT to detect individuals during the pre-infectious and infectious periods. For each IVLT, the observed clinical sensitivity of the Ag-RDT was plotted alongside inferred clinical sensitivity predicted for ANS specimens tested by a hypothetical assay with a similar LOD (10^6 copies/mL).

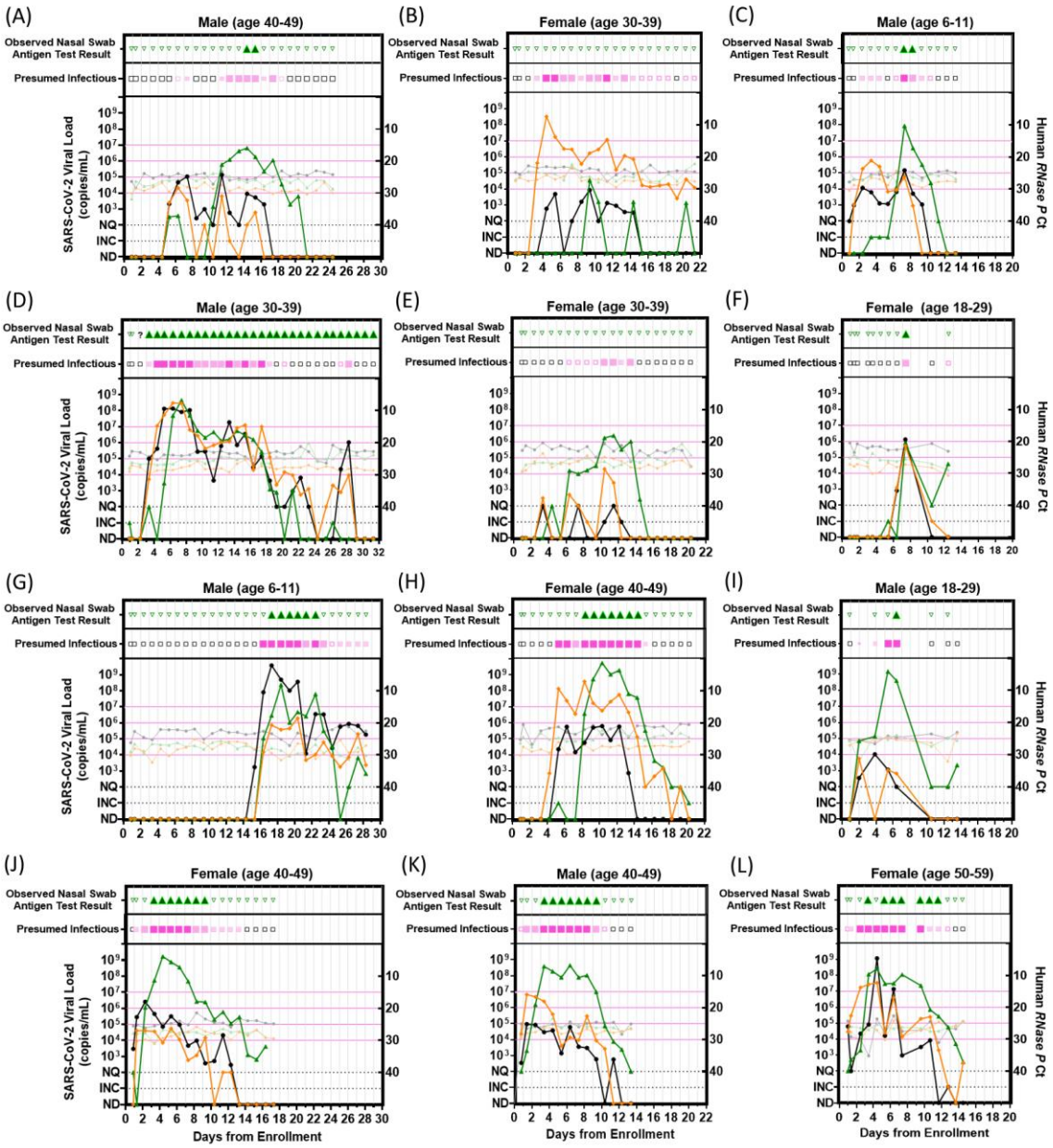

Figure continues on next page >>

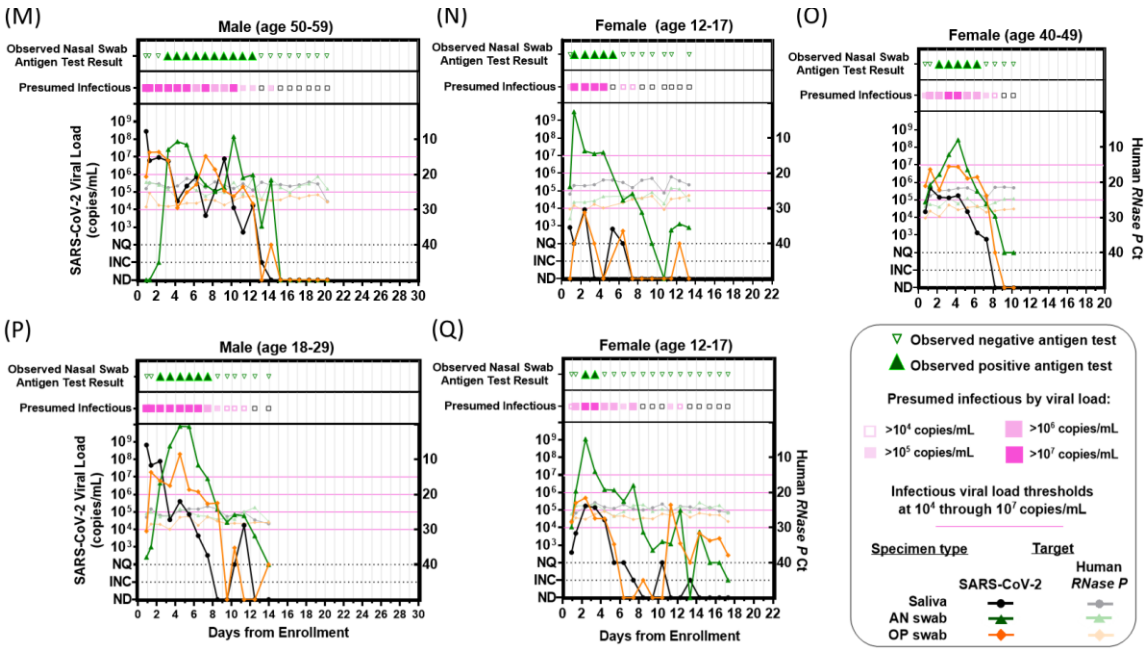

Figure 6-4. Longitudinal Viral Loads and Antigen Rapid Diagnostic Testing**.** Each panel **(A-Q)** represents a single participant throughout the course of enrollment, with observed ANS rapid antigen testing results, presumed infectious period (magenta) based on viral loads at or above each infectious viral-load threshold 10^4 to 10^7 copies/mL in any specimen type, SARS-CoV-2 viral loads (left y-axis) and human *RNase P* Ct values (right y-axis) by RT-qPCR in each specimen type. Viral-load data for participants A-N were reported previously.[26] INC, inconclusive; NQ, viral load detected but below the test LOD (250 copies/mL); ND, not detected for RT-qPCR measurements; AN, anterior-nares; OP, oropharyngeal. A single invalid antigen test is indicated with a "?" symbol in panel D.

The inferred clinical sensitivity predicted for ANS specimens tested by this hypothetical assay and the observed clinical sensitivity of the Ag-RDT were similar for both the pre-infectious and infectious periods, at all four IVLTs (**Figure 6-6A,D**). This congruency supported the use of quantitative viral loads to predict Ag-RDT performance. In the pre-infectious period, the Ag-RDT was positive in, at most, one of 34 timepoints (**Figure 6-6B**). In the infectious period, the Ag-RDT detected only 63% of presumed infectious individuals in the highest IVLT (10^7 copies/mL) (**Figure 6-6C**). Performance decreased as IVLT was lowered; at an IVLT of 10^4 copies/mL, the Ag-RDT detected only 48% of infectious individuals.

We also inferred the clinical sensitivity of other specimen types if tested by an assay with similar analytical sensitivity as the Ag-RDT. At an LOD of 10^6 copies/mL, no single specimen type (ANS, OPS, SA) achieved 95% inferred clinical sensitivity to detect infectious individuals, for any IVLT (**Figure 6-6C**). However, a computationally-contrived AN–OP combination swab specimen at an LOD of 10^6 copies/mL was predicted to perform significantly better than all other specimen types, including the observed performance of the ANS Ag-RDT (**Figure 6-6D**). But, at this low analytical sensitivity, the AN–OP swab was unable to detect pre-infectious timepoints.

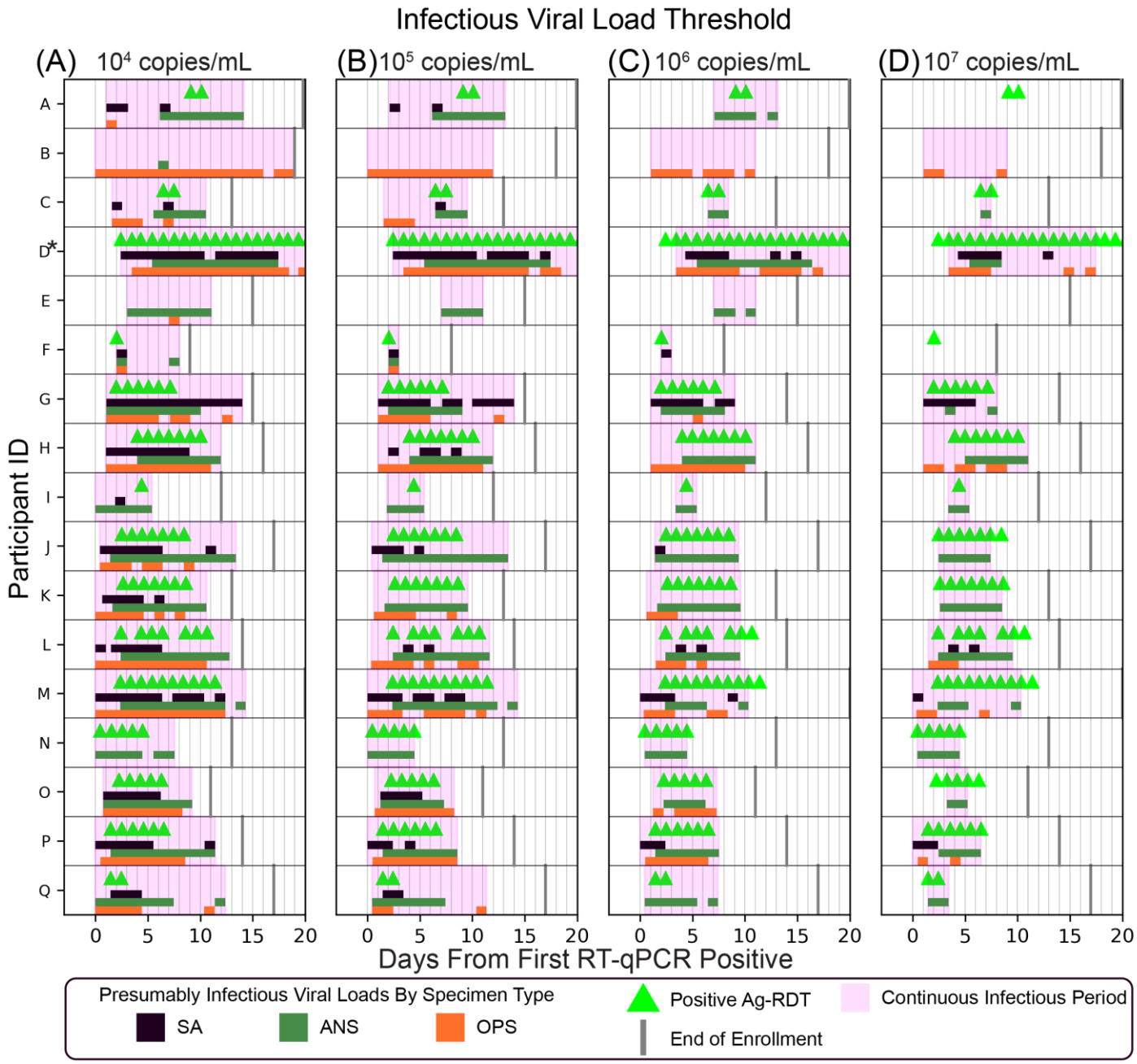

Figure 6-5. Periods of Presumed Infectiousness as a Factor of Infectious Viral-Load Threshold (IVLT). (**A-D)** Days starting from first RT-qPCR positive that each participant (A-Q; see **Figure 6-3**) had presumably infectious viral loads (with IVLTs of 10^4 to 10^7 copies/mL) in each specimen type (green bars, anterior nares swab [ANS]; orange bars, oropharyngeal swab [OPS]; black bars, saliva [SA]). Positive Ag-RDT tests are indicated with green triangles and the final date of study enrollment for each is indicated with grey lines. The timecourse for participant D (who experienced a series of false-positive antigen tests) is truncated, indicated by a * (see Supplementary Information).

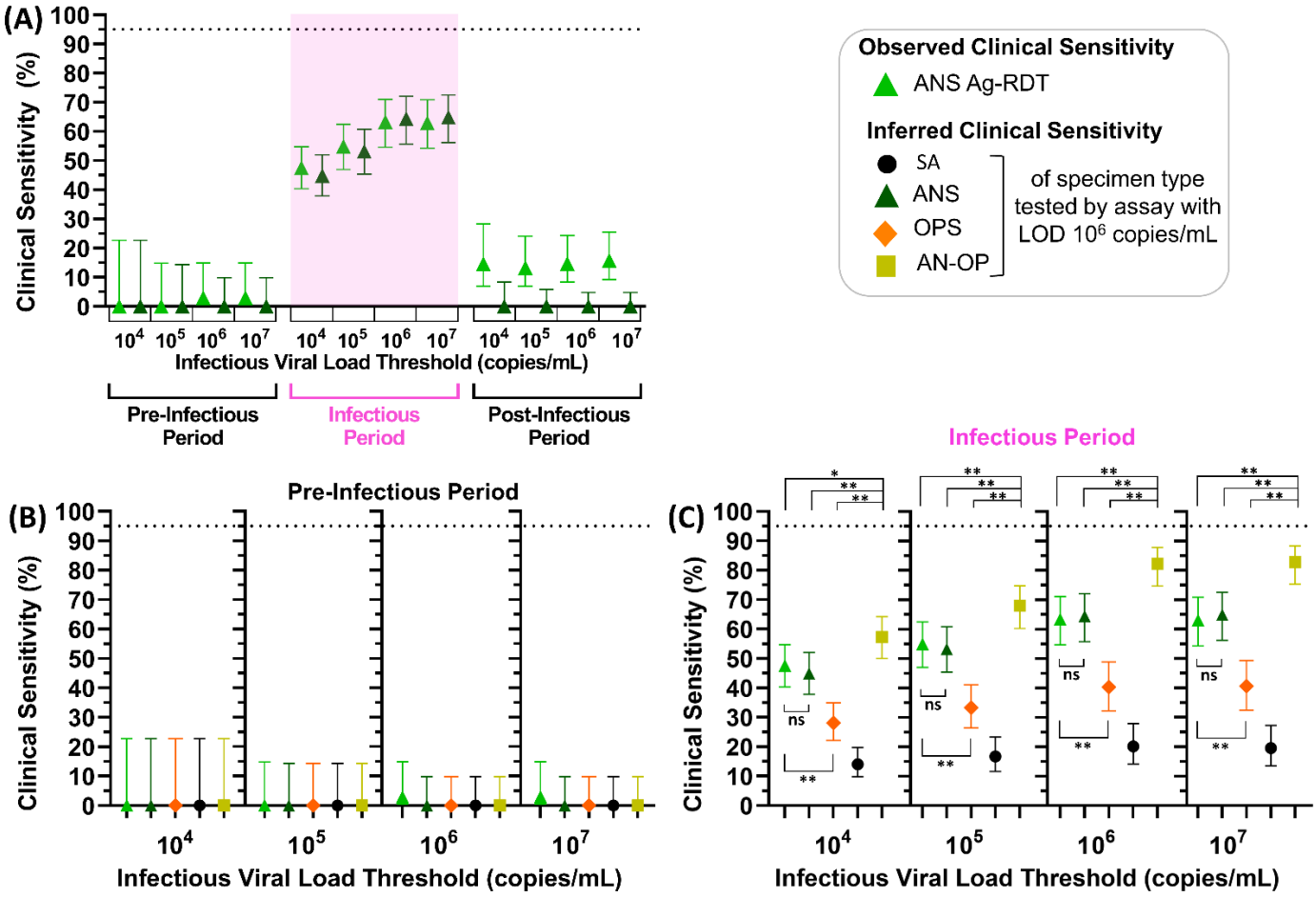

Figure 6-6. Observed and Inferred Performance of Low-Analytical-Sensitivity Daily Antigen Rapid Diagnostic Tests (Ag-RDTs) to Detect Presumed Infectious Individuals. Individuals were presumed infectious for the period between first specimen (of any type) with a viral load above the infectious viral load threshold (10^4, 10^5, 10^6, or 10^7 copies/mL) until all specimen types were below the IVLT; specimens collected prior to this period were considered pre-infectious, and after this period, post-infectious. **(A)** Observed clinical sensitivity of the ANS Ag-RDT (fluorescent green), and the inferred clinical sensitivity of an ANS test with an LOD of 10^6 copies/mL (green), for each stage of infection. Subsequent plots show the observed clinical sensitivity for detection of presumed infectious individuals by the ANS Ag-RDT (fluorescent green) and the inferred clinical sensitivity for ANS (green), OPS (orange), SA (black), and a computationally-contrived AN–OP combination swab specimen type (yellow) during the **(B)** pre-infectious period and **(C)** infectious period of infection. Inferred clinical sensitivity was based on measured viral loads in the given specimen type at or above an LOD of 10^6. Error bars indicate 95% confidence intervals. Comparison of the clinical sensitivities to detect infectiousness at IVLTs of 10^4 to 10^7 across specimen types was performed using the McNemar Exact Test, for given comparisons across specimen type. ANS Ag-RDT vs ANS with LOD 10^6 copies/mL was tested using a two-tailed McNemar Exact Test; all other combinations use a one-tailed McNemar exact test. *P*-values were adjusted using a Benjamini–Yekutieli correction to account for multiple hypotheses being tested. Comparisons resulting in *p*-values <0.01 are indicated by **, <0.05 are indicated by *, and >0.05 are indicated by "ns". Point estimates for these comparisons are provided in **Supplemental Table 6-4.** Additional analyses of the inferred clinical sensitivity of the anterior-nares—oropharyngeal combination swab can be found in a separate manuscript.[26] SA, saliva; ANS, anterior-nares swab; OPS, oropharyngeal swab; AN–OP, anterior-nares–oropharyngeal combination swab; LOD, limit of detection.

Conclusions

Our field evaluation of an ANS Ag-RDT revealed three key findings generally relevant to the use of Ag-RDTs and other tests with low and moderate analytical sensitivity (including some molecular tests that forgo nucleic-acid extraction and purification). First, the evaluated Ag-RDT showed low (44%) clinical sensitivity for detecting infected persons at any stage of infection. This poor clinical sensitivity is consistent with another field evaluation of this Ag-RDT used for twice-weekly screening testing at a college.[53] It is also consistent with FDA[54] and CDC guidance[55] that using two or more repeat ANS Ag-RDTs are needed to improve the clinical sensitivity of these tests.

There are two reasons for the observed low clinical sensitivity of the ANS Ag-RDT to detect infected individuals: (i) First, the low analytical sensitivity of Ag-RDTs requires high viral loads to yield a positive result. Although it has been proposed[12] that a rapid rise in viral load reduces the advantage of tests that can detect low viral loads (**Figure 6-7A**), this advantage remains when there is a more gradual rise in viral loads (**Figure 6-7B**) as we observed in some individuals (**Figure 6-4A,C**). (ii) The second, more impactful reason is that many early-infection timepoints had detectable virus in saliva or throat swabs, but not ANS. A nasal-swab reference test would miss these infected timepoints. Therefore, the true performance of an ANS Ag-RDT would be worse when compared to composite infection status based on multiple specimen types rather than nasal-swab alone (**Figure 6-7C**).

These two reasons for poor detection of infected individuals by Ag-RDTs have implications for the design and interpretation of other Ag-RDT evaluations. Because viral-load timecourses in different specimen types from an individual are asynchronous,[26] the true clinical sensitivity of an Ag-RDT will be lower than reported by field evaluations that compare only to an ANS reference test.[19,39,42-44,46-48,58] The PPA reported by the Ag-RDT manufacturer to the FDA (83.5%) was calculated relative to detection by a nasal RT-PCR reference test—and nearly all specimens (84 of 91) were from symptomatic individuals likely late in infection.[50] Our work suggests that governing bodies should require clinical sensitivity estimates for an Ag-RDT to detect infected individuals be based on a composite infection status from multiple upper-respiratory specimen types.

Our second key finding is that the Ag-RDT poorly detected presumably infectious individuals. The Ag-RDT detected ≤63% of presumed infectious timepoints. This low clinical sensitivity to detect infectious individuals is inconsistent with a common view[12] that proposes low-analytical-sensitivity tests have near-perfect detection of infectious individuals (**Figure 6-7D**).

Our data demonstrate that this common but idealized view misses two important points: (i) First, in the common view, the LOD of the Ag-RDT aligns with the IVLT (**Figure 6-7D**), but there is no fundamental reason why LOD should align perfectly with the IVLT. Replication-competent virus is reliably isolated from specimens with viral

loads of $\geq 10^4$ copies/mL (**Supplemental Table 6-1**), whereas Ag-RDT LODs span orders of magnitude (~10^5–10^7 copies/mL). As demonstrated here (**Figure 6-3**), if the chosen IVLT is at or above a test's LOD, that test will be predicted to have near-perfect clinical sensitivity to detect infectious individuals. However, if the true IVLT is below the LOD, clinical sensitivity may be reduced substantially (**Figure 6-7E**). Additionally, when viral loads rise gradually, there is more time between when an individual becomes infectious and when viral loads become detectable by the Ag-RDT. (ii) The second point that the common view misses is the potential for infectious virus in specimen types other than the one tested by the Ag-RDT. We observed presumably infectious viral loads in SA and OPS specimens at all IVLTs from 10^4 to 10^7 copies/mL, even while ANS viral loads were well below the Ag-RDT's LOD. As expected, the Ag-RDT was unable to detect presumably infectious individuals at these timepoints. In one individual (**Figure 6-4A**), ANS viral loads were undetectable or $<10^3$ copies/mL for the first five days of infection, resulting in negative Ag-RDT results despite presumably infectious viral loads in SA and OPS specimens. Because nasal Ag-RDTs can only detect individuals with high, presumably infectious viral loads in nasal swabs, individuals with infectious virus in other specimen types are missed (**Figure 6-7F**).

These two points have critical implications for evaluating an Ag-RDT's ability to detect infectious individuals. Some agent-based outbreak models[5,59-61] have inferred that low-analytical-sensitivity tests would be effective at mitigating SARS-CoV-2 transmission in a population. Individuals in these simulations are infectious and capable of transmitting infection when viral loads are above a chosen IVLT. These models will overestimate test effectiveness if infectiousness is based only on simulated viral loads in a single, tested specimen type, and/or if the IVLT chosen is near or above the LOD of the simulated test. Additionally, nearly all studies evaluating Ag-RDT concordance with infectiousness performed viral culture only on a single specimen type[16-19,35,36,38-44] overlooking potentially infectious virus in other types. One of these studies[38] is cited as a basis for CDC[55] recommendations to use repeat ANS Ag-RDTs to improve their clinical sensitivity.

Our third key finding is that use of a combination AN–OP specimen type can significantly improve the performance of Ag-RDTs to detect infectious individuals. Improved detection with an AN–OP combination swab for a different Ag-RDT was recently demonstrated among asymptomatic individuals at a testing center.[62] Many countries already authorized and/or implemented the use of combination specimen types for Ag-RDTs, yet this is not the case in the U.S., where all at-home Ag-RDTs use nasal swabs.

We acknowledge several study limitations. First, we only evaluated one Ag-RDT. Other Ag-RDTs have different LODs[6,63]; however, equivalence between the clinical sensitivity of this Ag-RDT directly observed versus inferred based on ANS viral loads supports that performance of other Ag-RDTs could also be inferred from quantitative viral-load data. Second, we infer but did not directly observe the clinical sensitivity for a combination AN–OP

swab. Finally, this study was performed in the context of two SARS-CoV-2 variants (Delta and Omicron) and one geographical area.

Ag-RDTs are useful tools for rapid identification of individuals with high viral loads in the specimen type tested. As discussed above, the utility of Ag-RDTs for detection of infected and presumably infectious individuals is often justified using several assumptions (**Figure 6-7**), in particular that viral loads in all specimen types from an individual at a given timepoint are similar. Our study demonstrates that this assumption is not justified. Re-evaluating assumptions based on new evidence will inform more effective testing strategies, both for SARS-CoV-2 and for other respiratory viral pathogens.

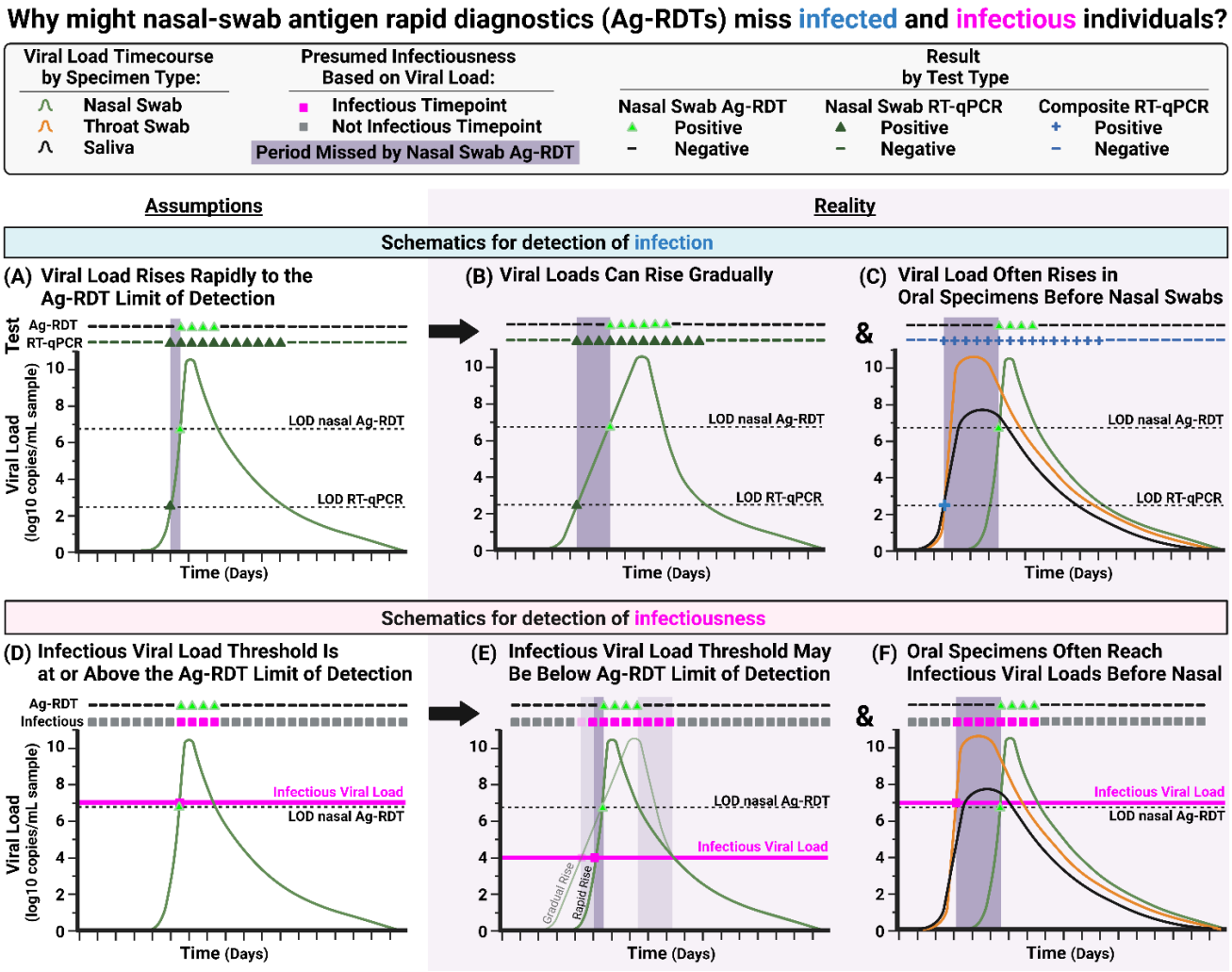

Figure 6-7. Conceptual Diagrams Illustrating Why Nasal-only Antigen Rapid Diagnostic Tests (Ag-RDTs) Are Likely to Miss Infected and Infectious Individuals. **(A)** Schematic of an idealized, hypothetical viral-load timecourse in which viral load rises quickly from detectable to the limit of detection (LOD) of a low-analytical-sensitivity test, such as Ag-RDTs. Such a pattern would result in a daily Ag-RDT being effective for detection of infection (diagram based on a commonly held view[12]). **(B)** Schematic of a viral-load timecourse based on longitudinal viral-load data[16-30] in which, for some individuals, early viral loads rise gradually, resulting in detection of the infected individual several days earlier by a high-analytical-sensitivity test than by the Ag-RDT. This mechanism for missed detection by COVID-19 Ag-RDTs has been previously hypothesized.[56] **(C)** Schematic of a viral-load timecourse based on observed paired, longitudinal viral-load data in which individuals exhibit a rise in viral load in oral (saliva or throat swab) specimens days before viral loads rise in nasal specimens.[17,18,20,21,25,26] When these additional specimen types are used to assign a composite infection status, the nasal Ag-RDT is revealed to have poor performance. **(D)** Schematic of an idealized, hypothetical viral-load timecourse (based on commonly held views[12,16,57]) in which viral load rises quickly from detectable to infectious, and the infectious viral load threshold is equivalent to the LOD of the Ag-RDT. Such a pattern would result in near-perfect detection of infectious individuals by the daily Ag-RDT. **(E)** Schematic of a viral-load timecourse in which the infectious viral load is lower than the LOD of the Ag-RDT. Here, infectious individuals would be missed by the Ag-RDT during the period viral load is between the infectious viral load threshold and the LOD of the Ag-RDT. This period will be longer if the rise in viral load is gradual (light-green line) rather than quick (dark-green line). **(F)** Schematic of a viral-load timecourse in which individuals exhibit high, presumably infectious viral loads in saliva or throat swab specimens while nasal swab viral loads remain very low, particularly at the beginning of infection. Here, the ANS Ag-RDT is unable to detect most infectious timepoints. The dashed LOD nasal Ag-RDT line indicates the inferred LOD for the nasal-swab Ag-RDT we evaluated (7.6×10^6 copies/mL). The dashed LOD RT-qPCR line indicates the LOD of the RT-qPCR assay used in this study (250 copies/mL). The pink Infectious Viral Load line indicates a threshold associated with the presence of replication-competent virus; individuals are considered infectious if any specimen type has a viral load above the threshold.

References

1. WHO. Antigen-detection in the diagnosis of SARS-CoV-2 infection [interim guidance]. 2021. https://www.who.int/publications/i/item/antigen-detection-in-the-diagnosis-of-sars-cov-2infection-using-rapid-immunoassays.

2. Drain PK. Rapid Diagnostic Testing for SARS-CoV-2. *N Engl J Med* 2022; **386**(3): 264-72.

3. Rader B, Gertz A, Iuliano AD, et al. Use of At-Home COVID-19 Tests - United States, August 23, 2021-March 12, 2022. *MMWR Morb Mortal Wkly Rep* 2022; **71**(13): 489-94.

4. Hayden MK, Hanson KE, Englund JA, et al. The Infectious Diseases Society of America Guidelines on the Diagnosis of COVID-19: Antigen Testing. *IDSA* 2022; **v.2 updated 12/20/2022**.

5. Han AX, Girdwood SJ, Khan S, et al. Strategies for Using Antigen Rapid Diagnostic Tests to Reduce Transmission of Severe Acute Respiratory Syndrome Coronavirus 2 (SARS-CoV-2) in Low- and Middle-Income Countries: A Mathematical Modelling Study Applied to Zambia. *Clin Infect Dis* 2022: ciac814.

6. Hardick J, Gallagher N, Sachithanandham J, et al. Evaluation of Four Point of Care (POC) Antigen Assays for the Detection of the SARS-CoV-2 Variant Omicron. *Microbiol Spectr* 2022: e0102522.

7. FDA. In Vitro Diagnostic EUAs - Other Tests for SARS-CoV-2. 2022. https://www.fda.gov/medical-devices/coronavirus-disease-2019-covid-19-emergency-use-authorizations-medical-devices/in-vitro-diagnostics-euas-other-tests-sars-cov-2.

8. Cubas-Atienzar AI, Kontogianni K, Edwards T, et al. Limit of detection in different matrices of 19 commercially available rapid antigen tests for the detection of SARS-CoV-2. *Sci Rep* 2021; **11**(1): 18313.

9. Mercer T, Almond N, Crone MA, et al. The Coronavirus Standards Working Group's roadmap for improved population testing. *Nat Biotechnol* 2022; **40**(11): 1563-8.

10. Deerain J, Druce J, Tran T, et al. Assessment of the Analytical Sensitivity of 10 Lateral Flow Devices against the SARS-CoV-2 Omicron Variant. *J Clin Microbiol* 2022; **60**(2): e0247921-e.

11. Lee Rose A, Herigon Joshua C, Benedetti A, Pollock Nira R, Denkinger Claudia M, Humphries Romney M. Performance of Saliva, Oropharyngeal Swabs, and Nasal Swabs for SARS-CoV-2 Molecular Detection: a Systematic Review and Meta-analysis. *J Clin Microbiol*; **59**(5): e02881-20.

12. Mina MJ, Parker R, Larremore DB. Rethinking Covid-19 Test Sensitivity — A Strategy for Containment. *N Engl J Med* 2020.

13. Tom MR, Mina MJ. To Interpret the SARS-CoV-2 Test, Consider the Cycle Threshold Value. *Clin Infect Dis* 2020; **71**(16): 2252-4.

14. Bullard J, Dust K, Funk D, et al. Predicting Infectious Severe Acute Respiratory Syndrome Coronavirus 2 From Diagnostic Samples. *Clin Infect Dis* 2020; **71**(10): 2663-6.

15. Larremore DB, Wilder B, Lester E, et al. Test sensitivity is secondary to frequency and turnaround time for COVID-19 screening. *Science Advances* 2021; **7**(1): eabd5393.

16. Kirby JE, Riedel S, Dutta S, et al. SARS-CoV-2 antigen tests predict infectivity based on viral culture: comparison of antigen, PCR viral load, and viral culture testing on a large sample cohort. *Clin Microbiol Infect* 2023; **29**(1): 94-100.

17. Ke R, Martinez PP, Smith RL, et al. Longitudinal analysis of SARS-CoV-2 vaccine breakthrough infections reveal limited infectious virus shedding and restricted tissue distribution. *Open Forum Infectious Diseases* 2022: ofac192.

18. Ke R, Martinez PP, Smith RL, et al. Daily longitudinal sampling of SARS-CoV-2 infection reveals substantial heterogeneity in infectiousness. *Nature Microbiology* 2022; **7**(5): 640-52.

19. Bonenfant G, Deyoe JE, Wong T, et al. Surveillance and Correlation of Severe Acute Respiratory Syndrome Coronavirus 2 Viral RNA, Antigen, Virus Isolation, and Self-Reported Symptoms in a Longitudinal Study With Daily Sampling. *Clin Infect Dis* 2022; **75**(10): 1698-705.

20. Adamson B, Sikka R, Wyllie AL, Premsrirut P. Discordant SARS-CoV-2 PCR and Rapid Antigen Test Results When Infectious: A December 2021 Occupational Case Series. *medRxiv* 2022: 2022.01.04.22268770.

21. Savela ES, Viloria Winnett A, Romano Anna E, et al. Quantitative SARS-CoV-2 viral-load curves in paired saliva and nasal swabs inform appropriate respiratory sampling site and analytical test sensitivity required for earliest viral detection. *J Clin Microbiol* 2021; **0**(ja): JCM.01785-21.

22. Cevik M, Tate M, Lloyd O, Maraolo AE, Schafers J, Ho A. SARS-CoV-2, SARS-CoV, and MERS-CoV viral load dynamics, duration of viral shedding, and infectiousness: a systematic review and meta-analysis. *Lancet Microbe* 2021; **2**(1): e13-e22.

23. Winnett A, Cooper MM, Shelby N, et al. SARS-CoV-2 Viral Load in Saliva Rises Gradually and to Moderate Levels in Some Humans. *medRxiv* 2020: 2020.12.09.20239467.

24. Lai J, German J, Hong F, et al. Comparison of Saliva and Mid-Turbinate Swabs for Detection of COVID-19. *medRxiv* 2022: 2021.12.01.21267147.

25. Killingley B, Mann AJ, Kalinova M, et al. Safety, tolerability and viral kinetics during SARS-CoV-2 human challenge in young adults. *Nat Med* 2022; **28**(5): 1031-41.

26. Viloria Winnett A, Akana R, Shelby N, et al. Extreme differences in SARS-CoV-2 viral loads among respiratory specimen types during presumed pre-infectious and infectious periods. *medRxiv (Accepted to PNAS Nexus)* 2022: MEDRXIV/2022/277113.

27. Walsh KA, Jordan K, Clyne B, et al. SARS-CoV-2 detection, viral load and infectivity over the course of an infection. *The Journal of infection* 2020; **81**(3): 357-71.

28. Stankiewicz Karita HC, Dong TQ, Johnston C, et al. Trajectory of Viral RNA Load Among Persons With Incident SARS-CoV-2 G614 Infection (Wuhan Strain) in Association With COVID-19 Symptom Onset and Severity. *JAMA Network Open* 2022; **5**(1): e2142796-e.

29. Kissler SM, Fauver JR, Mack C, et al. Viral dynamics of acute SARS-CoV-2 infection and applications to diagnostic and public health strategies. *PLoS Biol* 2021; **19**(7): e3001333-e.

30. Kissler SM, Fauver JR, Mack C, et al. Viral Dynamics of SARS-CoV-2 Variants in Vaccinated and Unvaccinated Persons. *N Engl J Med* 2021; **385**(26): 2489-91.

31. Stanley S, Hamel Donald J, Wolf Ian D, et al. Limit of Detection for Rapid Antigen Testing of the SARS-CoV-2 Omicron and Delta Variants of Concern Using Live-Virus Culture. *J Clin Microbiol* 2022; **60**(5): e00140-22.

32. Li R, Pei S, Chen B, et al. Substantial undocumented infection facilitates the rapid dissemination of novel coronavirus (SARS-CoV-2). *Science* 2020; **368**(6490): 489-93.

33. Robertson LS. Did people's behavior after receiving negative COVID-19 tests contribute to the spread? *Journal of public health (Oxford, England)* 2021; **43**(2): 270-3.

34. Pickering S, Batra R, Merrick B, et al. Comparative performance of SARS-CoV-2 lateral flow antigen tests and association with detection of infectious virus in clinical specimens: a single-centre laboratory evaluation study. *Lancet Microbe* 2021; **2**(9): e461-e71.

35. Chu VT, Schwartz NG, Donnelly MAP, et al. Comparison of Home Antigen Testing With RT-PCR and Viral Culture During the Course of SARS-CoV-2 Infection. *JAMA Internal Medicine* 2022; **182**(7): 701-9.

36. Pekosz A, Parvu V, Li M, et al. Antigen-Based Testing but Not Real-Time Polymerase Chain Reaction Correlates With Severe Acute Respiratory Syndrome Coronavirus 2 Viral Culture. *Clin Infect Dis* 2021; **73**(9): e2861-e6.

37. Korenkov M, Poopalasingam N, Madler M, et al. Evaluation of a Rapid Antigen Test To Detect SARS-CoV-2 Infection and Identify Potentially Infectious Individuals. *J Clin Microbiol* 2021; **59**(9): e00896-21.

38. Smith RL, Gibson LL, Martinez PP, et al. Longitudinal Assessment of Diagnostic Test Performance Over the Course of Acute SARS-CoV-2 Infection. *The Journal of Infectious Diseases* 2021; **224**(6): 976-82.

39. Bouton TC, Atarere J, Turcinovic J, et al. Viral Dynamics of Omicron and Delta Severe Acute Respiratory Syndrome Coronavirus 2 (SARS-CoV-2) Variants With Implications for Timing of Release from Isolation: A Longitudinal Cohort Study. *Clin Infect Dis* 2022: ciac510.

40. Kohmer N, Toptan T, Pallas C, et al. The Comparative Clinical Performance of Four SARS-CoV-2 Rapid Antigen Tests and Their Correlation to Infectivity In Vitro. *Journal of clinical medicine* 2021; **10**(2).

41. Steinlin-Schopfer J, Barbani MT, Kamgang R, Zwahlen M, Suter-Riniker F, Dijkman R. Evaluation of the Roche antigen rapid test and a cell culture-based assay compared to rRT- PCR for the detection of SARS-CoV-2: A contribution to the discussion about SARS-CoV-2 diagnostic tests and contagiousness. *Journal of clinical virology plus* 2021; **1**(1): 100020.

42. Ford L, Lee C, Pray IW, et al. Epidemiologic Characteristics Associated With Severe Acute Respiratory Syndrome Coronavirus 2 (SARS-CoV-2) Antigen-Based Test Results, Real-Time Reverse Transcription Polymerase Chain Reaction (rRT-PCR) Cycle Threshold Values, Subgenomic RNA, and Viral Culture Results From University Testing. *Clin Infect Dis* 2021; **73**(6): e1348-e55.

43. Shah MM, Salvatore PP, Ford L, et al. Performance of Repeat BinaxNOW Severe Acute Respiratory Syndrome Coronavirus 2 Antigen Testing in a Community Setting, Wisconsin, November 2020–December 2020. *Clin Infect Dis* 2021; **73**(Supplement_1): S54-S7.

44. Pray IW, Ford L, Cole D, et al. Performance of an Antigen-Based Test for Asymptomatic and Symptomatic SARS-CoV-2 Testing at Two University Campuses - Wisconsin, September-October 2020. *MMWR Morb Mortal Wkly Rep* 2021; **69**(5152): 1642-7.

45. Prince-Guerra JL, Almendares O, Nolen LD, et al. Evaluation of Abbott BinaxNOW Rapid Antigen Test for SARS-CoV-2 Infection at Two Community-Based Testing Sites - Pima County, Arizona, November 3-17, 2020. *MMWR Morb Mortal Wkly Rep* 2021; **70**(3): 100-5.

46. Soni A, Herbert C, Lin H, et al. Performance of Screening for SARS-CoV-2 using Rapid Antigen Tests to Detect Incidence of Symptomatic and Asymptomatic SARS-CoV-2 Infection: findings from the Test Us at Home prospective cohort study. *medRxiv* 2022: 2022.08.05.22278466.

47. Pilarowski G, Marquez C, Rubio L, et al. Field Performance and Public Health Response Using the BinaxNOWTM Rapid Severe Acute Respiratory Syndrome Coronavirus 2 (SARS-CoV-2) Antigen Detection Assay During Community-Based Testing. *Clin Infect Dis* 2021; **73**(9): e3098-e101.

48. Pollock NR, Jacobs JR, Tran K, et al. Performance and Implementation Evaluation of the Abbott BinaxNOW Rapid Antigen Test in a High-Throughput Drive-Through Community Testing Site in Massachusetts. *J Clin Microbiol* 2021; **59**(5).

49. Zymo Research. Quick SARS-CoV-2 rRT-PCR Kit. 2021. https://www.zymoresearch.com/products/quick-sars-cov-2-rrt-pcr-kit.

50. FDA. Quidel QuickVue At-Home OTC COVID-19 Test - Instructions for Use (IFU). 2021. https://www.fda.gov/media/147265/download

51. Levy JM, Frediani JK, Tyburski EA, et al. Impact of repeated nasal sampling on detection and quantification of SARS-CoV-2. *Sci Rep* 2021; **11**(1): 14903.

52. CLSI. EP12-A2 User Protocol for Evaluation of Qualitative Test Performance, 2nd edition; 2008.

53. Tinker SC, Prince-Guerra JL, Vermandere K, et al. Evaluation of self-administered antigen testing in a college setting. *Virol J* 2022; **19**(1): 202.

54. FDA. At-Home COVID-19 Antigen Tests-Take Steps to Reduce Your Risk of False Negative: FDA Safety Communication. 2022. https://www.fda.gov/medical-devices/safety-communications/home-covid-19-antigen-tests-take-steps-reduce-your-risk-false-negative-fda-safety-communication?utm_medium=email&utm_source=govdelivery (accessed Issued: August 11, 2022.

55. CDC. Guidance for Antigen Testing for SARS-CoV-2 for Healthcare Providers Testing Individuals in the Community. 2022. https://www.cdc.gov/coronavirus/2019-ncov/lab/resources/antigen-tests-guidelines.html.

56. Moreno GK, Braun KM, Pray IW, et al. Severe Acute Respiratory Syndrome Coronavirus 2 Transmission in Intercollegiate Athletics Not Fully Mitigated With Daily Antigen Testing. *Clin Infect Dis* 2021; **73**(Supplement_1): S45-S53.

57. Cevik M, Marcus JL, Buckee C, Smith TC. Severe Acute Respiratory Syndrome Coronavirus 2 (SARS-CoV-2) Transmission Dynamics Should Inform Policy. *Clin Infect Dis* 2021; **73**(Supplement_2): S170-S6.

58. James AE, Gulley T, Kothari A, Holder K, Garner K, Patil N. Performance of the BinaxNOW coronavirus disease 2019 (COVID-19) Antigen Card test relative to the severe acute respiratory coronavirus virus 2 (SARS-CoV-2) real-time reverse transcriptase polymerase chain reaction (rRT-PCR) assay among symptomatic and asymptomatic healthcare employees. *Infect Control Hosp Epidemiol* 2022; **43**(1): 99-101.

59. Kahn R, Holmdahl I, Reddy S, Jernigan J, Mina MJ, Slayton RB. Mathematical Modeling to Inform Vaccination Strategies and Testing Approaches for Coronavirus Disease 2019 (COVID-19) in Nursing Homes. *Clin Infect Dis* 2022; **74**(4): 597-603.

60. See I, Paul P, Slayton RB, et al. Modeling Effectiveness of Testing Strategies to Prevent Coronavirus Disease 2019 (COVID-19) in Nursing Homes—United States, 2020. *Clin Infect Dis* 2021; **73**(3): e792-e8.

61. Holmdahl I, Kahn R, Hay J, Buckee CO, Mina M. Estimation of Transmission of COVID-19 in Simulated Nursing Homes With Frequent Testing and Immunity-Based Staffing. *JAMA Network Open* 2021; **4**(5): e2110071.

62. Goodall BL, LeBlanc JJ, Hatchette TF, Barrett L, Patriquin G. Investigating the Sensitivity of Nasal or Throat Swabs: Combination of Both Swabs Increases the Sensitivity of SARS-CoV-2 Rapid Antigen Tests. *Microbiol Spectr* 2022; **10**(4): e0021722.

63. Kepczynski CM, Genigeski JA, Koski RR, Bernknopf AC, Konieczny AM, Klepser ME. A systematic review comparing at-home diagnostic tests for SARS-CoV-2: Key points for pharmacy practice, including regulatory information. *J Am Pharm Assoc (2003)* 2021; **61**(6): 666-77.e2.

Funding

This work was supported in part by a grant from the Ronald and Maxine Linde Center for New Initiatives at the California Institute of Technology (to R.F.I.) and the Jacobs Institute for Molecular Engineering for Medicine at the California Institute of Technology (to R.F.I.). A.V.W. is supported by a UCLA DGSOM Geffen Fellowship.

Acknowledgments

We sincerely thank the study participants for making this work possible. We thank Lauriane Quenee, Grace Fisher-Adams, Junie Hildebrandt, Megan Hayashi, RuthAnne Bevier, Chantal D'Apuzzo, Ralph Adolphs, Victor Rivera, Steve Chapman, Gary Waters, Leonard Edwards, Gaylene Ursua, Cynthia Ramos, and Shannon Yamashita for their assistance and advice on study implementation and/or administration. We thank Jessica Leong, Ojas Pradhan, Si Hyung Jin, Emily Savela, Bridget Yang, Ekta Patel, Hsiuchen Chen, Paresh Samantaray, Zeynep Turan, Cindy Kim, Trinity Lee, Vanessa Mechan, Katherine Stiefel, Rosie Zedan, Rahulijeet Chadha, Minkyo Lee, and Jenny Ji for volunteering their time to help with this study. We thank Prabhu Gounder, Tony Chang, Jennifer Howes, and Nari Shin for their support with recruitment. Finally, we thank all the case investigators and contact tracers at the Pasadena Public Health Department and Caltech Student Wellness Services for their efforts in study recruitment and their work in the pandemic response.

Disclosures

R.F.I. is a co-founder, consultant, and a director and has stock ownership of Talis Biomedical Corp.

All other authors declare that they have no competing interests.

Brief Author contributions

Detailed author contributions are in the Supplement.

Conceptualization: MF, Y-YG, RFI, NS, AVW

Methodology: RA, NS, AVW

Investigation: RA, AMC, YCC, SC, HD, MKK, JRBR, AER, NS, AVW, TY

Visualization: RA, NS, AVW

Funding acquisition: RFI, AVW

Project administration: RFI, NS

Supervision: YCC, RFI

Writing – original draft: RA, NS, AVW

Writing – review & editing: RA, AMC, RFI, AER, NS, AVW

Data and materials availability

The data underlying the results presented in the study can be accessed at

CaltechDATA: https://data.caltech.edu/records/20223.

Supplementary Methods

Study Population

This study was approved under Caltech IRB #20-1026. All adult participants provided written informed consent; all minor participants provided verbal assent accompanied by written permission from a legal guardian. Children ages 8-17 years old additionally provided written assent. Eligibility criteria were reported previously[13]; briefly, an individual was eligible to enroll if someone in their home had a recent known exposure or had tested positive for SARS-CoV-2 within the last five days. All participants were at least six years of age and all participants were fluent in English. Eligibility was determined by the Study Coordinators during a phone interview and/or completion of an online eligibility survey hosted on Qualtrics.

Additional Details about RT-qPCR Testing and Variant Sequencing

Briefly, each day, participants completed an online symptom survey, then self-collected saliva, then anterior-nares swab, then posterior oropharyngeal (throat) swab specimens for RT-qPCR testing. Extraction and RT-qPCR was performed at Pangea Laboratories using the FDA-authorized Quick SARS-CoV-2 RT-qPCR Kit.[30] This assay has a reported LOD of 250 copies/mL of sample, which we also verified prior to study initiation.[25] Details of the quantification of viral load were described previously.[25]

Viral sequencing and variant determination were also performed at Pangea; full methods previously described.[25] Extraction, RT-qPCR, and sequencing operators and supervisors at Pangea Laboratory were blinded to which participant a sample originated from, as well as the infection status and Ag-RDT results of all participants.

Ag-RDT

Participants performed the Ag-RDT according to manufacturer's instructions[1] and reported results and a photograph of their test strip via a secure REDCap server. This Ag-RDT was chosen because it is in use globally,[2] and performance evaluations have been published in several cross-sectional studies.[3-6]

LOD of the Ag-RDT

Conversion from the manufacturer-reported LOD of 1.91×10^4 TCID50/mL of based on commercial heat-inactivated SARS-CoV-2 particles[7] to copies/mL is not possible based on information provided in the FDA documentation for the Quidel QuickVue At-Home OTC COVID-19 Test.[7] Further, the manufacturer was unable to provide this value nor a lot number or certificate of analysis for the heat-inactivated particles. Thus, we were unable to convert this LOD value from TCID50/mL to copies/mL.

Data Used in the Analyses

A total of 2,174 timepoints had a valid, conclusive composite RT-qPCR result, of which 847 timepoints from 90 individuals were classified as infected. Of these 2,174 timepoints, 63 did not have associated Ag-RDT results reported by the participant and 4 had invalid results. Three positive Ag-RDT results were also excluded because they originated from a faulty lot of test strips (see Supplementary Information). A total of 2,107 (nasal swab), 2,108 (throat swab), and 2,114 (saliva) timepoints had valid ANS Ag-RDT and RT-qPCR results (**Figure 2A-F, Figure 3A-C**), and 2,104 timepoints had valid, paired ANS Ag-RDT and composite RT-qPCR results (**Figure 2G-H, Figure 3D-F**).

International Ag-RDT Use

Many countries have already authorized and/or implemented the use of combination specimen types for Ag-RDTs, including the United Kingdom, Canada, and Israel.[8-10]

Supplementary Analyses

Confidence intervals were calculated per the guidance in the Clinical Laboratory Standards Institute (CLSI) EPI12 A2 User Protocol for Evaluation of Qualitative Test Performance.[11]

Discordance in Participant Interpretation of Antigen Test Results

Participants interpreted and reported their own antigen test results (positive, negative, or invalid), and photographed their test strips immediately. In the event of an invalid result, study coordinators contacted participants to request they immediately take an additional test; invalid results were replaced with subsequent valid results, when applicable. Participants recorded their test results and uploaded photos of the test strips to a secure REDCap server immediately after testing. All photographs were inspected by at least two study coordinators blinded to RT-qPCR results. Results as reported by the participants were analyzed and reported here. In 2.5% of antigen tests (56 of 2,153 tests), a pink (positive) test line was visible to two study coordinators in photographs uploaded, but the result was reported as negative by the participant. In most cases the pink lines were faint and may have been overlooked by the participants. It is also possible that in some cases the test was photographed late; per the manufacturer's guidance, the test result is only valid at the 10-min mark. One participant with a dark pink line was queried and reported poor close-range vision; this participant had a housemate help with all further interpretations. In one case from one participant, an invalid result was reported, but a blue control line was visible to two study coordinators. In this manuscript, we used the participants' interpretations in all analyses. Although 2.5% of all rapid antigen test results had discordant interpretations, 14% (33 of 228) of participants had a discordant interpretation; this discordance underlines that user error can substantially affect sensitivity of these at-home tests in real-world settings.

Faulty Antigen Test Lot

In mid-January 2022 we observed that two asymptomatic participants had consecutive positive antigen test results, but negative results by RT-qPCR in all three specimen types tested. Further investigation revealed that the most recently taken false positives from these two participants were from the same antigen strip lot (Quidel QuickVue At-Home OTC COVID-19 Test #152000). A third participant (**Figure 6-4D**) also had a single false-positive test from this lot the same week. This lot was immediately pulled from circulation in the study, and reported to the manufacturer and to the FDA (via a MedWatch Voluntary Report). Following an IRB amendment, participants began photographing the antigen test strip lot number visible when they reported their Ag-RDT results. Known test results from this faulty lot were marked as invalid and excluded from analysis (**Figure 6-2**). In one of the 17 participants enrolled during the early period of infection (**Figure 6-4D**), the antigen test result from this lot is noted with a "?" on his plot, and the datapoint was excluded from subsequent analyses. An investigation of the high rate of false positives was investigated further in a laboratory study using antigen test buffer and commercial nasal fluid from healthy human donors. Full details of that investigation have been reported separately.[12]

In the participant in **Figure 6-4D**, we continued to observe consistent false-positive Ag-RDTs; with a variety of antigen lots. The participant also tested positive by the Quidel Ag-RDT while testing negative on an iHealth rapid antigen test taken outside of the study on the final day of sampling. This participant tested positive by the Quidel Ag-RDT even >30 days after his first detectable viral load, and when viral load was undetectable by RT-qPCR in all three specimen types. These antigen test strips were not from the lot that yielded consistently false-positive results. The reason for this participant's string of false positives remains unknown.

We observed a negative percent agreement (NPA) of 97% (1,343) antigen negative results of 1,385 ANS RT-qPCR negative results. This is slightly lower than the NPA of 99.2% (95% CI 97.2-99.8%) observed by the Ag-RDT manufacturer.[32] This decrease may be due to the inclusion of additional results from this faulty lot for which we were not able to collect test strip lot information.

Figure software

Figure 6-4 was created with GraphPad PRISM; **Figure 6-7** was created using BioRender.

Supplemental Table 6-1. Literature providing estimates for infectious viral load thresholds. Relevant literature with paired SARS-CoV-2 viral load and viral culture performed. These studies were reviewed to estimate the lowest viral load at which replication-competent virus was observed, to substantiate possible infectious viral load thresholds (IVLTs). If an exact number was provided in the manuscript, the method is listed as provided, otherwise an approximate value was obtained from review of data shown at the given location in the referenced manuscript. Study Type was listed as Clinical if culture data originated from human clinical specimens; if specimens were collected from humans inoculated with SARS-CoV-2 as part of a research study, the type is listed as Challenge Study. Laboratory study type indicates viral isolates were cultured and subsequently used to compare viral loads at which replication-competent virus was observable. Modeling study type indicates manuscripts without primary culture data that analyzed data from other studies to estimate an infectious viral load. Review indicates a manuscript synthesizing studies that include SARS-CoV-2 viral culture and/or viral load data and does not add new primary data.

Citation	**Study Type**	**Minimum Infectious Viral Load (RNA copies/mL)**	**Method**
Stanley S, Hamel Donald J, Wolf Ian D, et al. Limit of Detection for Rapid Antigen Testing of the SARS-CoV-2 Omicron and Delta Variants of Concern Using Live-Virus Culture. J Clin Microbiol 2022; 60(5): e00140-22.	Laboratory	$2.0x10^2$	Approximated from Figure 2
Marc A, Kerioui M, Blanquart F, et al. Quantifying the relationship between SARS-CoV-2 viral load and infectiousness. eLife 2021; 10: e69302.	Modeling	$1.0x10^6$	Provided (stated as parameter in methods)
Walsh KA, Jordan K, Clyne B, et al. SARS-CoV-2 detection, viral load and infectivity over the course of an infection. *The Journal of infection* 2020; **81**(3): 357-71.	Review	$1.0x10^5$	Provided (value provided approximated from primary literature)
van Kampen JJA, van de Vijver DAMC, Fraaij PLA, et al. Duration and key determinants of infectious virus shedding in hospitalized patients with coronavirus disease-2019 (COVID-19). Nature communications 2021; 12(1): 267.	Clinical	$5.0x10^5$	Approximated from Figure 1
Perera R, Tso E, Tsang OTY, et al. SARS-CoV-2 Virus Culture and Subgenomic RNA for Respiratory Specimens from Patients with Mild Coronavirus Disease. Emerg Infect Dis 2020; 26(11): 2701-4.	Clinical	$1.0x10^5$	Provided
Pickering S, Batra R, Merrick B, et al. Comparative performance of SARS-CoV-2 lateral flow antigen tests and association with detection of infectious virus in clinical specimens: a single-centre laboratory evaluation study. Lancet Microbe 2021; 2(9): e461-e71.	Laboratory	$1.2x10^6$	Provided
L'Huillier AG, Torriani G, Pigny F, Kaiser L, Eckerle I. Shedding of infectious SARS-CoV-2 in symptomatic neonates, children and adolescents. *medRxiv* 2020: 2020.04.27.20076778.	Clinical	$1.0x10^4$	Approximated from Figure 1

Jones Terry C, Biele G, Mühlemann B, et al. Estimating infectiousness throughout SARS-CoV-2 infection course. Science 2021; 373(6551): eabi5273.	Modeling	$1.0x10^5$	Approximated from Figure 2C (based on data from primary literature)
Quicke K, Gallichote E, Sexton N, et al. Longitudinal Surveillance for SARS-CoV-2 RNA Among Asymptomatic Staff in Five Colorado Skilled Nursing Facilities: Epidemiologic, Virologic and Sequence Analysis. *medRxiv* 2020: 2020.06.08.20125989.	Clinical	$1.0x10^3$	Approximated from Figure 2B
Puhach O, Adea K, Hulo N, et al. Infectious viral load in unvaccinated and vaccinated patients infected with SARS-CoV-2 WT, Delta and Omicron. *medRxiv* 2022: 2022.01.10.22269010.	Clinical	$2.0x10^6$	Approximated from Figure 1C
Bal A, Brengel-Pesce K, Gaymard A, et al. Clinical and microbiological assessments of COVID-19 in healthcare workers: a prospective longitudinal study. *medRxiv* 2020: 2020.11.04.20225862.	Clinical	$4.5x10^3$	Provided in Table S2
Ke R, Martinez PP, Smith RL, et al. Daily longitudinal sampling of SARS-CoV-2 infection reveals substantial heterogeneity in infectiousness. *Nature Microbiology* 2022; **7**(5): 640-52.	Clinical	$1.0x10^2$	Approximated from Figure 3C/1B and Figure e9
Boucau J, Marino C, Regan J, et al. Duration of Shedding of Culturable Virus in SARS-CoV-2 Omicron (BA.1) Infection. *N Engl J Med* 2022.	Clinical	$3.0x10^3$	Approximated from Figure 1A
Killingley B, Mann AJ, Kalinova M, et al. Safety, tolerability and viral kinetics during SARS-CoV-2 human challenge in young adults. *Nat Med* 2022; **28**(5): 1031-41.	Challenge Study	$2.0x10^2$	Approximated from Figure e2B
Wölfel R, Corman VM, Guggemos W, et al. Virological assessment of hospitalized patients with COVID-2019. *Nature* 2020; **581**(7809): 465-9.	Clinical	$1.0x10^3$	Approximated from Figure 1D
Rhee C, Kanjilal S, Baker M, Klompas M. Duration of Severe Acute Respiratory Syndrome Coronavirus 2 (SARS-CoV-2) Infectivity: When Is It Safe to Discontinue Isolation? *Clin Infect Dis* 2021; **72**(8): 1467-74.	Review	$5.0x10^5$	Approximated (based on data from primary literature)
Pekosz A, Parvu V, Li M, et al. Antigen-Based Testing but Not Real-Time Polymerase Chain Reaction Correlates With Severe Acute Respiratory Syndrome Coronavirus 2 Viral Culture. *Clin Infect Dis* 2021; **73**(9): e2861-e6.	Clinical	$3.2x10^4$	Approximated from Figure 1B
Cevik M, Tate M, Lloyd O, Maraolo AE, Schafers J, Ho A. SARS-CoV-2, SARS-CoV, and MERS-CoV viral load dynamics, duration of viral shedding, and infectiousness: a systematic review and meta-analysis. *Lancet Microbe* 2021; **2**(1): e13-e22.	Review	$1.0x10^6$	Provided (based on data from primary literature)

Berg MG, Zhen W, Lucic D, et al. Development of the RealTime SARS-CoV-2 quantitative Laboratory Developed Test and correlation with viral culture as a measure of infectivity. *J Clin Virol.* 2021;143:104945.	Clinical/Laboratory	$1.6x10^4$	Provided
Mollan KR, Eron JJ, Krajewski TJ, et al. Infectious Severe Acute Respiratory Syndrome Coronavirus 2 (SARS-CoV-2) Virus in Symptomatic Coronavirus Disease 2019 (COVID-19) Outpatients: Host, Disease, and Viral Correlates. *Clin Infect Dis.* 2022;75(1):e1028-e1036.	Clinical	$1.0x10^4$	Approximated
La Scola B, Le Bideau M, Andreani J, et al. Viral RNA load as determined by cell culture as a management tool for discharge of SARS-CoV-2 patients from infectious disease wards. *Eur J Clin Microbiol Infect Dis.* 2020;39(6):1059-1061.	Clinical	$1.0x10^5$	Provided

Supplemental Table 6-2. Demographic and Medical Information for Participants Shown in Figure 6-4. SARS-CoV-2 variant was determined by ANS swab in all cases except individual (B) who had low ANS viral loads so sequencing was from a throat swab. Variant for participant (I) is inferred from the household index case. See also Supp. **Table 6-3**. Some data for participants A-N were reported previously.[13]

Fig 3 panel	Status on enrollment				Months since vaccine			Active Medications	Medical conditions	Gender	Age range (in years)	Race	Ethnicity	SARS-CoV-2 Variant
	Saliva PCR	Throat PCR	Nasal PCR	Nasal antigen	1st dose	2nd dose	3rd dose							
(A)	**neg**	**neg**	**neg**	**neg**	9 [M]	8 [M]	<2 [M]	n/a	n/a	male	40-49	White	not Hispanic	Omicron BA.1.1
(B)	**neg**	**neg**	**neg**	**neg**	11 [JJ]	3 [P]	none	PPI, vitamin/ supplement	obesity, GI condition, anxiety or depression	female	30-39	White	not Hispanic	Omicron BA.1.1
(C)	**inc**	**neg**	**neg**	**neg**	<1 [P]	none	none	acetaminophen	n/a	male	6-11	Multiple Races	not Hispanic	Omicron BA.1.1
(D)	**neg**	**neg**	**neg**	**neg**	10 [M]	9 [M]	2 [M]	none	obesity	male	30-39	Asian or Pacific Islander	not Hispanic	Omicron BA.1.1
(E)	**neg**	**neg**	**neg**	**neg**	>11 [P]	<10 [P]	<3 [P]	allergy medication; acetaminophen, antihistamine, dextromethorphan, phenylephrine HCl, doxylamine	obesity	female	30-39	White	Hispanic	Omicron BA.1
(F)	**neg**	**neg**	**neg**	**neg**	10 [P]	9 [P]	none	vitamin/ supplement	n/a	female	18-29	White	not Hispanic	Omicron BA.1.1
(G)	**neg**	**neg**	**neg**	**neg**	<2 [P]	<1 [P]	none	vitamin/ supplement	n/a	male	6-11	White	not Hispanic	Omicron BA.1.1
(H)	**neg**	**neg**	**neg**	**neg**	10 [M]	9 [M]	2 [M]	vitamin/ supplement	n/a	female	40-49	White	not Hispanic	Omicron BA.1.1
(I)	**neg**	**neg**	**neg**	**neg**	10 [P]	9 [P]	none	antibiotic, vitamin/ supplement	obesity	male	18-29	White	Hispanic	Omicron BA.1.1 (index case)
(J)	*pos*	*pos*	**inc**	**neg**	9 [M]	8 [M]	<2 [M]	vitamin/ supplement	anxiety or depression	female	40-49	White	not Hispanic	Omicron BA.1.1
(K)	*pos*	*pos*	**inc**	**neg**	9.5 [M]	8.5 [M]	0.5 [P]	NSAID	n/a	male	40-49	White	not Hispanic	Omicron BA.1.1
(L)	*pos*	*pos*	*pos*	**neg**	11 [P]	10 [P]	2 [P]	allergy medication, diabetes medication, cholesterol medication	diabetes, high blood pressure, obesity, asthma, sleep apnea, GI condition	female	50-59	Multiple Races	not Hispanic	Omicron BA.1.1
(M)	*pos*	*pos*	**neg**	**neg**	10 [M]	9 [M]	2 [M]	SSRI	oveweight, anxiety or depression	male	50-59	White	not Hispanic	Omicron BA.1.1
(N)	*pos*	**neg**	*pos*	**neg**	5 [P]	4[P]	none	none	n/a	female	12-17	White	not Hispanic	Omicron BA.1.1
(O)	*pos*	*pos*	*pos*	**neg**	10 [P]	9 [P]	1 [P]	vitamin/ supplement	anxiety or depression	female	40-49	White	not Hispanic	Omicron BA.1.1
(P)	*pos*	*pos*	*pos*	**neg**	13 [P]	12 [P]	3.5 [P]	none	n/a	male	18-29	Asian	not Hispanic	Omicron BA.1.1
(Q)	*pos*	*pos*	*pos*	**neg**	9[P]	8[P]	<0.5 [P]	acetaminophen, antihistamine, dextromethorphan, phenylephrine HCl, doxylamine	obesity	female	12-17	White	Hispanic	Omicron BA.1

* Months from vaccine date are given relative to enrollment date

Vaccine abbreviations: [P], Pfizer-BioNTech COVID-19 Vaccine (COMIRNATY); [M], Moderna COVID-19 Vaccine (Spikevax); [JJ], Johnson & Johnson

NQ, not quantifiable; viral load was below the test LOD (250 SARS-CoV-2 RNA copies/mL)

** Participants were asked to report both sex at birth and current gender identity; all participants in this cohort responded cis-gender identities to sex at birth

Supplemental Table 6-3. Demographics of the 17-participant cohort shown in **Figure 6-4**. Additional detailed information on each participant can be found in **Supplemental Table 6-2**.

Sex*		
Male	8	47.1%
Female	9	52.9%
Age		
6-11	2	11.8%
12-17	2	11.8%
18-29	3	17.6%
30-39	3	17.6%
40-49	5	29.4%
50-59	2	11.8%
Race		
White	13	76.5%
Asian or Pacific Islander	2	11.8%
Multiple Races	2	11.8%
Ethnicity		
Hispanic	3	17.6%
Non-Hispanic	14	82.4%
Tobacco Smoker or Vape User History		
Current	0	0.0%
Former	2	11.8%
Never	15	88.2%
Active Medications and Supplements		
Vitamins/Supplements	7	41.2%
Acetaminophen/NSAIDs	4	23.5%
Allergy medications/Antihistamines	3	17.6%
Antibiotics/Antivirals	1	5.9%
Medical Comorbidities		
Asthma	1	5.9%
Anxiety or Depression	3	17.6%
Diabetes	1	5.9%
Overweight/Obesity	7	41.2%
GI condition	2	11.8%
SARS-CoV-2 Vaccination Status		
Partially Vaccinated	1	5.9%
Completed Vaccination	5	29.4%
Fully vaccinated and boosted	11	64.7%
No SARS-CoV-2 vaccines reported	0	0.0%

*Participants were asked to report both sex at birth and current gender identity; all participants in this cohort responded cis-gender identities to sex at birth

Specimen Type	LOD (copies/mL)		Specimen Type	LOD (copies/mL)	Infectious Viral Load Threshold (copies/mL) 10^4	10^5	10^6	10^7
ANS Ag-RDT	Observed	vs	ANS Inferred	10^6	47.5 vs 44.9%	54.8 vs 53.2	63.3 vs 64.3	63.0 vs 64.8
ANS Ag-RDT	Observed	vs	OPS Inferred	10^6	47.5 vs 28.1%	54.8 vs 33.3	63.3 vs 40.3	63.0 vs 40.6
ANS Ag-RDT	Observed	vs	AN-OP Inferred	10^6	47.5 vs 57.3%	54.8 vs 68.0	63.3 vs 82.2	63.0 vs 82.8
AN-OP Inferred	10^6	vs	ANS Inferred	10^6	57.3 vs 44.9%	68.0 vs 53.2	82.2 vs 64.3	82.8 vs 64.8
AN-OP Inferred	10^6	vs	OPS Inferred	10^6	57.3 vs 28.1%	68.0 vs 33.3	82.2 vs 40.3	82.8 vs 40.6

Infectious Period

Supplemental Table 6-4. Comparisons of the Observed and Inferred Performance of Low-Analytical-Sensitivity Diagnostic Tests (Ag-RDTs) to Detect Presumed Infectious Individuals. Individuals were presumed infectious for the period between first specimen (of any type) with a viral load above the infectious viral load threshold (10^4, 10^5, 10^6, or 10^7 copies/mL) until all specimen types were below the IVLT. Comparison of the clinical sensitivities to detect infectiousness at IVLTs of 10^4 to 10^7 across specimen types was performed using the McNemar Exact Test, for given comparisons across specimen type. ANS Ag-RDT vs ANS with LOD 10^6 copies/mL was tested using a two-tailed McNemar Exact Test; all other combinations use a one-tailed McNemar exact test. *P*-values were adjusted using a Benjamini–Yekutieli correction to account for multiple hypotheses being tested. Comparisons resulting in *p*-values <0.05 were considered statistically significant, and are indicated in red. SA, saliva; ANS, anterior-nares swab; OPS, oropharyngeal swab; AN–OP, anterior-nares–oropharyngeal combination swab; LOD, limit of detection.

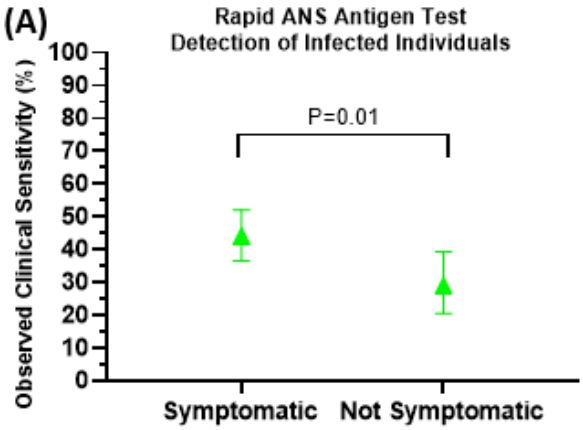

Supplemental Figure 6-1. Relationship Between Symptoms and Viral Load. The observed clinical sensitivity of the rapid antigen test to detect infection is plotted for timepoints when the cohort of 17 participants enrolled early in the course of the infection either reported at least one symptom (Symptomatic) or did not report any symptoms (Not Symptomatic). An upper-tailed Fished exact test was performed to determine whether Ag-RDT performance at symptomatic timepoints was significantly higher than timepoints when participants experienced no symptoms.

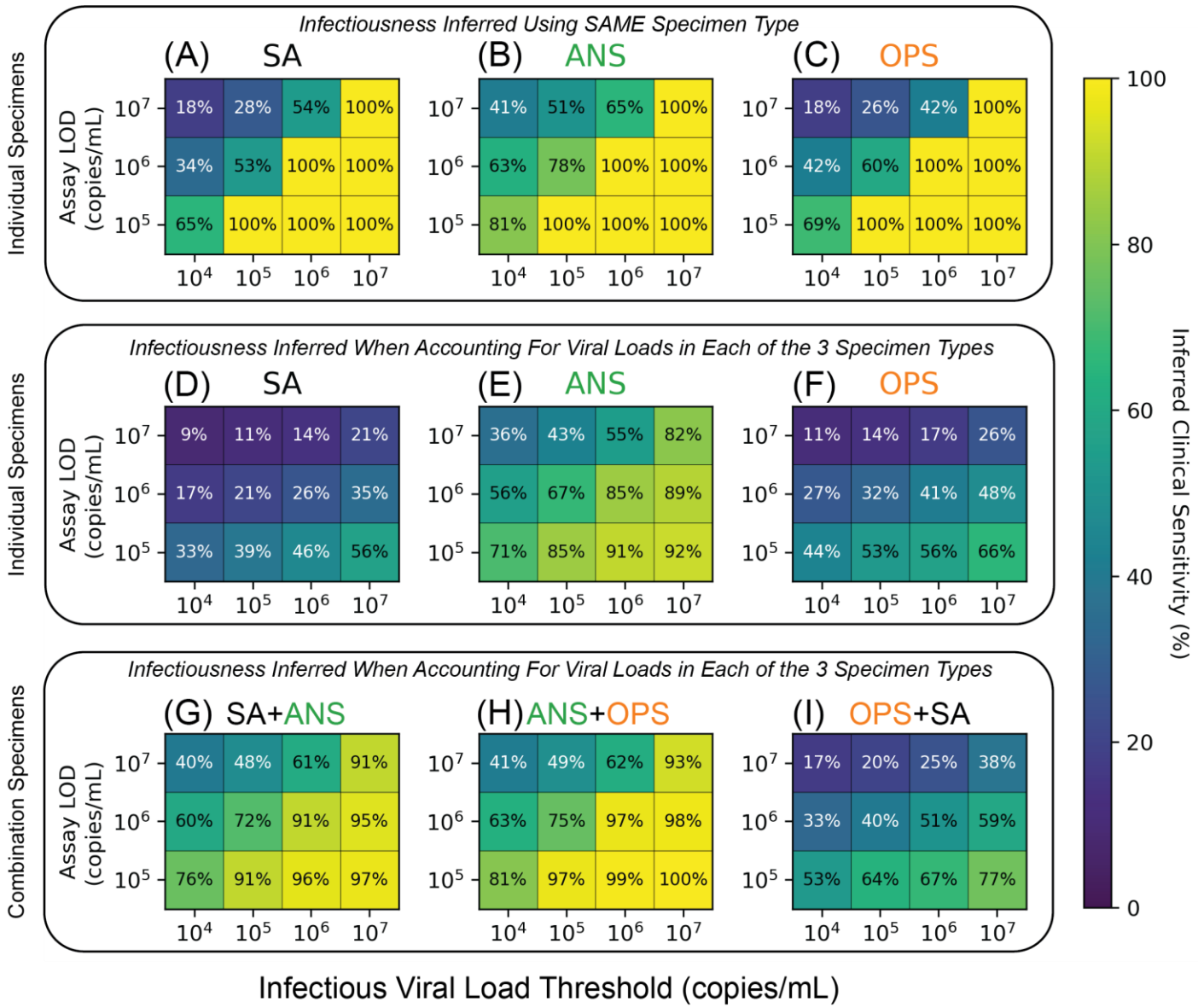

Supplemental Figure 6-2. Effect of Test LOD and Infectious Viral-Load Threshold (IVLT) on Inferred Clinical Sensitivity of Contrived Specimen Combinations. Clinical sensitivities of assays with varying LOD and IVLT for single specimen types **(A-F)** and contrived combination specimen types **(G-I)** Samples were deemed infectious if its own viral load surpassed the IVLT **(A-C)**, or if the viral load any sample collected from the same individual at the same timepoint surpassed the IVLT **(D-I)**. Contrived combination specimens **(G-I)** were calculated by taking the max viral load over the two specified specimen types.

Supplementary References

1. Quidel. Quidel QuickVue At-Home OTC COVID-19 Test - User Instructions. 2021. https://quickvueathome.com/wp-content/uploads/2021/05/EF1479701EN00_QV_At-Home_Web_Instructions_English_052421.pdf.

2. PATH. Global Availability of COVID-19 Diagnostic Tests. 2022. https://www.path.org/programs/diagnostics/covid-dashboard-global-availability-covid-19-diagnostic-tests/.

3. Kepczynski CM, Genigeski JA, Koski RR, Bernknopf AC, Konieczny AM, Klepser ME. A systematic review comparing at-home diagnostic tests for SARS-CoV-2: Key points for pharmacy practice, including regulatory information. *J Am Pharm Assoc (2003)* 2021; **61**(6): 666-77.e2.

4. Hardick J, Gallagher N, Sachithanandham J, et al. Evaluation of Four Point of Care (POC) Antigen Assays for the Detection of the SARS-CoV-2 Variant Omicron. *Microbiol Spectr* 2022: e0102522.

5. Bourassa L, Perchetti GA, Phung Q, et al. A SARS-CoV-2 Nucleocapsid Variant that Affects Antigen Test Performance. *J Clin Virol* 2021; **141**: 104900.

6. Tinker SC, Prince-Guerra JL, Vermandere K, et al. Evaluation of self-administered antigen testing in a college setting. *Virol J* 2022; **19**(1): 202.

7. FDA. Quidel QuickVue At-Home OTC COVID-19 Test - Instructions for Use (IFU). 2021. https://www.fda.gov/media/147265/download

8. National Health Service. How to use an NHS rapid lateral flow test for coronavirus (COVID-19). 2021. https://www.nhs.uk/conditions/coronavirus-covid-19/testing/how-to-do-a-test-at-home-or-at-a-test-site/how-to-do-a-rapid-lateral-flow-test/.

9. Ontario Health Canada. COVID-19 Rapid Antigen Tests: How to Collect a Sample. 2022. https://www.ontariohealth.ca/sites/ontariohealth/files/2022-02/COVID-19RapidAntigenTests-HowtoCollectaSample.pdf.

10. Reuters. Israel's Health Ministry recommends throat swab for COVID-19 tests while U.S. FDA warns against. 2022. https://www.ctvnews.ca/health/coronavirus/israel-s-health-ministry-recommends-throat-swab-for-covid-19-tests-while-u-s-fda-warns-against-1.5734130.

11. CLSI. EP12-A2 User Protocol for Evaluation of Qualitative Test Performance, 2nd edition; 2008.

12. Carter Alyssa M, Viloria Winnett A, Romano Anna E, Akana R, Shelby N, Ismagilov RF. Laboratory Evaluation Links Some False-Positive COVID-19 Antigen Test Results Observed in a Field Study to a Specific Lot of Test Strips. *Open Forum Infectious Diseases* 2023: 10.1093/ofid/ofac701/6972331.

13. Viloria Winnett A, Akana R, Shelby N, et al. Extreme differences in SARS-CoV-2 viral loads among respiratory specimen types during presumed pre-infectious and infectious periods. *PNAS Nexus.* doi: 10.1093/pnasnexus/pgad033

Author Contributions (listed alphabetically by last name):

Reid Akana (RA): Collaborated with AVW in creating digital participant symptom surveys; assisted with data quality control/curation with NS, HD, SC; created current laboratory information management system (LIMS) for specimen logging and tracking. Creation of iOS application for sample logging/tracking. Configured an SQL database for data storage. Created an Apache server and websites to view study data. Configured FTPS server to catalog PCR data. Wrote a Python package to access study data. Trained study coordinators on SQL. Troubleshooting and QC of LIMS. Made Figures 3, 5, S2, S3, S4, S5. Wrote and edited the manuscript with AVW and NS.

Alyssa M. Carter (AMC): Assisted with the inventory and archiving of >6,000 samples at Caltech; coordinated shipment of samples to Caltech with AER and JRBR; assisted with procurement of antigen tests; assisted with organizing volunteers and making participant kits; assisted AER in developing and implementing QC for participant kits. Led the in-lab investigation of antigen false-positive results; designed and performed experiments for lot analysis of the Quidel QuickVue At-Home Covid-19 tests. Provided feedback and edited the manuscript.

Yap Ching Chew (YCC): Primary liaison with Caltech team. Prepared and provided Zymo SafeCollect kits and related materials to Caltech team. Supervised the extraction, PCR, and QC teams at Pangea Laboratory. Sent PCR results daily to Caltech team. Arranged for Pangea team to perform viral-variant sequencing on selected samples; reported results and provided sequencing files.

Saharai Caldera (SC): Study coordinator; recruited, enrolled and maintained study participants with NS and HD; study-data quality control, curation and archiving with RA, NS, HD and MKK; supplies acquisition with AER, NS, HD and MKK.

Hannah Davich (HD): Lead study coordinator; co-wrote participant informational sheets with NS; developed recruitment strategies and did outreach with NS; participant kit creation and co-coordinated kit-making by volunteers with AER; recruited, enrolled and maintained study participants with NS and SC; managed the study-coordinator inventory; study-data quality control, curation and archiving with RA, NS, SC and MKK; supplies acquisition with AER, NS, SC and MKK.

Matthew Feaster (MF): Co-investigator; collaborated with AVW, MMC, NS, YG, RFI on study design and recruitment strategies; provided guidance and expertise on SARS-CoV-2 epidemiology and local trends.

Ying-Ying Goh (Y-YG): Co-investigator; collaborated with AVW, MMC, NS, MF, RFI on study design and recruitment strategies; provided guidance and expertise on SARS-CoV-2 epidemiology and local trends.

Rustem F. Ismagilov (RFI): Principal investigator; collaborated with AVW, MMC, NS, MF, YYG on study design and recruitment strategies; provided leadership, technical guidance, and oversight of all analyses; was responsible for obtaining the primary funding for the study.

Mi Kyung Kim (MKK): Study coordinator (part-time); maintaining participants with NS, HD, and SC; study-data quality control, curation and archiving with RA, NS, SC and HD; supplies acquisition with AER, NS, SC and HD; collected contact info for local health centers for recruitment outreach; assembled Table S2 with NS.

John Raymond B. Reyna (JRBR): Organized sample labeling and short-term storage of all samples at Pangea Laboratories. Arranged shipment of all samples to Caltech team. Assisted with processing of the specimens.

Anna E. Romano (AER): Co-coordinated kit-making by volunteers with HD; implemented QC process for kit-making; participated in kit making; managed logistics for the inventory and archiving of >6,000 samples at Caltech; supplies acquisition with HD, NS, SC and MKK; assisted with securing funding; compiled antigen lot data to assist false-positive antigen test investigation; organized and performed QC on sequencing data. Provided feedback and edited the manuscript.

Natasha Shelby (NS): Study administrator; collaborated with AVW, RFI, YG, MF on initial study design and recruitment strategies; co-wrote IRB protocol and informed consent with AVW; co-wrote enrollment questionnaire and post-study questionnaire with AVW; initiated the collaboration with Zymo and served as primary liaison throughout study; reviewed pilot sampling data and amended instructional sheets/graphics for specimen collections in collaboration with Zymo; co-wrote participant informational sheets with HD; hired, trained, and supervised the study-coordinator team; developed recruitment strategies and did outreach with HD; recruited, enrolled and maintained study participants with HD and SC; co-developed participant keep/drop criteria with AVW; performed the daily upload, review, and QC of PCR data received from Zymo; made the daily participant keep/drop decisions based on viral-load results and trajectories in each household; made all phone calls to alert presumptive positives of their status and provide resources; study-data quality control, curation and archiving with RA, HD, SC and MKK; archiving of all participant data and antigen-test photographs; supplies acquisition with AER, HD, SC and MKK; assisted with securing funding; managed the overall study budget; assembled Figure 1 with AVW; assembled Table S2 with MKK; assembled Table S3; created Figure 4 with AVW; managed citations and reference library; verified the underlying data with AVW and RA; co-wrote and edited the manuscript with AVW and RA.

Matt Thomson (MT): Assisted with statistical approach and analyses.

Colten Tognazzini (CT): Coordinated the recruitment efforts at PPHD with case investigators and contact tracers; provided guidance and expertise on SARS-CoV-2 epidemiology and local trends.

Alexander Viloria Winnett (AVW): Collaborated with NS, RFI, YG, MF on initial study design and recruitment strategies; co-wrote IRB protocol and informed consent with NS; co-wrote enrollment questionnaire and post-study questionnaire with NS; co-developed participant keep/drop criteria with NS; funding acquisition; designed and coordinated LOD validation experiments; selected and prepared specimen for viral-variant sequencing with NS, YC, and AER; assisted with the inventory and archiving of >6,000 specimen at Caltech with AER and AMC; minor role supporting outreach by HD and NS; minor role supporting kit-making by AER, HD and AMC; verified the underlying data with NS and RA; major contributor to reference organization and selection; assembled Figure 1 with NS; created Figure 4 with NS; performed analysis and prepared Figure 2, Figure 6, Figure 7, Figure S1, Table S1, and Table S4. Co-wrote and edited the manuscript with NS and RA.

Taikun Yamada (TY): Performed the RT-qPCR COVID-19 testing at Pangea Laboratory.

Chapter 7

LABORATORY EVALUATION LINKS SOME FALSE-POSITIVE COVID-19 ANTIGEN TEST RESULTS OBSERVED IN A FIELD STUDY TO A SPECIFIC LOT OF TEST STRIPS

This chapter was originally published in Carter AM*, Viloria Winnett A*, Romano AE, Akana R, Shelby N, Ismagilov RF. Laboratory Evaluation Links Some False-Positive COVID-19 Antigen Test Results Observed in a Field Study to a Specific Lot of Test Strips (Jan 2023). Open Forum Infectious Diseases. https://doi.org/10.1093/ofid/ofac701.

Abstract

During a household-transmission field study using COVID-19 antigen rapid diagnostic tests (Ag-RDT), a common test strip lot was identified among three participants with false-positive results. In blinded laboratory evaluation, this lot, exhibited a significantly higher false-positive rate than other lots. Because a positive Ag-RDT result often prompts action, reducing lot-specific false positives can maintain confidence and actionability of true-positive Ag-RDT results.

Introduction

Antigen rapid diagnostic tests (Ag-RDTs) are increasingly used for SARS-CoV-2 detection. Usage of at-home Ag-RDTs in the U.S. has increased nearly four-fold among those with self-reported COVID-19-like illness between the period of Delta (August 23–December 11, 2021) to Omicron (December 19–March 12, 2022) variant predominance.[1] Ag-RDTs are also used widely for test-to-enter events and serial screening testing in schools and workplaces; for example, in May 2022[2] the California Department of Public Health began recommending Ag-RDTs as the primary test for COVID-19 in schools[3].

Ag-RDTs typically have very high specificity; of the 51 Ag-RDTs currently authorized for at-home use in the USA as of September 2, 2022, all are required to demonstrate false-positive rates of ≤2%[4]. However, with widespread use imperfect specificity can result in many false positive results, and at low prevalence of infection, these false positives can represent a large fraction of or even dominate among all positive results[5].

As part of a COVID-19 household-transmission field study in Southern California initiated in November 2021, participants performed a daily at-home nasal swab Ag-RDT (Quidel QuickVue At-Home OTC COVID-19 Test) and self-collected saliva, anterior nares swab, and oropharyngeal swabs for RT-qPCR testing[6]. This test was selected for the field study[6] because it was one of the first Ag-RDTs to be granted FDA emergency use authorization[7] and is widely in use in the USA and internationally.

In January 2022, interim analysis of the field study showed a string of 24 Ag-RDT positive results from participants who had corresponding negative results in all three specimen types tested by RT-qPCR, causing an elevated clinical false-positive rate (**Figure 7-1A**). Further investigation revealed a common Ag-RDT strip lot number (152000) among three participants with false positive results. We then investigated the technical false-positive rate of Ag-RDT test strip lot 152000, and other lots acquired for use in the field study, in a controlled laboratory setting.

Methods

Participant Consent Statement

The Ag-RDT field study[6] was approved by the California Institute of Technology Institutional Review Board under protocol #20-1026. All adult participants in the study provided written informed consent and all minors provided verbal assent accompanied by written parental permission.

Laboratory Evaluation of Ag-RDT Test Strips

We created contrived specimens using heat-inactivated SARS-CoV-2 particles (BEI, Cat No. NR-52286, Lot 70034991) spiked into commercial SARS-CoV-2-negative human nasal fluid (Lee BioSolutions, Cat No. 991-13-P lot 03f4044 and Cat No. 991-13-P-PreC lot 09F3280) at concentrations above and below the inferred limit of detection (LOD) for this assay ($7x10^6$ copies/mL)[6] and applied them to two lots of test strips (152194 and 152532) which did not yield any false positive results among participants in the field study. Contrived specimens with SARS-CoV-2-negative human nasal fluid alone were also applied to four Ag-RDT strip lots (152194, 152532, 000202, as well as 152000, the lot common to participants with observed clinical false-positive results). The order of contrived specimens and Ag-RDT strip lots was randomized by the operator.

Contrived specimens (20 µL) were pipetted onto the swab that came with each Ag-RDT, and the swab was placed into the Ag-RDT tube containing buffer. Manufacturer instructions were then followed exactly[8], by mixing the swab in the buffer for one min, removing the swab, then placing an Ag-RDT strip in the tube and incubating at room temperature for 10 min. The result was then interpreted within 5 minutes by three readers blinded to the experimental conditions and test strip lot numbers; each trial with a single test strip therefore resulted in three independent reads. Readers were provided with the manufacturer instructions for result interpretation[8] and no additional guidance. Readers were unable to see the interpretations of other readers.

Statistical Methods

Clinical false-positive results were defined as positive Ag-RDT results reported by a study participant, at the same timepoint when saliva, nasal swab, and oropharyngeal swab specimens collected by the same participant all resulted negative by high-analytical-RT-qPCR testing. The clinical false positive rate was calculated as the number of clinical false-positive Ag-RDT results over all timepoints with false-positive and true-negative Ag-RDT results, using RT-qPCR as the reference standard. The clinical false-positive rate was binned by two-week periods for visualization (**Figure 7-1A**).

Technical false-positive Ag-RDT results were defined as reads interpreted as positive when contrived specimen containing only SARS-CoV-2 negative nasal fluid was tested. The technical false-positive rate was calculated as

the number of technical false-positive reads over all reads originating from specimen containing only SARS-CoV-2 negative nasal fluid. The technical false-positive rate was grouped by Ag-RDT strip lot (**Figure 7-1B**).

The 95% confidence interval of both the clinical and technical false-positive rate was calculated using the method described in the Clinical Laboratory Standards Institute EP12-A2 document[9]. Statistical testing was performed to assess differences in the clinical false-positive rates between time periods in the field study (**Figure 7-1A**), and to compare the technical false-positive rates between Ag-RDT strip lots in the laboratory evaluation (**Figure 7-1B**); for all analyses we used the Fisher's exact test, implemented in Python 3.8.8.

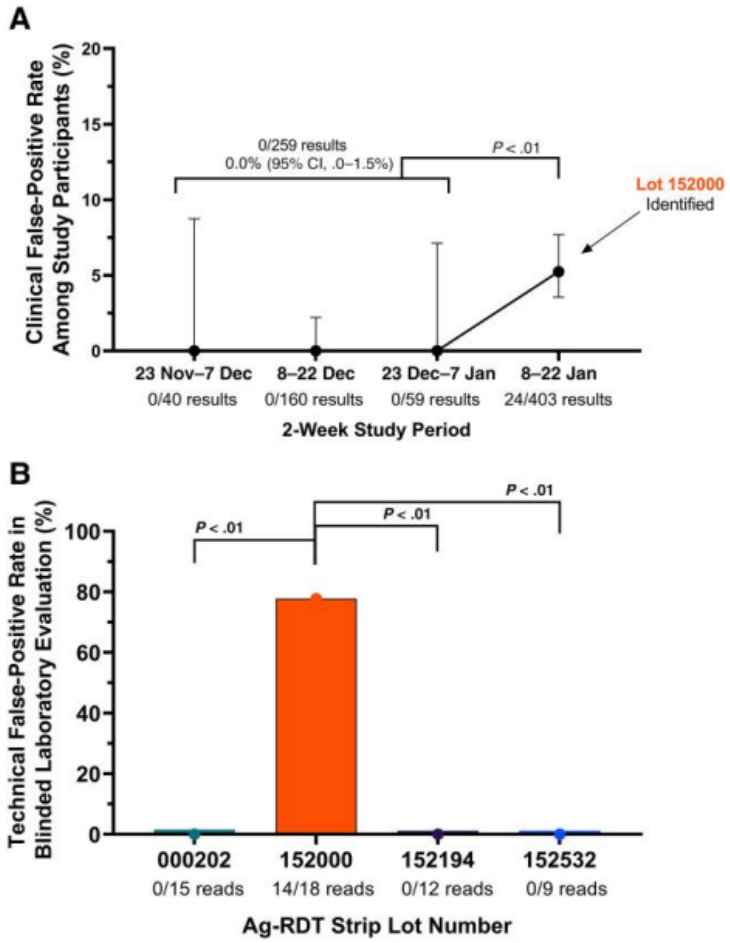

Figure 7-1. Clinical false-positive rate of Ag-RDTs among participants in a COVID-19 household-transmission field study and subsequent laboratory evaluation of technical false-positive rates among Ag-RDT strip lots. **(A)** The bi-weekly clinical false-positive rate for nasal-swab antigen rapid diagnostic testing (Ag-RDT), defined as a positive Ag-RDT at the same timepoint as negative results by RT-qPCR in saliva, nasal swabs, and oropharyngeal swab specimens. The proportions displayed below each month represent the number of clinical false-positive results over the total number of false-positive and true-negative Ag-RDT results in the field study during each period. Error bars represent 95% C.I. **(B)** Laboratory evaluation of the technical false-positive rate for four Ag-RDT strip lots was performed using SARS-CoV-2-negative human nasal fluid (see Methods). The proportion of technical false-positive reads to all reads by readers blinded to experimental conditions is displayed below each lot number. *P*-values were obtained using an upper-tailed Fisher's exact test. Additional details are provided in **Supplemental Table 7-1**.

Results

A significantly elevated clinical false-positive rate was observed among participants in a field study of a COVID-19 Ag-RDT, compared with what had previously been observed in the study ($P<0.01$, upper-tailed Fisher's exact test, **Figure 7-1A**). The elevated false-positive rate prompted the identification of a common Ag-RDT strip lot (152000) among three participants with multiple, daily clinical false-positive results. We then sought to evaluate the technical false-positive rate of this lot, and other lots acquired for use in the field study, through laboratory evaluation.

To confirm that this Ag-RDT could be performed and produce expected results in a laboratory setting, we created contrived specimens with and without SARS-CoV-2 particles. Contrived specimens were applied to two Ag-RDT strip lots that had not yielded clinical false-positive results in the field study. Positive reads were expected when nasal fluid with viral concentrations above the LOD were applied to Ag-RDT strips, and negative reads were expected when viral concentrations were below the inferred LOD, and when only SARS-CoV-2 negative nasal fluid (without any viral particles) was applied. Contrived specimens with SARS-CoV-2 concentrations between $1.0x10^7$ and $1.5x10^7$ copies/mL (above the inferred LOD of the Ag-RDT) were interpreted by readers as positive in eight out of nine reads (three independent trials each with three reads, one from each reader); contrived specimens with viral concentrations between $2.0x10^6$ and $4.1x10^6$ copies/mL (below the inferred LOD of the Ag-RDT) were interpreted by readers as negative in all six reads (**Supplementary Table 7-1**). These results confirmed that the Ag-RDT used in the field study yields expected positive and negative results with contrived specimens in a laboratory setting.

To assess the technical false-positive rate of different lots, SARS-CoV-2-negative human nasal fluid (without the addition of viral particles) was applied to Ag-RDT strips from four lots: 152194, 152532, 000202, and 152000 (the lot that produced clinical false positives among three different participants) (**Figure 7-1B**). No false-positive reads were reported for any trial performed on lots 152194, 152532, or 000202. However, 14 of 18 reads from lot 152000 were interpreted by readers as positive, yielding a technical false positive rate of 77%, (95CI 55-91%); one read from this lot was interpreted as invalid. Further, at least one reader interpreted a positive result for every trial with a lot 152000 test strip (**Supplementary Table 7-1**). The false-positive rate of Ag-RDT strip lot 152000 on laboratory evaluation was significantly higher than the false-positive rate observed for the other three test strip lots analyzed ($P<0.01$, upper-tailed Fisher's exact test).

Discussion

In a field study of a COVID-19 Ag-RDT in Southern California, a specific lot of test strips was found to be common among three participants (from three different households) with false-positive Ag-RDT results. These participants had negative test results in three paired high-analytical-sensitivity RT-qPCR assays (saliva, nasal swab, and oropharyngeal swab) that were collected at the same timepoint. Laboratory evaluation confirmed that

when SARS-CoV-2-negative nasal fluid was tested with this specific lot of Ag-RDT strips, readers blinded to randomized test conditions and strip lot numbers consistently interpreted results as positive. The laboratory evaluation supports that this lot was likely yielding false-positive results when in use by participants in our field study.

At-home Ag-RDTs are known to have low clinical sensitivity[6,10,11] and are likely to produce false-negative results. The low clinical sensitivity of Ag-RDTs is due to both their low-analytical-sensitivity (high limits of detection) and, in the USA, their authorized use exclusively with nasal swab specimens, which are not always representative of the patient infection status, especially early in the infection[6,12–16]. The Centers for Disease Control has recognized the lack of clinical sensitivity of Ag-RDTs and in September 2022 updated recommendations to Ag-RDT testing protocols to repeat testing 24 to 48 hours later[17].

False positives are less frequent. The manufacturer of the Quidel QuickVue At-Home OTC COVID-19 Test, which was not involved in the design or execution of this study, reports a 99.2 negative percent agreement[8], and Ag-RDTs generally have >97% clinical specificity in field evaluations[11,18]. By late 2020, the U.S. Centers for Disease Control and Prevention (CDC) recommended a confirmatory nucleic acid amplification test for Ag-RDT positive results in cases with low pre-test probability[19]. However as of April 2022, a single positive result now typically prompts immediate action from individuals, their close contacts, and healthcare personnel[20]. Notably, the Emergency Use Authorization for the Quidel QuickVue At-Home OTC COVID-19 Test[21] encourages individuals who test positive to self-isolate and contact their healthcare provider for follow-up care, which may include additional testing. Therefore, false-positive results can prompt unnecessary isolation and quarantine, needless treatment, consumption of additional testing resources, and diversion of contact tracing efforts from true positive cases[22]. Further, false-positive results undermine trust in positive Ag-RDT results, such that isolation, treatment, additional testing, and contact tracing may not be initiated when it is appropriate.

False-positive Ag-RDT results are not unique to the current COVID-19 pandemic. The Quidel QuickVue Influenza A + B Test, another Ag-RDT that uses nasal swab specimens, is reported by the manufacturer to have >97 negative percent agreement,[23] but during the 2009 Influenza A (H1N1) pandemic, the clinical performance of the test resulted in a 62.2 negative percent agreement, against RT-PCR.[24]

COVID-19 Ag-RDT false-positive results have been reported in a number of contexts[18,25,26]. In a recent evaluation of the Quidel QuickVue At-Home OTC COVID-19 test in a college community[27], eight of 11 participants with positive Ag-RDT results were found to be negative on RT-PCR testing within 24 hours. No definitive cause for these false-positive results was identified.

False-positive results may occur due to a variety of reasons,[22,25,28–30] including user error, invalid test conditions, improper storage or manufacturing errors that affect reagent chemistry, or off-target binding of human or microbial material (including viruses other than SARS-CoV-2): for example, infection of human rhinovirus A has produced false-positive results in SARS-CoV-2 Ag-RDTs.[26] However, both we and others[31,32] have found false-positive Ag-RDT results traceable to specific lots. Importantly, the overall false-positive rate observed among participants in our field study was 2.8% (95% CI 2.1-3.9%)[6]; monitoring only an overall false-positive rate across lots could mask specific lots with higher false-positive rates.

Lot issues can arise during manufacturing, transportation, or due to storage conditions after distribution[33,34]. In our study, Ag-RDTs were stored at room temperature and the mild winter climate in Southern California ensured temperatures were stable during shipment as well. Here, we demonstrate through a controlled laboratory evaluation that false-positive results captured in a field study of Ag-RDTs were not due to operator error but were lot specific. Therefore, efforts to monitor for lot-dependent false positives (and whether they originate from issues at the manufacturer or distributor/retailer level) can increase the confidence and actionability of positive Ag-RDT results.

Data Availability

The data underlying the results presented in the study are available at CaltechDATA at: https://doi.org/10.22002/fmz6a-0x036

Funding

This work was supported by the Ronald and Maxine Linde Center for New Initiatives at the California Institute of Technology and the Jacobs Institute for Molecular Engineering for Medicine at the California Institute of Technology. A UCLA DGSOM Geffen Fellowship to AVW.

Acknowledgements

We thank the study participants for making this work possible. We thank Study Coordinators Saharai Caldera for suggesting the laboratory evaluation and both Saharai and Hannah Davich for removing lot 152000 from circulation in the study. We thank Taikun Yamada, John Raymond B. Reyna, Paolo Piatti and Yap Ching Chew for performing and verifying the validity of RT-qPCR results as previously reported. Finally, we thank all the case investigators and contact tracers at the Pasadena Public Health Department and Caltech Student Wellness Services for their efforts in study recruitment and their work in the pandemic response.

Conflicts of Interest

RFI is a co-founder, consultant, and a director and has stock ownership of Talis Biomedical Corp.

References

1. Rader B, Gertz A, Luliano AD, et al. Use of At-Home COVID-19 Tests — United States, August 23, 2021–March 12, 2022. *Morb Mortal Wkly Rep*. 2022;71(13):489-494. doi:http://dx.doi.org/10.15585/mmwr.mm7113e1

2. Aragon T. Preliminary Testing Framework for K–12 Schools for the 2022–2023 School Year. Published May 27, 2022. Accessed October 13, 2022. https://www.cdph.ca.gov/Programs/CID/DCDC/Pages/COVID-19/Schools-Testing-Framework-K-12-Schools--2022-23.aspx

3. Aragon T. Testing Framework for K–12 Schools for the 2022–2023 School Year. Published August 19, 2022. Accessed October 25, 2022. https://www.cdph.ca.gov/Programs/CID/DCDC/Pages/COVID-19/Testing-Framework-for-K-12-Schools-for-the-2022-2023-School-Year.aspx

4. US Food and Drug Administration. In Vitro Diagnostics EUAs: Molecular and Antigen Home Use Test Template. Published online November 9, 2021. Accessed October 13, 2022. https://www.fda.gov/media/140615/download

5. Healy B, Khan A, Metezai H, et al. Covid-19 testing, low prevalence and the impact of false positive results. *The BMJ*. 2020;2020(369):m1808. doi:https://doi.org/10.1136/bmj.m1808

6. Viloria Winnett AV, Akana R, Shelby N, et al. Extreme differences in SARS-CoV-2 Omicron viral loads among specimen types drives poor performance of nasal rapid antigen tests for detecting presumably pre-infectious and infectious individuals, predicting improved performance of combination specimen antigen tests. Published online July 15, 2022:2022.07.13.22277513. doi:10.1101/2022.07.13.22277513

7. U.S. Food and Drug Administration. In Vitro Diagnostics EUAs - Antigen Diagnostic Tests for SARS-CoV-2. *FDA*. Published online December 15, 2022. Accessed December 16, 2022. https://www.fda.gov/medical-devices/coronavirus-disease-2019-covid-19-emergency-use-authorizations-medical-devices/in-vitro-diagnostics-euas-antigen-diagnostic-tests-sars-cov-2

8. Quidel. QuickVue At-Home OTC COVID-19 Test User Instructions. Accessed October 13, 2022. https://www.fda.gov/media/147250/download

9. CLSI. *EP12-A2 User Protocol for Evaluation of Qualitative Test Performance*. 2nd ed.; 2008.

10. Calderón RI, Jhaveri TA, Tovar MA, et al. Diagnostic Performance Assessment of Saliva RT-PCR and Nasopharyngeal Antigen for the Detection of SARS-CoV-2 in Peru. *Microbiol Spectr*. 10(4):e00861-22. doi:10.1128/spectrum.00861-22

11. Tsao J, Kussman AL, Costales C, Pinsky BA, Abrams GD, Hwang CE. Accuracy of Rapid Antigen vs Reverse Transcriptase–Polymerase Chain Reaction Testing for SARS-CoV-2 Infection in College Athletes During Prevalence of the Omicron Variant. *JAMA Netw Open*. 2022;5(6):e2217234. doi:10.1001/jamanetworkopen.2022.17234

12. Savela ES, Viloria Winnett AV, Romano AE, et al. Quantitative SARS-CoV-2 Viral-Load Curves in Paired Saliva Samples and Nasal Swabs Inform Appropriate Respiratory Sampling Site and Analytical Test Sensitivity Required for Earliest Viral Detection. *J Clin Microbiol*. 2022;60(2). doi:https://doi.org/10.1128/jcm.01785-21

13. Viloria Winnett AV, Akana R, Shelby N, et al. SARS-CoV-2 exhibits extreme differences in early viral loads among specimen types suggesting improved detection of pre-infectious and infectious individuals using combination specimen types. Published online July 15, 2022:2022.07.13.22277113. doi:10.1101/2022.07.13.22277113

14. Teo AKJ, Choudhury Y, Tan IB, et al. Saliva is more sensitive than nasopharyngeal or nasal swabs for diagnosis of asymptomatic and mild COVID-19 infection. *Sci Rep*. 2021;11(1):3134. doi:10.1038/s41598-021-82787-z

15. Wyllie AL, Fournier J, Casanovas-Massana A, et al. Saliva or Nasopharyngeal Swab Specimens for Detection of SARS-CoV-2. *N Engl J Med*. 2020;383(13):1283-1286. doi:10.1056/NEJMc2016359

16. Adamson B, Sikka R, Wyllie AL, Premsrirut P. Discordant SARS-CoV-2 PCR and Rapid Antigen Test Results When Infectious: A December 2021 Occupational Case Series. Published online January 5, 2022:2022.01.04.22268770. doi:10.1101/2022.01.04.22268770

17. U.S. Center for Disease Control and Prevention. Self-Testing At Home or Anywhere. Centers for Disease Control and Prevention. Published September 6, 2022. Accessed October 13, 2022. https://www.cdc.gov/coronavirus/2019-ncov/testing/self-testing.html

18. Nelson EJ, McKune SL, Ryan KA, et al. Antigen vs RT-PCR Tests for Screening Quarantined Students in Florida During the COVID-19 Pandemic SARS-CoV-2 Delta Variant Surge. *JAMA Pediatr*. 2022;176(5):525-526. doi:10.1001/jamapediatrics.2022.0080

19. Procop GW, Kadkhoda K, Rhoads DD, Gordon SG, Reddy AJ. Home testing for COVID-19: Benefits and limitations. *Cleve Clin J Med*. Published online February 12, 2021. doi:10.3949/ccjm.88a.ccc071

20. U.S. Centers for Disease Control and Prevention. Guidance for Antigen Testing for SARS-CoV-2 for Healthcare Providers Testing Individuals in the Community. Centers for Disease Control and Prevention. Published April 2, 2022. Accessed December 13, 2022. https://www.cdc.gov/coronavirus/2019-ncov/lab/resources/antigen-tests-guidelines.html

21. U.S. Food and Drug Administration. QuickVue At-Home OTC COVID-19 Test - Letter of Authorization. QuickVue At-Home OTC COVID-19 Test - Letter of Authorization. Published October 21, 2021. Accessed December 13, 2022. https://www.fda.gov/media/147247/download

22. Brooks ZC, Das S. COVID-19 Testing: Impact of Prevalence, Sensitivity, and Specificity on Patient Risk and Cost. *Am J Clin Pathol*. 2022;154(5):575-584. doi:https://doi.org/10.1093/ajcp/aqaa141

23. Quidel Corporation. Quidel QuickVue Influenza A+B Test. Published March 1, 2022. Accessed December 15, 2022. https://www.quidel.com/sites/default/files/product/documents/EF1350314EN00.pdf

24. Stevenson HL, Loeffelholz MJ. Poor Positive Accuracy of QuickVue Rapid Antigen Tests during the Influenza A (H1N1) 2009 Pandemic. *J Clin Microbiol*. 2010;48(10):3729-3731. doi:10.1128/JCM.01562-10

25. Itoh K, Kawamitsu T, Osaka Y, et al. False positive results in severe acute respiratory coronavirus 2 (SARS-CoV-2) rapid antigen tests for inpatients. *J Infect Chemother*. 2021;27(7):1089-1091. doi:10.1016/j.jiac.2021.03.011

26. Hase R, Kurita T, Mito H, et al. Potential for false-positive results with quantitative antigen tests for SARS-CoV-2: A case of a child with acute respiratory infection. *J Infect Chemother*. 2022;28(2):319-320. doi:10.1016/j.jiac.2021.10.032

27. Tinker SC, Prince-Guerra JL, Vermandere K, et al. Evaluation of self-administered antigen testing in a college setting. *Virol J*. 2022;19(1):202. doi:10.1186/s12985-022-01927-7

28. U.S. Food and Drug Administration. Potential for False Positive Results with Antigen Tests for Rapid Detection of SARS-CoV-2 - Letter to Clinical Laboratory Staff and Health Care Providers. FDA. Published November 3, 2020. Accessed December 13, 2022. https://www.fda.gov/medical-devices/letters-health-care-providers/potential-false-positive-results-antigen-tests-rapid-detection-sars-cov-2-letter-clinical-laboratory

29. Otake S, Miyamoto S, Mori A, Iwamodo T, Kasai M. False-positive results in SARS-CoV-2 antigen test with rhinovirus-A infection. *Pediatr Int.* 2021;63(9):1135-1137. doi:https://doi.org/10.1111/ped.14582

30. Patriquin G, Davidson RJ, Hatchette TF, et al. Generation of False-Positive SARS-CoV-2 Antigen Results with Testing Conditions outside Manufacturer Recommendations: A Scientific Approach to Pandemic Misinformation. *Microbiol Spectr*. 2021;9(2):e00683-21. doi:10.1128/Spectrum.00683-21

31. Gans JS, Goldfarb A, Agrawal AK, Sennik S, Stein J, Rosella L. False-Positive Results in Rapid Antigen Tests for SARS-CoV-2. *JAMA*. 2022;327(5):485-486. doi:10.1001/jama.2021.24355

32. U.S. Food and Drug Administration C for D and R. Ellume Recalls COVID-19 Home Test for Potential False Positive SARS-CoV-2 Test Results. FDA. Published November 16, 2021. Accessed December 13, 2022. https://www.fda.gov/medical-devices/medical-device-recalls/ellume-recalls-covid-19-home-test-potential-false-positive-sars-cov-2-test-results

33. Williams C. Did mishandling of Utah rapid antigen tests lead them to be pulled? Accessed October 13, 2022. https://www.ksl.com/article/50344932/did-mishandling-of-utah-rapid-antigen-tests-lead-them-to-be-pulled

34. Haage V, Ferreira de Oliveira-Filho E, Moreira-Soto A, et al. Impaired performance of SARS-CoV-2 antigen-detecting rapid diagnostic tests at elevated and low temperatures. *J Clin Virol*. 2021;138:104796. doi:10.1016/j.jcv.2021.104796

Supplemental Information

Supplemental Table 7-1. Complete laboratory evaluation of Ag-RDT test strips. Each trial of the laboratory evaluation assesses one Ag-RDT strip, listed with the corresponding lot number. SARS-CoV-2 concentration is the number of SARS-CoV-2 copies/mL of the test buffer when contrived specimens are applied (see methods). The incubation time is defined as the difference between the time at which the strip was taken out of the test buffer and the time at which the strip was placed in the buffer. The read window is defined as the difference between the time at which the last reader interpreted the results of the test and the time at which the strip was taken out of the buffer. The anticipated result for each trial is based off the concentration of particles applied to each strip. The three reads for each trial are listed and positive results are highlighted in red. The proportion of reads called positive is also listed, and any percentage above 0% when the anticipated result was negative is also highlighted in red.

Trial	Antigen Test Lot Number	SARS-CoV-2 Concentration Spike-in (copies/mL)	Incubation Time	Read Window	Anticipated Result	Reader 1	Reader 2	Reader 3	% Called Positive
1	152194	Quidel Positive Control Swab	11 min	2 min	Positive	Positive	Positive	Positive	100
2	152194	$2.0x10^6$ copies/mL	10 min	3 min	Negative	Negative	Negative	Negative	0
3	152194	$4.0x10^6$ copies/mL	10 min	3 min	Negative	Negative	Negative	Negative	0
4	152532	$1.0x10^7$ copies/mL	10 min	3 min	Positive	Positive	Positive	Positive	100
5	152532	$1.3x10^7$ copies/mL	10 min	3 min	Positive	Positive	Positive	Positive	100
6	152194	$1.5x10^7$ copies/mL	10 min	3 min	Positive	Negative	Positive	Positive	66.7
7	152194	0 copies/mL	11 min	2 min	Negative	Negative	Negative	Negative	0
8	152194	0 copies/mL	10 min	2 min	Negative	Negative	Negative	Negative	0
9	152194	0 copies/mL	10 min	4 min	Negative	Negative	Negative	Negative	0
10	152194	0 copies/mL	11 min	3 min	Negative	Negative	Negative	Negative	0
11	000202	0 copies/mL	10 min	2 min	Negative	Negative	Negative	Negative	0
12	000202	0 copies/mL	10 min	2 min	Negative	Negative	Negative	Negative	0
13	000202	0 copies/mL	11 min	2 min	Negative	Negative	Negative	Negative	0
14	000202	0 copies/mL	10 min	2 min	Negative	Negative	Negative	Negative	0
15	000202	0 copies/mL	11 min	3 min	Negative	Negative	Negative	Negative	0
16	152000	0 copies/mL	10 min	3 min	Negative	Positive	Positive	Negative	66.7
17	152000	0 copies/mL	10 min	3 min	Negative	Positive	Positive	Negative	66.7
18	152000	0 copies/mL	10 min	4 min	Negative	Positive	Positive	Negative	66.7
19	152000	0 copies/mL	10 min	3 min	Negative	Positive	Positive	Positive	100
20	152000	0 copies/mL	10 min	4 min	Negative	Positive	Positive	Positive	100
21	152000	0 copies/mL	10 min	4 min	Negative	Positive	Positive	Invalid	66.7
22	152532	0 copies/mL	10 min	4 min	Negative	Negative	Negative	Negative	0
23	152532	0 copies/mL	10 min	2 min	Negative	Negative	Negative	Negative	0
24	152532	0 copies/mL	10 min	3 min	Negative	Negative	Negative	Negative	0

Author Contributions

Reid Akana (RA) - Reader for laboratory evaluation blinded to experimental conditions. Wrote Python function to perform statistical testing. Reviewed manuscript draft.

Alyssa M. Carter (AMC) - Designed laboratory evaluation. Operator for laboratory evaluation. Reported issue with lot 152000 to Quidel and interacted with Quidel representatives. Outlined and co-wrote manuscript with AVW. Analyzed field study and laboratory evaluation data with AVW. Drafted Figure 1 with AVW. Prepared Supplementary Table 1. Major contributor to selection of references for manuscript with AVW

Anna E. Romano (AER) - Reviewed participant Ag-RDT photos from field evaluation to extract strip lot information. Performed interim analysis of Ag-RDT results by strip lot. Provided feedback on design of laboratory evaluation. Reader for laboratory evaluation blinded to experimental conditions. Reviewed manuscript draft.

Natasha Shelby (NS) - Study administrator. Interviewed all participants who received false-positive antigen results. Amended IRB protocol to add acquisition of antigen lot numbers. Filed Medline FDA report about lot #152000 and interacted with Quidel representatives. QC of data. Reader for laboratory evaluation blinded to experimental conditions. Reviewed and edited manuscript draft.

Alexander Viloria Winnett (AVW) – Provided feedback on design of laboratory evaluation. Reader for laboratory evaluation blinded to experimental conditions Reported issue with lot 152000 to Quidel and interacted with Quidel representatives. Major contributor to selection of references for manuscript with AMC. Managed reference library. Outlined and co-wrote manuscript with AMC. Analyzed field study and laboratory evaluation data with AMC. Drafted Figure 1 with AMC.

Chapter 8

INDEX CASES FIRST IDENTIFIED BY NASAL-SWAB RAPID COVID-19 TESTS HAD MORE TRANSMISSION TO HOUSEHOLD CONTACTS THAN CASES IDENTIFIED BY OTHER TEST TYPES

This chapter was originally published in Ji J*, Viloria Winnett A*, Shelby N, Reyes JA, Schlenker NW, Davich H, Caldera S, Tognazzini C, Goh YY, Feaster M, Ismagilov RF. Index Cases First Identified by Nasal-Swab Rapid COVID-19 Tests Had More Transmission to Household Contacts Than Cases Identified by Other Test Types. PLoS ONE. https://doi.org/10.1371%2Fjournal.pone.0292389.

Abstract

At-home rapid COVID-19 tests in the U.S. utilize nasal-swab specimens and require high viral loads to reliably give positive results. Longitudinal studies from the onset of infection have found infectious virus can present in oral specimens days before nasal. Detection and initiation of infection-control practices may therefore be delayed when nasal-swab rapid tests are used, resulting in greater transmission to contacts. We assessed whether index cases first identified by rapid nasal-swab COVID-19 tests had more transmission to household contacts than index cases who used other test types (tests with higher analytical sensitivity and/or non-nasal specimen types). In this observational cohort study, 370 individuals from 85 households with a recent COVID-19 case were screened at least daily by RT-qPCR on one or more self-collected upper-respiratory specimen types. A two-level random intercept model was used to assess the association between the infection outcome of household contacts and each covariable (household size, race/ethnicity, age, vaccination status, viral variant, infection-control practices, and whether a rapid nasal-swab test was used to initially identify the household index case). Transmission was quantified by adjusted secondary attack rates (aSAR) and adjusted odds ratios (aOR). An aSAR of 53.6% (95% CI 38.8–68.3%) was observed among households where the index case first tested positive by a rapid nasal-swab COVID-19 test, which was significantly higher than the aSAR for households where the index case utilized another test type (27.2% 95% CI 19.5–35.0%, *P*=0.003 pairwise comparisons of predictive margins). We observed an aOR of 4.90 (95% CI 1.65–14.56) for transmission to household contacts when a nasal-swab rapid test was used to identify the index case, compared to other test types. Use of nasal-swab rapid COVID-19 tests for initial detection of infection and initiation of infection control may not limit transmission as well as other test types.

Introduction

The majority of SARS-CoV-2 transmission events occur among household contacts.[1,2] Numerous studies have characterized household transmission of SARS-CoV-2[3-8] and identified factors that modulate the risk of transmission within households, such as larger household size being associated with higher risk.[9-12] Similarly, disparities by race and ethnicity have been observed, while controlling for socioeconomic differences.[11,13] Age of both the index case (first person in the household to become infected) and at-risk household contacts (who either remain uninfected or become infected secondary cases) has also been implicated in SARS-CoV-2 household-transmission patterns.[6,14-16] Furthermore, although vaccination does not fully prevent breakthrough infections,[17] vaccination has been shown to be protective and decrease the risk of infection.[8,18–22] Specific infection-control practices, such as wearing a mask around infected contacts, physical distancing, and quarantining sick individuals have also shown protective effects.[14,18,23–25] Lastly, SARS-CoV-2 variants such as Delta and Omicron have been shown in large studies to have greater transmissibility compared with ancestral variants.[8,18,19,26–33]

Early identification of an infectious individual is a critical step to reduce subsequent transmission, including within households. Because transmission of SARS-CoV-2 occurs during both the asymptomatic and symptomatic periods of infection,[34-37] diagnostic testing to quickly prompt infection control practices has been effective to limit additional exposures and transmission.[38] Conversely, infectious individuals that go unidentified or delay identification allow for greater exposure to contacts and thereby more transmission. [12,39,40]

Delayed detection can occur due to test turnaround times or when a test yields a false-negative result. Rapid tests (e.g., antigen and some molecular tests) offer fast turnaround times, but require higher levels of virus to reliably result positive; e.g., ~100,000 times more virus is needed to yield a positive result by the LumiraDx SARS-CoV-2 Ag Test than the PerkinElmer New Coronavirus Nucleic Acid Detection Kit.[41,42] Additionally, SARS-CoV-2 can infect different upper-respiratory compartments, so numerous specimen types are used to detect infection (e.g., anterior-nares nasal swab, mid-turbinate nasal swab, nasopharyngeal swab, oropharyngeal swab, tonsillar swab, buccal swab, lingual swab, gingival crevicular fluid, saliva). The rise and fall of viral loads in each specimen type throughout infection affects whether SARS-CoV-2 is detectable in that specimen type at the time of testing. A diagnostic test successfully detects infection when the viral load in the tested specimen type is above the limit of detection (LOD) of the test.

In our recent analysis[43] of viral loads from three specimen types (anterior-nares swab, oropharyngeal swab, and saliva) prospectively collected daily before or at the incidence of infection with the Omicron variant, we observed that longitudinal viral-load timecourses in different specimen types from the same person often exhibit extreme differences and do not correlate. Further, most people in that study[43] and our prior study of ancestral variants[44] had delayed accumulation of virus in nasal swabs compared with oral specimens. A delayed rise in nasal-swab viral loads has been observed in many studies,[45–48] including among participants in a SARS-CoV-2 human challenge study who received intra-nasal inoculation.[49] We[50] and others[43,46,48,51,52] found that this delayed rise in nasal viral loads, in combination with the high levels of virus required for detection by tests with low analytical sensitivity, leads to delayed detection of infected and infectious individuals by nasal-swab rapid antigen tests. Non-nasal upper respiratory specimen types and/or tests with high-analytical-sensitivity could detect these individuals earlier in the infection.[43]

In this study, we aimed to investigate whether test analytical sensitivity and differences in viral-load patterns among different specimen types may have implications for household transmission. We specifically tested whether the type of test (rapid nasal-swab vs all other COVID-19 tests) used to first identify household index cases was correlated with higher rates of transmission to household contacts. Data were collected from a two-year COVID-19 household transmission study in Southern California. We applied a two-level random intercept model, clustering by household and controlling for potential confounders[53] to assess the relationship between the use of

a nasal-swab rapid COVID-19 tests to first identify the household index case, and subsequent transmission to household contacts (**Figure 8-1**).

Methods

Participant Enrollment and Metadata

We conducted a case-ascertained COVID-19 household transmission observational cohort study in Southern California in two phases: between September 2020 and June 2021,[44,54] prior to the predominance of the Delta variant,[55] and between November 2021 and March 2022,[43] during the emergence and subsequent predominance of the Omicron variant[55] (**Supplemental Table 8-S1A**). The study was approved by the California Institute of Technology IRB (protocol #20-1026). Participants aged eight years and older provided written informed consent, and all minors additionally provided verbal assent accompanied by written parental permission. Only the study coordinators, study administrator, and study PI had access to identifying information; the rest of the investigators were blinded to participant identity (see Supplemental Information).

Upon enrollment, participants completed a questionnaire to provide information about demographics (see Supplementary Information). At the conclusion of their participation, participants were asked to complete another questionnaire to report any SARS-CoV-2 test results from outside of the study, updated infection status of each household member (including those unenrolled), and infection-control practices performed.

Laboratory Screening Testing

Specimens (saliva, anterior nares swabs, oropharyngeal swabs, **Figure 8-1A,B**) from participants underwent laboratory testing for SARS-CoV-2 infection, as previously described (Supplementary Information).[43,44,54] Participants reported COVID-19-like symptoms at each specimen collection timepoint. At least one specimen from most households underwent viral sequencing as previously described,[43,44] to ascertain the infecting SARS-CoV-2 variant of household members. For one household enrolled in early December 2022, sequencing was not performed but Delta variant was inferred based on the dominating variants circulating at the time[55] and for five households enrolled after mid-January 2022, sequencing was not performed, but Omicron variant was inferred based on local predominance.[55]

Statistical Analyses

We utilized the questionnaire data and laboratory testing data to investigate SARS-CoV-2 transmission within households**.** Households were included in this analysis if laboratory testing confirmed at least one household member was acutely infected with SARS-CoV-2 and more than a third of reported household members were enrolled in the study. Three households were excluded because they withdrew before three days of screening, 22 households were excluded because all members were negative for SARS-CoV-2 in all tested specimens, five households were excluded because of insufficient information about unenrolled household contacts, and one household was excluded because of inability to determine index case (**Figure 8-1B**). See Supplemental Information for details.

For each household, an index case was defined as the first member of the household (enrolled in the study or not) to test positive for SARS-CoV-2 infection, usually prior to enrollment. In one case where multiple members had the same first test date, the member with earlier self-reported onset of symptoms was considered the household index case. In five cases where symptom onset of household members was within one day of each other, we defined the index case as the individual with a known exposure to a non-household contact with laboratory-confirmed SARS-CoV-2 infection. In three cases with similar timing of exposure to infected, non-household contacts, the index case was defined as the individual whose viral load peaked first. All other members of the household who tested positive for SARS-CoV-2 prior to or during household enrollment in the study were considered secondary cases. Household members who never tested positive for SARS-CoV-2 prior to or while the household was enrolled in the study were considered uninfected. 143 of 149 (96%) participants classified as uninfected were enrolled and screened for at least five days; most (53%) were enrolled for at least nine days.

The test type of the household index case was interpreted as a "nasal-swab rapid test" when the household index case self-reported "shallow nasal swab (anterior nares or mid turbinate nasal swab)" as the specimen type and a result turnaround time of "within an hour" or "same day." Participants were not asked to report the specific test name, laboratory platform, or viral target (e.g., molecular, antigen), due to concerns that laypersons would not be aware of these terms (especially if the test was run by a clinic rather than direct-to-consumer). However, rapid tests (both antigen and molecular) have characteristically low analytical sensitivity because they forego the time-consuming and technically challenging extraction steps to purify and concentrate viral targets. Because our hypothesis was related to low-analytical-sensitivity rapid tests performed on specimens from nasal swabs, we simply distinguish rapid tests from those with longer turnaround times and presumably higher analytical sensitivity (**Figure 8-1D**).

We calculated unadjusted odds ratios (ORs) for a priori confounders,[56] infection-control practices, the use of nasal-swab rapid tests by index cases, and the risk of SARS-CoV-2 transmission to household contacts using

mixed-effect logistic regression (**Figure 8-2**, **Supplemental Table 8-S2**). We also used a two-level mixed-effects logistic regression model with random intercepts by household to account for clustering of individuals within households and including all covariables to estimate adjusted odds ratios (aOR) (**Figure 8-2, Supplemental Table 8-S3**). This type of model[57] was chosen to estimate the effects of predictors at both individual and household levels. The model adjusted for a sufficient set of the following potentially confounding variables: household size,[10–12] age,[6,15,16] race/ethnicity,[11,13] and vaccination status.[18–22] We also accounted for infecting SARS-CoV-2 viral variant.[18-20,28,32,33] Observations with missing data were omitted from respective analyses.

We used this model to assess the effect of household prevention practices and the COVID-19 test type used to first identify the household index case. An aOR >1.0 was associated with increased likelihood of household transmission, and deemed statistically significant if its associated *P*-value was ≤0.05 by Wald and likelihood ratio tests.

Predictive margins based on the results of the regression models were used to estimate unadjusted and adjusted secondary attack rates (SAR and aSAR). Binomial confidence intervals (CIs) were calculated as recommended by the Clinical Laboratory Standards Institute EP12-A guidance.[58] Differences among SARs and aSARs were assessed across strata.[59]

We separately assessed the conditional direct effects of viral variant and test type used to identify the household index case by modifying the model with or without each of these covariables (**Figure 8-3**). Calculations were performed in STATA/BE 17.0.

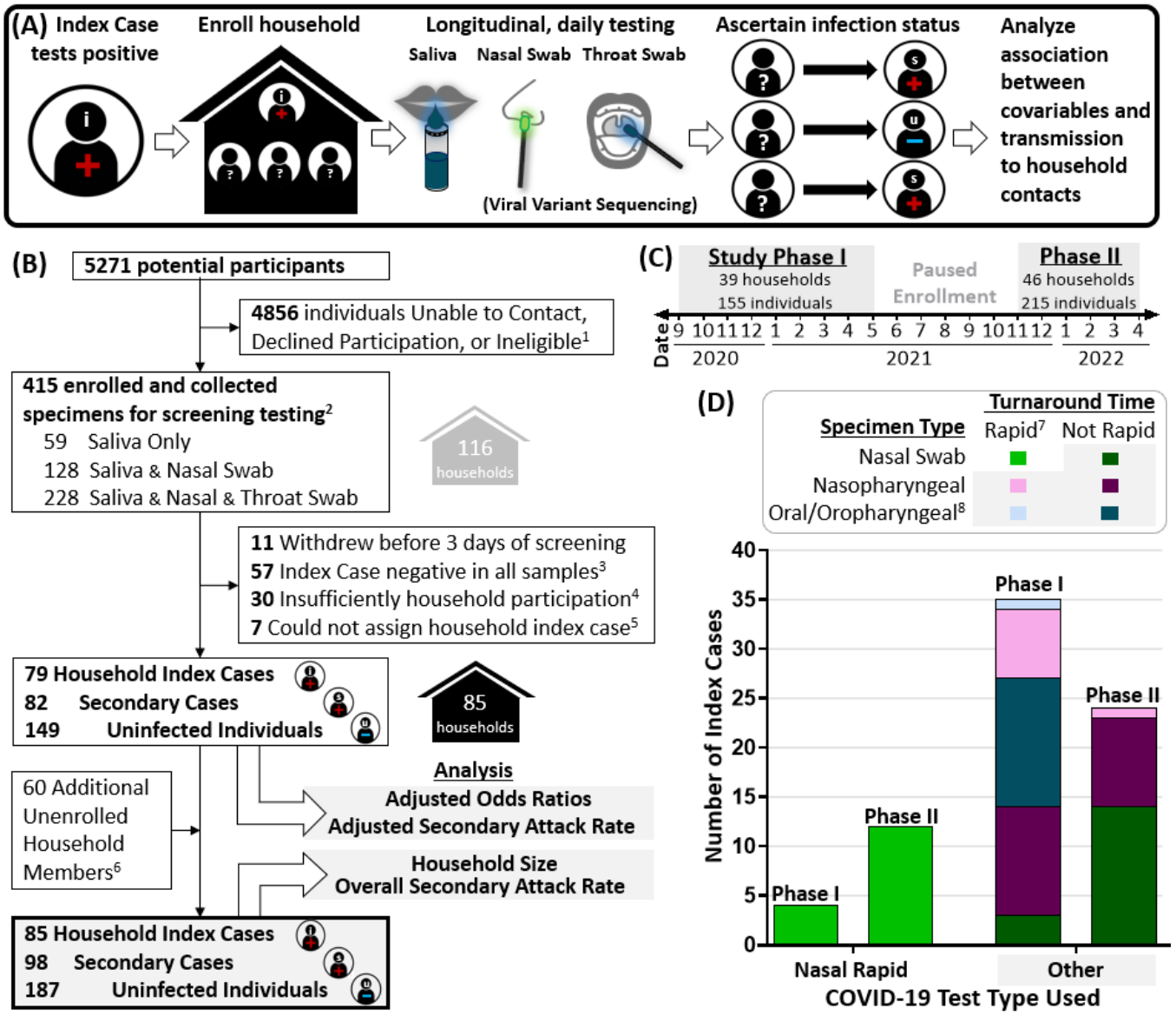

Figure 8-1. Overview of study design and analysis. **(A)** Study design beginning with recording the COVID-19 test type first used to identify index cases at study enrollment, enrollment of household contacts for daily, high-analytical-sensitivity laboratory screening, and analysis of potential factors modulating transmission. **(B)** CONSORT diagram for study enrollment. **(C)** Timeline of participant enrollment in study Phase I (September 2020—June 2021) and Phase II (November 2021—March 2022). Date is listed as numeric month over year. **(D)** Breakdown of self-reported COVID-19 test types (specimen type, and rapid or not) utilized to first identify household index cases. Test type was not reported by 10 of 85 index cases.

1. Individuals were ineligible for enrollment if they resided outside study jurisdiction, lived alone, or were more than seven days from positive result or symptom onset. 2. Participants in Phase I collected either saliva only, or paired saliva and nasal swabs; participants in Phase II collected paired saliva, nasal swabs, and throat swabs. 3. Households were considered not at risk if no member including the suspected index case had detectable SARS-CoV-2 in any sample tested upon enrollment. 4. Households in which a majority of unenrolled household members were considered to have insufficient information. 5. Households in which a single household index case could not be assigned. 6. Information about unenrolled household members was reported by enrolled participants. 7. Test type was defined as "Rapid" if the participant reported receiving results either within an hour or on the same day as the specimen was collected. Longer turnaround times were classified as "Not Rapid" tests. 8. Oral/oropharyngeal specimen type category included participants who self-reported that saliva, buccal swabs, or oropharyngeal swabs were collected for testing.

Results

We analyzed data from 370 individuals (enrolled and unenrolled participants) of which 85 were defined as household index cases (**Table 8-1**). Among index cases, nasal-swab rapid test use more than tripled from the first to second study phase (**Figure 8-1D**). Only three of 16 index cases first identified by a rapid nasal-swab rapid tests had a prior negative rapid nasal-test within three days of their positive result, suggesting repeat rapid nasal testing.[60] Across both study phases, we observed an overall, unadjusted SAR of 34.4% (95% CI 28.9%–40.2%, 98 of 285 household contacts) in this population.

Without accounting for index case testing, we observed several covariables associated with SARS-CoV-2 transmission in households (**Figure 8-2**). Household size greater than four members was associated with nearly a five-fold increase in the odds of infection (aOR=4.78, 95% CI 1.80–12.70). Whether a household contact had received at least one dose of a COVID-19 vaccine was found to reduce the odds of infection by 70% (aOR=0.30, 95% CI 0.08–1.17). Most infection-control practices were associated with reduced risk, such as not sharing a bedroom with (aOR=0.25, 95% CI 0.10–0.62) and wearing masks around (aOR=0.33, 95% CI 0.12-0.88) infected individuals.

Our results were also consistent with previous observations that infection with the Omicron variant is associated with greater transmission than ancestral variants.[8,18,19,31-33] Increased transmissibility of the Omicron variant compared to ancestral variants was observed in our study by both aOR (3.64, 95% CI 0.88–15.07), as well as aSAR stratified by whether the index case was infected with the Omicron variant (46.9%, 95% CI 32.3%-61.6%) or an ancestral variant (27.3%, 95% CI 17.7%-36.9%). Increased transmissibility of the Omicron variant was not observed in the univariable model (**Supplemental Table 8-S2**), likely because this model does not correct for a compensating, protective effect of vaccination, which was more prevalent among individuals from households infected with the Omicron variant (76.7%) than ancestral variants (17.5%, **Supplemental Table 8-S1**).

Identification of index cases by nasal-swab rapid tests was associated with higher transmission to household contacts than other test types, both when aggregated (**Figure 8-2C**) and for all other test type subgroups (**Supplemental Table 8-S3**), and in both univariable (OR=2.64, 95% CI 1.41–4.95, *P*=0.003, **Supplemental Table 8-S2**) and multivariable models (aOR=4.93, 95% CI 1.65–14.69, *P*=0.004, **Figure 8-2**). The multivariable model suggests that nasal-swab rapid test use by index cases increased the odds of transmission relative to other test types by almost five-fold (though both smaller and larger increases are also compatible with the data). Index cases who used nasal-swab rapid tests also had a higher aSAR of 53.5% (95% CI 38.7%–68.3%) compared to other test types (27.0%, 95% CI 19.3%–34.8%).

Because the use of nasal-swab rapid test use has increased in parallel with SARS-CoV-2 variants shown to have increased transmissibility, we examined the relationship of these two covariables on risk of transmission to

household contacts. The use of a nasal-swab rapid test to identify the index case was associated with a similar increased risk of transmission to household contacts) as infection with the Omicron variant (**Figure 8-3**). Introducing adjustment in the model for nasal-swab rapid test use by the index case decreased the aOR for infection with the Omicron variant from 3.63 (95% CI 0.88-15.0) to 2.40 (95% CI 0.63–9.22) (**Figure 8-3A**). The aOR of rapid nasal-swab test use also decreased from 5.50 (95% CI 1.78–17.04) to 4.90 (95% CI 1.65–14.59) without or with adjustment for viral variant, but nasal-swab rapid tests remained associated with at least a 1.5-fold increase in the odds of household contact infection (**Figure 8-3B**).

Table 8-1. Demographics, COVID-19 Vaccination Status, Viral Variant, and Smoking History of the 85-Household Cohort Used for Analyses.

		Index Case		Secondary Case		Uninfected		Total	
		N= 85		N= 98		N= 187		N= 370	
Self-Reported Gender Identity*		**n**	**(%)**	**n**	**(%)**	**n**	**(%)**	**n**	**(%)**
	Male	31	36.5	50	51.0	91	48.7	172	46.5
	Female	52	61.2	45	45.9	96	51.3	193	52.2
	Non-Binary/Other	0	0.0	0	0.0	0	0.0	0	0.0
	Unknown	2	2.4	3	3.1	0	0.0	5	1.4
Age Category (years)		**n**	**(%)**	**n**	**(%)**	**n**	**(%)**	**n**	**(%)**
	<10	4	4.7	19	19.4	33	17.6	56	15.1
	10 to 60	78	91.8	75	76.5	133	71.1	286	77.3
	>60	2	2.4	2	2.0	21	11.2	25	6.8
	Unknown	1	1.2	2	2.0	0	0.0	3	0.8
Self-Reported Race/Ethnicity**		**n**	**(%)**	**n**	**(%)**	**n**	**(%)**	**n**	**(%)**
	Asian or Pacific Islander	14	16.5	10	10.2	23	12.3	47	12.7
	Biracial	4	4.7	4	4.1	8	4.3	16	4.3
	Black/African American	2	2.4	3	3.1	11	5.9	16	4.3
	Native American/Alaska Native	4	4.7	1	1.0	7	3.7	12	3.2
	Unknown	20	23.5	39	39.8	68	36.4	127	34.3
	White, Hispanic	22	25.9	20	20.4	26	13.9	68	18.4
	White, Non-Hispanic	19	22.4	21	21.4	44	23.5	84	22.7
Vaccination Status***		**n**	**(%)**	**n**	**(%)**	**n**	**(%)**	**n**	**(%)**
	Unvaccinated	43	50.6	40	40.8	65	34.8	148	40.0
	Partial	0	0.0	2	2.0	3	1.6	5	1.4
	Complete	19	22.4	23	23.5	36	19.3	78	20.6
	Boosted	17	20.0	17	17.3	45	24.1	79	21.4
	Unknown	6	7.1	16	16.3	38	20.3	60	16.2
Household Viral Variant		**n**	**(%)**	**n**	**(%)**	**n**	**(%)**	**n**	**(%)**
	Ancestral	39	45.9	37	37.8	79	42.2	155	41.9
	Delta	12	14.1	14	14.3	22	11.8	48	13.0
	Omicron	28	32.9	45	45.9	64	34.2	137	37.0
	Unknown	6	7.1	2	2.0	22	11.8	30	8.1
Smoking/Vaping History History		**n**	**(%)**	**n**	**(%)**	**n**	**(%)**	**n**	**(%)**
	Never	60	70.6	58	59.2	105	56.1	223	60.3
	Former	13	15.3	14	14.3	24	12.8	51	13.8
	Current	5	5.9	4	4.1	6	3.2	15	4.1
	Unknown	7	8.2	22	22.4	52	27.8	81	21.9

**Both sex assigned at birth and current gender identity were self-reported by participants. One participant reported male assignment at birth and current gender identity of woman. Reported gender is listed.*

***63 individuals currently listed as "Unknown" did not select a race category but wrote-in "Latino"/"Latina"/"Latinx."*

****Participants reported date and manufacturer of each vaccine dose received; vaccination status was defined only by doses received at least seven days prior to enrollment in the study. Unvaccinated was defined as having received no COVID-19 vaccine doses. Partial vaccination was defined as receiving one dose of a multiple-dose series (e.g., Pfizer-BioNTech, Moderna). Complete vaccination was defined as receiving all doses of an initial COVID-19 vaccine series. Boosted was defined as the participant receiving any dose beyond an initial COVID-19 vaccine series. Vaccination and viral variant distributions varied by Study Phase; demographics by Study Phase are shown in* ***Supplemental Table 8-1****.*

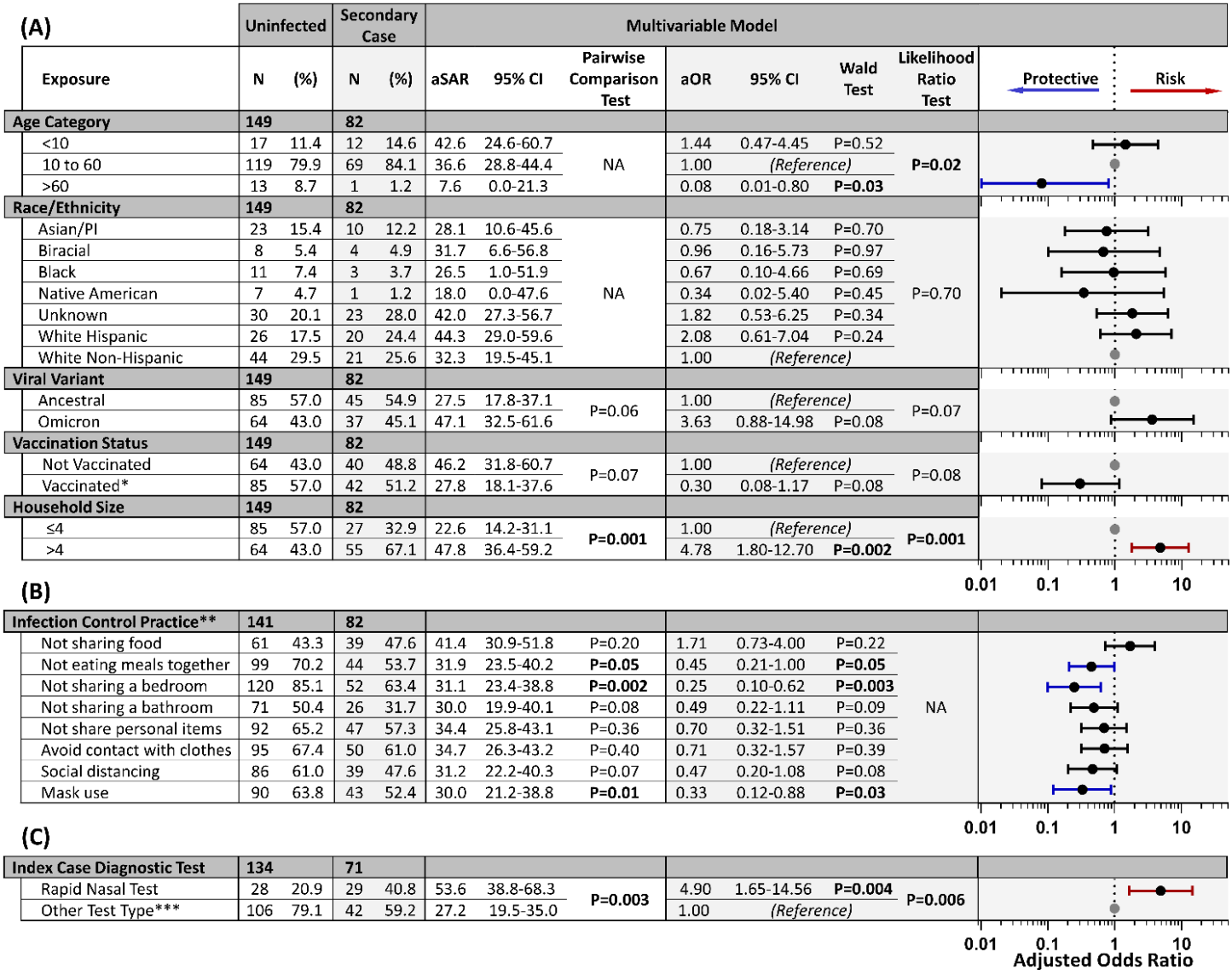

Figure 8-2. Results of Modeled Risk of Transmission to Household Contacts. Counts (N) of enrolled individuals who did not become infected during enrollment (uninfected) or became infected after the index case (secondary case) are provided for each covariable included in the multivariable model (**Figure 8-1C**). The adjusted secondary attack rate (aSAR) and adjusted odds ratio (aOR) point estimates with 95% confidence intervals from multivariable analysis are listed for each covariable and visualized to the right. Results of univariable analysis are provided in **Supplemental Table 8-2**. The Wald test *P*-values for the analyses likelihood ratio test is shown. Covariates with an aOR 95% CI >1 are shown in red, and those <1 are shown in blue. Reference groups are shown as a grey point. **(A)** Data for the five covariables included in the sufficient set. **(B)** Covariables related to infection-control practices controlling for the sufficient set. The aOR represents the conditional effect of the covariable in the model. **(C)** Association between COVID-19 test type used to identify the household index case, and subsequent transmission to household contacts. Unenrolled household index cases' test type was unknown, resulting in a lower total count for this category.

**Vaccinated is defined as having received at least one dose of a COVID-19 vaccine at least seven days prior to enrollment.*
***Participants were asked to respond whether or not they performed each action during interactions data coded. Data on infection control practices was not available for some participants. Observations with missing data were omitted, resulting in a lower total count for this category of covariables.*
****Analysis by Other Test Type subgroups is shown in **Supplemental Table 8-3**.*

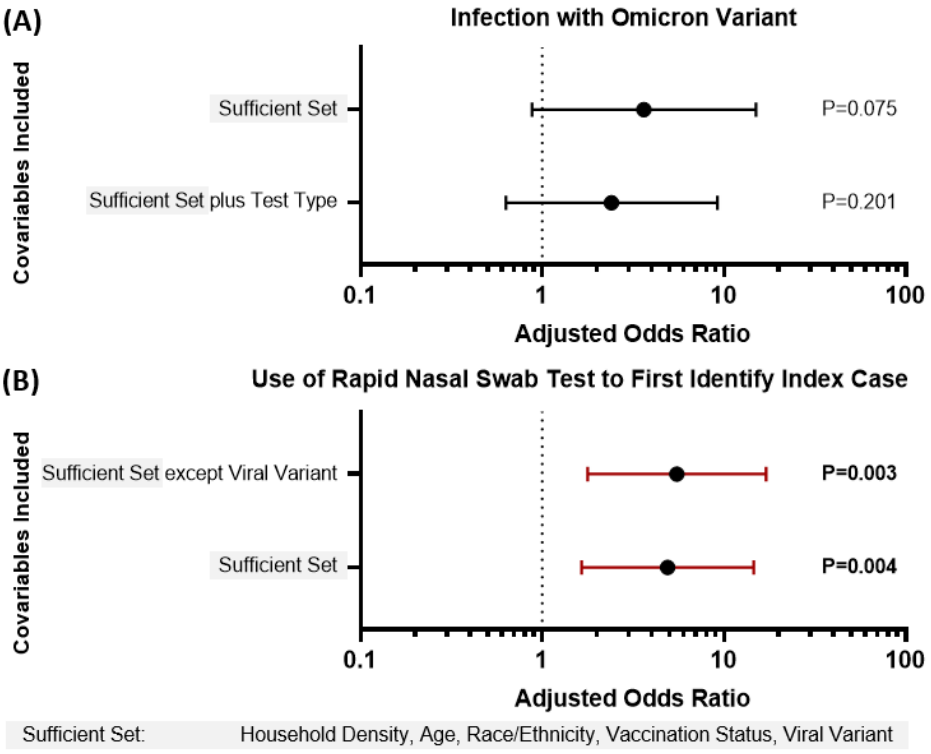

Figure 8-3. Effect Size Interactions of COVID-19 Test Type and Viral Variant on Transmission to Household Contacts. **(A)** The adjusted odds ratios (aOR) for infection with the Omicron variant (with ancestral SARS-CoV-2 variants as reference). Analysis was performed while controlling for the sufficient set of covariables in the model (grey box), as well as when additionally controlling for whether the index case was first identified using a nasal-swab rapid test or other COVID-19 test type. **(B)** The aOR for the use of nasal-swab rapid tests to first identify index cases, as opposed to other COVID-19 test type. Analysis was performed while controlling for the sufficient set of covariables in the model (shown in grey box), and with all covariables in the sufficient set except for viral variant. Wald test *P*-values are shown for each estimate of effect size. All error bars are 95% CI. Vertical dotted black line indicates an aOR of 1.0.

Discussion

Household contacts of index cases who used nasal-swab rapid antigen COVID-19 tests for primary infection detection had an increased risk of becoming infected compared with household contacts of index cases who used other test types. Greater transmission of SARS-CoV-2 to household contacts by individuals first identified by nasal-swab rapid tests is supported mechanistically by studies of SARS-CoV-2 viral load and nasal swab rapid test performance. First, a gradual rise in viral loads, as we[43,44,50,61] and others[52,62–64] have observed, often creates a several-day delay between when an individual likely becomes infectious and when viral loads reach levels detectable by low-analytical-sensitivity, rapid tests. Second, a delay in the rise of nasal viral loads relative to oral specimen types, as we [43,44,50] and others[45,49] have observed, renders nasal-swab rapid tests less able to detect individuals during the early phase of the infection.[46,50] During this early period of low nasal viral loads, we[43,50] and others[46] find that individuals exhibited high, presumably infectious viral loads in oral specimens. Relatedly, among data from a SARS-CoV-2 human challenge study,[49] we see that the majority of infected participants had replication-competent virus present in throat swabs at least one day prior to nasal-swabs. Therefore, nasal-swab

rapid tests may only yield positive results after exposure and transmission to contacts has occurred. These results together suggest that nasal-swab rapid tests are not as effective at identifying index cases to limit subsequent transmission as other test types.

Several additional findings from our model and dataset were consistent with prior studies. Household size was a significant risk factor for household transmission,[9–12] whereas vaccination[8,18–22] and infection-control practices[14,18,23–25] were protective. The overall SAR (34.4%) we observed was similar to what others have reported.[5,12,18,31,65,66] Relatedly, in one of those studies,[5] household transmission was monitored by daily high-analytical-sensitivity screening testing and the SAR calculated using only nasal-swab test data was lower than when both saliva and nasal-swab test data were used, which supports that even high-analytical-sensitivity nasal-swab testing may miss some infected individuals, and that the specimen type used for evaluation can impact estimates of transmission.

We also observed, as other epidemiological studies have,[8,18,19,31-33] that infection with the Omicron variant was associated with increased transmission compared with ancestral viral variants. However, the use of rapid nasal-swab tests (as opposed to other test types) to detect index cases had a similar conditional direct effect on transmission to household contacts as infection with the Omicron variant. Because the effect size of the Omicron variant association with transmission to household contacts decreased when controlling for nasal-swab rapid test use in our study, we speculate that a portion of the increased transmissibility attributed to the Omicron variant in published epidemiological studies may be partially attributable to the increased use of rapid nasal-swab tests in the USA that coincided with the predominance of this variant.[10,67] Although our results do not invalidate studies that conclude an increased transmissibility of the Omicron variant, they emphasize the potential impact of COVID-19 test type on estimates of transmissibility from epidemiological data.

Our findings are subject to limitations. First, vaccination status, demographic information, and infection-control practices are self-reported and may be subject to recall bias. Second, although questionnaires were written in simple terms (e.g., “shallow nasal swab” and “deep nasal swab”), participants could have misinterpreted test type. Third, age, gender, and infection status of each unenrolled household member was independently reported by each enrolled household member, which could lead to inaccurate reporting. Fourth, our potential misclassification of which household member was the index case may impact the analysis,[53] although in almost all (79 of 85) households, the index case was confirmed by timing of self-reported positive tests. Fifth, in our transmission model, we did not analyze ordinal levels of contact among household members (all household members were assumed to have equal contact). Instead, mitigating factors, including infection-control practices, were assessed for protective effects against transmission. Sixth, it is possible that high-analytical-sensitivity tests could have turnaround times which we classify as rapid. However, such misclassification would bias toward the null. Finally,

evidence suggests[52,68] and the CDC[60] recommends repeating rapid antigen tests over several days to improve clinical sensitivity. Although some index cases reported a negative test result in the days prior to their first positive result, most participants in our study did not use repeated rapid testing.

Conclusion

Rapid COVID-19 tests, such as antigen tests, are less expensive, portable, and offer faster results than high-analytical-sensitivity molecular tests. However, results from this observational study suggest that the use of nasal-swab rapid COVID-19 tests to first identify infection do not limit household transmission as well as other test types. The use of tests with low analytical sensitivity by an infected individual can have two effects on transmission: (i) a true-positive result can change behavior to increase infection-control practices in a timely manner, thus reducing transmission, or (ii) a false-negative result can result in a health certificate effect,[69] where individuals falsely assume they are not infected/infectious and reduce precautions, thereby increasing transmission. While imperfect testing may be better than no testing, understanding the optimal use and limitations of rapid tests is important not only for SARS-CoV-2, but other pathogens for which timely infection control and/or early treatment is critical.

Data Sharing Statement

Raw data is available at CaltechDATA: https://doi.org/10.22002/csh5w-rf132.

Acknowledgements

We thank the University of California, Los Angeles, Office of Advanced Research Computing, Statistical Methods and Data Analytics Group for recommendations on statistical methodology and implementation, and Dr. Andy Lin for guidance designing the analysis and feedback on the manuscript. This study is based on research funded in part by the Bill & Melinda Gates Foundation (INV-023124). The findings and conclusions contained within are those of the authors and do not necessarily reflect positions or policies of the Bill & Melinda Gates Foundation. This study was also funded in part by grants from the Ronald and Maxine Linde Center for New Initiatives at the California Institute of Technology (to RFI), a grant from the Jacobs Institute for Molecular Engineering for Medicine at the California Institute of Technology (to RFI), a DGSOM Geffen Fellowship at the University of California, Los Angeles (to AVW), and the John Stauffer Charitable Trust SURF Fellowship at the California Institute of Technology (to JJ).

Disclosures

R.F.I. is a cofounder, consultant, and a director and has stock ownership of Talis Biomedical Corp. All other co-authors report no competing interests.

References

1. Del Brutto OH, Costa AF, Mera RM, Recalde BY, Bustos JA, Garcia HH. Household Clustering of SARS-CoV-2 in Community Settings: A Study from Rural Ecuador. *Am J Trop Med Hyg.* 2020;103(3):1207-1210.

2. Lee EC, Wada NI, Grabowski MK, Gurley ES, Lessler J. The engines of SARS-CoV-2 spread. *Science.* 2020;370(6515):406-407.

3. Li F, Li YY, Liu MJ, et al. Household transmission of SARS-CoV-2 and risk factors for susceptibility and infectivity in Wuhan: a retrospective observational study. *Lancet Infect Dis.* 2021;21(5):617-628.

4. Donnelly MAP, Chuey MR, Soto R, et al. Household Transmission of Severe Acute Respiratory Syndrome Coronavirus 2 (SARS-CoV-2) Alpha Variant-United States, 2021. *Clin Infect Dis.* 2022;75(1):e122-e132.

5. Grijalva CG, Rolfes MA, Zhu Y, et al. Transmission of SARS-COV-2 Infections in Households - Tennessee and Wisconsin, April-September 2020. *MMWR Morb Mortal Wkly Rep.* 2020;69(44):1631-1634.

6. McLean HQ, Grijalva CG, Hanson KE, et al. Household Transmission and Clinical Features of SARS-CoV-2 Infections by Age in 2 US Communities. *medRxiv.* 2021.

7. Madewell ZJ, Yang Y, Longini IM, Jr., Halloran ME, Dean NE. Household Transmission of SARS-CoV-2: A Systematic Review and Meta-analysis. *JAMA Netw Open.* 2020;3(12):e2031756.

8. Madewell ZJ, Yang Y, Longini IM, Jr., Halloran ME, Dean NE. Factors Associated With Household Transmission of SARS-CoV-2: An Updated Systematic Review and Meta-analysis. *JAMA Netw Open.* 2021;4(8):e2122240.

9. Nash D, Qasmieh S, Robertson M, et al. Household factors and the risk of severe COVID-like illness early in the U.S. pandemic. *PLoS One.* 2022;17(7):e0271786.

10. Rader B, Scarpino SV, Nande A, et al. Crowding and the shape of COVID-19 epidemics. *Nat Med.* 2020;26(12):1829-1834.

11. Cerami C, Popkin-Hall ZR, Rapp T, et al. Household Transmission of Severe Acute Respiratory Syndrome Coronavirus 2 in the United States: Living Density, Viral Load, and Disproportionate Impact on Communities of Color. *Clin Infect Dis.* 2022;74(10):1776-1785.

12. Laajaj R, Webb D, Aristizabal D, et al. Understanding how socioeconomic inequalities drive inequalities in COVID-19 infections. *Sci Rep.* 2022;12(1):8269.

13. Niedzwiedz CL, O'Donnell CA, Jani BD, et al. Ethnic and socioeconomic differences in SARS-CoV-2 infection: prospective cohort study using UK Biobank. *BMC Med.* 2020;18(1):160.

14. Chu VT, Yousaf AR, Chang K, et al. Household Transmission of SARS-CoV-2 from Children and Adolescents. *N Engl J Med.* 2021;385(10):954-956.

15. Bi Q, Lessler J, Eckerle I, et al. Insights into household transmission of SARS-CoV-2 from a population-based serological survey. *Nat Commun.* 2021;12(1):3643.

16. Chen F, Tian Y, Zhang L, Shi Y. The role of children in household transmission of COVID-19: a systematic review and meta-analysis. *Int J Infect Dis.* 2022;122:266-275.

17. CDC. COVID-19 after Vaccination: Possible Breakthrough Infection. 2022; https://www.cdc.gov/coronavirus/2019-ncov/vaccines/effectiveness/why-measure-effectiveness/breakthrough-cases.html.

18. Baker JM, Nakayama JY, O'Hegarty M, et al. SARS-CoV-2 B.1.1.529 (Omicron) Variant Transmission Within Households - Four U.S. Jurisdictions, November 2021-February 2022. *MMWR Morb Mortal Wkly Rep.* 2022;71(9):341-346.

19. Lyngse FP, Mortensen LH, Denwood MJ, et al. Household transmission of the SARS-CoV-2 Omicron variant in Denmark. *Nat Commun.* 2022;13(1):5573.

20. Rosenberg ES, Dorabawila V, Easton D, et al. Covid-19 Vaccine Effectiveness in New York State. *N Engl J Med.* 2022;386(2):116-127.

21. Suthar AB, Wang J, Seffren V, Wiegand RE, Griffing S, Zell E. Public health impact of covid-19 vaccines in the US: observational study. *BMJ.* 2022;377:e069317.

22. Tande AJ, Pollock BD, Shah ND, et al. Impact of the Coronavirus Disease 2019 (COVID-19) Vaccine on Asymptomatic Infection Among Patients Undergoing Preprocedural COVID-19 Molecular Screening. *Clin Infect Dis.* 2022;74(1):59-65.

23. Brooks JT, Butler JC. Effectiveness of Mask Wearing to Control Community Spread of SARS-CoV-2. *JAMA.* 2021;325(10):998-999.

24. Chu DK, Akl EA, Duda S, et al. Physical distancing, face masks, and eye protection to prevent person-to-person transmission of SARS-CoV-2 and COVID-19: a systematic review and meta-analysis. *Lancet.* 2020;395(10242):1973-1987.

25. Ha BTT, Ngoc Quang L, Quoc Thanh P, Duc DM, Mirzoev T, Bui TMA. Community engagement in the prevention and control of COVID-19: Insights from Vietnam. *PLoS One.* 2021;16(9):e0254432.

26. LA County Public Health. Los Angeles County Public Health COVID-19 Vaccine Dashboard. 2022; http://publichealth.lacounty.gov/media/coronavirus/vaccine/vaccine-dashboard.htm.

27. Julin CH, Robertson AH, Hungnes O, et al. Household Transmission of SARS-CoV-2: A Prospective Longitudinal Study Showing Higher Viral Load and Increased Transmissibility of the Alpha Variant Compared to Previous Strains. *Microorganisms.* 2021;9(11).

28. Campbell F, Archer B, Laurenson-Schafer H, et al. Increased transmissibility and global spread of SARS-CoV-2 variants of concern as at June 2021. *Euro Surveill.* 2021;26(24).

29. Allen H, Vusirikala A, Flannagan J, et al. Household transmission of COVID-19 cases associated with SARS-CoV-2 delta variant (B.1.617.2): national case-control study. *Lancet Reg Health Eur.* 2022;12:100252.

30. Jorgensen SB, Nygard K, Kacelnik O, Telle K. Secondary Attack Rates for Omicron and Delta Variants of SARS-CoV-2 in Norwegian Households. *JAMA.* 2022;327(16):1610-1611.

31. Ogata T, Tanaka H, Tanaka E, et al. Increased Secondary Attack Rates among the Household Contacts of Patients with the Omicron Variant of the Coronavirus Disease 2019 in Japan. *Int J Environ Res Public Health.* 2022;19(13).

32. Song JS, Lee J, Kim M, et al. Serial Intervals and Household Transmission of SARS-CoV-2 Omicron Variant, South Korea, 2021. *Emerg Infect Dis.* 2022;28(3):756-759.

33. Jalali N, Brustad HK, Frigessi A, et al. Increased household transmission and immune escape of the SARS-CoV-2 Omicron compared to Delta variants. *Nat Commun.* 2022;13(1):5706.

34. He X, Lau EHY, Wu P, et al. Temporal dynamics in viral shedding and transmissibility of COVID-19. *Nat Med.* 2020;26(5):672-675.

35. Cheng HY, Jian SW, Liu DP, et al. Contact Tracing Assessment of COVID-19 Transmission Dynamics in Taiwan and Risk at Different Exposure Periods Before and After Symptom Onset. *JAMA Intern Med.* 2020;180(9):1156-1163.

36. Tindale LC, Stockdale JE, Coombe M, et al. Evidence for transmission of COVID-19 prior to symptom onset. *Elife.* 2020;9:e57149.

37. Buitrago-Garcia D, Egli-Gany D, Counotte MJ, et al. Occurrence and transmission potential of asymptomatic and presymptomatic SARS-CoV-2 infections: A living systematic review and meta-analysis. *PLoS Med.* 2020;17(9):e1003346.

38. Dora AV, Winnett A, Jatt LP, et al. Universal and Serial Laboratory Testing for SARS-CoV-2 at a Long-Term Care Skilled Nursing Facility for Veterans - Los Angeles, California, 2020. *MMWR Morb Mortal Wkly Rep.* 2020;69(21):651-655.

39. Hart WS, Maini PK, Thompson RN. High infectiousness immediately before COVID-19 symptom onset highlights the importance of continued contact tracing. *Elife.* 2021;10:e65534.

40. Li R, Pei S, Chen B, et al. Substantial undocumented infection facilitates the rapid dissemination of novel coronavirus (SARS-CoV-2). *Science.* 2020;368(6490):489-493.

41. Stanley S, Hamel DJ, Wolf ID, et al. Limit of Detection for Rapid Antigen Testing of the SARS-CoV-2 Omicron and Delta Variants of Concern Using Live-Virus Culture. *J Clin Microbiol.* 2022;60(5):e00140-00122.

42. FDA. SARS-CoV-2 reference panel comparative data. 2020; https://www.fda.gov/medical-devices/coronavirus-covid-19-and-medical-devices/sars-cov-2-reference-panel-comparative-data. Accessed March 8 2023.

43. Viloria Winnett A, Akana R, Shelby N, et al. Extreme differences in SARS-CoV-2 viral loads among respiratory specimen types during presumed pre-infectious and infectious periods. *PNAS Nexus.* 2023:10.1093/pnasnexus/pgad1033.

44. Savela ES, Viloria Winnett A, Romano AE, et al. Quantitative SARS-CoV-2 Viral-Load Curves in Paired Saliva Samples and Nasal Swabs Inform Appropriate Respiratory Sampling Site and Analytical Test Sensitivity Required for Earliest Viral Detection. *J Clin Microbiol.* 2022;60(2):e0178521.

45. Ke R, Martinez PP, Smith RL, et al. Daily longitudinal sampling of SARS-CoV-2 infection reveals substantial heterogeneity in infectiousness. *Nat Microbiol.* 2022;7(5):640-652.

46. Adamson B, Sikka R, Wyllie AL, Premsrirut P. Discordant SARS-CoV-2 PCR and Rapid Antigen Test Results When Infectious: A December 2021 Occupational Case Series. *medRxiv.* 2022:2022.2001.2004.22268770.

47. Lai J, German J, Hong F, et al. Comparison of Saliva and Midturbinate Swabs for Detection of SARS-CoV-2. *Microbiol Spectr.* 2022;10(2):e0012822.

48. Lin J, Frediani JK, Damhorst GL, et al. Where is Omicron? Comparison of SARS-CoV-2 RT-PCR and Antigen Test Sensitivity at Commonly Sampled Anatomic Sites Over the Course of Disease. *medRxiv.* 2022:2022.2002.2008.22270685.

49. Killingley B, Mann AJ, Kalinova M, et al. Safety, tolerability and viral kinetics during SARS-CoV-2 human challenge in young adults. *Nat Med.* 2022;28(5):1031-1041.

50. Viloria Winnett A, Akana R, Shelby N, et al. Why Daily SARS-CoV-2 Nasal Rapid Antigen Testing Poorly Detects Infected and Infectious Individuals. *medRxiv.* 2022:MEDRXIV/2022/277513.

51. Smith RL, Gibson LL, Martinez PP, et al. Longitudinal Assessment of Diagnostic Test Performance Over the Course of Acute SARS-CoV-2 Infection. *J Infect Dis.* 2021;224(6):976-982.

52. Chu VT, Schwartz NG, Donnelly MAP, et al. Comparison of Home Antigen Testing With RT-PCR and Viral Culture During the Course of SARS-CoV-2 Infection. *JAMA Intern Med.* 2022;182(7):701-709.

53. Accorsi EK, Qiu X, Rumpler E, et al. How to detect and reduce potential sources of biases in studies of SARS-CoV-2 and COVID-19. *Eur J Epidemiol.* 2021;36(2):179-196.

54. Winnett AV, Porter MK, Romano AE, et al. Morning SARS-CoV-2 testing yields better detection of infection due to higher viral loads in saliva and nasal swabs upon waking. *Microbiology Spectrum.* 2022.

55. Danza P, Koo TH, Haddix M, et al. SARS-CoV-2 Infection and Hospitalization Among Adults Aged >/=18 Years, by Vaccination Status, Before and During SARS-CoV-2 B.1.1.529 (Omicron) Variant Predominance - Los Angeles County, California, November 7, 2021-January 8, 2022. *MMWR Morb Mortal Wkly Rep.* 2022;71(5):177-181.

56. Tennant PWG, Murray EJ, Arnold KF, et al. Use of directed acyclic graphs (DAGs) to identify confounders in applied health research: review and recommendations. *Int J Epidemiol.* 2020;50(2):620-632.

57. Leyland A, Groenewegen P. *Multilevel modelling for public health and health services research: health in context.* Springer Nature; 2020.

58. CLSI. *EP12-A2 User Protocol for Evaluation of Qualitative Test Performance, 2nd edition.* 2008.

59. STATA. Pairwise comparisons of margins. 2022; https://www.stata.com/manuals13/rmarginspwcompare.pdf and https://www.stata.com/features/overview/pairwise-comparisons.

60. CDC. Guidance for Antigen Testing for SARS-CoV-2 for Healthcare Providers Testing Individuals in the Community. 2022; https://www.cdc.gov/coronavirus/2019-ncov/lab/resources/antigen-tests-guidelines.html.

61. Winnett A, Cooper MM, Shelby N, et al. SARS-CoV-2 Viral Load in Saliva Rises Gradually and to Moderate Levels in Some Humans. *medRxiv.* 2020:2020.2012.2009.20239467.

62. Kissler SM, Fauver JR, Mack C, et al. Viral dynamics of acute SARS-CoV-2 infection and applications to diagnostic and public health strategies. *PLoS Biol.* 2021;19(7):e3001333.

63. Kissler SM, Fauver JR, Mack C, et al. Viral Dynamics of SARS-CoV-2 Variants in Vaccinated and Unvaccinated Persons. *N Engl J Med.* 2021;385(26):2489-2491.

64. Stankiewicz Karita HC, Dong TQ, Johnston C, et al. Trajectory of Viral RNA Load Among Persons With Incident SARS-CoV-2 G614 Infection (Wuhan Strain) in Association With COVID-19 Symptom Onset and Severity. *JAMA Netw Open.* 2022;5(1):e2142796.

65. Toth DJA, Beams AB, Keegan LT, et al. High variability in transmission of SARS-CoV-2 within households and implications for control. *PLoS One.* 2021;16(11):e0259097.

66. Tosif S, Haycroft ER, Sarkar S, et al. Virology and immune dynamics reveal high household transmission of ancestral SARS-CoV-2 strain. *Pediatr Allergy Immunol.* 2022;33(7).

67. Drain PK. Rapid Diagnostic Testing for SARS-CoV-2. *N Engl J Med.* 2022;386(3):264-272.

68. Connor BA, Rogova M, Garcia J, et al. Comparative Effectiveness of Single vs Repeated Rapid SARS-CoV-2 Antigen Testing Among Asymptomatic Individuals in a Workplace Setting. *JAMA Netw Open.* 2022;5(3):e223073.

69. Batteux E, Bonfield S, Jones LF, et al. Impact of residual risk messaging to reduce false reassurance following test-negative results from asymptomatic coronavirus (SARS-CoV-2) testing: an online experimental study of a hypothetical test. *BMJ open.* 2022;12(3):e056533.

Supplemental Information

Supplemental Table 8-S1. Participant Demographics by (A) Study Phase and (B) Infecting SARS-CoV-2 Variant Demographics, vaccination status, and index case testing type of the 85-household cohort divided by (**A**) study phase and (**B**) infecting viral variant.

	(A) Study Phase				(B) Viral Variant			
	Phase I		Phase II		Omicron		Ancestral Variants	
	N= 155		N= 215		N= 163		N= 207	
Self-Reported Gender Identity*	**n**	**(%)**	**n**	**(%)**	**n**	**(%)**	**n**	**(%)**
Man	70	45.2	104	48.4	78	47.9	96	46.4
Woman	85	54.8	111	51.6	85	52.1	111	53.6
Third Gender	0	0.0	0	0.0	0	0.0	0	0.0
Age Category	**n**	**(%)**	**n**	**(%)**	**n**	**(%)**	**n**	**(%)**
<10	29	18.7	28	13.0	20	12.3	37	17.9
10 to 60	115	74.2	173	80.5	129	79.1	159	76.8
>60	11	7.1	14	6.5	14	8.6	11	5.3
Self-Reported Race/Ethnicity**	**n**	**(%)**	**n**	**(%)**	**n**	**(%)**	**n**	**(%)**
Asian or Pacific Islander	11	7.1	36	16.7	31	19.0	16	7.7
Biracial	8	5.2	8	3.7	6	3.7	10	4.8
Black/African American	9	5.8	7	3.3	7	4.3	9	4.3
Native American/Alaska	0	0.0	12	5.6	8	4.9	4	1.9
Unknown	61	39.4	66	30.7	44	27.0	83	40.1
White, Hispanic	38	24.5	30	14.0	22	13.5	46	22.2
White, Non-Hispanic	28	18.1	56	26.0	45	27.6	39	18.8
Vaccination Status***	**n**	**(%)**	**n**	**(%)**	**n**	**(%)**	**n**	**(%)**
Unvaccinated	133	85.8	15	7.0	4	2.5	144	69.6
Partial	3	1.9	2	0.9	2	1.2	3	1.4
Complete	1	0.6	77	35.8	52	31.9	26	12.6
Boosted	0	0.0	79	36.7	71	43.6	8	3.9
Unknown	18	11.6	42	19.5	34	20.9	26	12.6
Household Size	**n**	**(%)**	**n**	**(%)**	**n**	**(%)**	**n**	**(%)**
<= 4	97	62.6	85	39.5	65	39.9	117	56.5
> 4	58	37.4	130	60.5	98	60.1	90	43.5
Index Case Test Type	**n**	**(%)**	**n**	**(%)**	**n**	**(%)**	**n**	**(%)**
Rapid Nasal	17	11.0	72	33.5	62	38.0	27	13.0
Not Rapid Nasal	134	86.5	111	51.6	73	44.8	172	83.1
Unknown	4	2.6	32	14.9	28	17.2	8	3.9

**Both sex assigned at birth and current gender identity were self-reported by participants. One participant reported male assignment at birth and current gender identity of woman. Reported gender is listed.*

***63 individuals currently listed as "Unknown" did not select a race category but wrote-in "Latino"/"Latina"/"Latinx."*

****Participants reported date and manufacturer of each vaccine dose received; vaccination status was defined only by doses received at least seven days prior to enrollment in the study. Unvaccinated was defined as having received no COVID-19 vaccine doses. Partial vaccination was defined as receiving one dose of a multiple-dose series (e.g., Pfizer-BioNTech, Moderna). Complete vaccination was defined as receiving all doses of an initial COVID-19 vaccine series. Boosted was defined as the participant receiving any dose beyond an initial COVID-19 vaccine series.*

Supplemental Table 8-S2. Univariable Model. Simple Odds Ratios (OR) for covariables included in the models in Figure 8-2.

	Univariable Model					
Exposure	**SAR (%)**	**95% CI (%)**	**Pairwise Comparison Test**	**OR**	**95% CI**	**Wald Test**
Age Category						
<10	41.4	23.5-59.3		1.22	0.55-2.70	P=0.63
10 to 60	36.7	29.8-43.6		1.00	*(Reference)*	
>60	7.1	0.0-20.6	NA	0.13	0.02-1.04	P=0.05
Race/Ethnicity						
Asian/PI	30.3	14.6-46.0		0.91	0.37-2.25	P=0.84
Biracial	33.3	6.66-60.0		1.05	0.28-3.87	P=0.94
Black	21.4	0.0-42.9		0.57	0.14-2.27	P=0.43
Native American	12.5	0.0-35.4		0.30	0.03-2.59	P=0.27
Unknown	43.4	30.1-56.7		1.61	0.76-3.41	P=0.22
White Hispanic	43.5	29.2-57.8		1.61	0.74-3.52	P=0.23
White Non-Hispanic	32.3	20.9-43.7	NA	1.00	*(Reference)*	
Viral Variant						
Ancestral	34.6	26.4-42.8		1.00	*(Reference)*	
Omicron	36.6	27.2-46.0	P=0.75	1.09	0.63-1.88	P=0.75
Vaccination Status						
Not Vaccinated	38.5	29.1-47.8		1.00	*(Reference)*	
Vaccinated*	33.1	24.9-41.3	P=0.40	0.79	0.46-1.36	P=0.40
Household Density						
≤4	24.1	16.2-32.0		1.00	*(Reference)*	
>4	46.2	37.3-55.2	**P<0.001**	2.71	1.54-4.75	**P=0.001**
Infection Control Practice**						
Not sharing food	39.0	29.4-48.6	P=0.53	1.19	0.69-2.05	P=0.53
Not eating meals together	30.8	23.2-38.3	**P=0.01**	0.49	0.28-0.86	**P=0.01**
Not sharing a bedroom	30.2	23.4-37.1	**P<0.001**	0.30	0.16-0.58	**P<0.001**
Not sharing a bathroom	26.8	18.0-35.6	**P=0.005**	0.46	0.26-0.81	**P=0.007**
Not share personal items	33.8	25.9-41.7	P=0.24	0.72	0.41-1.25	P=0.24
Avoid contact with clothes	34.5	26.7-42.2	P=0.34	0.76	0.43-1.33	P=0.33
Social distancing	31.2	23.1-39.3	P=0.05	0.58	0.33-1.01	P=0.05
Mask use	32.3	24.4-40.3	P=0.10	0.62	0.36-1.09	P=0.10
Index Case Diagnostic Test						
Rapid Nasal Test	50.9	37.9-63.9		2.61	1.39-4.91	**P=0.003**
Other Test Type	28.4	21.1-35.6	**P=0.003**	1.00	*(Reference)*	

Supplemental Table 8-S3. Association of Test Type Subcategories with SARS-CoV-2 Transmission Among Household Contacts. Provides data and Odds Ratios (OR) on the association between COVID-19 test type used to identify the household index case and subsequent transmission to household contacts.

	Uninfected		Secondary Case		Multivariable Model					
Exposure	**N**	**(%)**	**N**	**(%)**	**aSAR**	**95% CI**	**aOR**	**95% CI**	**Wald Test**	**Likelihood Ratio Test**
Test Type	**149**		**82**							
Nasal Rapid	28	18.8	31	37.8	48.1	32.6-63.5	1.00	*(Reference)*		
Nasal Not Rapid	37	24.8	7	8.5	16.2	4.59-27.8	0.13	0.03-0.51	**P=0.003**	
Nasopharyngeal Rapid	17	11.4	4	4.9	19.5	0.25-38.7	0.17	0.03-1.06	P=0.06	
Nasopharyngeal Not Rapid	31	20.8	15	18.3	33.1	18.0-48.2	0.43	0.11-1.61	P=0.21	**P=0.05**
Oral Rapid	1	0.7	3	3.7	43.9	0.0-98.4	0.80	0.04-18.01	P=0.89	
Oral Not Rapid	17	11.4	10	12.2	43.4	20.7-66.1	0.78	0.15-3.88	P=0.76	
Unknown	18	12.1	12	14.6	45.9	26.9-64.9	0.89	0.24-3.28	P=0.86	

Supplemental Methods

Participants

Individuals fluent in English or Spanish aged six years and older from households of two or more persons were eligible for participation if at least one household member had tested positive, developed COVID-19-like symptoms,[1] or had a known exposure with a SARS-CoV-2 infected individual within seven days, and at least one other household member had either negative or unknown infection status during screening.

Upon enrollment, participants completed a questionnaire to provide information about demographics (based on the 2019 California Health Interview Survey tool)[2], medical information, and COVID-19 history (e.g., COVID-19-like symptoms[1], positive and negative test results, and COVID-19 vaccination information). For participants enrolled prior to February 22, 2021, vaccination was not asked, but unvaccinated status was inferred based on local vaccine availability.[3] Vaccination status was defined only by doses received at least seven days prior to enrollment. The questionnaire also asked about household size, the age and gender of other household members and their SARS-CoV-2 infection status, as well as current and anticipated infection-control practices (e.g., shared items and spaces, disinfection, distancing, and masking).

Sample collection

In Phase I of the study, participants self-collected either saliva or paired saliva and anterior-nares nasal swabs every morning upon waking and in the evening before bed in Spectrum SDNA 1000 devices.[4] In Phase II, participants self-collected paired saliva, anterior-nares nasal swabs, and oropharyngeal swabs in Zymo Research's SafeCollect devices[5,6] once daily (upon enrollment and thereafter each morning upon waking).

Supplemental References

1. CDC. Symptoms of Coronavirus. 2020:https://www.cdc.gov/coronavirus/2019-ncov/symptoms-testing/symptoms.html.
2. UCLA. California Health Interview Survey: 2019 Adult CAWI Questionnaire 2019.
3. LA County Public Health. Los Angeles County Public Health COVID-19 Vaccine Dashboard. 2022; http://publichealth.lacounty.gov/media/coronavirus/vaccine/vaccine-dashboard.htm.
4. FDA. Emergency use authorization (EUA) review memorandum sdna-1000 saliva collection device. 2021; https://www.fda.gov/media/142907/download.
5. Zymo Research. SafeCollect Saliva Collection Kit User Instruction Manual. 2021; https://files.zymoresearch.com/protocols/r1211e-dna_rna_shield_safecollect_saliva_collection_kit_user_instructions.pdf.
6. Zymo Research. SafeCollect Swab Collection Kit User Instruction Manual. 2021; https://files.zymoresearch.com/protocols/r1160_r1161-dna_rna_shield_safecollect_swab_collection_kit_user_Instructions.pdf.

Author Contributions

Listed alphabetically by surname

Saharai Caldera (SC)- Study coordinator; recruited, enrolled and maintained study participants with NS, JAR, HD and NWS; study-data quality control; validated data provided by participants in study instruments.

Hannah Davich (HD)- Lead study coordinator; recruited, enrolled and maintained study participants with NS, JAR, SC and NWS; developed recruitment strategies and did outreach with NS; study-data quality control; validated data provided by participants in study instruments; Compiled data from screening with NS for use in Figure 1B. Compiled data for household size and density metrics.

Matthew Feaster (MF)- Co-investigator; contributed to overall study design and recruitment strategies; provided guidance and expertise on SARS-CoV-2 epidemiology and local trends. Contributed to design of biostatistical analysis, particularly conceptualization of causal model represented in Figure 1C and parameterization/coding of covariables. Technical guidance on analysis method and interpretation. Reviewed manuscript. AC

Ying-Ying Goh (YYG)- Co-investigator; contributed to overall study design and recruitment strategies; provided guidance and expertise on SARS-CoV-2 epidemiology and local trends.

Rustem F. Ismagilov (RFI)- Principal investigator; provided leadership, technical guidance, oversight of all analyses, and was responsible for obtaining the primary funding for the study.

Jenny Ji (JJ)- Conceptualization of study with AVW and RFI. Performed extensive literature search on household transmission and co-wrote enrollment questionnaire with AW and NS. Data curation. Performed preliminary analyses. Coded and cleaned data from participant questionnaires. Validated underlying data. Parameterization of participant data for analysis. Assigned index case with AVW, NS, and NWS. Performed analyses in STATA. Prepared Figure 1, 2 and 3 with AVW. Prepared Table 1 with AVW. Study-specific literature review with AVW. Outlined manuscript with AVW. Revised manuscript with AVW.

Jessica A. Reyes (JAR)- Lead study coordinator; recruited, enrolled and maintained study participants with NS, HD, SC, and NWS; study-data quality control; validated data provided by participants in study instruments.

Natasha Shelby (NS)- Study administrator; contributed to initial study design and recruitment strategies; co-wrote enrollment questionnaire with AW and JJ; hired, trained, and supervised the study-coordinator team; recruited, enrolled and maintained study participants with JAR, JAR, NWS, HD and SC; study-data quality control; validated data provided by participants in study instruments; data curation; organized archiving of participant data; helped assemble CONSORT diagram (Figure 1B); assisted with assignment of household index cases with JJ, AVW, and NWS; managed reference library; reviewed and edited the manuscript.

Noah W. Schlenker (NWS)- Study coordinator; recruited, enrolled and maintained study participants with NS, JAR, HD and SC; study-data quality control; validated data provided by participants in study instruments; major role in assignment of household index cases with JJ, AVW, and NS.

Colten Tognazzini (CT)- Coordinated the recruitment efforts at PPHD with case investigators and contact tracers; provided guidance and expertise on SARS-CoV-2 epidemiology and local trends.

Alexander Viloria Winnett (AVW)- Conceptualization of study with JJ and RFI. Contributed to overall study design and recruitment strategies. Co-wrote enrollment questionnaire with NS and JJ; Data curation and analysis. Assigned vaccination status for each participant. Assigned infection status from viral load data. Assigned index case with JJ, NS, and NWS. Prepared Figure 1, 2 and 3 with JJ. Prepared Table 1 with JJ. Verified underlying data and analyses performed by JJ. Study-specific literature review with JJ. Outlined manuscript with JJ. Drafted initial manuscript. Revised manuscript with JJ.

Chapter 9

VALIDATING COMBINATION THROAT-NASAL SWAB SPECIMENS FOR CORONAVIRUS DISEASE 2019 TESTS WOULD IMPROVE EARLY DETECTION, ESPECIALLY FOR THE MOST VULNERABLE

This chapter was originally published in Viloria Winnett A, Stenzel T, Ismagilov RF. Validating Combination Throat-Nasal Swab Specimens for Coronavirus Disease 2019 Tests Would Improve Early Detection, Especially for the Most Vulnerable (July 2024). Clinical Infectious Diseases. https://doi.org/10.1093/cid/ciae381.

Abstract

Early detection of severe acute respiratory syndrome coronavirus 2 infection by diagnostic tests can prompt actions to reduce transmission and improve treatment efficacy, especially for vulnerable groups such as immunocompromised individuals. Recent evidence suggests that sampling the throat in addition to the nose improves clinical sensitivity during early infection for both antigen and molecular coronavirus disease 2019 tests. We urge test manufacturers to validate tests for use with throat swab, in combination with nasal swabs.

Main Text

Individuals with immunocompromise and other vulnerable groups at high risk for severe disease continue to rely heavily on COVID-19 testing. This reliance often includes screening contacts prior to in-person interactions, to prevent the risk of exposure to individuals with presymptomatic or asymptomatic infections. Even in the absence of symptoms or known exposure, individuals with immunocompromise may also test themselves regularly to identify early infection and quickly initiate treatment. For this population—approximately seven million people in the U.S. with primary immunodeficiencies or immunosuppressive treatment for cancer, transplants, or autoimmune disorders[1]—tests that detect early infection with high sensitivity are essential.

Among COVID-19 tests, the low cost, direct-to-consumer sale, and rapid results of at-home antigen rapid diagnostic tests (Ag-RDTs) make them an attractive and increasingly used diagnostic modality both for high-risk individuals and the general population.[2,3] While the United States Food and Drug Administration (FDA) has long been open to throat swab specimens for COVID-19 testing, all at-home Ag-RDTs are currently only authorized for use with self-collected nasal swabs.[4] However, nasal-swab Ag-RDTs have been demonstrated to have low to moderate (~50–80%) clinical sensitivity to detect infected individuals, especially when those individuals are asymptomatic and/or in the early stage of infection,[5] when transmission of SARS-CoV-2 often occurs.[6]

Several cross-sectional studies have demonstrated that Ag-RDTs exhibit higher clinical sensitivity when a combination of nasal (anterior nares) and throat (posterior oropharynx plus palatine tonsils) swabbing is used, compared with nasal-swab-only (**Figure 9-1A**). A small study in Nova Scotia evaluated the use of combined nasal and throat swabbing for two separate Ag-RDTs (Panbio COVID-19 Ag Rapid Test Device, BTNX Rapid Response COVID-19 Antigen Rapid Test) among asymptomatic individuals.[7]

Among 62 and 40 infected individuals respectively, a 24% (Panbio) and 18% (BTNX) improvement in clinical sensitivity was observed by combining nasal-swab and throat-swab Ag-RDT results over nasal-swab-only Ag-RDT results. This study also demonstrated a 13% increase in clinical sensitivity by testing a single combined throat-nasal swab compared with nasal swab alone among 38 infected individuals. A separate, large study of 827 infected individuals in Copenhagen recently demonstrated that combined nasal-swab and throat-swab Ag-RDT results improved clinical sensitivity by upwards of 16% over nasal-swab Ag-RDT results alone.[8]

Longitudinal viral load data suggests that infection stage influences the magnitude of the benefit of combined throat-nasal swab Ag-RDT compared with nasal-swab-only Ag-RDT. Daily viral loads quantified from prospectively collected nasal and throat swabs by individuals with incident SARS-CoV-2 infection revealed that virus often presents in the throat days before the nose.[9] A simplified representation based on available data[9,10] for the typical presentation of viral loads in the throat and the nose during early infection illustrates how the benefit of adding throat swabs to nasal swab Ag-RDTs is expected to be greatest during the first few days of infection (**Figure 9-1B**). Indeed, based on quantitative viral-load measurements in the throat and nose during the first four days of incident infection, we predicted[5] that a combined throat-nasal swab Ag-RDT would have approximately 25% greater clinical sensitivity than a nasal-swab-only Ag-RDT (**Figure 9-1C**). This prediction was similar to the benefits observed in the later studies performed in Nova Scotia[7] and Copenhagen.[8] Additionally, supplemental data from Copenhagen shows that the benefit of combined throat-nasal swab Ag-RDT results over nasal-swab-only Ag-RDT decreased with time from symptom onset among individuals for whom healthcare workers collected specimens, from 32% on the first day of symptoms to 13% thereafter.[8]

The benefit of combined throat-nasal sampling extends to molecular COVID-19 tests as well. Among 14 individuals with naturally acquired incident SARS-CoV-2 infection, 10 (71%) had viral loads above 1000 copies/mL in throat swabs for at least a day before viral loads in the nose rose to over 1000 copies/mL.[9] For many individuals, the delay was longer: over a third of participants (five of 14) had virus in the throat at least three days before the nose, and up to seven days for one individual.[9] In a separate study of individuals who underwent intranasal inoculation with SARS-CoV-2, 10 of 18 (55%) participants with sustained infection had detectable virus in the throat for at least one day before virus was detectable in the nose by PCR.[10] Notably, replication-competent (infectious) virus was successfully cultured from throat

swabs prior to nasal swabs in 12 of these 18 individuals (67%). These data suggest if nasal swabs alone are used, even molecular COVID-19 tests with high analytical sensitivity (low limits of detection down to 1000 copies/mL) could yield false negative results for individuals who may be capable of transmitting SARS-CoV-2.[11] Analyses of paired viral load dynamics from the cohort with naturally acquired infection suggested that using combined throat-nasal swabs rather than a nasal-swab-only swab with a high analytical sensitivity molecular COVID-19 tests would result improve clinical sensitivity by over 40% during the first days of SARS-CoV-2 infection.[9] However, because a subset of individuals may present with rising viral loads in the nose before the throat, combination throat-nasal swab tests are likely to yield higher clinical sensitivity than throat swabs alone. Indeed, the current Infectious Diseases Society of America Guidelines on the Diagnosis of COVID-19[12] recommend against the use of throat swabs alone for both molecular diagnostic tests[13] and Ag-RDTs.[14]

Cross-sectional analyses of participant populations later in infection (after the first few days) are unlikely to observe the benefit of combining throat-nasal swabbing on Ag-RDT clinical sensitivity. For example, reanalyzing viral loads between days 0 and 12 of infection from our study[5] cross-sectionally predicted only a marginal benefit (6%) for combined throat-nasal swab Ag-RDT over the observed clinical sensitivity of a nasal-swab-only Ag-RDT (43%). This small, predicted benefit is similar to that observed in a later cross-sectional study of 96 infected individuals in San Francisco.[15] In that study, a combined throat-nasal swab Ag-RDT increased clinical sensitivity from 54% (nasal-swab only Ag-RDT) to 59%.[15] We note that the high PCR-positivity rate (83%) among the 115 participants screened may suggest a study population skewed towards later infection. The clinical sensitivity of a combined throat-nasal swab Ag-RDT may also be influenced by throat swab specimen collection technique,[16] or if a test designed for use with nasal swabs exhibits lower analytical sensitivity when used with throat swabs.[12,17]

Maximizing the clinical sensitivity of COVID-19 tests—both Ag-RDTs and molecular diagnostic tests—for early detection is paramount, particularly given surges in emerging variants with potential for evasion of humoral immunity.[18] To improve performance, Ag-RDTs and molecular COVID-19 tests need to be analytically and clinically validated by manufacturers for use with combination throat-nasal swab specimens, including clinical-validation studies on (at least) symptomatic patient specimens. This combination throat-nasal swab test could use a single swab sampling both the throat and the nose, or (to address consumer hesitancy) separately collected swabs from the nose and throat which could be placed

into the same elution media. Based on past FDA flexibilities offered for the validation of COVID-19 tests for Emergency Use Authorizations (EUAs) (**Supplemental Table 9-S1**), the FDA is likely to accept non-inferiority studies, perhaps even only on symptomatic patients (historically ~30 positives and 30 negatives required for the EUA). For clearance, the FDA may accept evaluation of the combined throat-nasal swab against a standard single swab, and showing in at least symptomatic patients that the combination swab is not inferior (has equivalent or better sensitivity) on the requisite number of positive patients, usually 120 positive patients and 500 negative patients for an over-the-counter test. The best way for developers to determine what the FDA expects is through the Q-Submission process,[19] which is a no-charge FDA submission. The developers can ask their questions of the FDA and receive a response within 70 calendar days.[19] Although it may not be required for test validations, it would be particularly useful for studies to include populations for whom early detection is most impactful, such as the immunocompromised and those residing in congregate settings (e.g., skilled nursing facilities, dormitories). These populations would demonstrate just how useful combination throat-nasal swabs are for populations at high risk of transmission or severe disease. We also suggest studies to investigate whether the use of combined throat-nasal swabs provide similar benefit for diagnostic testing of other upper respiratory viral infections, such as influenza and respiratory syncytial virus.

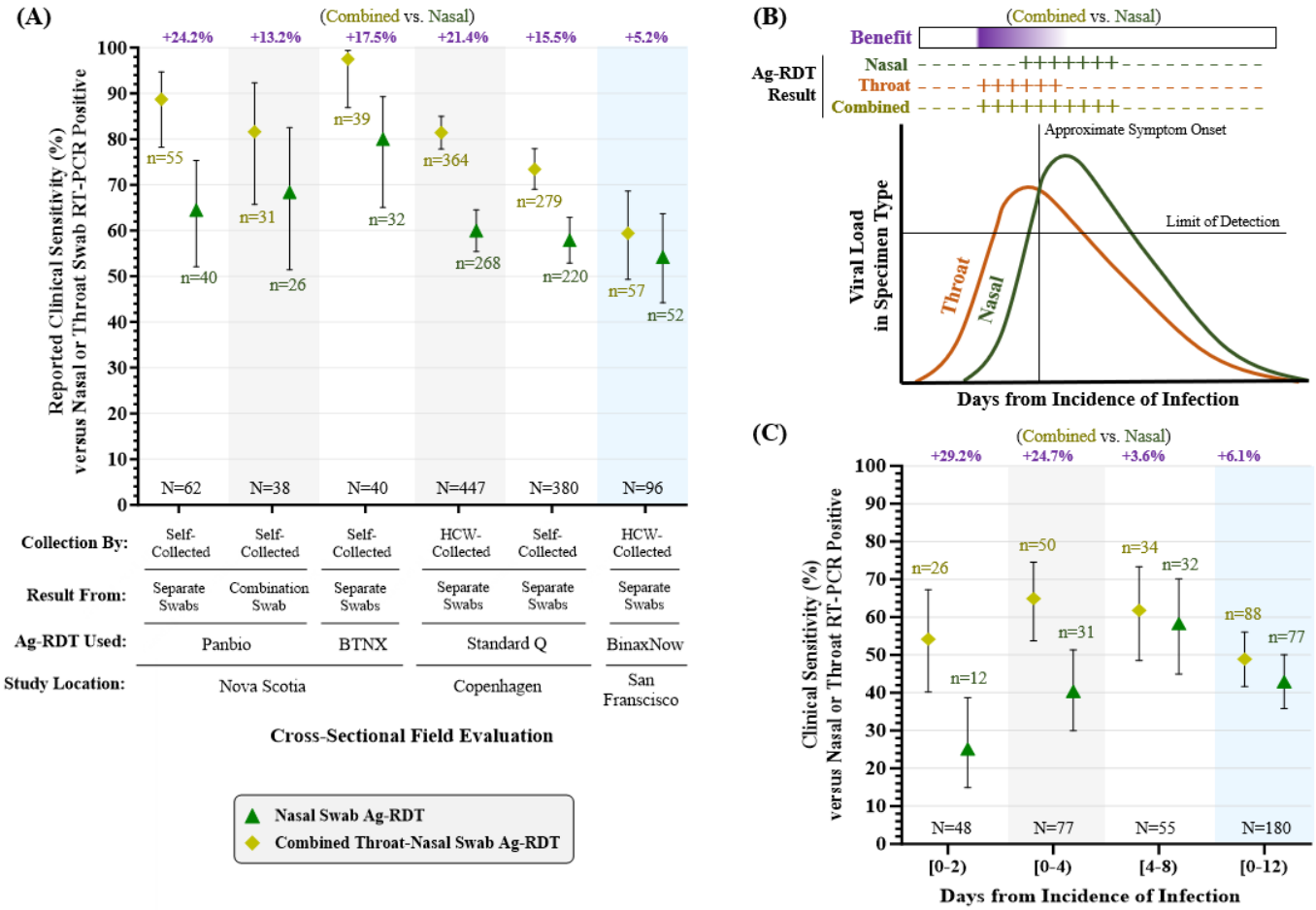

Figure 9-1. (A) Summary of studies reporting the clinical sensitivity of combined throat-nasal swab antigen rapid diagnostic tests (Ag-RDTs) compared with nasal-swab-only Ag-RDTs. The difference between clinical sensitivity of combined throat-nasal swab Ag-RDT results over nasal-swab-only Ag-RDT results alone is shown in purple. Data are reproduced from cross-sectional field evaluations in Nova Scotia,[7] Copenhagen,[8] and San Francisco.[15] These field evaluations had slight differences in design, which we highlight: "HCW-collected" refers to nasal and throat swabs specimen collection performed by a by a healthcare worker, whereas "Self-collected" refers to collection by the study participant. "Separate Swabs" refers to designs where test results represent the composite outcome of testing a nasal swab and a throat swab, separately, whereas "Combination Swab" refers to designs where the test result was determined by directly testing a single swab that had sampled both the nose and throat. **(B)** Conceptual schematic depicting the typical presentation of longitudinal SARS-CoV-2 viral loads in nasal and throat swab specimens from the incidence of infection, based on data from a study of individuals with naturally acquired infection in Los Angeles[9] and individuals inoculated with SARS-CoV-2 in London.[10] The hypothetical nasal, throat, and combined throat-nasal swab Ag-RDT results are expected based on this typical presentation of viral loads, to illustrate why the increased clinical sensitivity of a combined throat-nasal swab Ag-RDT over a nasal-swab-only Ag-RDT would be greatest during early in infection and wane during later infection. The horizontal line indicates the limit of detection for Ag-RDTs. **(C)** Clinical sensitivity of combined throat-nasal swab Ag-RDT (inferred from viral loads) and nasal-swab Ag-RDT results (participant reported) during different periods of infection, based on data from a nasal-swab Ag-RDT field evaluation with paired viral load quantification in Los Angeles.[5] Blue shading in panels A and C highlight how cross-sectional evaluations that include timepoints late in the infection may underestimate the benefit of a combined throat-nasal swab Ag-RDT over nasal-swab-only Ag-RDT.

Funding: This work was supported by the Bill & Melinda Gates Foundation (INV-023124) and the Ronald and Maxine Linde Center for New Initiatives at the California Institute of Technology.

Conflicts of Interest: The authors declare no conflicts of interest.

References

1. Harpaz R, Dahl RM, Dooling KL. Prevalence of Immunosuppression Among US Adults, 2013. *JAMA.* 2016;316(23):2547-2548.

2. Ji J, Viloria Winnett A, Shelby N, et al. Index cases first identified by nasal-swab rapid COVID-19 tests had more transmission to household contacts than cases identified by other test types. *PLOS ONE.* 2023;18(10):e0292389.

3. Drain PK. Rapid Diagnostic Testing for SARS-CoV-2. *New England Journal of Medicine.* 2022;386(3):264-272.

4. FDA. In Vitro Diagnostics EUAs - Antigen Diagnostic Tests for SARS-CoV-2. 2024; https://www.fda.gov/medical-devices/covid-19-emergency-use-authorizations-medical-devices/in-vitro-diagnostics-euas-antigen-diagnostic-tests-sars-cov-2.

5. Viloria Winnett A, Akana R, Shelby N, et al. Daily SARS-CoV-2 Nasal Antigen Tests Miss Infected and Presumably Infectious People Due to Viral Load Differences among Specimen Types. *Microbiology spectrum.* 2023;11(4):e0129523.

6. Wu P, Liu F, Chang Z, et al. Assessing Asymptomatic, Presymptomatic, and Symptomatic Transmission Risk of Severe Acute Respiratory Syndrome Coronavirus 2. *Clinical Infectious Diseases.* 2021;73(6):e1314-e1320.

7. Goodall BL, LeBlanc JJ, Hatchette TF, Barrett L, Patriquin G. Investigating the Sensitivity of Nasal or Throat Swabs: Combination of Both Swabs Increases the Sensitivity of SARS-CoV-2 Rapid Antigen Tests. *Microbiology spectrum.* 2022;10(4):e0021722.

8. Todsen T, Jakobsen KK, Grønlund MP, et al. COVID-19 Rapid Antigen Tests With Self-Collected vs Health Care Worker–Collected Nasal and Throat Swab Specimens: A Randomized Clinical Trial. *JAMA Network Open.* 2023;6(12):e2344295-e2344295.

9. Viloria Winnett A, Akana R, Shelby N, et al. Extreme differences in SARS-CoV-2 viral loads among respiratory specimen types during presumed pre-infectious and infectious periods. *PNAS nexus.* 2023;2(3):pgad033.

10. Killingley B, Mann AJ, Kalinova M, et al. Safety, tolerability and viral kinetics during SARS-CoV-2 human challenge in young adults. *Nature medicine.* 2022;28(5):1031-1041.

11. Porter MK, Viloria Winnett A, Hao L, et al. The ratio between SARS-CoV-2 RNA viral load and culturable viral titer differs depending on stage of infection. *Access Microbiology.* 2023.

12. Hanson KE, Caliendo AM, Arias CA, et al. Infectious Diseases Society of America Guidelines on the Diagnosis of COVID-19 (June 2020). *Clinical Infectious Diseases.* 2024;78(7):e106-e132.

13. Hanson KE, Caliendo AM, Arias CA, et al. The Infectious Diseases Society of America Guidelines on the Diagnosis of COVID-19: Molecular Diagnostic Testing (January 2021). *Clinical Infectious Diseases.* 2024;78(7):e170-e207.

14. Hanson KE, Altayar O, Caliendo AM, et al. The Infectious Diseases Society of America Guidelines on the Diagnosis of COVID-19: Antigen Testing (June 2021). *Clinical Infectious Diseases.* 2024;78(7):e208-e229.

15. Schrom J, Marquez C, Pilarowski G, et al. Comparison of SARS-CoV-2 Reverse Transcriptase Polymerase Chain Reaction and BinaxNOW Rapid Antigen Tests at a Community Site During an Omicron Surge : A Cross-Sectional Study. *Annals of internal medicine.* 2022;175(5):682-690.

16. Todsen T, Bohr A, Hovgaard LH, et al. Valid and Reliable Assessment of Upper Respiratory Tract Specimen Collection Skills during the COVID-19 Pandemic. *Diagnostics (Basel, Switzerland).* 2021;11(11).

17. Cubas-Atienzar AI, Kontogianni K, Edwards T, et al. Limit of detection in different matrices of 19 commercially available rapid antigen tests for the detection of SARS-CoV-2. *Scientific Reports.* 2021;11(1):18313.

18. Willett BJ, Grove J, MacLean OA, et al. SARS-CoV-2 Omicron is an immune escape variant with an altered cell entry pathway. *Nature Microbiology.* 2022;7(8):1161-1179.

19. FDA. The Q Submission Program: Final Guidance, June 2023. 2023; https://www.fda.gov/regulatory-information/search-fda-guidance-documents/requests-feedback-and-meetings-medical-device-submissions-q-submission-program.

Supplementary Information

Supplemental Table 9-S1. Demonstration of flexibilities exhibited by the U.S. Food and Drug Administration (FDA) in the emergency use authorization (EUA) of COVID-19 tests.

	Title	Description of flexibility	Reference
1	Authority for Emergency Use Authorization (EUA)	Under law, the EUA authorities allow a lower bar for test development and validation. The FDA made full use of this flexibility during the COVID-19 pandemic, as well as in other emergencies.	https://www.fda.gov/regulatory-information/search-fda-guidance-documents/emergency-use-authorization-medical-products-and-related-authorities
2	Validation specimen type	With few patient specimens available early in the COVID-19 pandemic, contrived positive specimens were used for clinical evaluation.	https://www.fda.gov/media/136112/download?attachment (See *Clinical evaluation*)
3	Scaling of manufacturing	To accommodate emergency response needs in the production of COVID-19 EUA tests, the FDA is permitted to waive otherwise-applicable current good manufacturing practice (CGMP) requirements (e.g., storage or handling).	https://www.fda.gov/regulatory-information/search-fda-guidance-documents/emergency-use-authorization-medical-products-and-related-authorities (See Section IV.C)
4	Specimen Pooling	To increase capacity, pooling of specimens for testing by a previously authorized test was allowed without FDA review of pooled specimen performance, if single specimen validation data supported compatibility.	https://www.fda.gov/medical-devices/covid-19-emergency-use-authorizations-medical-devices/in-vitro-diagnostics-euas-molecular-diagnostic-tests-sars-cov-2#amendment (See *Pooling and Serial Testing Amendment for Certain Molecular Diagnostic Tests for SARS-CoV-2*)
5	Extension of test expiration dates	Expiration dates for at-home, over-the-counter (OTC) COVID-19 tests were extended when test manufacturers provided data demonstrating a longer shelf-life than was known when the test was first authorized.	https://www.fda.gov/medical-devices/coronavirus-covid-19-and-medical-devices/home-otc-covid-19-diagnostic-tests (See *Authorized At-Home OTC COVID-19 Diagnostic Tests and Expiration Dates*) https://www.fda.gov/regulatory-information/search-fda-guidance-documents/emergency-use-authorization-medical-products-and-related-authorities#expdate (See Section IV.B)
6	Multi-analyte tests	Multi-analyte (multi-pathogen) tests were authorized under COVID-19 EUA.	https://www.fda.gov/media/176728/download?attachment

7	Performance accounting for study population	Positive Percent Agreement during clinical evaluation was modeled to adjust for the viral load of participants in the study population.	https://www.fda.gov/media/157544/download?attachment (See *Section 2.6*)
8	At-home testing	Simulated home test environments for over-the-counter (OTC) test validation were considered.	https://www.fda.gov/media/157544/download?attachment (See *Section 2.6*)
9	Asymptomatic screening	Screening of asymptomatic patients using tests were allowable for tests that did not initially include asymptomatic claims.	https://www.fda.gov/medical-devices/covid-19-emergency-use-authorizations-medical-devices/in-vitro-diagnostics-euas-antigen-diagnostic-tests-sars-cov-2#SerialTesting (See *Antigen EUA Revisions for Serial (Repeat) Testing*)
10	Serial testing	The FDA exhibited flexibility to allow asymptomatic claims with serial testing.	https://www.fda.gov/medical-devices/covid-19-emergency-use-authorizations-medical-devices/in-vitro-diagnostics-euas (See *Umbrella EUA for SARS-CoV-2 Molecular Diagnostic Tests for Serial Testing* and *Antigen EUA Revisions for Serial (Repeat) Testing*)
11	Performance with serial testing	Cumulative Positive Percent Agreement through serial testing, rather than one-time testing, was considered in the review of test performance for EUA.	https://thehill.com/opinion/healthcare/515628-fda-were-constantly-working-on-covid-testing-options/ https://www.fda.gov/medical-devices/covid-19-emergency-use-authorizations-medical-devices/in-vitro-diagnostics-euas-antigen-diagnostic-tests-sars-cov-2#SerialTesting

Chapter 10

INTERFERON STIMULATION IS SYNCHRONIZED ACROSS MULTIPLE UPPER RESPIRATORY MUCOSAL SURFACES DURING EARLY SARS-COV-2 INFECTION

Introduction

Interferons play a key role in the human immune response to viral pathogens. Following their initial discovery in 1957,[1] interferons have been classified into three groups: Type I interferons (including IFN-α, IFN-β, IFN-ε, IFN-κ, and IFN-ω), Type II interferon (IFN-γ)[2], and Type III interferons (IFN-λ1, IFN-λ2, IFN-λ3, IFN-λ4).[3] Interferons bind to cell surface receptors, activating the JAK-STAT signaling pathway, which leads to the transcriptional activation of interferon-stimulated genes (ISGs).[4] ISGs coordinate various functions to directly and indirectly restrict viral infection, influencing both individual cells and cell populations.[5] For example, IFNs enhance the expression of MHC molecules for antigen presentation, induce the expression of interferon-induced proteins with tetratricopeptide repeats (IFITs) that bind viral mRNAs to block their translation, and activate macrophages to increase Fc and complement receptors, thereby enhancing phagocytosis of viral particles. IFNs also stimulate the production of chemokines to recruit leukocytes to the site of infection.

Recognition of viral components by cellular sensing mechanisms initiates the production of interferons. Pattern recognition receptors (PRRs) such as Toll-like receptors (TLRs), retinoic acid-inducible gene I (RIG-I)-like receptors (RLRs), cyclic GMP-AMP synthase (cGAS), and IFI16, as well as NOD-like receptors (NLRs), recognize viral pathogen-associated molecular patterns (PAMPs). TLRs detect viral nucleic acids on the cell surface or in endosomes, while RLRs, cGAS and IFI16 sense viral nucleic acids in the cytosol. Recognition prompts engagement with adaptor proteins, such as mitochondrial antiviral signaling protein (MAVS) for RLRs, TIR-domain-containing adapter-inducing interferon-beta (TRIF) and myeloid differentiation primary response 88 (MyD88) for TLRs, and stimulator of interferon genes (STING) for cGAS/IFI16. Engagement of these adaptor proteins activate transcription factors such as IRF3, IRF7, and NF-κB, leading to the production of interferons.

The human upper respiratory mucosa uses interferon signaling to initiate and amplify a protective antiviral response, though the spatial dynamics of this process in vivo have not been thoroughly studied. It is well established that cells

within the mucosa will produce interferons that stimulate the production of ISGs in both an autocrine manner, and a paracrine manner among neighboring cells.[6,7] This paracrine signaling induces a local antiviral state, which decreases the susceptibility of surrounding cells to infection.[8,9] Current models for this paracrine interferon function suggest that interferon signaling is localized,[10,11] forming a declining gradient with distance from the infected cell.[12] This localization has been metaphorically described as "ring vaccination" and "contact tracing," public health strategies that focus resources on infected individuals and their immediate contacts.[13] However, the length scale of this feed-forward interferon signaling in response to viral infection of the upper respiratory mucosa has not been explored.

The length scale of the early interferon response in the upper respiratory mucosa is a key component of mucosal immunity, with important implications for the design and delivery of mucosal vaccines. Mucosal vaccines are intended to immunize the mucosal sites of primary infection to induce sterilizing immunity that effectively blocks infection.[14] In contrast to systemic vaccines, where neutralizing antibody titers in the blood serve as correlates of protection, the correlates for evaluating mucosal vaccine candidates remain uncertain.[15] Moreover, since respiratory viruses can infect various anatomical areas of the respiratory mucosa, the clinically meaningful markers of a protective response may vary between these sites. Since interferon stimulation is a well-studied mechanism that is known to restrict viral proliferation and has been implicated in SARS-CoV-2 disease severity,[16] it may serve as a meaningful correlate of protection for mucosal vaccine responses. However, for the interferon response to be useful in the evaluation of mucosal vaccine candidates, we must first understand the localization of this interferon response. However, as Maurice et al. comment, while "studying acute localized infections is easily accomplished in the mouse model system, studying a defined localized primary infection is much more challenging in human cohorts".[17]

In previous chapters of this thesis, I have shown that SARS-CoV-2 can exhibit extreme differences in viral load dynamics among different upper respiratory anatomical sites, particularly during early infection when the interferon response is typically initiated. Given that viral components stimulate interferon production and that current models describe paracrine interferon signaling to nearby cells, **I hypothesized that early interferon stimulation is restricted to upper respiratory sites with detectable viral proliferation and absent from sites without detectable SARS-CoV-2 RNA.** To test this hypothesis, we developed a method to sequence human mRNA molecules from paired upper respiratory specimens collected daily or twice-daily by individuals who initially tested negative for SARS-CoV-2 RNA when they began collecting specimens, but later exhibited sustained infection. Additionally, human mRNA was sequenced from longitudinal specimens collected by individuals who did not

exhibit evidence of SARS-CoV-2. Human mRNA sequences from each specimen were then processed to quantify gene expression. Gene expression data from different specimen types collected throughout acute SARS-CoV-2 infection were combined with quantitative viral load measurements. This approach assessed whether the interferon response is localized to anatomical sites of active viral proliferation.

Materials and Methods

Participant Cohort and Specimen Collection

Among 370 participants enrolled in the Caltech COVID-19 Study (see prior **Chapter VIII**), 16 who collected paired specimen types were identified as having Sustained Incident Infection (SII). Infection was defined as sustained if the participant had at least two timepoints in one specimen type with viral loads above 10,000 copies/mL. Infection was defined as incident if the participant had either undetectable or very low (below 1000 copies/mL) viral loads in all specimen types for at least one timepoint preceding sustained infection. Seven participants from Phase I and nine participants from Phase II met SII criteria (**Table 10-1**). Participants in Phase I collected saliva and nasal swabs twice per day (in the morning immediately upon waking, and in the evening prior to performing dental hygiene at bedtime), while participants in Phase II collected saliva, nasal swabs, and throat swabs daily (in the morning immediately upon waking). All specimens were collected in guanidinium thiocyanate RNA-preservation buffer (Spectrum SDNA 1000 in Phase I [Spectrum Inc], and DNA/RNA Shield in Phase II [Zymo Research Corp.]). A cohort of 16 participants without sustained infection was identified based on matching Study Phase, age, sex, COVID-19 vaccination status, and medical comorbidities to the 16 participants with SII. These individuals were in households where at least one person had sustained infection with SARS-CoV-2 and therefore may have been exposed. This cohort is referred to as Test Negative (TN), to acknowledge the potential for exposure resulting in subclinical, undetected, or abortive infections. For individuals with SII, all specimens with sufficient volume were selected for processing, while for TN individuals, at least five specimens of each type were selected for processing. This yielded a total of 567 saliva, 565 nasal swab, and 236 throat swab specimens to undergo processing. All specimens from individuals in the SII cohort and a subset of specimens from individuals in the TN cohort underwent SARS-CoV-2 viral load quantification (**Figure 10-1**) as described in **Chapters III and IV**.

Specimen Processing for Human mRNA Sequencing

Selected specimens were thawed from -80° C to room temperature, and 300uL of primary specimen volume was aliquoted into designated 96-deep-well plates compatible with automated processing on a KingFisher Flex 96 (ThermoFisher Scientific Cat# 95040450). Each plate contained specimens of a given specimen type (e.g., all nasal swab, or all saliva, or all throat swab) from the same study phase (e.g., all Phase I specimens, or all Phase II specimens). Additionally, each plate contained 300uL of nuclease-free water as a negative control, 300uL volume from a single-stock of HeLa cell culture lysate in DNA/RNA Shield as a positive control, and 300uL volume from a single-stock of saliva in DNA/RNA Shield pooled from 10 unique participants (not within the SII or TN cohorts) as a positive control in a relevant, challenging clinical specimen matrix.

Specimens underwent RNA extraction and purification via the Quick-DNA/RNA HT kit (Zymo Research Corp, Cat R2150) including a DNase digestion on the KingFisher Flex 96. RNA was eluted in a 50uL volume. 2uL of elution volume was used to ensure successful DNA digestion (Qubit™ dsDNA Quantification Assay, Cat Q32851) and 5uL of elution volume underwent RT-qPCR (TaqMan™ Fast Virus 1-Step Master Mix for qPCR, ThermoFisher Scientific Cat# 4444434) for two human mRNA-specific targets in the MYH9 and ACTB genes (ThermoFisher Scientific, Hs01066381_m1 with FAM fluorophore, and ThermoFisher Scientific Hs99999903_m1 with VIC fluorophore). For specimens with Ct values below 35 for both human mRNA targets, 8.5uL of elution volume underwent library preparation (Illumina RNA Prep with Enrichment (L) Tagmentation, Illumina Cat 20040537) with 17 amplification cycles. cDNA libraries concentration were quantified (Qubit™ dsDNA Quantification Assay, Cat Q32853) as well as library fragment size distribution (Agilent Agilent D1000 ScreenTape on Agilent TapeStation 2200, Cat 50675582). Triplex pools for human exome enrichment were created by pooling 200ng of cDNA from each constituent libraries, originating from specimens collected by the same participant when possible. 7.5uL of select cDNA libraries with concentrations incompatible with triplex pooling (ie. <30ng/uL) were underwent singeplex enrichment. Enrichment (Illumina RNA Prep with Enrichment (L) Tagmentation, Illumina Cat 20040537) was performed using the Twist Exome 2.0 Plus panel (Illumina Cat 20077595) with 17 amplification cycles. Human exome enriched libraries were then pooled for 150 base pair, paired end sequencing on a NovaSeq 6000, targeting 40 million reads per sample for saliva specimens, and 25 million reads per sample for nasal swab and throat swab specimens.

Mapping and Gene Expression Quantification

Sequencing reads were mapped to the full human genome primary assembly (GRCh38.p14, Gencode V46) using STAR v2.7.10b with default parameters. Read and mapping quality was assessed using Qualimap v2.2.2, and gene counts were quantified using FeatureCounts v2.0.1. Raw gene counts were normalized using the trimmed mean of m-values with singleton pairing implemented in edgeR v4.2.1.

Statistical Analysis

Interferon Stimulation Module Scores (ISMS) were generated for each sample as described in Yoshida et al. Nature 2021.[18] Briefly, the arithmetic mean log1p transformed expression values for 26 genes (BST2, CMPK2, EIF2AK2, EPSTI1, HERC5, IFI35, IFI44L, IFI6, IFIT3, ISG15, LY6E, MX1, MX2, OAS1, OAS2, PARP9, PLSCR1, SAMD9, SAMD9L, SP110, STAT1, TRIM22, UBE2L6, XAF1, and IRF7) and for a random set of 1,000 control genes was calculated, and the difference between mean expression of these genes in each sample was defined as the module score. ISMS for each specimen could then be plotted over time for each specimen type from each participant to observe changes in interferon stimulation throughout SARS-CoV-2 infection. Spearman correlation coefficients were calculated to assess a monotonic correlation between log10-transformed viral load and interferon stimulation over time within specimens of a given type (e.g., saliva, nasal swab, throat swab) from each participant. Nonparametric distributions of paired observations were compared using Wilcoxon Signed Rank Test, with or without Bonferroni correction. Statistical testing was implemented in Python 3.12.4 using SciPy v1.14.1.

Table 10-1. Cohort of Participants from the Caltech COVID-19 Study for whom specimens underwent human mRNA sequencing. Participants with Participant ID (PID) values that begin with "P" were enrolled in Phase I while those that begin with "Z" were enrolled in Phase II of the study. Participants with Status of "Case" indicate that the participant had Sustained Incident Infection, while the subsequent demographically-matched "Control" was Test Negative (see Methods). COVID Vaccination status was determined by participant self-report, and classified as Complete if they reported receipt of the full series as authorized for a given vaccine ("Moderna" being authorized under the name "Spikevax" and prior investigations under the name "mRNA-1273," "Pfizer" being the Pfizer-BioNTech mRNA COVID-19 vaccine authorized under the name "Comirnaty" and prior investigations under the name "BNT162b2," and "Janssen" being the Johnson & Johnson COVID-19 vaccine authorized under the name "Jcovden" and prior investigations under the name "Ad26.COV2.S"). Saliva, Nasal, and Throat samples refer to the number of specimens of each type for which mRNA sequencing was attempted. Active medications, medical comorbidities ("Comorb"), smoking history ("SmokingHx") and health status were self-reported by participants upon enrollment in the study.

PID	Status	Age	Sex	COVIDVaccination	Saliva Samples	Nasal Samples	Throat Samples	Medications	Comorb	SmokingHx	Health Status
P088	Case	7	Female	None	31	36	NA	Vitamin	None	Never	Excellent
P165	Control	7	Female	None	13	13	NA	Vitamin	None	Never	Very Good
P099	Case	55	Male	None	37	38	NA	Vitamin	None	Prior	Fair
P138	Control	55	Male	None	10	11	NA	Vitamin	None	Never	Very Good
P163	Case	57	Female	None	38	35	NA	Aspirin, Vitamin	None	Never	Very Good
P065	Control	51	Female	None	11	11	NA	Unspecified antihypertensive, vitamin	HTN	Never	Fair
P179	Case	13	Female	None	43	42	NA	Vitamin	None	Never	Good
P123	Control	13	Female	None	10	10	NA	None	None	Never	Excellent
P177	Case	34	Female	Incomplete (T-15d)	36	38	NA	OCP, Vitamin	None	Never	Good
P086	Control	38	Female	None	12	14	NA	Vitamin	None	Never	Very Good
P161	Case	30	Male	None	29	28	NA	None	DBM	Never	Fair
P178	Control	34	Male	None	6	7	NA	Vitamin	None	Prior	Very Good
P083	Case	51	Male	None	27	28	NA	cetaminophen, Fluticasone propionate	Obesity	Prior (curr. vape)	Good
P068	Control	56	Male	None	11	11	NA	Vitamin	None	Never	Very Good
Z187	Case	40	Female	Boosted (3-Moderna)	21	21	21	Vitamin	None	Never	Excellent
Z167	Control	45	Female	Boosted (3-Pfizer)	11	11	10	None	None	Never	Very Good
Z106	Case	33	Male	Boosted (3-Moderna)	27	27	27	None	None	Prior	Very Good
Z197	Control	34	Male	Boosted (3-Moderna)	9	9	9	None	None	Never	Excellent
Z072	Case	45	Male	Boosted (3-Moderna)	21	21	22	None	None	Never	Excellent
Z122	Control	42	Male	Boosted (3-Moderna)	8	8	9	Vitamin	None	Prior	Very Good
Z144	Case	33	Female	Boosted (1-Janssen, 1-Moderna	22	22	22	Vitamin	Anxiety	Never	Good
Z015	Control	36	Female	Boosted (1-Janssen, 1-Pfizer)	6	7	6	None	None	Prior	Good
Z086	Case	7	Male	Incomplete (1-Pfizer, T-16d)	14	14	14	Acetaminophen	None	Never	Excellent
Z014	Control	11	Male	None	8	10	8	None	None	Never	Good
Z196	Case	37	Female	Boosted (3-Pfizer)	18	18	18	Unspecified allergy	None	Never	Fair
Z091	Control	32	Female	Boosted (3-Moderna)	6	6	6	None	None	Never	Fair
Z115	Case	20	Female	Complete (2-Pfizer)	11	11	11	OCP, Vitamin	None	Never	Good
Z002	Control	27	Female	Complete (2-Pfizer)	7	6	6	Acetaminophen, Ibuprofen	None	Never	Good
Z073	Case	8	Male	Complete (2-Pfizer)	28	27	27	None	None	Never	Excellent
Z134	Control	6	Male	Complete (2-Pfizer)	8	8	8	None	None	Never	Excellent
Z114	Case	20	Male	Complete (2-Pfizer)	8	7	8	Unspecified antibiotic ear drops	None	Never	Fair
Z047	Control	27	Male	Complete (2-Pfizer)	5	5	5	None	None	Never	Fair

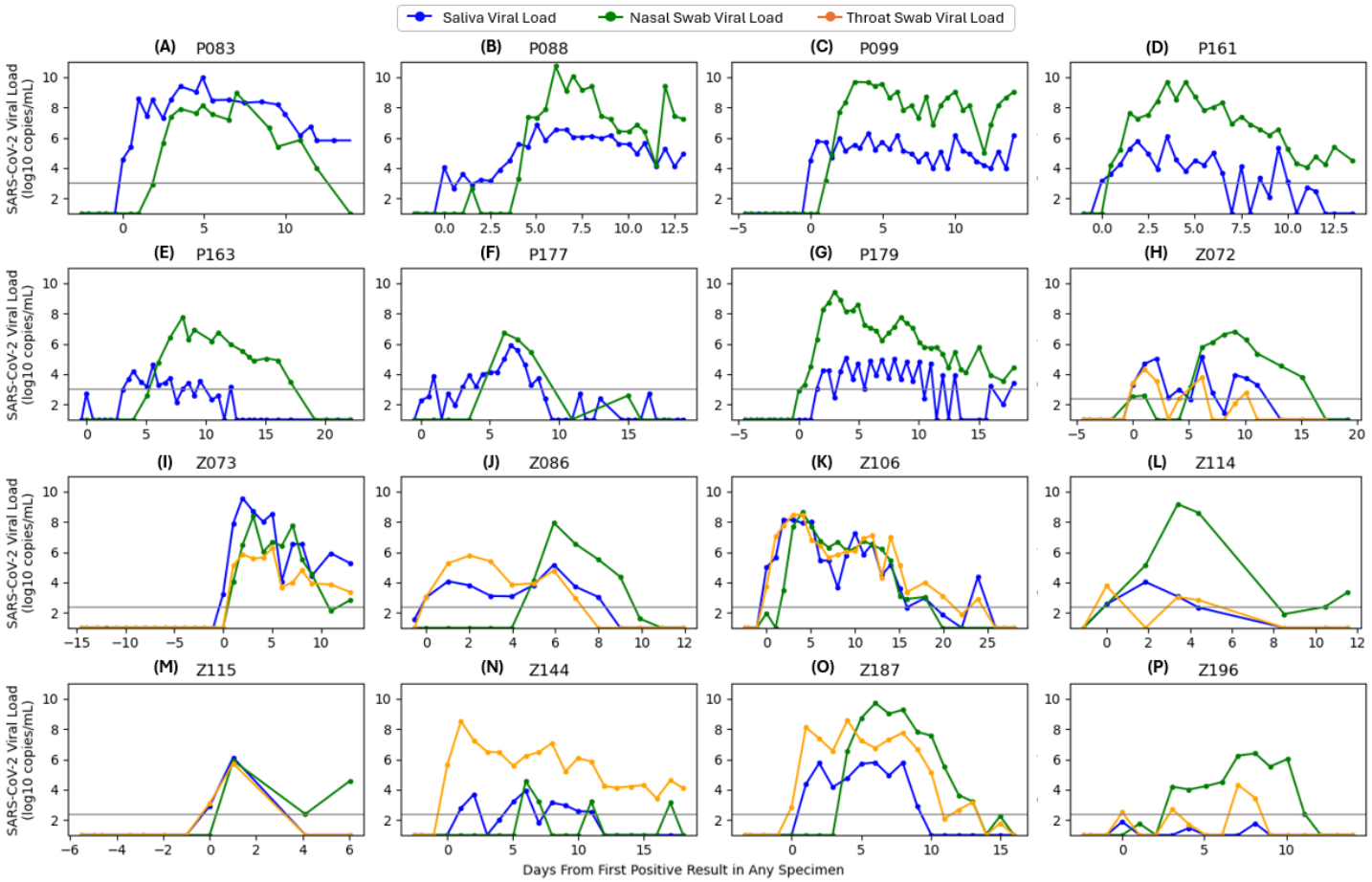

Figure 10-1 Viral load timecourses in paired specimen types from individuals with incident SARS-CoV-2 infection. Participants with Participant ID (PID) values that begin with "P" were enrolled in Phase I while those that begin with "Z" were enrolled in Phase II of the study. Participants with Status of "Case" indicate that the participant had Sustained Incident Infection. Each panel **(A-P)** shows data from specimens collected by a single participant with sustained incident infection, for all available specimen types. Panels are ordered by Participant ID, and the panel label is held consistent for each participant in **Figures 10-1, 10-5, 10-6, and 10-7**. SARS-CoV-2 viral loads are plotted over time relative to the day that SARS-CoV-2 RNA was first detected in any specimen type (x-axis). Saliva (oral cavity) viral loads are shown in blue, nasal swab (anterior nares) in green, and throat swab (oropharynx) in orange. The horizontal grey line indicates the Limit of Detection (LoD) of the assay used for SARS-CoV-2 detection; in Phase I the LoD was 1,000 copies/mL of specimen, and in Phase II the LoD was 250 copies/mL of specimen.

Results

High quality gene expression data was obtained from 1,177 human upper respiratory clinical specimens

It is notoriously challenging to generate high quality human gene expression data from self-collected upper respiratory clinical specimens. Challenges arise in the purification of nucleic acids due to the presence of cellular and environmental (e.g., food) debris, and viscosity due to the high mucus content of the samples. These characteristics can reduce the efficiency DNA digestion, leading to the persistence of genomic DNA which is carried through to sequencing but does not reflect gene expression. Relatedly, RNA collected at mucosal surfaces may be fragmented due to enzymatic or chemical degradation, which can limit the efficiency of their capture or amplification by some specimen preparation methods. Additionally, mucosal surfaces harbor high loads of bacteria, such that RNA present within clinical specimens may be dominated by bacterial rRNA. For this reason, a large portion of reads from metatranscriptomic sequencing of upper respiratory clinical specimens map to bacterial genomes, and relatively few reads mapping to the human genome; analysis of human gene expression is routinely performed on only 1 million human reads per sample,[19,20] though it has been established that robust analyses of human gene expression typically require tens of millions of human reads.[21,22] We evaluated several methods for RNA purification and sequencing library preparation to overcome these challenges and optimized a workflow to generate high quality human gene expression data.

Ten million human-mapping reads per sample was determined by empirical analysis to be sufficient for robust gene expression analyses. Twenty-one samples which generated over 66 million human-mapping reads per sample were used to evaluate the impact of lower sequencing depth. For each sample, 40 million, 20 million, 10 million, 5 million, and 1 million human-mapping reads were randomly selected, and gene expression in each computationally down selected subset was compared. Each sample clustered with itself, regardless of sequencing depth, and separate from other samples when Principal Component Analysis was applied and visualized for Principal Components 1 to 5 (which represented >95% of variance explained). Clustering by PCA would be dominated by genes with high levels of expression that vary among the different samples, indicating that major features of gene expression do not change in this range of sequencing depth. However, genes with lower expression may be both relevant and important for the analysis of mucosal immune function. To assess the impact of sequencing depth on lower-abundance genes, I assessed at what sequencing depth genes with fewer than 0.1 copies per million began to exhibit 0 counts per million (or dropout). I observed dropout of genes with fewer than 0.1 copies per million when the sample had five million

human-mapping reads or less, but consistent detection of these genes when greater than five million human-mapping reads were available. Analyses of gene expression typically rely not only on the presence of genes, but the gene expression quantification, to identify differential expression. To assess the impact of sequencing depth on gene expression values, I assessed what portion of genes exhibited significant differential expression when five million human-mapping reads per sample were available, compared to when 10 million human-mapping reads per sample were available. Only 2.7% of genes (1700 of 63420 genes) exhibited significant differences ($P_{unadj}<0.05$, Wilcoxon Signed Rank Test) when comparing five million human-mapping reads to 10 million human mapping reads for each sample. Unadjusted P-values were used for this analysis, to provide a more liberal estimate of the number of genes with significantly different expression; with P-value adjustment for multiple hypothesis testing correction, even fewer genes would exhibit differential expression between sequencing depths of five million and 10 million human-mapping reads per sample. These results supported that samples which generated at least 10 million human mapping reads per sample were likely to yield robust representation of gene expression, including for genes which may have low abundance but high biological consequence—including interferon stimulated genes.

Data obtained from our optimized workflow provided high quality measurements of human gene expression with low technical noise. Of 1,368 clinical specimens for which preparation was attempted, 86% yielded more than 10 million human-mapping reads per sample, and an average of 22 million human-mapping reads per sample (**Figure 10-2A**). For each sample, the fraction of reads mapping to non-intronic (exonic, intergenic) regions was calculated in order to assess the potential for genomic DNA contamination of the sequencing data. Some reads mapping to intronic regions are also expected, given that some reads may originate from nascent pre-mRNA molecules which have not undergone splicing, and that SARS-CoV-2 is known to interfere with splicing and promote intron retention (Banerjee et al. Cell 2020). For 85% of samples reads were predominantly exonic (**Figure 10-2B**), and average of 60.5% (Standard Deviation 15%) of reads from each sample mapped to known exonic regions. These data supported that reads obtained are likely to be reflective of gene expression. The workflow for specimen processing was designed for compatibility with automated instrumentation, in order to decrease operator-dependent variability, and in each batch of specimens that were processed, a positive control consisting of pooled human saliva from a single-stock was included. Gene expression data from this positive control in each batch represents technical replicates, and was analyzed to assess technical noise from processing. As expected, variation (attributable to technical noise) among replicate gene expression measurements was dependent on the level of expression, with lower variability among genes with higher expression. However, for over 95% of genes with abundances as low as 10 copies per

million, standard deviation was only 0.2; this corresponds to less than 1.5-fold changes due to technical noise among replicate measurements of genes at low abundance (**Figure 10-2C**). Technical noise was lower for genes with greater expression values. For genes with mean abundances below two copies per million, the gene was not detected (zero counts) in one or more technical replicates, resulting in the striped pattern observed in the top left quadrant when mean log10 copies per million is plotted against standard deviation; individual stripes occur due to an increasing prevalence of zero counts for that gene (for example, the first stripe contains genes which had a zero count in one of 17 replicates, and the second stripe contains genes which had a zero count in two of 17 replicates, etc).

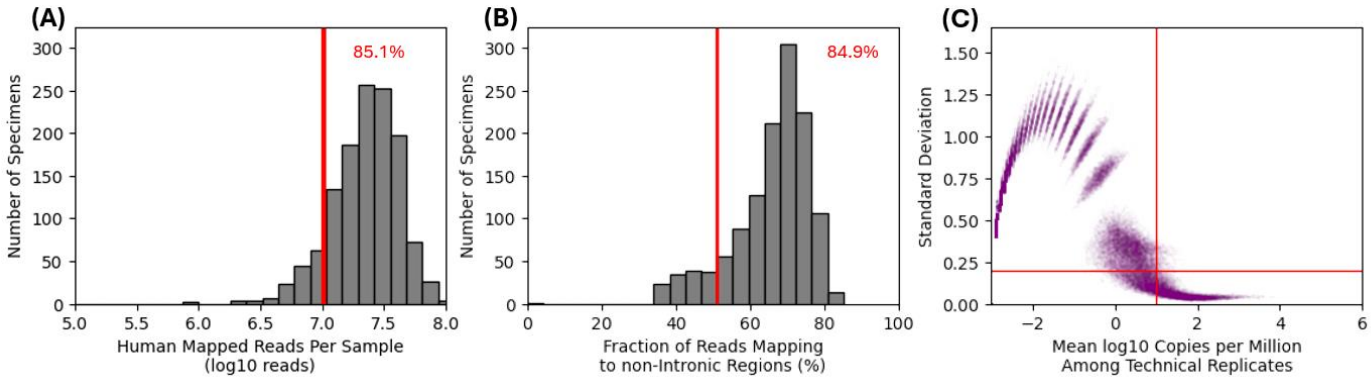

Figure 10-2 Human-exome enriched sequencing of upper respiratory clinical specimens generates gene expression data of high technical quality. **(A)** Histogram of log10 human-mapped reads per sample. Red line indicates 10 million human-mapped reads per sample. Red text shows the fraction of samples with more than 10 million human-mapped reads per sample. **(B)** Histogram visualizing the fraction (percent) of reads from each sample which mapped to non-intronic (exonic, intergenic) regions. Red line indicates 50% non-intronic mapped reads. Red text shows the fraction of samples which had more than 50% of reads mapping to non-intronic regions. **(C)** Specimens were processed in 17 independent batches, which each contained volume from a single-stock of human saliva pooled from 10 unique saliva specimens. Measurements from this pooled saliva control therefore represent technical replicates. Raw counts per gene for each pooled saliva replicate were normalized by library size to represent gene expression in copies per million reads. For each gene, the average of log10-transformed expression values among the replicates was calculated (x-axis) and plotted against the standard deviation of log10-transformed expression values (y-axis) among the 17 pooled saliva technical replicates. Vertical red line indicates an expression value of 10 copies per million. Technical replicate expression values for 95.1% of genes at or above this level of abundance had a standard deviation less than 0.2 (horizontal red line).

Longitudinal gene expression data demonstrates substantial upregulation of interferon stimulated genes during acute viral infection

In order to ascertain the magnitude of change in expression observed for interferon stimulated genes (ISGs) during acute viral infection, I visualized the expression of canonical interferon stimulated genes (STAT1, MX1, OAS1) and quantitative viral load data from each specimen type from each participant over time. Most participants exhibited large changes in ISG expression that closely followed the progression of SARS-CoV-2 proliferation. A subset of four participants with representative changes in gene expression are shown in **Figure 10-3**. Baseline expression of these canonical ISGs (prior to observed upregulation) varied by participant and specimen type and was fairly stable, changing by than one order of magnitude before becoming upregulated by several orders of magnitude. This upregulation was observed in all specimen types for these individuals. In some individuals with low viral loads, the expression changes of ISGs were notably smaller (data not shown). For several individuals, including the participant shown in **Figure 10-3D**, expression of these ISGs appear to be upregulated in a relatively synchronized fashion among all specimen types despite low or undetectable viral loads in one or more specimen types during early infection. This result suggests that early interferon stimulation is not restricted to upper respiratory sites with detectable viral proliferation and can be present in sites without detectable SARS-CoV-2 RNA.

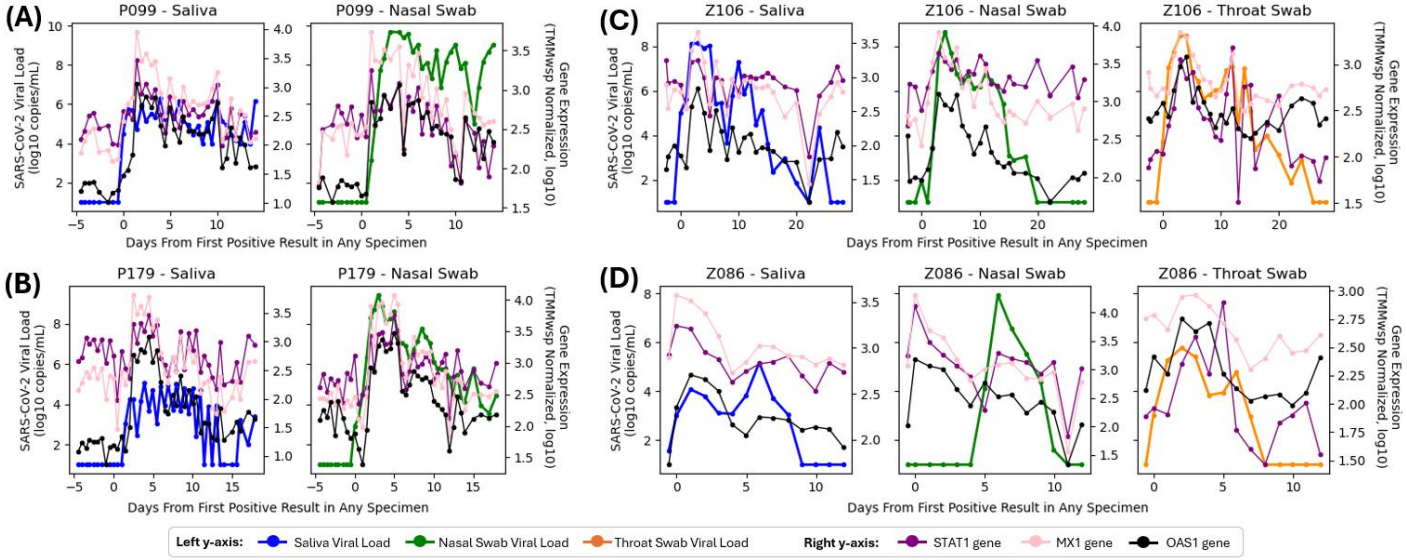

Figure 10-3. Canonical interferon stimulated genes exhibit massive upregulation during the early phase of SARS-CoV-2 infection in all specimen types. For a representative set of four participants **(A–D)** with Sustained Incident Infection, SARS-CoV-2 viral load (left y-axis) is plotted over time in each specimen type collected (saliva in blue, nasal swab in green, and throat swab in orange). Additionally, the observed gene expression values (TMMwsp normalized and log10 transformed, right y-axis) for STAT1 (purple), MX1 (pink), and OAS1 (black) are overlayed.

Interferon stimulation is conserved and specific to individuals with sustained infection

While individual gene expression may suggest interferon stimulation, expression changes among sets of genes more robustly demonstrate this response. Additionally, analysis methods that consider the expression of interferon-stimulated gene sets relative to the expression of randomly selected genes provide a more rigorous and unbiased evaluation of interferon stimulation.

I implemented a method to calculate an Interferon Stimulation Model Score (ISMS) for each sample.[18] This method uses a validated list of 26 known interferon stimulated genes, and compares the arithmetic mean of their expression to that of a randomly selected set of 100 "control" genes, which serves as a baseline to account for random gene expression variation.

I compared whether the ISMS differentiated participants in the Sustained Incident Infection (SII) cohort (**Figure 10-4A**) from those in the Test Negative (TN) cohort (**Figure 10-4B**). Increases in ISMS were highly specific to individuals with sustained infection, with marked differences between SII and TN cohorts across specimen types. Among individuals with SII, ISMSs rose to values greater than one before gradually declining over time. ISMSs remained low and stable among TN individuals. To quantify specificity, I considered threshold of minimum ISMS in a minimum number of timepoints for each individual (**Figure 10-4C,D**). Among saliva samples, 14 of 16 (88%) individuals in the SII cohort had at least two samples with an ISMS greater than 0.75, while this was the case for zero of 16 (0%) individuals in the TN cohort. ISMSs of 0.5 in at least two saliva samples were observed for 100% of SII participants and 19% of TN participants. Similarly, among nasal swab samples, 14 of 16 (88%) individuals in the SII cohort and two of 16 (13%) individuals in the TN cohort had at least two samples with an ISMS greater than 0.25. ISMS scores were systematically lower in throat swabs compared to other specimen types, which may reflect differential ISG upregulation between specimen types. Among throat swab samples, eight of nine (89%) individuals in the SII cohort and 1 of 9 (11%) individuals in the TN cohort had at least two samples with an ISMS greater than 0.25. Notably, a single Test Negative participant exhibited a consistently high ISMS in throat swabs (**Figure 10-4B**), which highlights the variability in baseline mucosal immune function across individuals and underscores the value of longitudinal measurements to detect changes from baseline.

Visualization of ISMS dynamics among individuals with SII suggest that interferon stimulation is initiated in all upper respiratory mucosal sites shortly after the first SARS-CoV-2 positive result in any specimen type. Given that

viral load dynamics are asynchronous among upper respiratory mucosal sites for most participants in this cohort (**Figure 10-1**), the synchronicity of interferon stimulation among specimen types suggests that early interferon stimulation is not restricted to upper respiratory sites with detectable viral proliferation but can indeed be present in sites without detectable SARS-CoV-2 RNA.

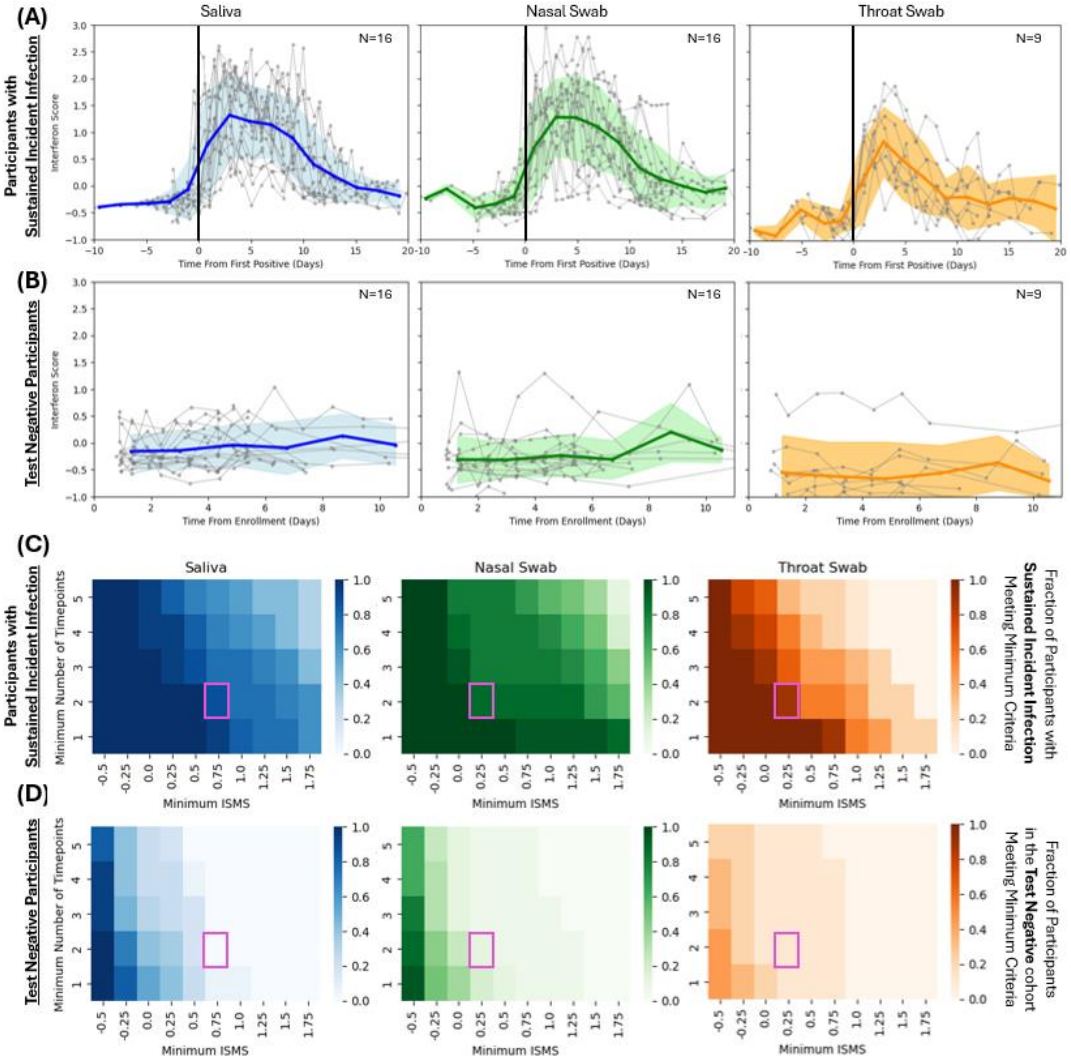

Figure 10-4. Interferon Stimulation Module Scores distinguish participants with Sustained Incident Infection from Test Negative participants. **(A)** shows Interferon Stimulation Module Scores in each specimen type, for participants with Sustained Incident Infection over time relative to the day of first SARS-CoV-2 positive result in any specimen type. Vertical black lines indicate time 0. **(B)** shows Interferon Stimulation Module Scores in each specimen type, for demographically-matched participants in the Test Negative cohort, over time relative to the day of enrollment. Thin grey lines indicate data from individual participants, while thick lines with shading indicate the daily median ISMS with interquartile range. N indicates the number of individual participants from whom data is shown. **(C)** Heatmap visualizing the percent of participants with Sustained Incident Infection who had ISMS values above a minimum threshold (x-axis) in a minimum number of timepoints throughout their enrollment (y-axis), for each specimen type. **(D)** Heatmap visualizing the percent of participants in the Test Negative cohort who had ISMS values above a minimum threshold (x-axis) in a minimum number of timepoints throughout their enrollment (y-axis), for each specimen type. Magenta boxes indicate specific comparisons described in Results.

Interferon stimulation is synchronized across anatomical sites in the upper respiratory mucosa independently of local SARS-CoV-2 viral load

Prior analyses demonstrated that select ISGs in an upper respiratory mucosal site can be upregulated prior to the rise of viral load in that site (**Figure 10-3D**) and that on a population level, the Interferon Stimulation Module Score exhibits a synchronized rise in all upper respiratory mucosal sites immediately after viral RNA is detected in any specimen type (**Figure 10-4A**). These results are inconsistent with the hypothesis that early interferon stimulation is restricted to upper respiratory sites with detectable viral proliferation and absent from sites without detectable SARS-CoV-2 RNA. However, to rigorously test this hypothesis, I next assessed ISMS dynamics at each anatomical site in individuals with Sustained Incident Infection, in relation to local viral load dynamics..

In most SII participants, nasal viral load rose later than viral load in saliva or throat swabs. Among 16 individuals in the SII cohort, 11 exhibited a delay in the rise of viral load in the nose, compared to saliva or throat swabs, four had detectable viral RNA in the nose at the same time as saliva or throat swabs, and one individual had detectable virus in the nose prior to saliva (**Figure 10-1**). If interferon stimulation during early infection is absent from upper respiratory mucosal sites without detectable SARS-CoV-2 RNA, then ISMSs in the nose should remain low prior to the rise of SARS-CoV-2 viral load in the nose.

In 81% (13 of 16) of individuals with SII, interferon stimulation in the nose (ISMS > 0.25) occurred before viral loads in the nose exceeded 1,000 copies/mL (**Figure 10-5A,B,C,E,F,G,H,I,J,K,N,O,P**). One participant (**Figure 10-5M**) exhibited a high ISMS of 2.07 on the same day that SARS-CoV-2 viral load in the nose was above 1,000 copies/mL, which was one day after SARS-CoV-2 was first detected in any specimen type. For two participants (**Figure 10-5D,L**), the rise in nasal swab viral load occurred prior to the rise in ISMS; one of these participants (**Figure 10-5D**) was the only participant for whom the rise in nasal swab viral load preceded the rise in saliva viral load. These findings challenge the hypothesis that early interferon stimulation is confined to sites with detectable viral proliferation, indicating that ISMS can rise even in locations without detectable viral RNA.

In contrast to the nose, interferon stimulation in the mouth and throat generally followed detectable viral load. Seven of 9 (78%) participants had viral loads above 1,000 copies/mL in the throat prior to ISMSs of 0.25 (**Figure 10-6H-N**). For one participant (Z187, **Figure 10-6O**), these thresholds were met on the same day, and for the other participant (Z196, **Figure 10-6P**) an ISMSs of 0.25 was observed several days prior to throat swab viral loads above

1,000 copies/mL. In the latter participant, throat swab viral loads never exceeded 10^5 copies/mL. Test Negative participants had higher ISMSs in saliva than in nose or throat samples (**Figure 10-4B**), and therefore an ISMS of 0.25 in saliva had lower specificity for sustained infection than this value in nasal or throat swabs (**Figure 10-4D**). To achieve a similar level of specificity for sustained infection, I set an ISMS threshold of 0.5 to assess the timing of interferon stimulation relative to the rise of viral load in saliva. Fifty percent (eight of 16) of participants had saliva viral loads exceeding 1,000 copies/mL prior to ISMS reaching 0.5 (**Figure 10-7B,C,G,H,I,K,N,O**), while in 19% (3 of 16) participants, these events occurred at the same timepoint (**Figure 10-7D,L,M**). For 31% (five of 16) participants, interferon stimulation preceded the rise in saliva viral load (**Figure 10-7A,E,F,J,P**), with three of these five participants exhibiting ISMS > 0.5 before viral RNA was detected in any specimen type (**Figure 10-7A,E,F**). For one participant (Z196, **Figure 10-7P**), salivary viral load never exceeded 1,000 copies/mL.

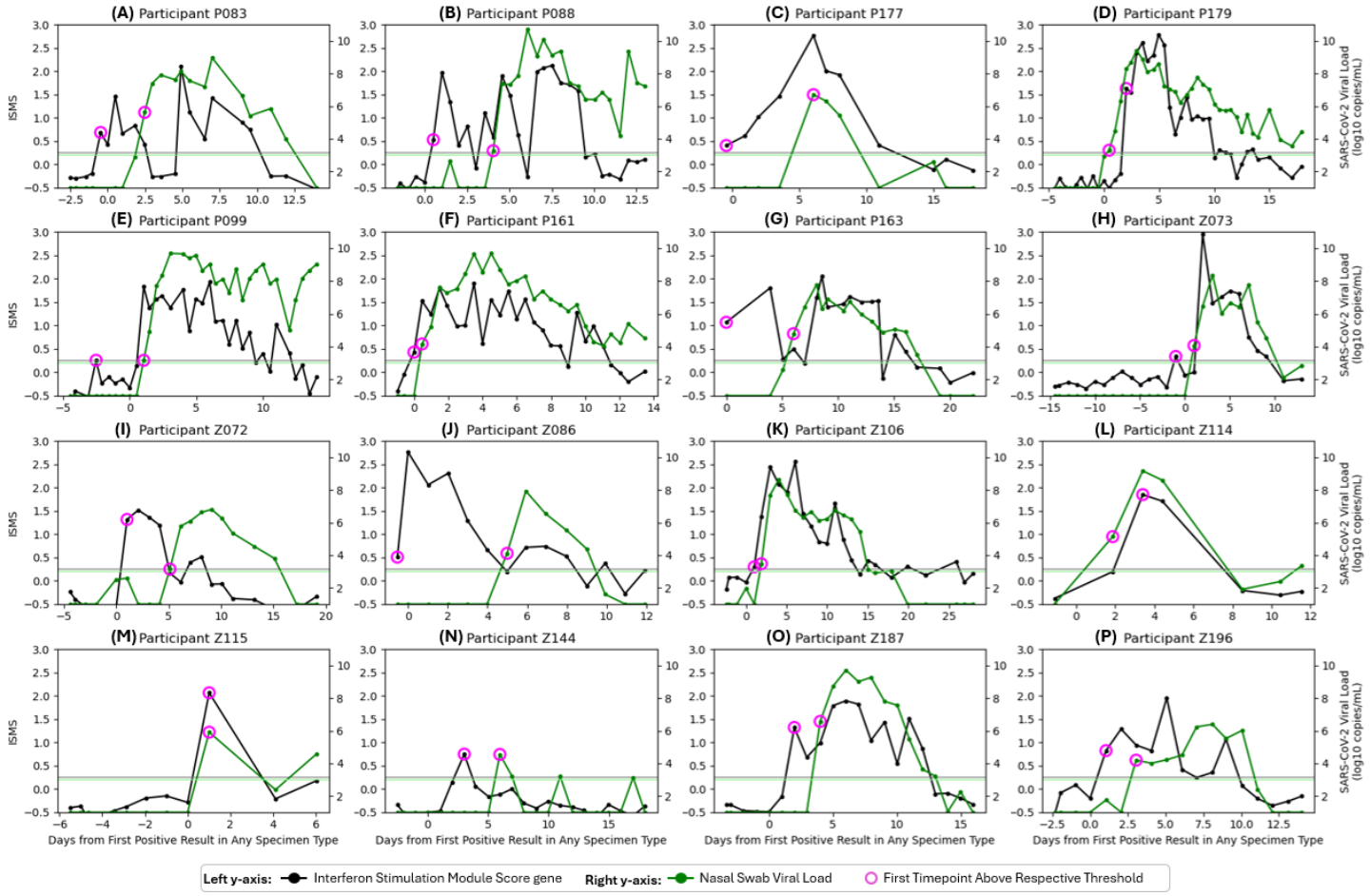

Figure 10-5. **Interferon Stimulation in the nose frequently occurs prior to detectable viral proliferation in the nose of individuals with sustained incident infection**. Each panel **(A–P)** shows data from nasal swab specimens collected by a single participant with sustained incident infection. Panels are ordered by Participant ID, and the panel label is held consistent for each participant in **Figures 10-1, 10-4, 10-5, and 10-6**. Interferon Stimulation Module Scores in the nose are plotted in black (left y-axis), and SARS-CoV-2 viral loads are plotted in green (right y-axis), over time relative to the day that SARS-CoV-2 RNA was first detected in any specimen type (x-axis). The horizontal grey line indicates an ISMS threshold of 0.25, and the horizontal light green line indicates a nasal viral load threshold of 1,000 copies/mL. The earliest datapoint with values above each threshold are indicated by a magenta circle.

Figure 10-6. The timing of detectable viral proliferation and interferon stimulation in the oropharynx of individuals with sustained incident infection. Each panel **(H–P)** shows data from throat swab (oropharyngeal) specimens collected by a single participant with sustained incident infection. Panels are ordered by Participant ID, and the panel label is held consistent for each participant in **Figures 10-1, 10-5, 10-6, and 10-7**. Interferon Stimulation Module Scores in the nose are plotted in black (left y-axis), and SARS-CoV-2 viral loads are plotted in orange (right y-axis), over time relative to the day that SARS-CoV-2 RNA was first detected in any specimen type (x-axis). The horizontal grey line indicates an ISMS threshold of 0.25, and the horizontal light orange line indicates a oropharyngeal viral load threshold of 1,000 copies/mL. The earliest datapoint with values above each threshold are indicated by a magenta circle.

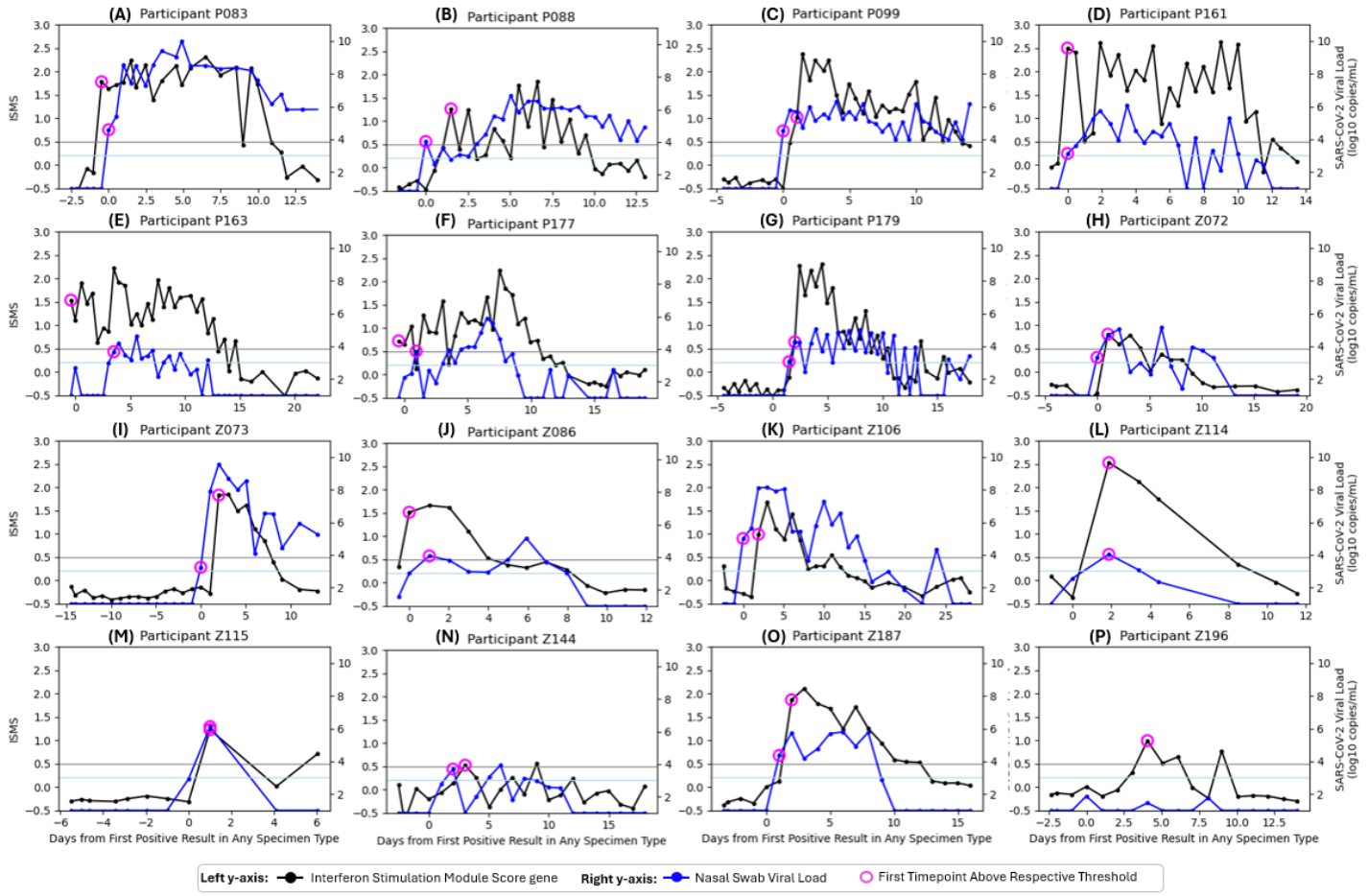

Figure 10-7. The timing of detectable viral proliferation and interferon stimulation in the oral cavity of individuals with sustained incident infection. Each panel **(A–P)** shows data from saliva specimens collected by a single participant with sustained incident infection. Panels are ordered by Participant ID, and the panel label is held consistent for each participant in **Figures 10-1, 10-5, 10-6, and 10-7**. Interferon Stimulation Module Scores in the nose are plotted in black (left y-axis), and SARS-CoV-2 viral loads are plotted in blue (right y-axis), over time relative to the day that SARS-CoV-2 RNA was first detected in any specimen type (x-axis). The horizontal grey line indicates an ISMS threshold of 0.5, and the horizontal light blue line indicates a saliva load threshold of 1,000 copies/mL. The earliest datapoint with values above each threshold are indicated by a magenta circle.

To determine whether interferon stimulation during early infection was synchronized across upper respiratory mucosal sites, I compared the timing of interferon stimulation (ISMS above 0.25 in the nose and throat, and above 0.5 in the oral cavity) with the onset of detectable viral proliferation (SARS-CoV-2 >1000 copies/mL) at the same site or any site. Interferon stimulation in the nose occurred closer to the timepoint of detectable viral proliferation in any site than in the nose itself (Padj=0.003, Wilcoxon Signed Rank Test with Bonferroni Correction, **Figure 10-8A**), suggesting that nasal interferon response is more influenced by viral proliferation at any upper respiratory site than by local proliferation. Since viral proliferation was typically first observed in the oropharynx (**Figure 10-8B**) and oral cavity (**Figure 10-8C**), interferon stimulation in these sites coincided with the earliest detectable viral load at any site. In addition to the initiation of interferon stimulation, I also assessed the correlation of longitudinal ISMSs among specimen type pairs from each participant. For all specimen type pairs (nasal and saliva in **Figure 10-8D**, nasal and throat in **Figure 10-8E**, saliva and throat in **Figure 10-8F**), ISMS values correlated significantly better than those in a null model where values were shuffled randomly across time (Padj=0.009, Padj=0.035, Padj=0.012 for each pairwise comparison, Wilcoxon Signed Rank Test with Bonferroni Correction). These correlations between ISMS across specimen type pairs further support that interferon stimulation is synchronized across multiple anatomical sites in the upper respiratory mucosa during acute viral infection.

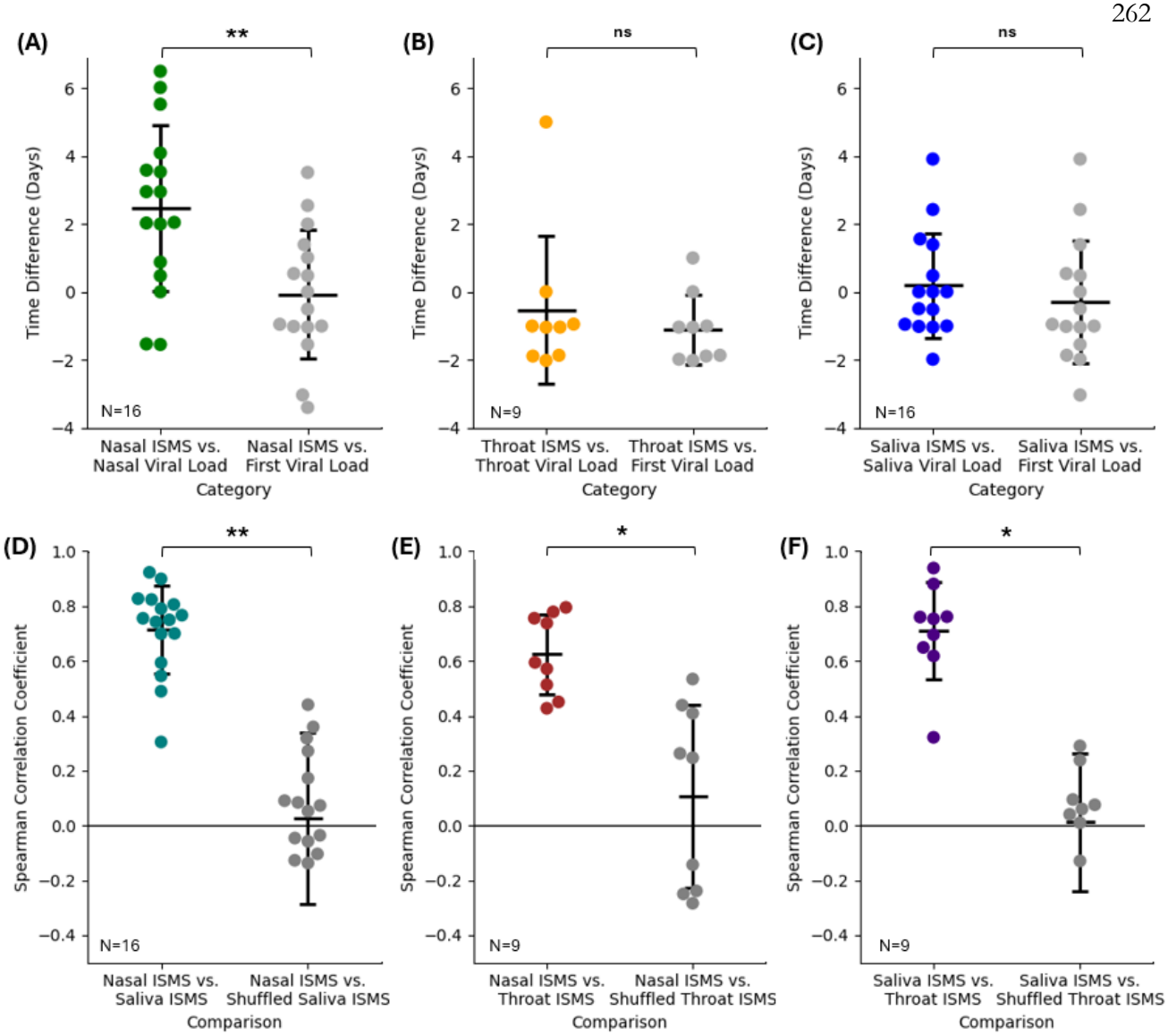

Figure 10-8. Interferon Stimulation is synchronized across anatomical sites in the upper respiratory mucosa. (A) For each participant, the time difference between the initiation of interferon stimulation in the nose (first timepoint with Interferon Stimulation Module Score [ISMS] > 0.25 in nasal swabs) and first detectable viral proliferation in the nose (SARS-CoV-2 viral load >1000 copies/mL) was calculated. The time difference between the initiation of interferon stimulation in the nose (first timepoint with Interferon Stimulation Module Score [ISMS] > 0.25 in nasal swabs) and first detectable viral proliferation in any upper respiratory sampling site (SARS-CoV-2 viral load >1000 copies/mL) was also calculated. The distribution of time differences in each group was then compared using Wilcoxon Signed Rank Test with Bonferroni correction. Similar analyses were performed on data from the **(B)** oropharynx (throat) and the **(C)** oral cavity (saliva). N indicates the number of participants assessed in each plot. ISMS: Interferon Stimulation Module Score. * indicates adjusted P value <0.05, ** indicates adjusted P value < 0.01, while ns indicates non-significant.

Discussion

High quality, longitudinal human transcriptomic data from paired specimen types starting prior to acute viral infection is extraordinarily rare. To our knowledge, the only other dataset with similar features that exists was obtained following intentional inoculation of an early SARS-CoV-2 variant strain (SARS-CoV-2/human/GBR/484861/2020, a D614G-containing pre-alpha wild-type virus) into young (age 18–29 years) and healthy volunteers in the United Kingdom.[23–25] While this human challenge study has provided valuable insight into the mechanisms of infection and defense against SARS-CoV-2, the study is limited by the experimental infection route, the demographic diversity of participants, the viral variant used, and the lack of prior COVID-19 exposure or vaccination. In contrast, our dataset includes individuals age seven to 57, infected with a variety of viral variants (including both ancestral and the currently predominant Omicron variant), and individuals with prior COVID-19 vaccination. Additionally, gene expression analyses from the human challenge study have only been reported for paired nasopharyngeal swabs and blood, while our dataset includes three paired upper respiratory specimen types—saliva (oral cavity), nasal swab (anterior nares), and throat swab (oropharynx).

The localization of interferon stimulation across the upper respiratory tract during the early phase of acute viral infection has important implications for our understanding of mucosal immunology and for mucosal vaccine design. Current models of interferon stimulation propose that interferon production is concentrated at the site of viral infection and decreases with distance, inducing an antiviral state in nearby cells.[13] While this localized response limits excess inflammation, it may leave more distant mucosal cells vulnerable to viral infection. If viral spread is primarily diffusion-limited, a localized interferon response could effectively contain the infection. However, if viral spread involves additional mechanisms, such as virus-induced cell migration,[26] localized interferon production may be insufficient to prevent sustained infection. Sterilizing immunity, or the ability to prevent sustained viral infection, would limit viral transmission not only among cells within an individual, but prevent among individuals. For this reason, induction of sterilizing immunity is a central objective of mucosal vaccines.[14,15] Understanding the localization of interferon and other immune responses across anatomically distinct mucosal sites is necessary to develop mucosal vaccines that effectively induce sterilizing immunity.

Our findings challenge the hypothesis that interferon stimulation is restricted to upper respiratory sites with detectable viral RNA. Instead, we observed synchronized interferon stimulation across multiple sites—specifically, the oropharynx, oral cavity, and nasal passages—following viral proliferation in any one of these sites. This synchronization was evident through both ISG expression patterns and ISMS analysis, and through analysis of both aggregate and individual-level data. Synchronization of interferon stimulation during early viral infection was demonstrated by the timing of initiation of the interferon response relative to detectable viral proliferation, as well as through longitudinal correlation over the course of acute viral infection.

There are two potential explanations for the observed interferon stimulation in sites without detectable viral proliferation during early acute infection. First, viral infection may have occurred nearly simultaneously at multiple mucosal sites, triggering independent, localized interferon responses, with viral proliferation remaining below detectable thresholds in some sites. Alternatively, the mucosal immune system may have coordinated a broad-range interferon response across sites, even in the absence of local viral proliferation. Either explanation advances our understanding of respiratory viral infection and the host mucosal immune response.

Current models of respiratory virus transmission typically assume a single initial site of cellular infection, followed by viral spread to adjacent tissues.[11,27,28] However, our first explanation challenges this model, suggesting that initial infection can occur simultaneously at multiple upper respiratory sites. Moreover, the ability to maintain viral proliferation below detectable limits in some sites, but not others, suggests the presence of specific immune mechanisms that more effectively suppress viral replication in certain areas. Identification of these features can inform correlates of protection for mucosal vaccines. Interestingly, that nasal viral loads eventually rose indicates that effective viral suppression only lasted for a few days. This begs us to ask what occurs at that transition point. It is notable that among the thirteen individuals who exhibited interferon stimulation prior to viral proliferation in the nose, in eight individuals (62%) the rise in nasal viral load was immediately preceded by a relative decline in ISMS (**Figure 10-5A,B,G,I,J,N,O,P**). This could indicate a lack of immune effector cell recruitment to the nose due to high viral loads in the mouth or throat, or potentially viral-mediated perturbation of interferon-mediated antiviral mechanisms.[29]

Alternatively, interferon stimulation may be coordinated across the upper respiratory mucosa, independent of local viral proliferation. This challenges models of short-distance, compartmentalized paracrine interferon signaling, which is assumed to be diffusion-limited. Instead, interferon stimulation may function as a feed-forward mechanism, inducing an antiviral state across multiple at-risk sites. Signal amplification over long distances (e.g., from the throat to the nose) may be mediated by epithelial cells,[10] although tissue-resident leukocytes, such as plasmacytoid dendritic cells (pDCs), likely play a central role. In this way, networks of cells can serve as beacon towers that light "signal fires" to communicate over longer distances, as human societies have done for at least 3,000 years.[30]

While neutralizing antibodies have long been recognized as a key defense against sustained viral infection, recent studies highlight the crucial role of cell-mediated immunity, particularly the bystander activation of CD8+ T cells. Interferon signaling can induce a bystander activation state in CD8+ T cells, enabling them to exhibit cytotoxic functions without the need for direct antigen recognition. Early research suggested that prolonged exposure to high-dose antigen was required to activate cytotoxic T lymphocytes.[31] However, Tough et al.[32] demonstrated that brief proliferation of CD8+ T cells could be stimulated by Type I IFN in the absence of antigen, a phenomenon termed "bystander proliferation," which was initially thought to be of limited biological importance.[33,34] Later studies revealed that antigen-independent cytokine stimulation of CD8+ T cells primed them for rapid effector functions, including the secretion of IFNγ and granzyme B upon subsequent antigen encounter.[35,36] This "bystander activation" state also promotes the recruitment and activation of innate immune cells[37] and modulates the balance between memory and effector T cell responses.[7,38]

The importance of bystander activation has been demonstrated in several models. For instance, inhibition of bystander activation during early Listeria monocytogenes infection in mice resulted in worsened disease outcomes,[36] and bystander activation of lung-resident memory T (T_{mem}) cells was shown to enhance neutrophil recruitment, helping to mitigate bacterial pneumonia.[39] Similar patterns have been observed in viral infections: early induction of bystander activation in CD8+ T cells was detected in the spleen following reovirus infection in mice.[40] In humans, a lack of bystander-activated CD8+ T cells during the first week of symptomatic SARS-CoV-2 infection has been linked to more severe disease.[41] These studies suggest that bystander-activated CD8+ T_{mem} play a critical role in orchestrating the immune response during the early

stages of acute viral infection,[17,42] preventing superinfection,[43] as well as maintaining T_{mem} cell populations.[38] Recent evaluations of mucosal vaccines have further highlighted the role of T_{mem} cells in suppressing early viral proliferation, which is critical for achieving sterilizing immunity.[44]

Three limitations of this study must be noted. First, this study is observational in nature. Experimental animal models will be necessary to confirm the synchronization of mucosal immune responses observed here. Second, although over one thousand specimens were analyzed, they were collected from a relatively small number of participants due to the logistical challenges of obtaining daily paired upper respiratory samples from individuals with sustained infection. The cohort is diverse in age, sex, vaccination status, and infecting viral variant, but insufficient in size to control for these differences. However, the findings presented were highly conserved across this group of participants. Third, it was only possible to generate this unique dataset through the self-collection of non-invasive specimen types, but these specimen types may not fully capture or reflect intra-mucosal gene expression. Advancements in technologies to non-invasively sample intra-mucosal dynamics are necessary to enable a more precise understanding of human mucosal immunobiology.

References

1. Isaacs A, Lindenmann J. Virus interference. I. The interferon. *Proc R Soc Lond B Biol Sci*. 1957;147(927):258-267. doi:10.1098/rspb.1957.0048

2. Wheelock EF. Interferon-Like Virus-Inhibitor Induced in Human Leukocytes by Phytohemagglutinin. *Science*. 1965;149(3681):310-311. doi:10.1126/science.149.3681.310

3. Kotenko SV, Gallagher G, Baurin VV, et al. IFN-lambdas mediate antiviral protection through a distinct class II cytokine receptor complex. *Nat Immunol*. 2003;4(1):69-77. doi:10.1038/ni875

4. Darnell JE, Kerr IM, Stark GR. Jak-STAT pathways and transcriptional activation in response to IFNs and other extracellular signaling proteins. *Science*. 1994;264(5164):1415-1421. doi:10.1126/science.8197455

5. Schneider WM, Chevillotte MD, Rice CM. Interferon-stimulated genes: a complex web of host defenses. *Annu Rev Immunol*. 2014;32:513-545. doi:10.1146/annurev-immunol-032713-120231

6. Platanias LC. Mechanisms of type-I- and type-II-interferon-mediated signalling. *Nat Rev Immunol*. 2005;5(5):375-386. doi:10.1038/nri1604

7. Krummel MF, Mahale JN, Uhl LFK, et al. Paracrine costimulation of IFN-γ signaling by integrins modulates CD8 T cell differentiation. *Proc Natl Acad Sci U S A*. 2018;115(45):11585-11590. doi:10.1073/pnas.1804556115

8. Czerkies M, Kochańczyk M, Korwek Z, Prus W, Lipniacki T. Respiratory Syncytial Virus Protects Bystander Cells against Influenza A Virus Infection by Triggering Secretion of Type I and Type III Interferons. *J Virol*. 2022;96(22):e0134122. doi:10.1128/jvi.01341-22

9. Otter CJ, Renner DM, Fausto A, Tan LH, Cohen NA, Weiss SR. Interferon signaling in the nasal epithelium distinguishes among lethal and common cold coronaviruses and mediates viral clearance. *Proc Natl Acad Sci*. 2024;121(21):e2402540121. doi:10.1073/pnas.2402540121

10. Miura TA. Respiratory Epithelial Cells as Master Communicators during Viral Infections. *Curr Clin Microbiol Rep*. 2019;6(1):10-17. doi:10.1007/s40588-019-0111-8

11. Lamers MM, Haagmans BL. SARS-CoV-2 pathogenesis. *Nat Rev Microbiol*. 2022;20(5):270-284. doi:10.1038/s41579-022-00713-0

12. Van Eyndhoven LC, Singh A, Tel J. Decoding the dynamics of multilayered stochastic antiviral IFN-I responses. *Trends Immunol*. 2021;42(9):824-839. doi:10.1016/j.it.2021.07.004

13. Lavigne GM, Russel H, Sherry B, Ke R. Autocrine and paracrine interferon signalling as 'ring vaccination' and 'contact tracing' strategies to suppress virus infection in a host. *Proc R Soc B Biol Sci*. 2021;288(1945). doi:10.1098/rspb.2020.3002

14. Medzhitov R, Iwasaki A. Exploring new perspectives in immunology. *Cell*. 2024;187(9):2079-2094. doi:10.1016/j.cell.2024.03.038

15. Knisely JM, Buyon LE, Mandt R, et al. Mucosal vaccines for SARS-CoV-2: scientific gaps and opportunities—workshop report. *Npj Vaccines*. 2023;8(1):1-7. doi:10.1038/s41541-023-00654-6

16. Lucas C, Wong P, Klein J, et al. Longitudinal analyses reveal immunological misfiring in severe COVID-19. *Nature*. 2020;584(7821):463-469. doi:10.1038/s41586-020-2588-y

17. Maurice NJ, Taber AK, Prlic M. The ugly duckling turned to swan - a change in perception of bystander activated memory CD8 T cells. *J Immunol Baltim Md 1950*. 2021;206(3):455-462. doi:10.4049/jimmunol.2000937

18. Yoshida M, Worlock KB, Huang N, et al. Local and systemic responses to SARS-CoV-2 infection in children and adults. *Nature*. 2022;602(7896):321-327. doi:10.1038/s41586-021-04345-x

19. Saravia-Butler AM, Schisler JC, Taylor D, et al. Host transcriptional responses in nasal swabs identify potential SARS-CoV-2 infection in PCR negative patients. *iScience*. 2022;25(11). doi:10.1016/j.isci.2022.105310

20. Kim J, Tierney BT, Overbey EG, et al. Single-cell multi-ome and immune profiles of the Inspiration4 crew reveal conserved, cell-type, and sex-specific responses to spaceflight. *Nat Commun*. 2024;15(1):4954. doi:10.1038/s41467-024-49211-2

21. Hart SN, Therneau TM, Zhang Y, Poland GA, Kocher JP. Calculating Sample Size Estimates for RNA Sequencing Data. *J Comput Biol*. 2013;20(12):970-978. doi:10.1089/cmb.2012.0283

22. Kukurba KR, Montgomery SB. RNA Sequencing and Analysis. *Cold Spring Harb Protoc*. 2015;2015(11):951-969. doi:10.1101/pdb.top084970

23. Killingley B, Mann AJ, Kalinova M, et al. Safety, tolerability and viral kinetics during SARS-CoV-2 human challenge in young adults. *Nat Med*. 2022;28(5):1031-1041. doi:10.1038/s41591-022-01780-9

24. Lindeboom RGH, Worlock KB, Dratva LM, et al. Human SARS-CoV-2 challenge uncovers local and systemic response dynamics. *Nature*. 2024;631(8019):189-198. doi:10.1038/s41586-024-07575-x

25. Wagstaffe HR, Thwaites RS, Reynaldi A, et al. Mucosal and systemic immune correlates of viral control after SARS-CoV-2 infection challenge in seronegative adults. *Sci Immunol*. 2024;9(92):eadj9285. doi:10.1126/sciimmunol.adj9285

26. Woodall MNJ, Cujba AM, Worlock KB, et al. Age-specific nasal epithelial responses to SARS-CoV-2 infection. *Nat Microbiol*. 2024;9(5):1293-1311. doi:10.1038/s41564-024-01658-1

27. Jackson CB, Farzan M, Chen B, Choe H. Mechanisms of SARS-CoV-2 entry into cells. *Nat Rev Mol Cell Biol*. 2022;23(1):3-20. doi:10.1038/s41580-021-00418-x

28. Zeng C, Evans JP, King T, et al. SARS-CoV-2 spreads through cell-to-cell transmission. *Proc Natl Acad Sci*. 2022;119(1):e2111400119. doi:10.1073/pnas.2111400119

29. Banerjee AK, Blanco MR, Bruce EA, et al. SARS-CoV-2 Disrupts Splicing, Translation, and Protein Trafficking to Suppress Host Defenses. *Cell*. 2020;183(5):1325-1339.e21. doi:10.1016/j.cell.2020.10.004

30. Earley-Spadoni T. Landscapes of warfare: Intervisibility analysis of Early Iron and Urartian fire beacon stations (Armenia). *J Archaeol Sci Rep*. 2015;3:22-30. doi:10.1016/j.jasrep.2015.05.008

31. Oehen S, Brduscha-Riem K. Differentiation of naive CTL to effector and memory CTL: correlation of effector function with phenotype and cell division. *J Immunol Baltim Md 1950*. 1998;161(10):5338-5346.

32. Tough DF, Borrow P, Sprent J. Induction of bystander T cell proliferation by viruses and type I interferon in vivo. *Science*. 1996;272(5270):1947-1950. doi:10.1126/science.272.5270.1947

33. Ehl S, Hombach J, Aichele P, Hengartner H, Zinkernagel RM. Bystander Activation of Cytotoxic T Cells: Studies on the Mechanism and Evaluation of In Vivo Significance in a Transgenic Mouse Model. *J Exp Med*. 1997;185(7):1241-1252.

34. Zarozinski CC, Welsh RM. Minimal Bystander Activation of CD8 T Cells during the Virus-induced Polyclonal T Cell Response. *J Exp Med*. 1997;185(9):1629-1640.

35. Marshall HD, Prince AL, Berg LJ, Welsh RM. IFN-αβ and self-MHC divert CD8 T cells into a distinct differentiation pathway characterized by rapid acquisition of effector functions. *J Immunol Baltim Md 1950*. 2010;185(3):1419-1428. doi:10.4049/jimmunol.1001140

36. Chu T, Tyznik AJ, Roepke S, et al. Bystander-Activated Memory CD8 T Cells Control Early Pathogen Load in an Innate-like, NKG2D-Dependent Manner. *Cell Rep*. 2013;3(3):701-708. doi:10.1016/j.celrep.2013.02.020

37. Soudja SM, Chandrabos C, Yakob E, Veenstra M, Palliser D, Lauvau G. Memory-T-cell-derived interferon-γ instructs potent innate cell activation for protective immunity. *Immunity*. 2014;40(6):974-988. doi:10.1016/j.immuni.2014.05.005

38. Odumade OA, Knight JA, Schmeling DO, Masopust D, Balfour HH, Hogquist KA. Primary Epstein-Barr virus infection does not erode preexisting $CD8^+$ T cell memory in humans. *J Exp Med*. 2012;209(3):471-478. doi:10.1084/jem.20112401

39. Ge C, Monk IR, Pizzolla A, et al. Bystander Activation of Pulmonary Trm Cells Attenuates the Severity of Bacterial Pneumonia by Enhancing Neutrophil Recruitment. *Cell Rep*. 2019;29(13):4236-4244.e3. doi:10.1016/j.celrep.2019.11.103

40. Holay N, Kennedy BE, Murphy JP, et al. After virus exposure, early bystander naïve CD8 T cell activation relies on NAD+ salvage metabolism. *Front Immunol*. 2022;13:1047661. doi:10.3389/fimmu.2022.1047661

41. Bergamaschi L, Mescia F, Turner L, et al. Longitudinal analysis reveals that delayed bystander CD8+ T cell activation and early immune pathology distinguish severe COVID-19 from mild disease. *Immunity*. 2021;54(6):1257-1275.e8. doi:10.1016/j.immuni.2021.05.010

42. Wherry EJ, Ahmed R. Memory CD8 T-cell differentiation during viral infection. *J Virol*. 2004;78(11):5535-5545. doi:10.1128/JVI.78.11.5535-5545.2004

43. Urban SL, Berg LJ, Welsh RM. Type 1 interferon licenses naïve CD8 T cells to mediate anti-viral cytotoxicity. *Virology*. 2016;493:52-59. doi:10.1016/j.virol.2016.03.005

44. Adam A, Kalveram B, Chen JYC, et al. A single-dose of intranasal vaccination with a live-attenuated SARS-CoV-2 vaccine candidate promotes protective mucosal and systemic immunity. *NPJ Vaccines*. 2023;8(1):160. doi:10.1038/s41541-023-00753-4

45. Yoshida M, Worlock KB, Huang N et al. Local and systemic responses to SARS-CoV-2 infection in children and adults. *Nature*. 2022; 602, 321–327. https://doi.org/10.1038/s41586-021-04345-x

CONCLUSIONS

Synthesis and Implications of Findings

The quantitative, longitudinal measurements of SARS-CoV-2 viral load from individuals with sustained incident infection suggest that the proliferation of virus within a single human follows distinct dynamics at different anatomical sites in the upper respiratory mucosa (**Chapter III**). These distinct dynamics result in extreme differences in viral load among specimen types from the same person (**Chapter IV**), which in turn, substantially impacts the clinical sensitivity of COVID-19 diagnostic tests in a manner that depends on the specimen type tested and the analytical sensitivity of the test (**Chapter III, Chapter VI**). For both pre-Delta and Omicron variants of SARS-CoV-2, we observed that viral loads in the nose generally increased several days after viral loads in saliva and the throat. This delay contributed to the poor clinical sensitivity of nasal swab specimens, particularly with Ag-RDTs and molecular tests during early infection, when individuals are typically asymptomatic but infectious. Cell culture experiments and cross-sectional human specimen analyses suggested that the relationship between SARS-CoV-2 viral RNA concentration and concentration of replication-competent virus was static, and a high viral load was requisite for infectiousness. However, in humans with a dynamic mucosal immune response, this relationship is dynamic: SARS-CoV-2 viral load appears to be more indicative of replication-competent virus in early infection than later infection (**Chapter V**), presumably due to increasing production of antibodies that effectively neutralize replication competent virus but do not affect viral RNA. The poor performance of nasal swab rapid tests in detecting early infection (compared to other specimen types) was associated with higher levels of household transmission (**Chapter VII**). However, Testing both nasal and throat specimens with validated molecular or Ag-RDT tests is likely to improve the detection of early infection, allowing for timely isolation and reduced transmission (**Chapter IX**).

Unlike the asynchronous viral load dynamics, gene expression data indicate that mucosal interferon stimulation is synchronized across the upper respiratory tract, independent of detectable viral proliferation at specific sites (**Chapter X**). A synchronous mucosal immune response could indicate either (1) primary infection with SARS-CoV-2 does not occur at a single site in the upper respiratory mucosa and then spread to other areas, but rather that inoculation occurs near-simultaneously at multiple sites during naturally

acquired SARS-CoV-2 infection or (2) that there is rapid initiation of a global antiviral response coordinated across upper respiratory mucosal surfaces. Either explanation advances our mechanistic understanding of respiratory viral infection in humans. The former explanation contrasts with current models of respiratory viral transmission, which assume a single site of initial infection, while the latter explanation would contrast with current models of interferon signaling, which assume paracrine function that induces a localized antiviral state among close by, neighboring cells.

Future Work

Daily gene expression human transcriptomic data from paired upper respiratory specimen types starting prior to acute viral infection is extraordinarily rare. Generation of this precious dataset was only made possible by four key intersecting factors: advances in nucleic acid purification and sequencing technologies for challenging respiratory specimens, the high prevalence of COVID-19 during the pandemic, increased public health resources for testing and rapid contact tracing, and the willingness of individuals to isolate after exposure and to participate in research. Below, I outline several promising analyses that can be conducted using this valuable dataset:

Matrix Factorization to Identify Gene Program Sequence, and Novel Human Interferon Stimulated Genes

Cellular and tissue function are dependent on a regulated network of gene expression. As such, identification of gene programs—sets of genes with a functional relationship and interrelated expression patterns—and the sequence by which different gene programs are activated can shed light on the tissue level response to acute viral infection in humans. The sequence of stimulation of these gene programs likely plays an important role in coordination of the mucosal immune response. For example, early interferon stimulation activates gene programs comprised of ISGs, which recruit additional leukocytes and initiate an adaptive immune response. Many ISGs known to date are cell-type specific,[1,2] and thus studies of different cell types or anatomical compartments are likely to identify previously unrecognized, putative ISGs, especially in the upper respiratory mucosa. ISGs which are rapidly upregulated in humans upon viral infection are unlikely to have been observed in studies that only analyze gene expression at later stages of infection. I anticipate that identifying early mucosal immune response programs containing known ISGs will uncover new early-response ISGs or suggest putative functions for genes currently lacking annotation. To identify latent

features (interpreted as gene programs) within this transcriptomic dataset, I will employ a signal processing technique known as Orthogonal Non-negative Matrix Factorization (ONMF).[3,4]

Very Early Biomarkers of Respiratory Viral Infection to Improve Diagnostics for Early Detection

Features of the early mucosal immune response to SARS-CoV-2 are discernable even before viral RNA rises to levels detectable by some of the highest analytical sensitivity diagnostic assays available. Conserved changes in gene expression that occur during the early mucosal immune response to viral infection can serve as candidate biomarker for diagnostic assays that enable earlier detection of infected individuals than currently available diagnostics. Earlier detection can prompt earlier isolation that reduces viral transmission, and earlier initiation of antiviral treatment to maximize treatment efficacy I will apply computational methods—including differential expression, cross-correlation, and impulse modeling[5]—to identify genes that change expression during the early stages of infection, before viral RNA becomes detectable. I will prioritize candidate biomarkers that exhibit large, conserved expression changes across individuals and are compatible with RT-qPCR assays. To increase the diagnostic utility, I will also assess biomarkers for conservation during human infection with other respiratory viruses, such as influenza and RSV, using publicly available datasets.

Conservation and Migration of Leukocyte Populations Across Upper Respiratory Mucosal Sites

The mucosal immune response to viral infection results from the function of cells present within, recruited to, or emigrating from the mucosa. Since SARS-CoV-2 can proliferate to high levels ($>10^8$ copies/mL) in multiple anatomical sites of the upper respiratory mucosa simultaneously, the mucosal immune system must balance recruitment of leukocytes across these anatomical sites to combat infection. How leukocyte populations change in different areas of the upper respiratory mucosa during different phases of acute viral infection, and the impact of those populations on viral clearance in the mucosa has not been established. By deconvoluting cell type abundance estimates[6] from bulk gene expression data from annotated single-cell gene expression data, I will monitor changes in the cell populations in different areas of the upper respiratory mucosal throughout acute SARS-CoV-2 infection.

Re-activation of Latent Viral Elements in the Respiratory Mucosa During Acute Viral Infection

Re-activation of latent viral elements (e.g., human endogenous retroviruses, and latent exogenous viruses) within human cells has important health implications, but the mechanistic knowledge of what prompts re-activation and where re-activation occurs in humans is lacking. Re-activation of viral elements is more frequent with age[7] and known to have oncogenic potential.[8,9] More recently, viral re-activation has been linked to immunopathologies including systemic lupus erythematosus, Crohn's disease, and potentially long COVID. Acute infection by a variety of pathogens (including other viruses) has been associated with re-activation of latent viral elements,[10] likely due to perturbation of immune regulation.[11] This re-activation can amplify the innate immune response, with either beneficial or detrimental effects.[12,13] Vaccination against viral infection can induce re-activation of viral elements,[14] which may cause rare but debilitating post-vaccine syndromes (e.g., Guillon-Barré). However, it is not known what specific cellular changes precede the re-activation of these elements in humans during acute viral infection, and whether re-activation is localized to the anatomical site of infection or if infection prompts re-activation across multiple sites. Such mechanistic understanding of re-activations is critical to elucidating their true impact on human health. With this knowledge, researchers can tailor vaccine design for improved safety and efficacy and identify novel mechanisms to prevent viral element re-activation or limit their negative sequelae.

Longitudinal specimens from paired anatomical sites collected by humans throughout the full course of an acute viral infection are necessary to answer these questions, but such samples are incredibly challenging to obtain. Instead, most studies of re-activation of viral elements use cell culture or animal models, and those that use human samples are limited by cross-sectional sampling and/or single specimen types (typically peripheral blood mononuclear cells). Single specimen types cannot answer whether re-activation is localized, or global, and cross-sectional sampling cannot reveal what occurred prior to re-activation.

Using the unique sample set described in **Chapter X** and advanced viral mapping tools,[20] I will map and estimate the abundance of genomic viral elements[15] in our human RNA-seq data to assess whether viral element re-activation is localized during acute viral infection and identify transcriptional and infection-related events preceding re-activation of viral elements.

Regulation of non-coding RNAs During Acute Viral Infection

Beyond coding RNA sequences, there is an increasing appreciation for the role of non-coding RNA molecules in the regulation of cellular function. These include species such as microRNAs, long non-coding RNAs, small interfering RNAs, and small nucleolar RNAs. Changes in non-coding RNA expression during acute viral infection could uncover novel intracellular antiviral mechanisms, or mechanisms by which viral infection interferes with cellular function.[16] I will attempt to study perturbations in non-coding RNA expression associated with acute SARS-CoV-2 infection, and their impact on cellular regulatory networks.

Closing Thoughts

Homo sapiens have always been, and for the foreseeable future will be, at risk of infection. Subsequently, we will be at risk of outbreaks, epidemics, and pandemics. At this moment, an epidemic of a poxvirus (Mpox) is expanding[17] and conjuring memories of the battle against smallpox,[18] and vector borne diseases are expanding their geographic distribution.[19] We must learn from and improve upon our response to the microbial neighbors that threaten our health to reduce the tragedy of future pandemics. I hope that my work adds a small, but solid brick to the foundation laid by numerous scientists before me, including those who developed technologies for studying nucleic acid sequences to enhance the detail with which we can study our world.

References

1. van Boxel-Dezaire AHH, Rani MRS, Stark GR. Complex modulation of cell type-specific signaling in response to type I interferons. *Immunity*. 2006;25(3):361-372. doi:10.1016/j.immuni.2006.08.014

2. Mostafavi S, Yoshida H, Moodley D, et al. Parsing the interferon transcriptional network and its disease associations. *Cell*. 2016;164(3):564-578. doi:10.1016/j.cell.2015.12.032

3. Lee DD, Seung HS. Learning the parts of objects by non-negative matrix factorization. *Nature*. 1999;401(6755):788-791. doi:10.1038/44565

4. Liu Y, Wen Z, Li M. The Power of Matrix Factorization: Methods for Deconvoluting Genetic Heterogeneous Data at Expression Level. *Curr Bioinforma*. 2020;15(8). doi:10.2174/1574893615666200120110205

5. Sander J, Schultze JL, Yosef N. ImpulseDE: detection of differentially expressed genes in time series data using impulse models. *Bioinformatics*. 2017;33(5):757-759. doi:10.1093/bioinformatics/btw665

6. Newman AM, Steen CB, Liu CL, et al. Determining cell type abundance and expression from bulk tissues with digital cytometry. *Nat Biotechnol*. 2019;37(7):773-782. doi:10.1038/s41587-019-0114-2

7. Hurme M. Viruses and immunosenescence - more players in the game. *Immun Ageing A*. 2019;16:13. doi:10.1186/s12979-019-0152-0

8. Chen J, Foroozesh M, Qin Z. Transactivation of human endogenous retroviruses by tumor viruses and their functions in virus-associated malignancies. *Oncogenesis*. 2019;8(1):6. doi:10.1038/s41389-018-0114-y

9. Donzel M, Bonjour M, Combes JD, et al. Lymphomas associated with Epstein-Barr virus infection in 2020: Results from a large, unselected case series in France. *EClinicalMedicine*. 2022;54:101674. doi:10.1016/j.eclinm.2022.101674

10. Ansari S, Gupta N, Verma R, et al. Antiviral activity of the human endogenous retrovirus-R envelope protein against SARS-CoV-2. *EMBO Rep*. 2023;24(7):e55900. doi:10.15252/embr.202255900

11. Reese TA, Wakeman BS, Choi HS, et al. Helminth infection reactivates latent γ-herpesvirus via cytokine competition at a viral promoter. *Science*. 2014;345(6196):573-577. doi:10.1126/science.1254517

12. Grandi N, Tramontano E. Human Endogenous Retroviruses Are Ancient Acquired Elements Still Shaping Innate Immune Responses. *Front Immunol*. 2018;9:2039. doi:10.3389/fimmu.2018.02039

13. Balestrieri E, Minutolo A, Petrone V, et al. Evidence of the pathogenic HERV-W envelope expression in T lymphocytes in association with the respiratory outcome of COVID-19 patients. *EBioMedicine*. 2021;66:103341. doi:10.1016/j.ebiom.2021.103341

14. Daouk SK, Kamau E, Adachi K, Aldrovandi GM. Zoster Meningitis in an Immunocompetent Child after COVID-19 Vaccination, California, USA. *Emerg Infect Dis*. 2022;28(7):1523-1524. doi:10.3201/eid2807.220600

15. Luebbert L, Sullivan DK, Carilli M, et al. Efficient and accurate detection of viral sequences at single-cell resolution reveals putative novel viruses perturbing host gene expression. *bioRxiv*. Published online May 4, 2024:2023.12.11.571168. doi:10.1101/2023.12.11.571168

16. Ziegler CGK, Miao VN, Owings AH, et al. Impaired local intrinsic immunity to SARS-CoV-2 infection in severe COVID-19. *Cell*. 2021;184(18):4713-4733.e22. doi:10.1016/j.cell.2021.07.023

17. Kozlov M. Growing mpox outbreak prompts WHO to declare global health emergency. *Nature*. 2024;632(8026):718-719. doi:10.1038/d41586-024-02607-y

18. Adetifa I, Muyembe JJ, Bausch DG, Heymann DL. Mpox neglect and the smallpox niche: a problem for Africa, a problem for the world. *Lancet Lond Engl*. 2023;401(10390):1822-1824. doi:10.1016/S0140-6736(23)00588-3

19. Paz S. Climate change: A driver of increasing vector-borne disease transmission in non-endemic areas. *PLOS Med*. 2024;21(4):e1004382. doi:10.1371/journal.pmed.1004382

20. Laura L, Sullivan DK, Carilli M, Hjörleifsson KE, Viloria Winnett A, Chari T, Pachter L. *bioRxiv*;2023. doi: https://doi.org/10.1101/2023.12.11.571168

END